The role of R-spondin3 in coronary artery formation and novel roles for retinoic acid signaling in cardiac development and repair

Fabio da Silva

École doctorale Sciences de la Vie et de la Santé (ED85)
Unité de recherche : INSERM U1091/CNRS UMR7277 / UCA

Thèse de doctorat

Présentée en vue de l'obtention du
grade de docteur en interactions moléculaires et cellulaires
de
L'UNIVERSITE COTE D'AZUR

par
Fabio Da Silva

Etude du rôle de R-spondin3 dans la formation des artères coronaires et des nouvelles fonctions dans la signalisation de l'acide rétinoïque au cours du développement et de la réparation cardiaques.

Dirigée par Andreas Schedl

Soutenue le 13 Octobre 2017
Devant le jury composé de :

Andreas	Schedl	Dr., iBV	Directeur de thèse
Kay	Wagner	Dr., iBV	Président du Jury
Pascal	Dollé	Dr., IGBMC	Examinateur
Ramón	Muñoz Chápuli	Dr., Universidad de Málaga	Rapporteur
Robert	Kelly	Dr., IBDM	Rapporteur
Sigolène	Meilhac	Dr., Institut Pasteur	Examinatrice

TABLE OF CONTENTS

RESUMÉ/ABSTRACT..... 3

ACKNOWLEDGEMENTS..... 5

CHAPTER I: INTRODUCTION

-**Part I**: Heart morphology and functions..... 7
-**Part II**: Cardiogenesis and cell lineages of the heart..... 12
-**Part III**: Coronary vessel development..... 20
-**Part IV**: Cardiac regeneration..... 29
-**Part V**: Wnt signaling in cardiac development and repair..... 36
-**Part VI**: The R-spondin protein family..... 45
-**Part VII**: Retinoic Acid signaling in the heart..... 60

CHAPTER II: THE ROLE OF R-SPONDIN3 IN CORONARY ARTERY FORMATION

-**Part I**: Project description..... 87
-**Part II**: Schematic of project description..... 90
-**Part III**: Manuscript entitled: "Coronary artery formation is driven..... 91
by localized expression of R-spondin3". Cell Reports *20*, 1745-1754.
-**Part IV**: Future perspectives..... 111

CHAPTER III: NOVEL FUNCTIONS FOR RETINOIC ACID SIGNALING IN CARDIAC DEVELOPMENT AND REPAIR

-**Part I**: Project description..... 115

-**Part II**: Schematic of project description…….. 119
-**Part III**: Manuscript entitled: “Retinoic acid signaling promotes …….. 120
cardiomyocyte survival in cardiac development and repair”. *In preparation.*
-**Part IV**: Future perspectives…… 173

CHAPTER IV: CONCLUSION

-General conclusion…….. 178

CHAPTER V: BIBLIOGRAPHY

-References for chapters I, II, III and IV……180

RESUMÉ

Les maladies coronariennes sont l'une des principales causes de décès dans le monde. Comment les artères coronaires sont modelées et quelles sont les molécules de signalisation qui régissent ce processus, sont des mécanismes mal compris. Dans la première partie de ma thèse, j'ai identifié le modulateur de signalisation Wnt *Rspo3* comme un régulateur crucial de la formation de l'artère coronaire dans le cœur en développement. *Rspo3* est spécifiquement exprimé autour des branches coronaires à des moments critiques dans leur développement. L'ablation temporelle de *Rspo3* à E11.5 conduit à une diminution de la signalisation de β-caténine et à une réduction de la prolifération spécifique des artères. En conséquence, les branches coronariennes sont défectueuses et l'arbre artériel ne se forme pas correctement. Ces résultats identifient un mécanisme par lequel l'expression localisée de RSPO3 induit la prolifération des artères coronaires à leurs branches permettant leur formation.

Le traitement des patients qui se remettent d'un infarctus du myocarde (IM) est difficile car les cardiomyocytes ont une capacité très limitée à proliférer et à régénérer le cœur endommagé. La voie de signalisation de l'acide rétinoïque (AR) est essentielle pour le développement cardiaque et joue un rôle protecteur dans les cœurs endommagés. Les mécanismes exacts et les types de cellules impliqués dans cette réponse protectrice ne sont pas clairs. Pour la deuxième partie de ma thèse, j'ai utilisé une nouvelle lignée rapportrice de l'AR inductible au TAM développée dans notre laboratoire et j'ai observé une réponse spécifique des cardiomyocytes pendant la fin de la gestation et après l'IM. L'ablation de la signalisation de l'AR par délétion génétique des enzymes Raldh1/2/3 entraîne une augmentation de l'apoptose myocytaire à la fin du développement tardif et après l'IM. Le séquençage des ARNs des cardiomyocytes primaires révèle que le traitement à l'AR réprime l'expression de *Ace1*, indiquant un nouveau lien entre la signalisation AR et le système Rénine Angiotensine dans le contexte de la réparation cardiaque.

ABSTRACT

Coronary artery disease is one of the leading causes of death worldwide. How coronary arteries are remodeled and the signaling molecules that govern this process are poorly understood. For the first part of my thesis, I have identified the Wnt-signaling modulator *Rspo3* as a crucial regulator of coronary artery formation in the developing heart. *Rspo3* is specifically expressed around the coronary stems at critical time-points in their development. Temporal ablation of *Rspo3* at E11.5 leads to decreased β-catenin signaling and a reduction in arterial-specific proliferation. As a result, the coronary stems are defective and the arterial tree does not form properly. These results identify a mechanism through which localized expression of RSPO3 induces proliferation of the coronary arteries at their stems and permits their formation.

Treating patients recovering from myocardial infarction (MI) is difficult since cardiomyocytes have a very limited capacity to proliferate and regenerate the damaged heart. The Retinoic Acid (RA) signaling pathway is essential for cardiac development and plays a protective role in damaged hearts. The exact mechanisms and cell types involved in this protective response is unclear. For the second part of my thesis, I have utilized a novel inducible RA reporter line developed in our lab and I have observed a cardiomyocyte-specific response during mid-late gestation as well as after MI. Ablation of RA signaling through genetic deletion of the *Raldh1/2/3* enzymes leads to increased myocyte apoptosis both during late development and after MI. RNA sequencing analysis of primary cardiomyocytes reveals atRA treatment represses *Ace1* expression, providing a novel link between RA signaling and the Renin Angiotensin System in the context of heart repair.

ACKNOWLEDGEMENTS

Before embarking on the long and difficult journey of defending a PhD, I had no idea how to think, act or perform like a researcher. I had no idea how to be a scientist. How to be an independent thinker capable of approaching a difficult question, formulating a hypothesis and carrying out the necessary experiments to either prove or disprove my initial hypothesis. But practice makes perfect. And with time I learned to work efficiently, to be innovative and to conduct my work with scientific rigour. However, this transformation into what I am today would not have been possible without the support of many people.

I would like to start off by thanking my supervisor, Andreas Schedl, for always believing in me and for encouraging me to pursue my research interests, wherever they took me. Being the only one working on the heart was undoubtedly difficult, but the experience molded me into a stronger, more capable researcher. Most other supervisors would not have supported this, but Andreas did, so, from the bottom of my heart, thank you! I would also like to thank Fariba Jian Motamedi for her tremendous dedication and enormous skill in performing the myocardial infarction surgeries. This VERY IMPORTANT part of the project would, without a shadow of a doubt, not have been possible without her. I would also like to thank Ana Sofia Rocha, my initial supervisor, who pretty much taught me everything I know. She showed me the ropes and encouraged me to always strive for the best. More importantly, she taught me to be critical not only of my own work, but of the scientific literature in general. Until today, I utilize the knowledge I gained from Ana, and I am sure I will continue to do so for the rest of my scientific career. It goes without saying that my PhD would have been a lot more difficult and less productive were it not for the continuous help of Kay Wagner. His technical expertise and willingness to teach were great assets to me, and I would have been lost without his guidance. Dr. Robert Kelly's advice as an expert in the field was also invaluable, and I am grateful to him for taking the time

to help me. And of course, I would like to thank all of the members of my lab. The lab meetings were great, the friendships, even better!

Completing a PhD requires a lot of technical and theoretical knowledge, as well as many, many, many hours of work. It also requires emotional and mental fitness. Without the help of my family, I do not think I would have had the will and right mindset to accomplish all that I have during my PhD. So I would like to thank my mother, father, brother and grandmother for always being there for me during the past four years. You guys kept me sane and focused. Without your moral support I would have had a much harder time getting through the many tough moments presented to me during my PhD. And last, but DEFINITELY not least, I would like to thank my lovely wife. Thanks for waiting and thanks for always being there for me. You are, and always will be, my rock. This PhD is dedicated to you, *meu amor*.

CHAPTER I: INTRODUCTION

I. Heart morphology, functions and disease

"The heart is, as it were, the hearthstone and source of the innate heat by which the animal is governed."

The heart has played an important part in understanding the human body since antiquity. In his treatise, *On the usefulness of the Parts of the Body,* the Greek physician Aelius Galenus described the heart as the body's innate source of heat and as the organ most closely related to the soul. Since then our understanding of the anatomy, physiology and function of the heart has evolved significantly. Yet cardiovascular-related diseases remain the number one cause of death worldwide. Hence, there is a need for a deeper understanding of the human heart and its associated pathologies.

The human heart is a muscular organ located in the midline of the thoracic cavity. It is hollow and cone shaped and consists of four separate chambers. The wall of the heart is comprised of three layers: the outer pericardium, the middle myocardium, and the inner endocardium (Figure 1A). The pericardium is the outer most layer that is composed of connective tissue and serves to protect the heart by reducing friction. The myocardium is made up of cardiac muscle and is surrounded by blood vessels and specialized nerve fibers. The function of the myocardium is to contract in a coordinated fashion in response to nervous pulses transmitted by the cardiac conduction system. The endocardium is the inner most layer of the heart and is made up mainly of blood vessels. The endocardium acts as a barrier between the blood and the heart. (Clark, 2005).

The heart plays a central role in the cardiovascular system, acting as a mechanical pump that distributes blood throughout the entire body. The heart's four chambers consist of two atria and two ventricles. Deoxygenated blood from the body enters the heart via the right atrium through

the superior and inferior vena cavae. This blood is pumped into the right ventricle and then through the pulmonary artery into the lungs, where it is oxygenated and delivered back to the left atrium via the pulmonary veins. The oxygenated blood is then pumped to the left ventricle and eventually through the aorta to the rest of the body (Figure 1B). Anatomically, the left ventricle contains a much thicker muscular layer than the right since it pumps blood to all body parts and has a much higher resistance to blood flow. The atria are separated by a solid wall known as the interatrial septum and the ventricles are separated by the interventricular septum. This separation is necessary to avoid mixing of oxygenated (left) and deoxygenated (right) blood. One way blood flow in the heart is ensured by a system of bi or tricuspid valves that are attached to the ventricular walls by strong fibers known as chordae tendinae. The atrioventricular valves, which consist of the bicuspid mitral valve (right) and the tricuspid atrioventricular valve (left), ensure one-way blood flow between the atria and ventricles. The pulmonary and aortic valves (tricuspid semilunar valves) ensure one way blood flow from the ventricles to the pulmonary artery and aorta respectively (Clark, 2005).

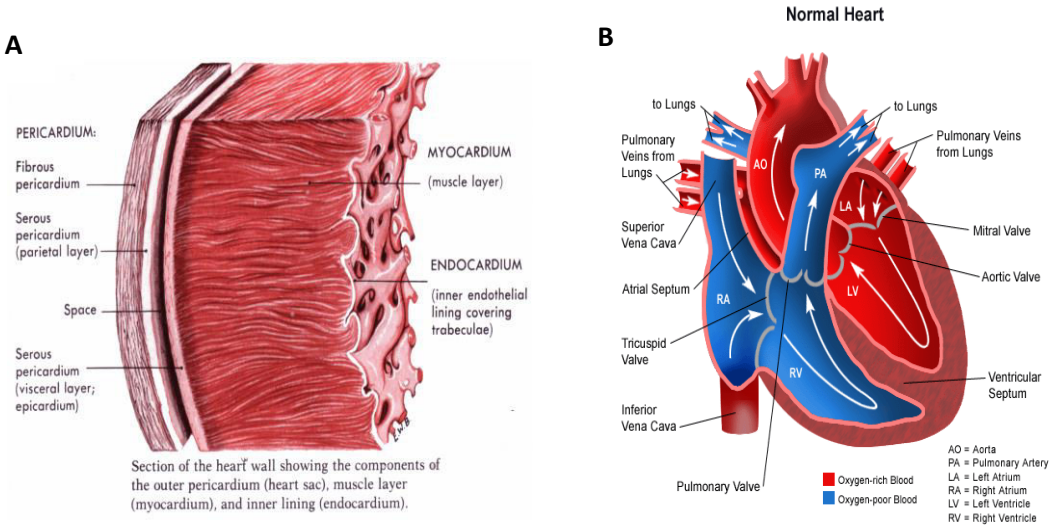

Figure 1. *Anatomy of the heart.* **A,** Cross section of the heart wall showing the various layers of the heart. **B,** diagram showing the various compartments and components of the heart. White arrows delineate the flow of blood through the atria, ventricles and great arteries (aorta and pulmonary artery). (Clark, 2005)

Coordinated contraction of the atria and ventricles is achieved by a specialized subset of cardiac muscle cells that innervate the myocardium. These cells, collectively known as the cardiac conduction system, are responsible for conducting an electrical pulse that stimulates muscle contraction within the heart. The pulse begins at the sinoatrial node (SAN), which is located in the right atrium near the superior right vena cava and is composed of a specialized mass of cells capable of autonomously initiating pulses. The pulse then passes along fibers of the conduction system, promoting atrial contraction, until it reaches the atrioventricular (AV) node. The AV node delays the pulse slightly, allowing the atria to refill with blood before ventricular contraction. From the AV node the pulse passes into a large AV bundle (bundle of His) and then spreads into the Purkinje fibers, which extend into the ventricles and permit the pulse to stimulate contraction of the ventricular myocardium (Clark, 2005).

In order to ensure the heart's nutritional and oxygen requirements are met, blood is supplied to the myocardium by a dedicated system of coronary arteries, veins and capillaries. Coronary circulation begins after left ventricular contraction, with the movement of blood from the aorta into two coronary orifices located just above the aortic valves. Connected to these orifices are the left and right coronary arteries, which extend into the ventricles and then branch off into a network of smaller arteries, arterioles and capillaries that supply the entire myocardium with oxygenated blood. After supplying the heart muscle with oxygen and nutrients the blood is then distributed to a system of venules and veins, which empty out into the right atrium via the coronary sinus (Reese et al, 2002).

Congenital heart disease (CHD) is a structural abnormality of the heart and/or great vessels that is present at birth. It is the most common birth defect, affecting nearly 1% of newly born infants. Moreover, it is estimated that around 30% of prenatal loss can be attributed to heart malformations (Brunneau, 2008). CHD is usually characterized based on a combination of anatomic and physiological phenotypes. These include conotruncal impairments such as ventricular and/or atrial septa defects, outflow tract malformations, defects resulting from abnormal left-right relationships,

valve abnormalities, and a broad range of other abnormalities (Zeidi and Brueckner, 2017). A special subset of CHDs involves defective development and/or anatomic variation of the coronary arteries. These diseases, known as coronary artery anomalies (CAA), can lead to serious clinical repercussions such as sudden cardiac death (Angelini, 2007). Overall, approximately one third of CHD patients have severe defects that require surgical intervention in the first year of life. Despite progress in medical and surgical treatments, CHD remains the leading cause of mortality from birth defects in the developed world and among the world's poorest populations CHD has a greater contribution to cardiovascular disease than ischaemic heart disease or stroke (Zeidi and Brueckner, 2017). The majority of CHDs are genetic and caused by mutations in genes that are essential for proper heart formation during embryonic development (Brunneau, 2008). Hence, understanding these pathways is essential in order to improve the diagnosis and treatment of patients with CHDs.

Cardiovascular diseases resulting from stroke and acute myocardial infarction (MI) are among the leading causes of death worldwide killing up to 17.5 million people a year (Mozaffarian et al., 2015). Myocardial infarction (MI) results from occlusion of a coronary artery after atherosclerotic plaque rupture and thrombosis (Antman and Braunwald, 2001). The resulting lack of blood flow to the myocardium leads to rapid cellular death, which then triggers a massive inflammatory response (Frangogiannis, 2014). The inflammatory response gradually clears out the injury site leaving sparse tissue with enlarged capillaries. Eventually the gap fills with granulation tissue, which, after a certain period of time, begins to mesh into a dense non-functional scar. To compensate for the loss of functional tissue, the myocardium surrounding the infarct area undergoes a hypertrophic response and a series of remodeling steps, leading to ventricular dilation. Although the initial reaction to MI is protective and acts to limit the spread of the damage, the excessive scar formation and ventricular remodeling acts as a barrier to proper electromechanical coupling between healthy regions of the heart; thus, compromising efficient and synchronous contraction of the myocardium (Aisagbonhi et al, 2015). The issue is further

aggravated by the fact that cardiomyocytes, the principle cell-type comprising the contractile myocardium, have a very limited capacity to proliferate and regenerate the damaged area (Roij, 2016). Hence, the heart cannot recover and over time its function continues to decrease, eventually leading to heart failure and death. Interestingly, many of the molecular programs essential for proper heart formation during embryonic development are reactivated following myocardial infarction (Roij, 2016). These pathways influence several aspects of the inflammatory response, ventricular remodeling and cell death. Understanding the contributions of these pathways to myocardial infarction is, thus, an integral part of designing novel regenerative treatments for patients suffering from myocardial infarction.

The mouse serves as an excellent model to study the molecular cues involved in cardiac development and disease. It is a well characterized mammalian species and many of the signaling pathways active during cardiac development and repair in the mouse play a similar role in humans (Roij, 2016). Furthermore, myocardial infarction can be easily modeled in the mouse and the wide variety of transgenic lines available allow us to study and manipulate the various pathways activated during cardiac remodeling and repair (Aisagbhoni et al., 2015). Hence, by combining the knowledge gained from murine developmental studies and MI models, scientists can gain a deeper understanding of the molecular mechanisms activated in the post ischaemic heart in order to design novel regenerative treatments for patients suffering from cardiovascular diseases.

II. Cardiogenesis and cell lineages of the heart

Cardiogenesis:

The embryonic heart is the first organ to function and it is essential for the distribution of oxygen and nutrients during embryogenesis (Vincent and Buckingham, 2010). In the mouse, heart development begins at Embryonic day 6.5 (E6.5) with specification of the cardiogenic mesoderm

in bilateral territories of the lateral mesoderm. At E7.5, cardiac progenitor cells extend towards the midline to form the cardiac crescent. The cardiac crescent is composed of two distinct populations of pre-cardiac cells, the so-called first and second heart fields. At E8.0, the cardiac crescent fuses at the midline and gives rise to the linear heart tube (Brade et al., 2016).

The linear heart tube is a primitive structure containing two tissues, the inner endocardium and the outer myocardium, which are separated by a thick extracellular matrix termed the cardiac jelly. Shortly after it is formed, the linear heart tube initiates a characteristic rightward looping that realigns and expands the heart, giving rise to a complex structure with four domains (MacGrogan et al., 2010). This looping and expansion of the heart tube occurs via two mechanisms: cell proliferation, and recruitment of additional cells (Brade et al., 2013). The additional cells are added to the arterial and venous poles of the heart and they originate primarily from the secondary heart field. SHF progenitors mainly contribute to the outflow tract (OFT), the right ventricle (RV) and a large portion of the inflow region (atria) (Buckingham et al., 2005; Kelly, 2012). The left ventricle (LV) is mainly derived from the first heart field. From E9.5-10.5 the atrioventricular canal, which separates the developing atria and ventricles, begins to form along with the valve primordia. Chamber development also progresses with trabeculae formation in the left and right ventricles (MacGrogan et al., 2010).

At E10.5 the developing heart is populated by two sources of extra cardiac cells: the proepicardium and the cardiac neural crest (Brade et al., 2010). The proepicardium gives rise to the epicardium, which consists of a single layer of cells that completely surrounds the heart. From E11.5-14.5, many epicardial cells undergo epithelial to mesenchymal transition and migrate into the heart, giving rise to various cell-types such as vascular smooth muscle cells, cardiac fibroblasts and a subset of endothelial cells (Brade et al., 2010). Additionally, the epicardium supports cardiomyocyte proliferation by secreting soluble growth factors to the underlying myocardium (Perez Pomares and de la Pompa, 2011). At E9.5 a subpopulation from the cranial neural crest, termed the cardiac neural crest cells (CNCC), begins to migrate towards the

pharyngeal arches. As they enter the heart, CNCCs differentiate into smooth muscle cells of the distal outflow tract and proximal coronary arteries (Brade et al., 2013; Arima et al., 2012). The cardiac neural crest also plays an essential role in signaling to the myocardium and promoting septation of the great arteries (pulmonary artery and aorta) as well as the atrial and ventricular chambers (Brade et al., 2013).

By E14.5 the heart is fully septated and the chambers and cell types are well-defined. The heart continues to proliferate, grow and mature throughout development and the post-natal period until 7 days post birth (P7), at which point the cardiomyocytes drastically slow down their proliferation rates. As the pup matures, the heart continues to grow but does so mainly via hypertrophy rather than hyperplasia (Xiao et al, 2017).

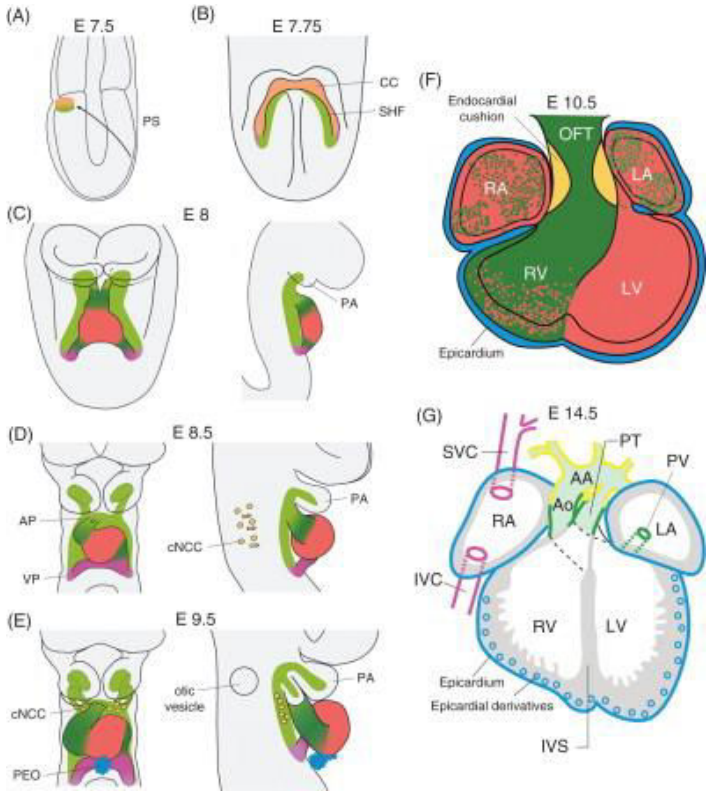

Figure 2. *Different steps in heart development.* **A-B**, Specification of cardiogenic mesoderm from primitive streak (PS) and formation of the cardiac crescent (CC). **C–E**, Formation and looping of the heart tube with contributions of cardiac neural crest cells (cNCC), which migrate from the pharyngeal arches (PA) to the arterial pole (AP). The proepicardial organ (PEO) forms in the vicinity of the venous pole (VP). **F,** The looped heart tube, with the cardiac compartments—OFT, outflow tract; RA, right atrium; LA, left atrium; RV, right ventricle; LV, left ventricle. **G,** The mature heart which has undergone septation—IVS, interventricular septum; AA, aortic arch; Ao, aorta; PT, pulmonary trunk; PV, pulmonary vein; SVC, superior caval vein; IVC, inferior caval vein. The first heart field (FHF) and its myocardial contribution are shown in red, the SHF and its derivatives in dark green (myocardium) and pale green (vascular endothelial cells), cNCC in yellow, and PEO derivatives in blue (Vincent and Buckingham, 2010).

Overall the heart is a complex organ formed of various cell types. These include atrial and ventricular cardiomyocytes, vascular smooth muscle of the great arteries and coronary vessels, endothelial cells of the vasculature and endocardium, cardiac fibroblasts, epicardial cells and interstitial cells of the AV and semilunar valves. Cardiomyocytes make up the majority of the heart by volume but constitute only around 25-35% of the total number of cells. The rest is made up of other cell types such as cardiac fibroblasts and endothelial cells. Originally it was thought that fibroblasts were the principle non-myocyte cell type, constituting up to 50% of the cells in the heart. However, these estimates were probably overestimated due to the lack of specific markers for fibroblasts. Recent work with novel antibodies more specific to fibroblasts placed their number at around only 10% of all cells. In this study, endothelial cells were determined to be the principle non-myocyte cell type making up around 45% of the total number of cells (Pinto et al., 2016). Overall, the cell types of the heart arise at different times during cardiac formation and originate from different sources. Characterizing the origin and characteristics of these sources along with their precise contributions to the cell types of the heart has required a tremendous amount of work and has been the subject of much debate.

Cardiogenic mesoderm:

The cardiogenic mesoderm, which harbors the so called first and secondary heart fields, forms the major proportion of the ventricular, atrial, and outflow tract myocardium. Additionally, these progenitors contribute cells to the endocardium, the conduction system and the aortic and pulmonary cushions (Kelly et al., 2012). Mesoderm induction is regulated by numerous signaling pathways such as Nodal, bone morphogenetic protein (BMP) and WNT signals, as well as fibroblast growth factors (FGF) (Kimmelman et al., 2006; Noseda et al., 2011) . Expression of the T box transcription factor Brachybury/T (*Bry*), a direct target of Wnt/β-catenin signaling, marks

mesodermal cells ingressing through the primitive streak. Commitment of these cells towards a cardiac fate requires inhibition of canonical WNT/β-catenin signaling and activation of non-canonical WNT signaling (Gessert and Kuhl, 2011). After ingression through the PS, cardiac progenitor cells migrate to the anterior lateral position caudal to the head folds to form the cardiac crescent. At this time-point the first and second heart fields can be distinguished by their positions in the crescent (FHF progenitors more anterior and lateral in respect to SHF). Although the FHF cells already differentiate at this stage, the SHF cells remain in a proliferative progenitor state. It is only after entering the heart at a later time-point that they differentiate into mature cells (Kelly et al., 2012).

Although no genes are uniquely expressed in the early FHF progenitors, the SHF precursors are marked by expression of the LIM-homeobox transcription factor islet-1 (Kelly, 2012). Islet-1 expression is dependent on canonical WNT signaling (Cohen et al., 2008), and it is essential for the survival, proliferation and migration of SHF progenitors. As SHF progenitor cells migrate into the heart and differentiate, Islet-1 expression is extinguished (Cai et al., 2003). Several studies have shown that the molecular signature *Isl1+/Nkx2.5+/Flk1+* marks a specific pool of primitive SHF progenitors that are multipotent and give rise to both myocytic and vascular cells. In particular, *Isl1+/Nkx2.5+* descendants that have lost Flk expression form cardiomyocytes and smooth muscle cells (SMCs) and extensively contribute to the proepicardial organ (Zhou et al., 2008), whereas the *Isl1+/Flk1+* subset differentiates to form endothelial cells and SMCs (Moretti et al., 2006). Interestingly, the SHF can be further subdivided into two different fields: the anterior heart field (AHF) and the posterior heart field (PHF). The AHF is marked by expression of genes such as *Fgf10* and *Mef2c,* and it contributes to the outflow tract and right ventricle. The PHF expresses *islet-1* but not any of the specific AHF heart field markers, and it contributes mainly to the atria (Zaffran et al.,2014). A critical transcription factor expressed in the PHF is *Tbx5*, which contributes to atrial septation and differentiation.

The fate of SHF progenitors is controlled by many different signaling pathways. FGF signaling promotes progenitor cell proliferation within the SHF and SHH-mediated signaling from the endoderm along with midline (neural tube) canonical WNT signaling maintain stemness and prevent differentiation of the SHF progenitors (Kelly 2012). BMPs, notch and non-canonical WNT signals promote differentiation of the SHF progenitors (Vincent and Buckingham, 2010). Epigenetic factors and microRNAs also play important roles in the progression of SHF progenitors to differentiated myocyte and non-myocyte cell types (Liu and Olson, 2010).

The Proepicardium:

The epicardium comprises the outer most layer of the heart and is essential for proper cardiac development. The epicardium, arises between E9.5 and E11.5 and is derived from a cluster of cells known as the proepicardium (PE). Apart from providing the heart with a protective outer layer, the epicardium is essential for coronary vessel development and formation of the compact myocardial layer. Defects in epicardial development generally lead to severe cardiac deformations and embryonic death around mid-late gestation (Brade et al., 2013).

The PE arises from the coelomic mesenchyme of the septum transversum in close proximity to the venous pole of the heart at E8.5 (Manner et al., 2001). PE induction, growth and maintenance depends upon opposing interactions between FGF signaling, which induces a proepicardial fate in the posterior splanchnic mesoderm, and BMP signaling, which drives myocardial differentiation of this population (Schlueter and Brand, 2012). The majority of PE progenitors are marked by expression of T-box18 (Tbx18) and Wilm's tumour protein1 (*Wt1*) (Brade et al., 2012), with many of the *Wt1* progenitors being derived from *Nkx2.5*+ and *Isl1*+ precursors (Zhou et al., 2008). An additional subpopulation of cells marked by the transcription factors Semaphorin3d (Sema3D) and Scleraxis (*Scx*) has been described, suggesting the PEO is a heterogeneous organ (Katz et al., 2012). Beginning at E9.5, free floating vesicles from the PE migrate towards the heart and upon contact flatten and spread out on the naked myocardium

(Brade et al., 2013). Cell adhesion molecules such as vascular adhesion molecule (VCAM) and b4-a1-integrin play a crucial role in this process, which is completed around E11.5 (Yang et al., 1995).

After the epicardium has been formed a complex array of signaling pathways work together to drive: (1) epicardial epithelial to mesenchymal transition and formation of epicardial-derived cells (EPDCs), (2) differentiation of EPDCs into different cell lineages, (3) compact zone proliferation, and (4) coronary vessel development. *Wt1* and *Tbx18* signaling are key factors for normal progression of epicardial EMT as well as subsequent EPDC migration and differentiation (Brade et al., 2013). FGFs, Notch and retinoic acid play prominent roles in promoting cardiomyocyte proliferation and formation of the compact zone (Sucov et al., 2009). Although there has been much debate about the exact contribution of EPDCs to different cell lineages, there is a general consensus that the majority of cardiac fibroblasts and vascular smooth muscle cells of the heart are derived from the epicardium (Brade, 2013). Whether or not cardiomyocytes are derived from the epicardium is not clear. Lineage tracing with a *Tbx18-Cre* suggests a small portion of cardiomyocytes derive from the epicardium, but these studies are muddled by the fact that cardiomyocyte-specific expression *Tbx18* is detected between E10.5-16.5 (Brade et al., 2013). In terms of contribution to the vasculature of the heart, the majority of the endothelium seems to be derived from different sources (venous endothelium of the sinus venosus (Red Horse et al., 2010) and ventricular endocardium (Wu et al., 2012)). However, recent studies show that a small portion of endothelial cells are in fact derived from the *Scx+/Sema3D+* population of the PEO (Katz et al., 2012).

The Cardiac Neural Crest:

CNCCs are a subpopulation of the cranial neural crest cells that delaminate from the neural tube and migrate on preset routes to the heart, reaching the pharyngeal arches 3,4, and 6 by E10.5 (Brade et al., 2013). The induction of CNCC progenitors is promoted by various molecular

cues such as BMP/TGF-β, FGF, WNT/β-catenin, FGF and retinoic acid signaling (Vincent and Buckingham, 2010). Their migration towards the heart is promoted by ligands of the ephrin family, sempahorins, connexin-43 and many other chemical attractants (Kuriyama and Mayor, 2008). Once the CNCCs reach the pharyngeal arches, endothelin, TGF-β and PDGF signaling promote their role in patterning the aortic arch arteries (Hutson and Kirby, 2007). In addition, to aortic arch patterning, CNCCs also play a role in promoting OFT development and septation. Defective CNCC induction and/or migration has been shown to lead to shortening and defective loop formation of the OFT. These phenotypes are generally caused by altered SHF progenitor addition to the developing OFT (Brade et al., 2013). The cellular contribution of CNCCs to the heart remains an ongoing debate, but it is generally thought that they differentiate into smooth muscle cells of the distal outflow tract and proximal coronary arteries, as well as a portion of insulating-glial cells of the cardiac conduction system (Brade et al., 2013).

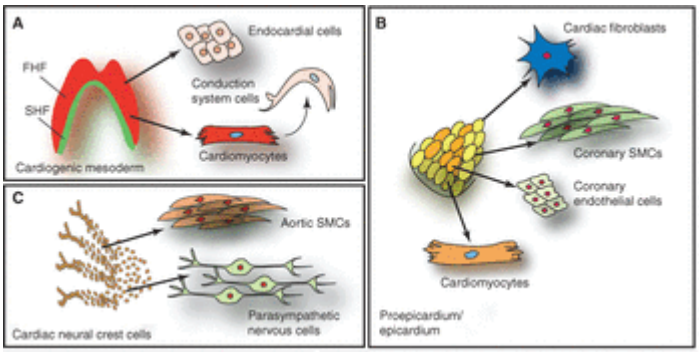

Figure 3. *Embryonic heart progenitor contributions to different cardiac compartments and cell types during heart morphogenesis in mouse development*. **A,** Cardiogenic mesoderm, **B,** proepicardium/epicardium, and **C**, cardiac neural crest cell lineage diversification (Brade et al., 2013).

Important transcription factors in cardiac development:

One of the first markers of cardiac progenitor cells is *Mesp1*, which is required for the delamination of these cells from the primitive streak (Vincent and Buckingham, 2010). A *Mesp1*-

Cre line crossed to a *Rosa26* conditional reporter marks all of the mesoderm-derived cardiac cells of the heart (Saga et al., 2009). It has been proposed that *Mesp1* acts as a master regulator of cardiovascular cell fates by down regulating pluripotency and early mesodermal genes and up regulating key transcription factors such as *Gata4* or *Nkx2-5*. Mesp1 has also been reported induce cardiogenesis by inhibiting canonical WNT signaling through promoting the expression of the WNT inhibitor Dkk1 (Vincent and Buckingham, 2010).

Other important transcription factors include *Gata4* and *Nkx2-5*, which are expressed in the cardiac crescent where myocardial cell differentiation first takes place. T-box transcription factors such as *Tbx5* and *Hand1/2* (basic helix-loop-helix), as well as *Mef2c* (MADS-box) factors are also involved in cardiogenic differentiation. In the context of master regulators, *Gata4* and *Tbx5*, along with the chromatin remodeling complex *Baf60c/Smarcd3*, can induce beating myocardial tissue when ectopically expressed in mesoderm. *Gata4* and *Baf60c* induce *Nkx2-5* expression which acts with Gata4 to initiate the cardiac program, while *Tbx5* plays an important role in inducing full differentiation (Takeuchi and Bruneau, 2009). By manipulating the expression of these along with many other transcription factors many groups have been able to generate functional myocardial cells from precursor populations. In fact, recent work using viral vectors to induce the expression of the transcription factors *Gata5, Mef2c* and *Tbx5* (GMT), showed that functional cardiomyocytes could be reprogrammed from adult fibroblasts (Qian et al., 2012). Hence, the clinical significance of not only delineating the cell lineages of the heart but understanding the transcriptional programs involved in their differentiation and maturation becomes clear and opens up numerous avenues towards novel regenerative treatments.

III. Development of the Coronary vasculature

Overview of coronary vessel development

Early in embryogenesis, the heart contains a thin layer of myocardial muscle that is easily oxygenated by blood flowing through its lumen. As the heart grows and the compact myocardial layer is formed, blood vessels emerge in order to support cell proliferation. Coronary vessel development begins with the formation of an immature vascular plexus on the dorsal part of the atrioventricular groove. This vascular plexus then undergoes branching morphogenesis followed by massive expansion to cover the entire heart (Red Horse et al., 2010). The plexus eventually connects with the aorta at the coronary orifices and coronary circulation is initiated (Figure 4) (Sharma et al., 2017). Following the initiation of blood flow the vascular plexus is remodeled into mature arteries, capillaries and veins. The result is a mature circulation system that supports efficient oxygenation of the myocardium.

The mature coronary vascular system is composed of various cell types that originate from different sources. In total, they comprise up to 60% of the non-myocyte population of cells (Pinto et al., 2016). All coronary vessels are lined by a single layered endothelium comprised of endothelial cells with specialized functions. Surrounding the endothelial layer are mural cells, which include smooth muscle cells covering arteries, and pericytes around capillaries. Veins also contain a smooth muscle layer but at a lower density than arteries. In mice large arteries are located deep within the myocardium (intramyocardial) and veins are closer to the surface (subepicardial). Capillaries are located throughout the entire heart (Sharma et al., 2017).

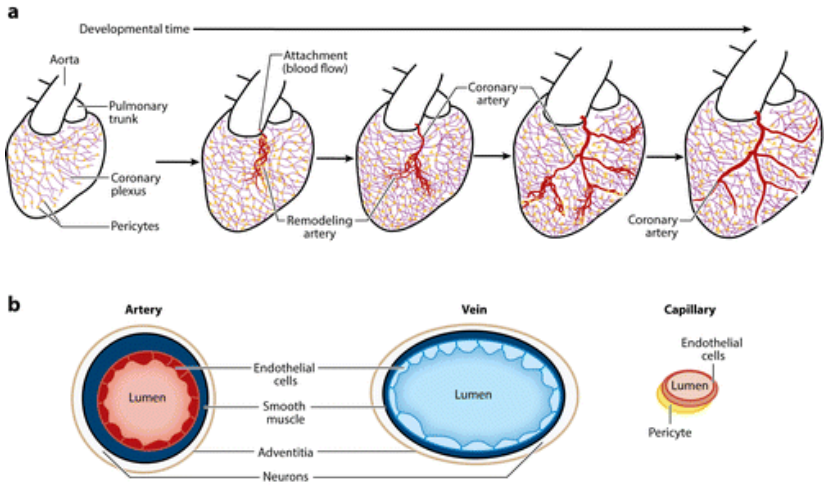

Figure 4. *Structure and cellular components of the coronary vasculature*. **A,** Schematic of the developmental events leading to mature coronary arteries. First, a coronary plexus (*purple*) covered in pericytes (*yellow*) migrates over the surface of the heart and into the myocardium. Then, plexus vessels attach to the aorta to initiate blood flow, triggering arterial remodeling (*red*) that ultimately leads to mature arteries. **B,** Depiction of the major cell types comprising the coronary vasculature. (Sharma et al., 2017)

Origins of the coronary endothelium:

The origin of the coronary vessels has been a topic of great interest for over a century. Initial observations of coronary connections lead scientists to believe coronary arteries and veins budded from the aortic orifices and sinus venosus respectively (Bennett, 1936; Goldsmith and Butler, 1937). However, through a series of transplantation studies in the chick, it was demonstrated that the coronary endothelium originated from an extra cardiac source, namely the proepicardial organ (Manner, 1999; Poelmann et al., 1993). For many years the PEO origin of coronary endothelial cells was accepted as a universal model for most complex organisms, including the mouse. However, with the advent of novel *Cre* recombinase lineage tracing systems, the PEO origin model for the mouse was challenged and gradually replaced by a more complex one (Sharma et al., 2017).

In order to gain a full appreciation for the intricate work on tracing the origins of the coronary endothelium, it is important to first introduce genetic lineage tracing techniques and to discuss their advantages and limitations. Lineage tracing in mammalian systems relies on *Cre*-loxP recombination and specific reporter lines. This method involves creating transgenic mice that

express *Cre* recombinase under a specific enhancer/promoter which restricts *Cre* expression to particular cell lineages. Selection of an enhancer or promoter region is usually achieved by identifying an endogenous gene that is exclusively expressed in the cell type of interest. The *Cre* is generally inserted as a constitutive transgenic, or as a "Knock-In" within the gene of interest. More sophisticated techniques utilize a *Cre*-fused to two mutated estrogen receptors (ERT2). Under basal conditions the ERs prevent *Cre* translocation into the nucleus. However, when an exogenous source of tamoxifen (which binds the ER receptor) is provided, the complex can enter the nucleus and excise loxP-flanked genes. This technique is beneficial since it allows for temporal control of *Cre* expression in addition to spatial control. *Cre* lines are then crossed with reporters that contain a marker protein such as GFP or β-galactosidase under the control of a broadly expressed promoter (eg. CAG). These constructs are generally knocked into an accessible genomic location such as the *Rosa26* locus. In the absence of *Cre* recombinase, a loxP flanked stop cassette blocks reporter expression. *Cre* expression in the progenitor cell leads to excision of the stop cassette, allowing expression of the reporter protein. Because this labeling is permanent and heritable, the cell and all of its descendants are marked. However, the results obtained from genetic lineage tracing must be interpreted carefully. In order for the system to work, expression of the endogenous gene must be limited to the cell of interest. Even if low levels are detected in potential progeny/descendants of the cell of interest, reporter activation can occur. This would mean that the labelled progeny are not descended from the original cell of interest since they promoted *Cre* expression on their own (Tian et al., 2015).

In order to test whether the coronary endothelium was in fact derived from the PEO, epicardial-specific cre lines (*WT1-Cre*, *Tbx18-Cre*) were generated and tested in the mouse. However, very few endothelial cells were labelled by these lines (Cai et al., 2008; Zhou et al., 2008), suggesting an alternative origin for the murine coronary endothelium. Following these revelations several studies were conducted to address this mystery. Through this work it was determined that the endothelial cells of the coronary vessels originated for three different sources:

the sinus venosus, the ventricular endocardium and a specialized subset of cells in the proepicardium (Sharma et al., 2017).

The sinus venosus (SV) is a transient structure in cardiovascular development that receives venous blood from the embryo and shuttles it to the atrium. As the heart matures, the SV becomes integrated into the right atrium, forming the coronary sinus. Recent work from Red Horse et al., 2010, has demonstrated the importance of vascular sprouting from the SV in coronary vessel development. Through a combination of single-cell labeling and clonal analysis the authors were able to show a lineage relationship between SV endothelium and the coronary veins, capillaries and arteries. Because the SV is initially venous, the study proposed a mechanism through which sprouting of SV venous endothelial cells is accompanied by dedifferentiation into progenitor cells capable of adopting a venous or arterial fate. These cells then spread throughout the surface of the heart to form an immature vascular plexus located in the subepicardial space. Vessels destined to become arteries then migrate towards the inner myocardium and undergo arterial differentiation, while those that remain in place adopt a venous identity. To support the SV origin of the endothelial cells, Tian et al., 2013, developed an *Apelin-Cre*ERT2 line capable of tracing endothelial cells originating from the SV. Using this line they were able to show that the majority of the coronary vasculature was indeed derived from the SV as predicted by Red Horse et al.

In parallel to the experiments by Red Horse et al. and Tian et al., data began to emerge which proposed an alternative source of coronary endothelial cells: the ventricular endocardium. Through a series of clonal and histological observations it was demonstrated that endothelial lined structures filled with blood cells, termed “blood islands”, were capable of budding from the ventricular endocardium onto the surface of the heart (Tian et al., 2013). These so called “blood islands” were observed to arise at the surface of the dorsal and ventral midline, from where they would migrate deeper into the myocardium and form coronary vessels. Evidence suggested that the blood cells within these structures emerge because the endocardium is hemogenic and able

to differentiate into hematopoietic cells. Lineage tracing experiments using an endocardial-specific *Nfatc1-Cre* line confirmed these observations. In these studies a large portion of coronary arteries and capillaries, but very few veins, were labelled by the *Nfatc1-Cre* line (Wu et al., 2012).

A third source of coronary endothelium in the mouse heart was revealed with *Cre*-based lineage-tracing studies on a subset of epicardial cells positive for the markers *Scx or Sema3D*. These cells, which were not labeled with the initial epicardial *Cre* lines, represent a separate population within the PEO that only partially overlap with *Tbx18*+ and *Wt1*+ cells. Lineage tracing using *Scx-Cre* or *Sema3D-Cre* lines revealed these cells could give rise to a portion of coronary endothelial cells. More specifically, the *Sema3D-Cre* line labeled endothelial cells of the sinus venosus, whereas the *Scx-Cre* gave rise to endocardium (Katz et al., 2012).

The above studies provided evidence that the coronary endothelium derived from three different sources. However, there was still much confusion over the levels of contribution from each source. A subsequent report aimed to address this issue by quantifying lineage-tracing data from all three sources using the *Apelin-Cre*ER (SV), *Nfatc1-Cre* (endocardial) and *Sema3d-Cre* (PEO) lines. The results revealed a striking compartmentalization of the areas populated by different progenitors. Sinus venosus cells gave rise to the majority of vessels on the dorsal and right lateral sides and almost half of the vessels on the left lateral side, with minimal contribution to the mid-ventral aspect and in the ventricular septum. Complementary to the sinus venosus traced cells, endocardium lineage tracing gave rise to vessels in the left mid-ventral aspect and ventricular septum. *Sema3D-Cre* and *Scx-Cre* derived cells were significantly lower when compared to the two aforementioned sources (<20%) and were distributed evenly among the outer circumference of the heart (Chen et al., 2014). However, more recent work using a *Gata4-Cre* to perform lineage tracing from the septum transversum demonstrated that the contribution of the PEO is larger than previously calculated, reaching over 20% of coronary endothelial cells in certain parts of the heart (Cano et al., 2015).

Although the simultaneous use of sinus venosus and endocardial lineage-tracing reagents clearly showed complementary contributions between these two progenitors, it was determined that there was a small percentage of cross labeling with the *Cre* lines. In particular, the *Nfatc1*-Cre line was shown to recombine in the sinus venosus and in parts of the coronary endothelium itself (Zhang et al., 2016). To address this issue a more specific endocardial *Cre* line (*Nrp3-CreER*) was developed to fully exclude sinus venosus labeling in endocardial lineage traces. It was observed that this line labelled very few coronary vessels; thus, demonstrating that the majority of coronary vessels believed to be derived from the endocardium, were actually derived from the sinus venosus.

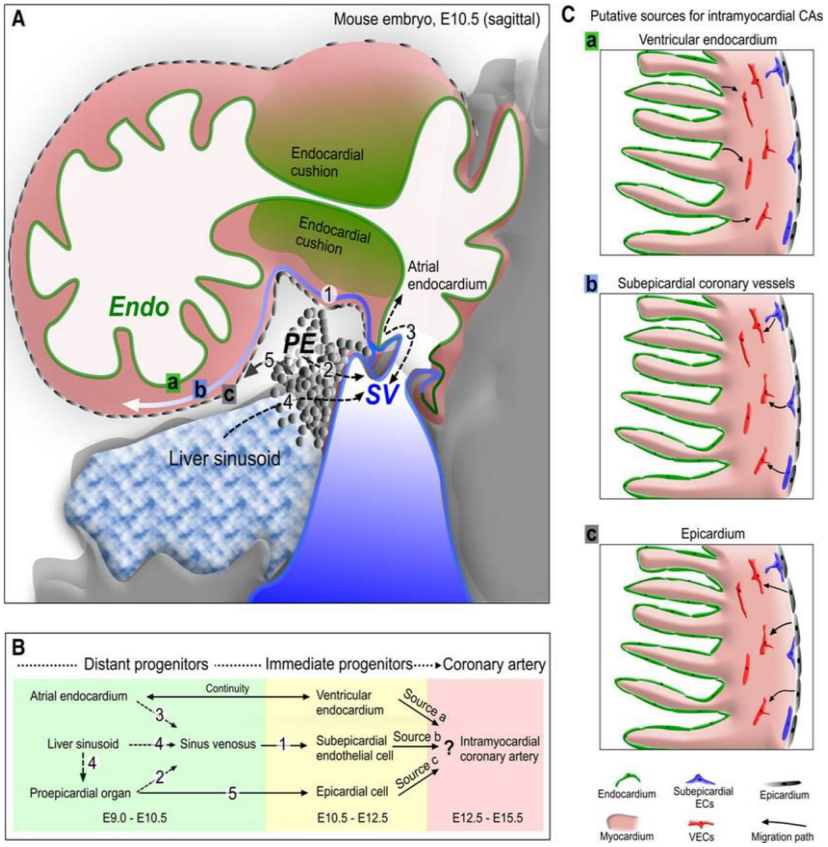

Figure 5, *Origin of coronary endothelial cells*. **A** and **B**, The 3 major sources of coronary vessels: the proepicardium (PE), sinus venosus (SV), and endocardium (Endo) are intimately associated with each other during heart development. The PE is a transient structure (gray color) that is wedged into the atrioventricular groove between liver sinusoids and SV, and eventually gives rise to the epicardium covering the heart. The SV (blue) is the venous inflow tract. Venous cells from SV sprout onto the heart and produce subepicardial coronary vessels. The endocardium (green) lines the heart lumen. Black-dashed arrows denote movement from one compartment to another, potentially complicating lineage-tracing experiments. Numbers in **B** correspond to those in **A** showing location of migration events. **C**, Three putative sources for intramyocardial coronary arteries (CAs) in the developing heart. Arrows indicate corresponding migration path. EC indicates endothelial cell; VEC, vascular endothelial cell. (Tian et al., 2015)

Coronary Artery Smooth Muscle

Another important cell type for coronary vessels are smooth muscle cells. During the remodeling phase of vascular plexus formation, smooth muscle cells are layered around the coronary arteries to provide mechanical support (Sharma et al., 2017). Coronary artery segments closer to the aorta that are exposed to higher blood pressure have multiple layers of smooth muscle while more distal ones have only a single layer. Lineage tracing with several epicardial-specific cre lines (*Wt1-Cre*, *Tbx*18-*Cre*, *Gata*5-*Cre Tcf21-Cre*ER) has revealed that the majority of vascular smooth muscle is derived from the epicardium (Cai et al., 2008; Zhu et al., 2008; Acyara et al., 2012). More specific lineage tracing experiments using *Ng2-Cre* and *Notch3-Cre* lines demonstrated the intermediate progenitors for smooth muscle to be cardiac pericytes (Volz et al, 2015). Much like the endothelial cells of the heart, the vascular smooth muscle of the coronary arteries also has multiple origins. Lineage tracing experiments with the *Wnt1-Cre*, which labels the CNCC, showed that the smooth muscle around the proximal coronary arteries is derived from the preotic neural crest (Jiang et al., 2000). Recently, a third source for coronary smooth muscle has been discovered. In this study it was determined that the endocardial-derived cardiac cushion mesenchyme can also provide a source of coronary mural cells (smooth muscle and pericytes). These cells were observed at a higher frequency in the ventricular septum when compared to the left and right lateral walls (Chen et al., 2016).

Molecular programs driving coronary vessel development

Coronaries are believed to derive from vascular sprouts originating in the SV. Mechanistically, it is not clear exactly how this happens but many signaling pathways have been shown to be involved in this process. For instance, *Vegfr3*, which is generally involved in angiogenic sprouting, is expressed at the site where SV cells enter the heart (Red Horse et al., 2010). Myocardial-specific *Angiopoetin1* signaling to the SV promotes migration of venous cells

into the heart. *Angiopoetin1* is also reported to be involved in venous differentiation as deletion of *Ang1* in the myocardium resulted in defective venous, but not arterial formation (Arita et al., 2014). *Vegfc* is another essential signaling factor involved in SV sprouting. Ablation of *Vegfc*, which is normally expressed in the epicardium, leads to delayed vascular sprouting and reduced vessel density near the outflow tract. This was determined to be due to migration defects rather than a decrease in proliferation (Chen et al., 2014). Calcineurin-*Nfat* signaling is also essential for vascular plexus formation as deletion of *Cnb1* delays vascular growth near the SV (Zeini et al., 2009). Mechanistically this is attributed to defective tube formation during the initial stages of plexus formation. Myocardial FOG2 expression has also been shown to promote plexus formation by promoting the expression of angiogenic factors and inhibiting anti-angiogenic ones (Ma et al., 2008). FGFs indirectly support coronary vessel development by promoting myocardial growth, which, through the expression of angiogenic growth factors (*Vegf*-a,b,c and *Ang2*), promotes vascular sprouting (Lavine et al., 2006). Sonic hedgehog (*Shh*) signaling plays an important role in arterial venous differentiation. Ablation of SHH receptors in either the epicardium or myocardium leads to less arteries and veins respectively (Lavine et al., 2008).

The derivation of coronary arteries from the so called “blood islands” of the endocardium is attributed to myocardial-derived VEGFA signaling to VEGFR2-expressing endocardial cells. Knockout of either molecule in their associated cell types diminishes the number of coronary arteries in the compact myocardium (Wu et al., 2012). Recent studies have begun to decipher the mechanisms involved in epicardial-endothelial transition. One study suggests that the Hippo pathway transcription factors Yap/Taz promote the proliferation, epithelial–mesenchymal transformation (EMT), and differentiation of *Sema3d*+ cells into coronary endothelial cells (Singh et al., 2016).

Another important aspect of coronary vessel formation involves proper connection of the coronary arteries to the aortic orifices. The proximal left and right coronary arteries are derived from the primitive vascular plexus in a well-defined “ïn growth model”. That is, rather than budding

from the aorta, as was initially thought many years ago, the proximal coronaries grow into the aortic orifices and establish a connection as early as E12.5 (Tian et al., 2013). The establishment of this connection is essential for plexus maturation as it initiates blood flow, which triggers the arterialization of undifferentiated plexus vessels (Sharma et al., 2017). *Vegfc* and the chemokine *Cxcr4* are highly expressed in the walls of the outflow tract and their receptors, *Vegfr2* and *Cxcl12* are expressed by endothelial cells of the plexus (Chen et al., 2014; Ivins et al., 2015). Deletion of either *Vegfc* or *Cxcr4* leads to defective stem formation and severe plexus defects. In both cases the phenotype is attributed to migration deficiencies, although with Vegfc the defect in stem formation may be secondary to reduced vessel density around the outflow tract.

The differentiation of precursor cells from the epicardium and neural crest into smooth muscle is also a complex process regulated by many factors. To form vascular smooth muscle, epicardial cells must undergo EMT that allows them to leave the surface of the heart and migrate into deeper layers (Sharma et al., 2017). In terms of cellular differentiation, evidence indicates that the decision made by EPDCs to form smooth muscle rather than cardiac fibroblasts occurs right at the surface, where it is coupled to the EMT process. Canonical Wnt signaling has been shown to play a role in supporting epicardial EMT and deletion of β-catenin with the *Gata5-Cre* leads to defective smooth muscle layer formation (Zamora et al., 2007). Deletion of *Pdgfrβ* and Myocardin-related transcription factors A and B also leads to defective smooth muscle differentiation (Trembley., 2015). Retinoic acid signaling (by controlling *Tcf21* expression) delays smooth muscle long enough for the coronary endothelium to form functional tubes (Braitsch et al., 2012). *Edn/Ednra1* signaling promotes the differentiation of smooth muscle from the preoptic neural crest and defects in this pathways result in ectopic connections of the coronary arteries with the aorta (Jiang et al., 2000). *Notch3* stimulates the induction of contractile proteins in pericytes surrounding the developing coronary arteries, which is in response to *Jagged1* expression in the endothelium (Volz et al., 2015).

Overall, coronary vascularization is a precisely timed and fine-tuned process, and one that is regulated by many cell lineages and signaling pathways. Important cell types involved in coronary vascularization include venous cells of the SV, endocardial cells, epicardial cells, the cardiac neural crest and cardiac myocytes. Together, these cells coordinate coronary plexus formation and maturation via various autocrine and paracrine molecular cues. Disruption of these processes leads to defects in coronary circulation and serious consequences such as embryonic lethality.

IV. Cardiac Regeneration

Acute myocardial infarction leads to rapid cell death and replacement of healthy tissue with a non-functional scar. Despite the availability of medical therapies, heart function continues to decline after MI, resulting in heart failure and eventual death (Frangogiannis, 2014). A central problem with treating heart disease is that adult mammals do not sufficiently regenerate cardiomyocytes to compensate for lost cardiomyocytes (Senyo et al, 2014). Recent work has elucidated some of the mysteries behind cardiomyocyte regeneration during homeostasis and repair. This knowledge has been used to generate novel strategies for treating heart disease based on stimulating endogenous repair mechanisms and reprogramming cardiomyocytes from other cell types.

Cardiomyocyte proliferation

Historically, the heart has been viewed as a post mitotic organ in which the primary parenchymal cells, cardiomyocytes, do not proliferate (Senyo et al., 2014). In a study performed in the 1950s, scientists measured the increase in cardiomyocyte cross sectional area in the left ventricular papillary and concluded that cardiomyocyte enlargement could fully account for myocardial growth between birth and adulthood (Linzbach, 1950). In mice, cardiomyocytes are

thought to proliferate vigorously until postnatal day 5, after which point they begin exiting the cell cycle. By postnatal day 7, hearts lose regenerative capacity and between P10 and P21, CMs become terminally differentiated and quiescent. This transition is accompanied by a downregulation of cell cycle factors such as *Cyclin/cdk* complexes and up regulation of cell cycle inhibitors such as P21/P27 (Naqvi et al., 2014). An interesting feature of mammalian cardiomyocytes is that many undergo bi-nucleation, a common marker of terminal differentiation. In mice, bi-nucleation occurs in 80-90% of cardiomyocytes between postnatal day 5 and 10. In humans, 30% of CMs are bi-nucleated in the newborn heart and although there is no rapid increase in bi-nucleation during the postnatal period, CM ploidy is active well into adulthood (Senyo et al., 2014)

Recent studies using novel technological advances have since challenged the notion that adult mammalian CMs are quiescent. One of the first indications that adult CMs could proliferate came from a study by Soonpaa et al. 1997, wherein mice were injected with tritiated thymidine and analyzed two hours later. From these experiments, the authors detected a 0.0005% labeling frequency of cardiomyocytes. In another series of studies, long-term bromo-deoxyuridine (BrdU) labeling demonstrated a basal CM proliferation rate of 1% per year in adult mice (Li et al., 1996; Malliaras et al., 2013). Perhaps the most stunning evidence for cardiomyocyte proliferation in humans was revealed by Carbon 14 (C14) dating studies. C14 birth dating makes use of the transient increase of C14 in the biosphere that occurred in the 1950s-1960s due to above ground nuclear testing. The C14, which was taken up by through diet and incorporated into genomic DNA, can be used as a time-stamp to calculate the mean birth date of a stable cell population. This can then be compared with the age of the source individual to calculate the generation rate of new cells (Senyo et al., 2014). By using this technique, the Frisen group was able to demonstrate that new cardiomyocytes formed at a rate of approximately 1.5% per year at age 25 years; however, this rate tended to decrease substantially in the latter half of life (Bergmann et al., 2009). This data was confirmed through the use of imaged-based assays in tissue samples procured from donor

hearts prior to heart transplantation. From this study the authors calculated a CM proliferation rate of about 1.9% at 20 years of age. Furthermore, through direct stereological quantification of cardiomyocytes in humans, the authors also demonstrated that CM number increases from 1.1 to 3.7 billion during a 20 year time period after birth (Mollova et al., 2013). A similar change is reported in rodents (Li et al., 1996) although a new study indicates that a large proportion of this increase happens during the pre-adolescent period (P15), during which time mice experience a 40% increase in CM number (Naqvi et al., 2014).

To assay the role of a potential progenitor cell contribution to CM proliferation, multiple groups have used the α-Myosin Heavy Chain (MHC) *Cre*ER^{T2} crossed with a GFP reporter line. In a study by Hsieh et al., 2007, it was demonstrated that during normal aging in mice, the percentage of preexisting cardiomyocytes remained unchanged. Influx of cardiomyocytes generated from undifferentiated progenitor cells should have resulted in a decrease in the percentage of GFP-positive CMs but this “dilution” was not observed, indicating that the majority of new CMs generated after birth in the mammalian heart arose from endogenous cell proliferation. Regarding one specific progenitor cell type marked by *c-Kit* expression, conflicting results have emerged. Ellison et al. 2013, reported a 0.15% generation rate for *c-kit* derived cardiomyocytes in a 4-week period of normal aging. This, however, contrasted with results from Zaruba et al. 2010, who, by using a more direct lineage tracing approach with a *c-Kit* knock in *Cre*, determined that C-KIT positive cells did not generate novel cardiomyocytes to a significant degree.

In adult mouse models of myocardial damage, the story becomes more complex. After experimental myocardial infarction, border zone CMs exhibit a 10-fold increase in cell cycle activity (Senyo et al., 2014). Using the MHC transgenic model, Malliaras et al. demonstrated a dilution of GFP positive cells after damage, indicating a larger role for progenitor cells than endogenous proliferation. However, by combining the *Cre* model with stable isotope mapping, Senyo et al. 2013 observed cell cycle activity in preexisting cardiomyocytes at the injury border. These contrasting observations may be attributed to varied long-term viability of GFP- and GFP+

populations, although an evaluation of short term apoptosis or proliferation rates did not show any differences. In addition, there is growing evidence that activation of the surrounding epicardium may contribute to myocardial repair after injury (Senyo et al., 2012). Epicardial cells that demonstrate an epithelial to mesenchymal transition can lead to myocardial vascularization and, possibly, to cardiomyocyte formation (Huang et al., 2012). However, there is much controversy regarding the latter and treatments aimed at promoting epicardial-cardiomyocyte differentiation have had conflicting results (Smart et al., 2011; Zhou et al., 2012).

In an attempt to explain the limited proliferative capacity of adult CMs, two possibilities have been proposed: (1) the presence of the differentiated sarcomeric cytoskeleton prohibits cell division and; (2) the binucleated and polyploid phenotype prevents cell cycle re-entry (Senyo et al., 2014). To address the first point, cardiomyocyte mitotic figures have been reported in adult zebrafish and neonatal mice during cardiac regeneration following MI (Jopling et al., 2010; Porello et al., 2011). Both neonatal and adult zebrafish cardiomyocytes are capable of disassembling their sarcomeres in order to reenter the cell cycle, indicating that presence of sarcomeres may not be prohibitive to cardiomyocyte division. Hence, this theory has its limitations. In support of the binucleation theory, it has been demonstrated that exogenously induced proliferation of differentiated adult mouse cardiomyocytes *in vitro* occurs primarily in the mononucleated portion (Bersell et al., 2009). Furthermore, most adult zebrafish are mononucleated which is consistent with their proliferative activity during regeneration (Wills et al., 2008). A similar feature is observed in Newt cardiomyocytes (Bettencourt-Dias et al., 2003), indicating that binucleation is indeed correlated with the inability of CMs to proliferate.

Novel regenerative approaches for patients suffering from heart damage

The majority of cardiac regenerative approaches have involved stimulating endogenous repair mechanisms and transplantation of cells with potential progenitor features into infarcted myocardium. Types of stem cells used include bone marrow derived stem cells, human embryonic

stem cells and induced pluripotent stem cells. Reprogramming of adult progenitor cells *in vivo* is an additional technique that has shown much promise.

The observation that neonatal mice exhibit regenerative capacity in response to surgical procedure has sparked interest in modulating adolescent-adult cardiomyocyte proliferation (Senyo et al., 2014). Forced expression of CYCLINB1/B2 and knockdown of *p21/p27* have been shown to increase CM proliferation *in vitro* (Bicknell et al., 2004; Di Stefano et al., 2011). *In vivo*, CYCLIN D2 overexpression resulted in increased cardiomyocyte DNA synthesis and reduced scarring after MI in mice (Pasumarthi et al., 2005). Similarly, transgenic expression of CYCLIN A2 increased cardiomyocyte cycling and myocardial regeneration (Chaudry et al., 2004). Delivery of *neuregulin* (NRG10), *fibroblast growth factor* (FGF1) with pharmacologic p38 MAP kinase blockade, and periostin peptide have all been demonstrated to promote myocardial repair as well (Bersell et al., 2009; Engel et al., 2006; Kuhn et al., 2007). Thus, the modulation of endogenous repair pathways provides a novel therapeutic avenue for regenerative treatments, although it is no quite clear how these would fare in clinical trials.

Bone marrow-derived stem cells (BMDSCs) are able to differentiate into a wide variety of cells including cardiomyocytes and can be used for autologous transplantation in patients suffering from heart disease (Senyo et al., 2014). Many trials, such as the REPAIR-AMI, have shown improved outcomes in heart function after BMDSC transplantation (Assmus et al., 2010). However, two recent clinical trials have been somewhat discouraging. Neither the TIME trial nor the POSEIDON trial showed any significant improvement in ventricular function after transplantation (Traverse et al., 2012; Hare et al., 2012). A large multinational trial (BAMI) is being conducted in Europe to further address this issue.

Embryonic stem cells (ESCs) provide the possibility of generating an unlimited amount of cardiomyocytes *in vitro*. By treating ESCs with ACTIVIN-A and BMP4 one can generate a highly purified population of ESC-derived CMs, that when transplanted *in vivo*, demonstrate enhanced survival rates (Laflamme et al., 2007). Human ESC-derived CMS can also electromechanically

couple with host cells to allow synchronous contraction between the grafted cells and host tissue (Shiba et al., 2012). However, one of the risks associated with this technique is the formation of teratomas from incompletely differentiated ESCs. This was observed in immunosuppressed rhesus monkeys transplanted with ESC-derived CMs (Blin et al., 2010). Ethical concerns concerning the use of ESCs along with lack of supply have also been limiting factors in using this approach (Garbern and Lee, 2013).

The discovery that embryonic and mouse fibroblasts could be induced to become pluripotent stem cells revolutionized regenerative biology. Like ESCs, induced pluripotent stem cells (iPSCs) can be reprogrammed into CMs *in vitro*. Unlike ESCs, there are no ethical issues associated with iPSCs and since they are generally derived from adult tissues, their supply is unlimited (Garbern et al., 2013). Different types of CMs–atrial, ventricular, nodal- can be derived with these strategies depending upon the types of growth and transcription factors used (Zhang et al., 2009). However, the lack of efficiency and cost associated with these strategies makes it difficult to treat patients within a therapeutic time. And, as with ESCs, there is a risk of teratoma development (Garbern et al., 2013).

In vivo cardiac reprogramming from one cell type to another is a promising alternative to ESC and iPSC-derived CM strategies. The Srivastava group devised a method to directly reprogram fibroblasts to cardiomyocyte-like cells with a combination of three transcription factors (GATA4, MEF2C and TBX5) (leda el al., 2010). Using a retroviral system to deliver these to 2 month old male mice subjected to myocardial infarction, they were able to promote the trans-differentiation of various resident fibroblasts into cardiomyocyte-like cells. The treatment resulted in improved myocardial function (Qian et al., 2012). Subsequent studies using microRNAs or alternative transcription factors have shown similar results (Garbern et al., 2013). However, all of these methods show low efficiency and incomplete efficacy. Furthermore, it is possible that incomplete programming can lead to adverse effects such as rhythm disturbances, making it difficult to assess the overall therapeutic benefit of these strategies (Garbern et al., 2013).

A major challenge in cell therapy approaches is how to improve the delivery of reprogrammed cells. Whether it is intravenous, intracoronary or intra-myocardial, all of these methods are limited by poor local retention (Garbern et al., 2013). In order to address this issue, tissue engineering approaches combining cells with biomaterials have been taken. Hydrogels and biodegradable scaffolds seeded with cells have both shown promising results (Ye et al., 2011; Schmidt et al., 2007). However, these approaches are still in development and need to be improved.

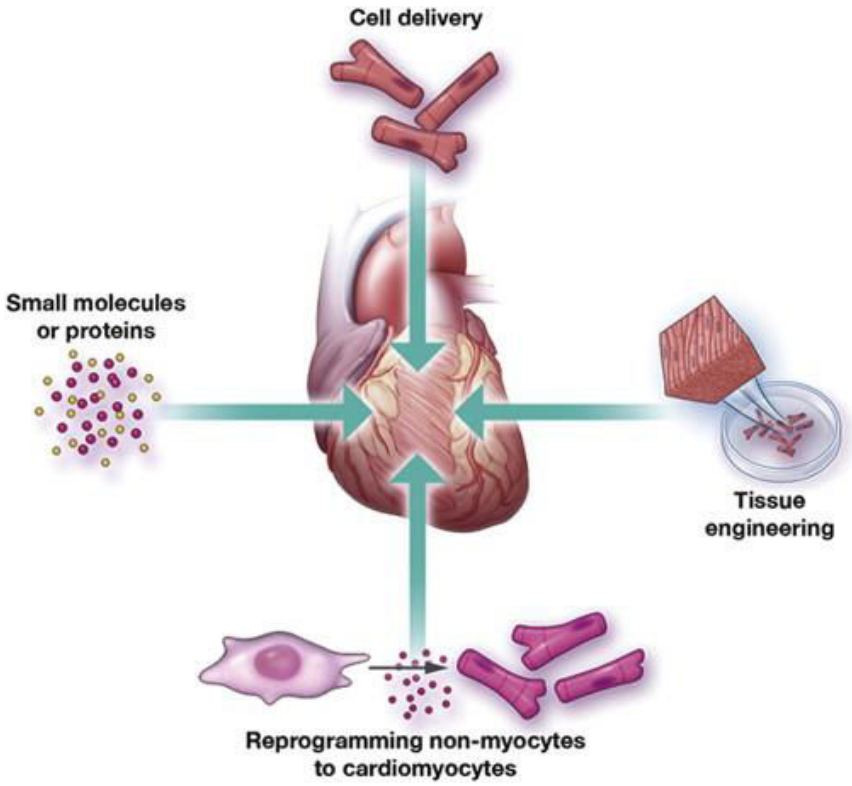

Figure 6, *Cardiac Regeneration strategies*. **A,** Cell therapy with cultured cells injected into the myocardium or coronary arteries. **B,** Tissue engineering approaches that combine cells with biomaterials to create functional tissue in vitro for transplantation into the heart. **C,** reprogramming non-cardiomyocytes into cardiomyocytes in situ. **D,** Small molecules such as growth factors or microRNAs that are delivered to promote wound healing via cardiomyocyte proliferation or angiogenesis (Garbern and Lee, 2013).

V. Wnt signaling in cardiac development and repair

The *Wnt1* gene, originally known as *Int1*, was identified in 1982 as a gene activated by integration of mouse mammary tumour virus proviral DNA in virally induced breast tumours (Nusse and Varmus, 1982). The drosophila Wingless GENE (*Wg*) which controls segment polarity during larval development, was later on shown to be a homolog of *Int1* (Rijsewick et al., 1987), hence accounting for the name *Wnt1*. By 1994, a series of epistasis experiments in *Drosophila* delineated the core components of the WNT signaling cascade (Peifer et al., 1994; Siegfreed et al., 1992). WNT signaling is an essential pathway involved in cellular proliferation, polarity, and differentiation during embryonic development and tissue homeostasis. As a result, mutations in the WNT pathway are often linked to human birth defects, cancer and other diseases (Clevers and Nusse, 2012). The most studied WNT pathway is canonical WNT signaling, which functions by regulating the levels of the transcriptional co-activator *β-catenin*. Non-canonical WNT pathways such as WNT/PCP and WNT/Calcium signaling have also been described and have been reported to play essential roles in various cellular processes.

Canonical WNT signaling

WNT/β-catenin signaling is a complex pathway that has taken several decades and a tremendous amount of work to be deciphered. In the absence of WNT, cytoplasmic β-catenin protein is degraded by a destruction complex composed of the proteins Axin, *adenomatous polyposis coli* gene product (APC), casein kinase 1 (CK1), Dishevelled (DVL), and glycogen synthase kinase 3 (GSK3β). Axin and APC serve as scaffolding proteins while CK1 and GSK3 sequentially phosphorylate the amino terminal region of β-catenin. Phosphorylated β-catenin is recognized and ubiquitinated by the E3 ubiquitin ligase β-TRCP, targeting it for proteosomal destruction. The continual elimination of β-catenin prevents it from accumulating in the cytoplasm and reaching the nucleus. As a result, WNT target genes are repressed by the DNA-bound T cell

factor/lymphoid enhancer factor (TCF/LEF) family of proteins, which, in the absence of β-catenin, are bound to groucho proteins (MacDonald et al., 2009).

The Wnt/β-catenin pathway is activated when a WNT ligand binds to a seven-pass transmembrane Frizzled (FZD) receptor, which then forms a heterodimer with the low-density lipoprotein receptor related protein (LRP). The WNT–FZD–LRP5/6 trimeric complex recruits Dishevelled (DVL) and Axin through the intracellular domains of FZD and LRP5/6 respectively, resulting in inhibition of β-catenin phosphorylation. The free β-catenin is then able to translocate to the nucleus to form complexes with TCF/LEF transcription factors, thereby activating WNT target gene expression (MacDonald et al., 2009).

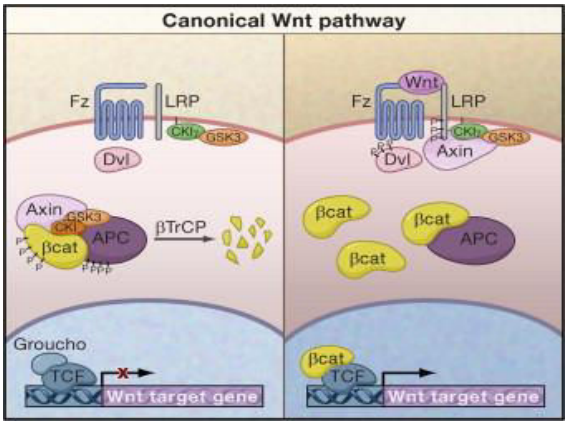

Figure 6, *Schematic demonstrating the various components involved β-catenin degradation/stabilization* (Clevers and Nusse 2010).

Non Canonical WNT Signaling

A key feature of non-canonical WNT signaling pathways is that they act in a β-catenin independent manner. The two most well characterized non canonical pathways are the planar cell polarity (PCP) pathway and the WNT/Ca pathway. The Wnt/PCP pathway plays an important role in regulating cell polarity while the WNT/Ca pathway promotes intracellular calcium signaling. In both these pathways the FZD receptor acts independently of LRP, and the Dishevelled protein, through its three different domains, DIX, PDZ ad DEP, plays a very essential role (Sugimara and Li, 2010).

The non-canonical WNT/PCP pathway emerged from a study in Drosophila in which WNT mutations affected the orientation of several structures such as hair, sensory bristles and the ommatidia in the eye (Mlodzik, 2002). Like the canonical pathway, WNT/PCP is activated by WNTs. Once bound by a WNT ligand, FZD recruits DVL, which then uses its PDZ and DIX domains to form a complex with Dishevelled-associated activator of morphogenesis 1 (DAAM1). DAAM1 activates the small G-protein RHO through a guanine exchange factor. RHO activates Rho-associated kinase (ROCK) which is a principal regulator of the cytoskeleton. In parallel, DVL forms a complex with RAC1 and mediates profilin binding to actin. RAC1 activates JNK and promotes actin polymerization while profilin binding to actin results in cytoskeletal remodeling (Sugimara and Li, 2010).

The observation that the WNT/FZD interaction could also stimulate intracellular Ca release lead to the discovery of the second major non canonical signaling cascade: the WNT/Ca pathway. Upon WNT ligand binding, the activated FZD receptor directly interacts with DVL, through its PDZ and DEP domains, and a trimeric G-protein. The co-stimulation of DVL and the G-protein activates PLC, which cleaves PIP2 into DAG and IP3. When IP3 binds its receptor on the ER, calcium is released. Intracellular release of calcium activates Ca sensitive proteins such as protein kinase C (PKC), and calcium/calmodulin-dependent kinase II (CAMKII). These, in turn, activate Calcineurin, which dephosphorylates and stabilizes NFAT. NFAT acts as potent transcription factor, regulating multiple processes such as T-cell proliferation and differentiation. The deregulation of NFAT leads to several defects in embryogenesis and adult homeostasis (Sugimara and Li, 2010).

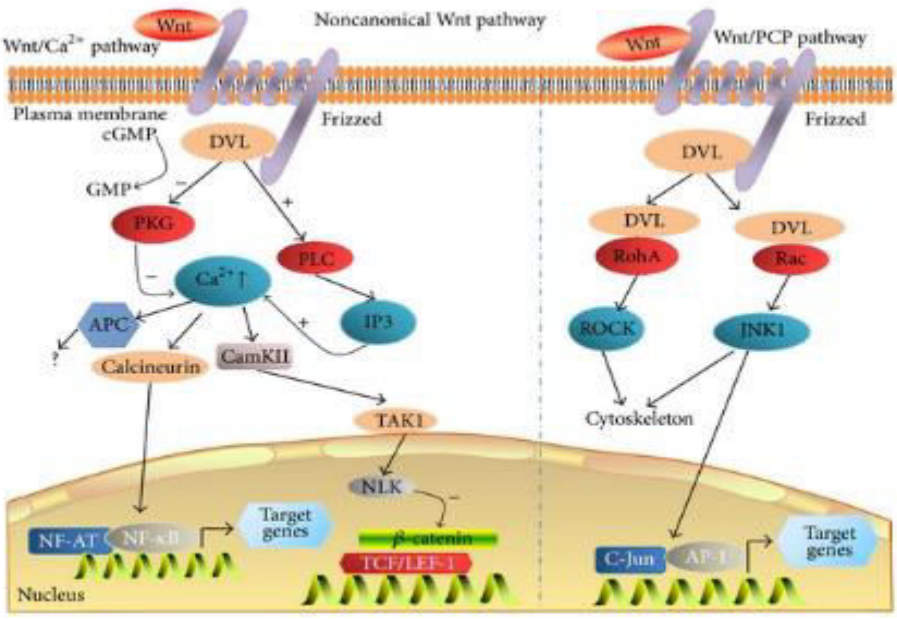

Figure 6, *Schematic demonstrating the key players involved in non canonical Wnt signaling pathways*. Left; Wnt/Calcium pathway, and Right; Wnt/PCP pathway (Shi et al., 2016).

WNT ligands

WNT ligands are cysteine rich proteins of approximately 40kDa in size amino acids that contain an N-terminal signal peptide for secretion. In mammals there are 19 WNT ligands comprising 12 different sub-families (Tanaka et al., 2002). WNT ligands have unique expression patterns and can activate either canonical or non-canonical Wnt pathways (Table1). In order to function properly, WNTs must undergo several post-translational changes. These include N-glycosylation and various lipid modifications. These lipid modifications are required for efficient signaling and may be important for secretion. They are carried out in part by the multi-pass transmembrane O-acyltransferase Porcupine (*Porc*) (Hoffman et al., 2000). Loss of *Porc* leads to WNT retention in the ER. Wntless (*Wls*) and Sprinter (*Srt*) are two additional proteins involved in WNT secretion. *Wls* is a multipass transmembrane protein that localizes to the Golgi, endocytic compartments and the plasma membrane. In *Wl* mutant cells WNT ligands accumulate in the Golgi and are not secreted. *Srt* mediates membrane protein trafficking between endosomes and the Golgi apparatus. Loss of *Srt* causes *Wls* to be degraded in the lysosomes and results in reduced WNT secretion. Overall, these studies have led to an emerging picture of WNT biogenesis

wherein WNT is glycosylated and lipid modified by *Porc* in the ER, and is escorted by *Wls* from the Golgi to the plasma membrane for secretion (MacDonald et al., 2009).

WNTs acting through canonical pathway	**WNTs acting through non-canonical pathways**
Wnt1, Wnt2, Wnt2b, Wnt3a, Wnt4, Wnt7a*, Wnt7b, Wnt8a, Wnt8b, Wnt9a, Wnt10a, Wnt10b, Wnt11b**	*Wnt4*, Wnt5a, Wnt5b, Wnt6, Wnt7a*, Wnt9b, Wnt11a, Wnt11b**

Table 1, Table listing the different WNT ligands and the WNT pathways to which they have been associated.
*Have been demonstrated to act via canonical and non-canonical pathways (de Lau et al., 2012).

WNT extracellular movement

It is often assumed that WNT signals are capable of exerting their actions across large distances in tissues. Indeed, when acting in concert with lipoprotein particles and specific binding partners such as SWIM, the WG protein has been shown function via long range signaling in the wing of drosophila embryos (Panakova et al., 2005). However, it should be noted that this kind of event is rare and in the majority of cases WNT ligands act as short range signals. In mammals, WNT signaling occurs predominantly between cells that are close to each other, such as in adult stem cell niches (Clevers and Nusse, 2012).

WNT receptors

The Frizzled (*Fzd*) seven-pass transmembrane receptors along with the LDL receptor-related proteins 5 and 6 (LRP5 and LRP6) represent the two distinct families of receptors that are critical for Wnt/β-catenin signaling. The mammalian genome harbors 10 *Fzd* genes, most of which display functional redundancy and have variable capacities to activate β-catenin signaling (Logan and Nusse, 2004). Frizzled receptors contain a hydrophobic groove that provides a docking platform for the lipid component of Wnt ligands. Of the two LRP receptors (5 and 6), LRP6 plays

a more dominant role and is essential for embryogenesis. LRP5 is dispensable for embryogenesis but plays an important role in adult bone homeostasis (He et al., 2004). In some cases, as in mouse gastrulation, their functions are partially redundant. Most data suggests that the two classes of receptors are initially separate in the cell membrane. After binding WNT, FZD forms a complex with LRP, leading to activation of canonical WNT signaling (Macdonald et al., 2009).

WNT antagonists and agonists

There are several families of secreted proteins that antagonize or modulate WNT/β-catenin signaling. sFRPs (secreted Frizzled related proteins), and WIF (Wnt inhibitory protein) bind to WNT, and *Fzd* respectively and function as WNT antagonists for both canonical and non-canonical WNT signaling (Clevers and Nusse, 2012). The WNT binding property suggests that sFRPs and WIF may also regulate WNT stability and diffusion/distribution extracellularly; however, this is not entirely clear. Two additional classes of WNT inhibitors are the Dickkopf (*Dkk*) and *Wise* Families. Both *Dkk1* and *Wise* are thought to function by directly disrupting the WNT-induced FZD-LRP6 complex. Shisa proteins represent a distinct family of WNT antagonists. They function by trapping FZD proteins in the ER thereby preventing them from reaching the cell surface. Norrin and R-spondin (*Rspo*) proteins are two families of agonists for WNT/β-catenin signaling. Norrin is a specific ligand for FZD receptors and acts through FZD4 and LRP5/6 during retinal vascularization. R-spondin proteins exhibit synergy with WNT ligands and have a vast array of functions during embryogenesis and tissue homeostasis (MacDonald, 2009). The R-spondins will be explored in greater detail in an upcoming section.

Canonical Wnt Reporter lines

Several reporter mice have been designed to track WNT-responsive cells *in vivo* and *in vitro*. The *Tcf* optimal promoter (TOP)-beta-galactosidase (TOPGAL) transgenic mice were made fusing three LEF/TCF binding sites to *c-fos* minimal promoter (Das Gupta and Fuchs, 1999). A

second reporter line, the β-catenin activated transgene (BAT) driving the expression of nuclear beta-galactosidase, was designed by fusing seven TCF/LEF binding sites upstream of a 0.13 kb fragment containing the minimal promoter-TATA box of the *Siamois* gene (Maretto et al., 2003). A third line using a stable knock in of *LacZ* in frame with the endogenous start codon of the *Axin2* gene has been generated as well. AXIN2 induces β-catenin degradation in a negative feedback loop and is considered a universal target of the canonical WNT signaling pathway (Lustig el at., 2002). In recent times, the faithfulness of these three lines has been brought into question as experiments have shown differential responses in the developing embryo (Alam et al., 2011). Thus, in order to track WNT-responsive cells one must rely on a combination of techniques that involve: several different reporter lines, expression of transcriptional targets of β-catenin (e.g. *Axin2*), and, if possible, detection of nuclear β-catenin.

Wnt signaling in cardiac development

WNT/β-catenin signaling plays an essential role in various stages of vertebrate heart development. The mammalian heart is formed soon after gastrulation from the mesodermal layer of the primitive streak (Buikema et al., 2014). WNT signaling is required for the gastrulation process and in β-catenin knockout embryos the mesoderm fails to develop (Hagel et al., 2005). During normal cardiac development mesodermal cells from the primitive streak migrate anteriorly to form the cardiac cresent. In order for these cells to specify into cardiogenic progenitors β-catenin signaling must be repressed. This is generally thought to be achieved through *Mesp1*-induced expression of DKK1, a WNT inhibitor (Brenner et al., 2008). Once the cardiac crescent is formed the so called First and Secondary Heart fields can be defined. The SHF is defined by the expression of specific markers such as *Fgf10* and Islet-1 (*Isl1*) (Kelly et al., 2012*). Isl1*+ cardiac progenitors play an essential role in sourcing the right ventricular myocardium and outflow tract. β-catenin has been show to promote the clonal expansion of *Isl1*+ progenitors in the SHF. One

study identified β-catenin role in the SHF to act through FGF signaling (Cohen et al., 2008), while another demonstrated *Isl1* to be a direct target of β-catenin (Lin et al., 2007).

However, more recent studies have shown that the relationship between β-catenin and *Islet1* expression is more complex than previously reported. In a study by Kwon et al., 2009, β-catenin stabilization in the SHF progenitors was performed by crossing a β-catenin gain of function mutant with the *Islet1*-Cre. The resulting increase in β-catenin activity lead to a decrease in *Islet1* expression in cardiac progenitors. A similar decrease was also observed in *Notch1* null mutants, as NOTCH1 normally negatively regulates β-catenin accumulation. In a study performed a few years later by Cohen et al., 2012, the deletion of the non-canonical Wnt ligands *Wnt5a* and *Wnt11* lead to a decrease in Islet1 progenitors and reduced SHF expansion. It was demonstrated that *Wnt5a* and *Wnt11*, by acting through the Wnt/PCP pathway, negatively regulate β-catenin stabilization in order to prevent the inhibitory effect on Islet1 expression generally caused by excessive β-catenin levels. Hence, the balance between β-catenin signaling, *Islet1* expression and SHF progenitor expansion is tightly regulated and deviations can lead to serious consequences in early cardiac development.

During mid-late gestation (E11.5-14.5) the outer layer of the myocardium, referred to as the compact myocardium, proliferates and expands at a much faster rate than the inner trabecular layer. Recent work has shown that β-catenin plays an important role in this regional expansion. Deletion of β-catenin in the compact myocardium leads to a reduction in the compact zone thickness and developmental arrest at E12.5. Conversely, ubiquitous activation of β-catenin in the ventricular myocytes lead to an overall increase in myocyte-specific proliferation and an abnormal expansion of the compact layer (Buikema et al., 2013). Additionally, β-catenin signaling has been shown to play an important role in coronary artery formation by regulating the epithelial to mesenchymal transition of smooth muscle cells from the epicardium. *Gata5*-Cre (epicardial-specific) deletion of β-catenin lead to defective development of the smooth muscle layer around the coronary arteries, resulting embryonic death around E15.5-18.5 (Zamora et al., 2007).

Wnt signaling in cardiac repair

In addition to its role during heart development, WNT/β-catenin signaling has also been implicated in the regulation of cardiac remodeling and injury responses. Several studies have shown that the expression of WNT ligands and of the feedback regulators DKK1 and DKK2 are induced in response to myocardial injury (Ozhen and Weidinger, 2015). β-catenin levels have also been reported to increase in rat hearts one day after thoracic aortic constriction (Haq et al., 2009). Using the *Axin2-LacZ* line, upregulation of pathway activity was reported in endothelial cells, c-kit positive progenitors, fibroblasts and smooth muscle cells after surgical ligation of the left anterior descending artery (LAD). With the TOPGAL line, upregulation of pathway activity could be detected 4 days after LAD in subepicardial endothelial cells (Oerlemans et al., 2010). In this study, *LacZ*+ myofibroblasts accumulated in the infact area one week post MI, and it was shown that they were derived from endothelial cells that appeared to undergo an endothelial to mesenchymal transition (Aisagbhoni et al., 2011). In a different study, TOPGAL activity was reported in the epicardium in response to ischaemia-reperfusion (Duan et al., 2012).

Several inhibitors and activators of β-catenin signaling have been used in order to modulate the cardiac remodeling steps that occur post MI. At the membrane level, overexpression of the WNT inhibitor Secreted Frizzled Related Protein (SFRP1) caused a reduction in infarct size and improved cardiac function (Barandon et al., 2003). The injection of recombinant SFRP2 two days post-MI showed similar results (He at al., 2010). In contrast, αMHC-driven overexpression of SFRP1 caused decreased cardiac function and increased scar size (Barandon et al., 2005). Genetic deletion of *Sfrp2* showed reduced fibrosis and improved cardiac function when analyzed two weeks after LAD ligation (Kobayashi et al., 2009). Synthesized peptides targeting and antagonizing FZD1 and FZD2 showed a reduction in infarct area and increased repair (Laeramans, 2011).

At the level of β-catenin degradation, inhibition of both the alpha and beta forms of GSK-3 showed no difference in cardiac function or infarct size (Webb et al., 2010). Specific targeting of the GSK-3 beta isoform with small inhibitory molecules (Lithium Chloride and SB216763) or with a genetic knock out model was associated with preserved cardiac function, less apoptosis and increased capillary density in the infarcted area (Woulfe et al., 2010). Down regulation of β-catenin in cardiac fibroblasts increased left ventricular dilatation *in vivo* and decreased fibroblast proliferation *in vitro* (Kaga et al., 2006). αMHC-specific deletion of β-catenin (Zelarayan, 2008) was superior over αMHC β-catenin stabilization (Hahn et al., 2006), with significantly improved functional outcomes in the former. Overall, these conflicting results may be due to the differences in timing, dosage and strategies used. In addition, while we know that stage-specific timing of β-catenin expression is extremely important for cardiac development, the same may be true for cardiac repair.

VI. The R-spondin protein family

The R-spondins are members of a superfamily of thromobospondin type 1 repeat (TSR-1) containing proteins (de Lau et al., 2012). The original prototype member of the TSR-1 family was isolated from platelets that had been stimulated with thrombin, hence the name “thrombin-sensitive protein” (Baenziger et al., 1973). The prefix R in the R-spondin subfamily derives from the fact that R-spondin1 is transiently expressed in the boundary region between the roof plate and neuroepithelium during embryonic development. Hence the name R(oof plate-specifc)-spondin. In addition to the TSR-1 domain, all R-spondins are characterized by the presence of a positively-charged carboxy terminal region, a hydrophobic signal peptide near the N-terminus that ensures secretion from the cell, and two furin-like cysteine rich repeats. Furin repeats are common among growth factors such as epidermal growth factor (EGF), hepatocyte growth factor (HGF) and neurotrophic factors (de Lau et al., 2012). In total, there are four R-spondin family members.

Rspo3 was the first to be discovered in 2002 (Chen et al., 2002), whereas descriptions of *Rspo1* (Kamata et al., 2004) and *Rspo2* followed in 2004 (Kazanskaya et al., 2004). *Rspo4* was the last member to be discovered in 2006 (Kim et al., 2006). R-spondin homologs are highly conserved among all vertebrates but are not present in invertebrates such as *D. Melanogaster* or *C. elegans* (de Lau et al., 2012).

Mammalian R-spondins have a similar 5 exon gene organization and protein domain structure. The human and murine family members share a 40-60% pair-wise similarity. The amino terminal signal peptide is encoded by the first exon, whereas the two furin repeats are encoded by exons 2 and 3. The TSP-1 domain is encoded by exon 4, and exon 5 encodes a region that is solely characterized by its high density of basic amino acids. As with WNT ligands, R-spondins act as short-distance effectors. Because of their TSR-1 domain, R-spondins bind the extracellular matrix of cells once they are secreted, meaning that they tend exert their actions in an autocrine or nearby-paracrine manner (de Lau, 2012).

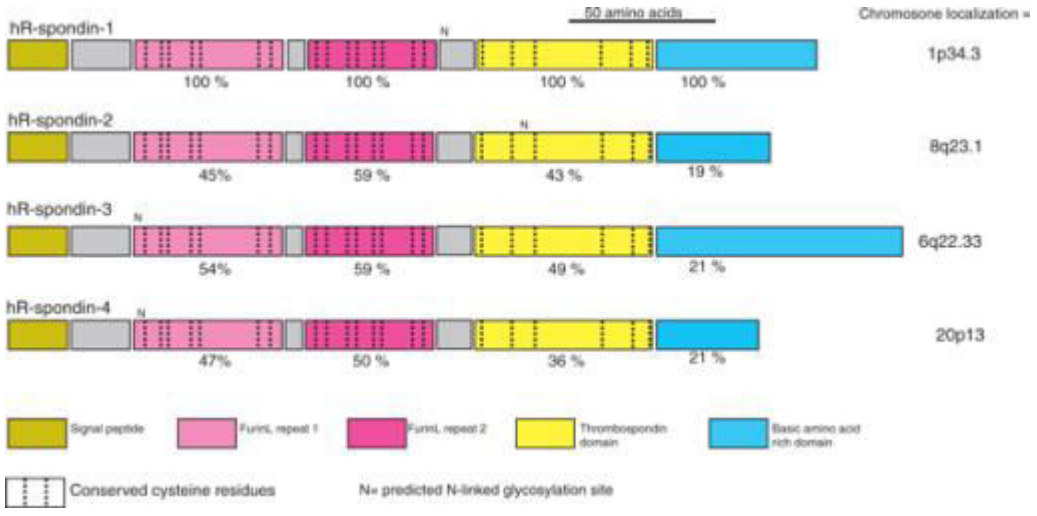

Figure 7, *Graphic demonstrating the different domains in the four human R-spondin proteins* (de Lau et al., 2012).

Through extensive functional analysis of the R-spondin proteins *in vitro* it was discovered that R-spondins synergistically activate β-catenin signaling in the presence of WNT ligands (Kazanskaya et al., 2004). They also showed sensitivity to the presence of the extracellular WNT inhibitor DKK1. The first *in vivo* evidence linking R-spondins with canonical Wnt signaling came from studies in frog embryos. Depletion of *Rspo2* at the eight cell stage in blastomeres resulted in disorganized somites and a reduction of myotomes at the site of injection. Depletion at the gastrula stage resulted in failed activation of the muscle development genes *MyoD* and *Myf5* (Kim et al., 2008). These phenotypes strikingly phenocopied the effects seen from manipulating the WNT pathway and lead to the conclusion that R-spondins were indeed involved in canonical Wnt signaling (Cossu and Borello, 1999). β-catenin activation by R-spondins has also been observed in experimentally induced tumours as well as in human carcinomas such as colon cancer (Nusse, 2005).

The knowledge that R-spondins were involved in the canonical Wnt signaling pathway prompted researchers to study their functions during embryonic development. By combining analysis of their dynamic expression profiles with gene depletion models in various organisms, the pleiotropic roles for R-spondins during embryogenesis began to be deciphered.

R-spondin 1: Sex Reversal

R-spondin1 plays an essential role in gonadal sex determination. Mutations in RSPO1 lead to an extremely rare human syndrome that combines SRY-independent XX male sex reversal with palmoplantar hyperkeratosis (PPK) and a predisposition to squamous cell carcinoma of the skin (de Lau et al., 2012). A later analysis of *Rspo1* knockout mice confirmed that an absence of R-spondin1 at the gonadal differentiation stage lead to partial sex reversed phenotypes (Parma et al., 2006). A similar phenotype is seen in *Wnt4* knockout mice, most likely because of upstream *Rspo1*-induced *Wnt4* activation. Thus, a *Wnt4/Rspo1* axis is operational in bipotential gonads of

XX individuals during gonadal development. Mechanistically this is thought to occur though the suppression of FGF9-induced SOX9 (a masculinizing gene directly activated by SRY) production (Tomizuka et al., 2008).

R-spondin2: Limbs, lungs and hair follicle development

During development, R-spondin2 is expressed in the lung buds as well as in the apical ectodermal region of the limbs (Nam(a) et al., 2007). Accordingly, *Rspo2* KO mice show defects in both limb (Nam(b) et al., 2007) and lung development (Bell et al., 2008). Mechanistically, *Rspo2* is thought to promote limb bud formation by inducing the expression of the apical ridge maintenance factors FGF4 and FGF8. The lung defects seen in *Rspo2*-deficient mice are associated with reduced branching of bronchioles and are a direct result of reduced β-catenin signaling. An additional study in dogs revealed that *Rspo2* is involved in hair follicle development (Cadieu et al., 2009).

R-spondin3: Placenta, vasculature, adrenal, liver and heart development

Genetic ablation of *Rspo3* in the mouse leads to developmental arrest around E10. Analysis of *Rspo3* deficient embryos revealed severe vascular defects in the placenta (Aoki et al., 2007), which was determined to be a result of decreased β-catenin mediated VEGF signaling (Kazanskaya et al., 2008). Since then, *Rspo3* has been shown to have important roles in the secondary heart field progenitors of the developing heart (Cambier et al., 2014), zonation of the liver during development and adulthood (Rocha et al., 2015), in the developing and adult adrenal (Vidal et al., 2016), and in the post-natal vasculature of the lungs and retina (Scholz et al., 2016). Interestingly, of the four R-spondins, R-spondin 3 is the only one capable of directly activating both the non-canonical Wnt/PCP (Ohkawara et al., 2011) and Wnt/Ca pathways (Scholz et al., 2016). A more detailed explanation of Rspo3's role during embryonic development and in adult homeostasis will be provided in an upcoming section.

Rspo4: nail development

R-spondin4 is directly linked with nail development as homozygous and compound heterozygous *Rspo4* mutations have been found in individuals with anonychia, a genetic disease characterized by the absence of finger nails and toe nails (Ishii et al., 2008). In the mouse *Rspo4*'s role in nail development was associated with β-catenin signaling (Blaydon et al., 2006)

LGR Receptors

The identification of R-spondin receptors has not been easy and has proceeded with plenty of trial and error. Originally, it was proposed that R-spondins interacted with FZDs, LRPs and/or WNTs. However, none of these theories proved to be correct and were eventually dropped due to lack of evidence (de Lau et al., 2012). Recently, three separate reports identified *Lgr4*, *Lgr5* and *Lgr6* as the principal receptors for the R-spondin protein family (de Lau et al., 2011, Carmen et al., 2011, Glinka et al., 2011). LGR proteins are a unique class of seven-transmembrane G-protein coupled receptors characterized by a large extracellular region (ectodomain) that harbors multiple copies of a leucine-rich repeat protein interaction domain. LGRs are subdivided into 3 families, A, B and C, with *Lgr4, Lgr5* and *Lgr6* belonging to the B family. All three have been shown to bind the four R-spondin family members with high affinity in *in vitro* settings (de Lau et al., 2012).

The LGR receptors display unique patterns of expressions during embryonic development that correlate to their functions. Strong *Lgr4* expression has been observed in various organs during embryogenesis such as the kidney, adrenal gland, reproductive organs, eyes, developing nervous system and heart (Mazerbourg et al., 2004). Interestingly, in many of these organs *Lgr4* expression was determined to be very broad, and almost ubiquitous. Ablation of *Lgr4* in the embryo lead to multiple defects and *Lgr4* null mice died postnatally due to kidney failure (Mazerbourg et al., 2004, Kinzel et al., 2014). In one study a portion of *Lgr4* mutants were reported to die during late-gestation (E15-16), although the reasons for this were not entirely clear (Kinzel

et al., 2014). *Lgr5* was first identified as a WNT target gene in colon cancer cell lines harbouring WNT-activating mutations. Further examination of *Lgr5* expression revealed it was expressed in the healthy crypts of the intestine, alongside many WNT pathway components and target genes. Overall, *Lgr5* shows a complex expression pattern during embryogenesis and in the adult (Barker et al., 2013). LGR5+ cells are seen in the adult eye, mammary gland, and skin along with the developing kidney and gonads. In general, LGR5 is thought to mark stem cell niches in various organs (de Lau et al., 2012). *Lgr5* KO mice have gastrointestinal distension and die postnatally due to respiratory distress resulting from underdeveloped lungs (Barker et al., 2013). Developmental *Lgr6* expression is most prominent in the hair placodes, rare cells in the brain, the mammary gland and the airways of the lungs. *Lgr6* KOs are viable and fertile (Barker et al., 2013).

The RSPO/LGR/ZNRF3/RNF43 axis

Recent work has revealed that WNT signaling regulation is more complex than previously imagined. In the absence of R-spondins, WNT stabilization of β-catenin is quickly saturated, leading to decreased activation of the system (de Lau et al., 2012). This is accomplished by two E3 ubiquitin ligases, RNF43 and ZNRF3. These two ligases, which are direct targets of β-catenin, are responsible for ubiquitinating the cytosolic domain of FZD receptors. By doing so they promote the internalization and degradation of the WNT receptors, thereby shutting down β-catenin signaling. However, in situations where excessive β-catenin signaling is necessary, the R-spondins “come to the rescue” and negatively regulate ZNRF3 and RNF43 (Yu and Virshup, 2014). Recent work has shown that R-spondins are capable of simultaneously binding the ectodomains of LGR and RNF43/ZNRF3 proteins through their furin repeats (Zebisch et al. 2013; Chen et al., 2013). By doing so they promote the membrane clearance of the ubiquitin ligases, thereby increasing the availability of FZD receptors. In summary, RSPOs indirectly activate β-catenin signaling by reducing the degradation of Wnt receptors, a mechanism that is consistent

with the observation that RSPOs only activate canonical Wnt pathways in the presence of Wnt ligands.

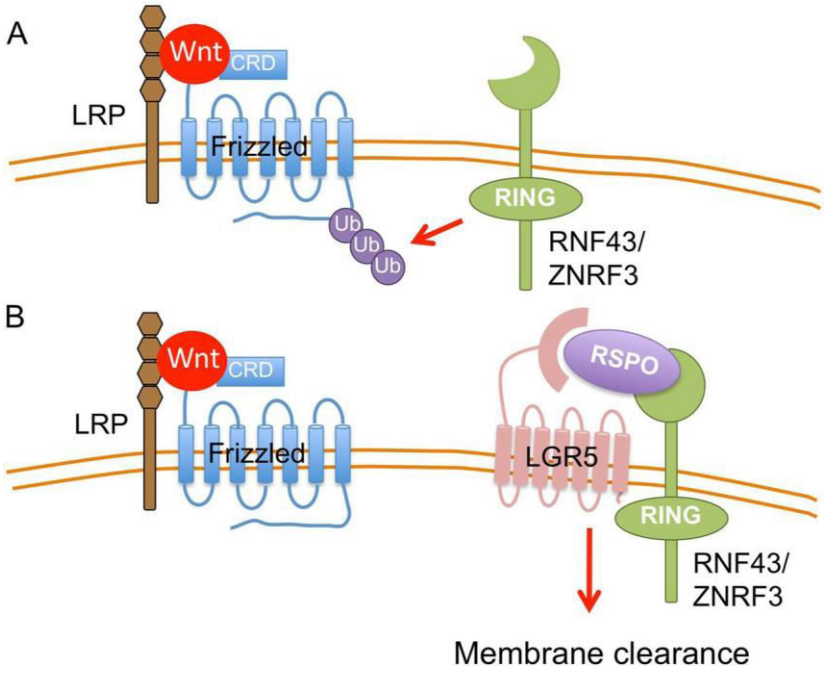

Figure 8, *Schematic demonstrating the role of R-spondins in increasing the availability of Wnt receptors* (de Lau et al., 2012). **A,** In the absence of R-spondin (RSPO), the E3 Ubiquitin ligases RNF43 and ZNRF3 ubiquitinate frizzled receptors, which promotes their degradation. **B,** Upon RSPO binding of LGR and RNF43/ZNRF3, the complex is cleared from the membrane and frizzled receptor is no longer cleared from the plasma membrane (Yu and Virshup, 2014).

Novel concepts regarding the role of R-spondins in Wnt signaling

In general, R-spondins are thought to facilitate Wnt signaling by increasing the availability of Wnt receptors. On their own, they are unable to stabilize β-catenin levels and are believed to play a supportive role. However, during development R-spondins show very distinct and specific patterns of expression that overlap very highly with known areas of high Wnt signaling. In many cases, this contrasts with many Wnt ligands that tend to show more broad patterns of expression (de Lau et al., 2012). Furthermore, many Wnt ligands show high amounts of functional redundancy, while this is rarely the case with R-spondins (*Rspo2* and *Rspo3* play redundant roles

in limb development, representing one of the few exceptions). Perhaps the most well studied model involving Wnt ligands, R-spondins and β-catenin signaling is the intestine. In the intestine, β-catenin signaling promotes stem-cell renewal of Lgr5+ crypt cells and maintains the progenitor pool. A reduction of canonical Wnt signaling generally leads to differentiation of the stem cell niche. Surprisingly, individual mutations in Wnt ligands have failed to reveal homeostatic phenotypes in the intestinal epithelium. On the other hand R-spondin3 fusion transcripts have been directly correlated with colon cancer resulting from excessive β-catenin signaling (Picco et al., 2017).

A recent study by Yan et al., 2017, looked more closely at the role of Wnt ligands and R-spondins in intestinal stem cell (ISC) renewal. By using gain of function studies with RSPO ligands and a novel non-lipidated Wnt analogue, the authors revealed that R-spondins and Wnts have distinct roles in ISCs. On their own, Wnt ligands were unable to induce Lgr5+ stem cell renewal. In stark contrast, RSPO ligand treatment on its own was able to maintain and promote ISC proliferation. The authors then proposed a model in which the role of Wnt ligands in maintaining the ISC niche is to confer a basal competency by promoting the expression of RSPO receptors and allowing R-spondins to drive stem cell expansion.

R-spondin3 in the placenta

The placenta is a vital organ that is necessary for the survival of mammalian embryos in the uterine environment. In order to ensure proper development of the placenta, three critical events must take place: (1) chorioallantoic fusion, (2) simple branching between the allantoic mesoderm and underlying fetal blood vessels with chorionic trophoblast cells must occur, and (3) a functional labyrinth with highly branched villi, which enable efficient exchange of gases, nutrients and waste products between mother and fetus, must develop properly. In a study by Aoki et al. 2007, targeted deletion of *Rspo3* lead to embryonic death around E10. Analysis of mutant embryos revealed severe defects in the placental labyrinth. Chorioallantoic fusion occurred normally in *Rspo3* mutants, but there was no penetration of the fetal blood vessels into the chorion.

Analysis of *Rspo3* expression revealed high it was highly expressed in the allantoic component of the labyrinth.

A follow up study performed in mouse and *Xenopus* revealed the mechanistic functions of *Rspo3*in the placenta. In *Xenopus* embryos, *Rspo3* expression was observed in the primitive streak, allantois, and several other sites of vasculogenesis and angiogenesis. By performing morpholino antisense knockdown of *Rspo3,* the authors observed severe vascular defects. Through a series of *in vivo* and *in vitro* studies it was determined that *Rspo3* was essential for promoting angioblast specification in blood cell precursors. This was attributed to β-catenin-mediated VEGFA expression. Targeted deletion of *Rspo3* in the mouse led to placental vascular defects and early embryonic death as was observed by Aoki et al 2007. *Rspo3* expression was detected in and around the endothelial cells of the allantoic labyrinth, in areas with high *Vegfa* and *Vegfr2* expression. By crossing *Rspo3* mutant mice with the BATGAL reporter line, a significant decreased in β-catenin signaling was detected. Decreased *Vegfa* expression was also observed. By performing various *in vitro* assays it was demonstrated that *Rspo3* promoted angiogenesis, endothelial proliferation, tube formation and increased sprouting in human endothelial cell lines. Hence, *Rspo3* was described as playing an essential role in the development of the placental vasculature.

R-spondin 3 and zonation: the adrenal gland and the liver

Since the initial studies carried out in the placenta, the functions of *Rspo3* in several other organs both during development and in adult homeostasis have been revealed. Two organs in which *Rspo3* has been shown to play an essential role are the adrenal gland and the liver. In both these organs *Rspo3* was demonstrated to promote and maintain zonation in the embryo and adult respectively.

The adrenal gland is a zonated endocrine organ that is essential for controlling body homeostasis. In a study by Vidal et al. 2016, *Rspo3* expression was detected in the capsular cells

underlying the outermost mesothelial layer of the organ. Ubiquitous deletion of *Rspo3* in the embryo at E11.5 followed by analysis 5 days later revealed smaller adrenals with a drastic reduction of the zona glomerulosa, a region underlying the adrenal capsule. Other regions of the adrenal were not affected suggesting a very localized and regional effect of *Rspo3* signaling. Mechanistically, the strong phenotype resulting from *Rspo3* deletion was attributed to decreased Sonic-hedgehog and *Wnt4* expression, two very important signaling molecules previously shown to be involved in zona glomerulosa development (Ching et al., 2009; Heikkiki et al., 2002). More importantly, *Rspo3*'s function was also shown to be essential in the adult adrenal as conditional deletion of *Rspo3* in 8 week old mice led to a severe reduction of the zona glomerulosa. Both during development and adult homeostasis, *Rspo3* was demonstrated to act through the canonical WNT/β-catenin pathway as *Rspo3* deletion lead to decreased expression of *Axin2* and many other direct β-catenin targets. In summary, this study established that *Rspo3* expression in the adrenal gland is necessary to establish zonation during development as well as to maintain the properties of the zona glomerulosa throughout life.

Another organ in which zonation plays an important role is the liver. In order for it to function properly, a spatial separation of the different metabolic pathways in the liver must be established and maintained throughout life. Disruption in liver zonation can lead to the development of severe disorders such as hyperammonemia (Rocha et al., 2015). In a study performed by Rocha et al., *Rspo3* was shown to be specifically expressed within the central vein endothelium of the liver. Conditional deletion of *Rspo3* disrupted both the activation and maintenance of central vein fate in post-natal and adult mice respectively. Moreover, forced transgenic expression of *Rspo1* in adult hepatocytes lead to portal-central vein conversion. Hence, R-spondins were determined to be key players in imprinting central vein fate in both the developing and adult liver. As in the adrenal, *Rspo3* was determined to function via the Wnt/β-catenin pathway.

R-spondin3 in the developing heart

The first evidence that *Rspo3* played a role in cardiac development came from a study by Cambier et al. in 2014. The goal of this study was to better characterize the role of the cardiac transcription factor *Nkx2-5* in heart development. Mice null for *Nkx2-5* die in utero at E10 due to cardiac malformations resulting from the loss of second heart field progenitors (Lyons et al., 1995). Close analysis of *Nkx2-5* null mice reveals the absence of a right ventricle and a poorly developed outflow tract. To study the role of *Nkx2-5* in the SHF, *Nkx2-5* floxed mice were crossed with the Islet-1-*Cre* line. SHF-specific ablation of *Nkx2-5* phenocopied the defects observed in null mutants. Microarray analysis of deregulated genes in conditional *Nkx2.5* mutant hearts revealed a drastic decrease in *Rspo3* expression. This observation was confirmed by *in situ* hybridization which showed high *Rspo3* expression in the SHF under normal conditions, and near complete ablation in conditional *Nkx2-5* conditional mutants. By performing Chromatin immunoprecipitation (ChIP), Electric mobility shift assays (EMSA) and transgenic promoter activation studies the authors were then able to demonstrate that *Rspo3* was a direct transcriptional target of *Nkx2.5*. To determine the role of *Rspo3* in the SHF, *Rspo3* was deleted with the *Islet1-Cre*. Strikingly, conditional *Rspo3* ablation led to severe secondary heart field defects and embryonic death at E11.5. The defects were attributed to decreased proliferation of Islet-1 progenitors resulting from a reduction in canonical WNT signaling. The authors then performed a series of rescue experiments in which the activation of β-catenin signaling via lithium chloride administration and transgenic *Rspo3* overexpression both rescued the *Nkx2.5* conditional mutant phenotype. In summary, *Nkx2.5*'s role in promoting SHF expansion was attributed to the direct regulation of *Rspo3*-induced β-catenin signaling.

R-spondin3 and non-canonical WNT signaling

One of the most interesting features about *Rspo3* is its ability to activate non canonical WNT signaling pathways. In a study by Ohkawara et al. 2011, RSPO3 was shown to directly bind the receptor Syndecan4 (SDC4) and activate the PCP pathway in *Xenopus* embryos. Furthermore, *Sdc4* and *Rspo3* were determined to be essential for two WNT/PCP driven processes: gastrulation and head cartilage morphogenesis. *Rspo3/Sdc4* mediated WNT/PCP activation was found to be dependent upon *Wnt5a* and was transduced via *Fzd7*, *Dvl* and JNK. Mechanistically, *Rspo3* was shown to function by inducing *Sdc4*-dependent, clathrin-mediated endocytosis, an internalization process the authors then demonstrated to be essential for WNT/PCP signal transduction. To date, an interaction between *Rspo3* and *Sdc4* has not been demonstrated in mammals. Furthermore, the Syndecan receptors display functional redundancy in the mouse, so whether or not the findings of this study are relevant to mammalian systems remains to be seen.

Rspo3 has also been shown to activate the WNT/Calcium pathway. In a study performed by Scholz et al. 2016, the authors studied the function of *Rspo3* in the embryonic and post-natal endothelium. To do so they first deleted *Rspo3* with a constitutive endothelial-specific *Cre* line. Strikingly, *Rspo3* ablation in the endothelium replicated the placental vasculature defects previously observed in *Rspo3* null mutants, suggesting the primary *Rspo3*-expressing cell types in the allantois layer to be endothelial cells. The authors then performed an inducible endothelial specific deletion of *Rspo3* in post-natal pups and observed reduced micro-vessel density and increased vascular apoptosis in the retina. Implantation of tumour cells into nude mice also demonstrated reduced vessel density in *Rspo3*-deficient tumours when compared to controls. Microarray analysis of lung endothelial cells devoid of *Rspo3* revealed upregulation of three E3 ubiquitin ligases, RNF213, USP18 and TRIM30α. Interestingly, RNF213 had been previously shown to be associated with a genetic disease in the brain vasculature known as Moya moya. Even more interesting was that these ligases were previously known to interact with the

downstream WNT/Calcium effector NFAT1. To confirm these observations, the authors performed co-immunoprecipitation experiments with specific antibodies and determined that all three ligases did indeed bind NFAT1, but not β-catenin. Hence, RSPO3 seemed to be able to regulate NFAT1 protein levels by inhibiting the expression of RNF213, USP18 and Trim30α. To confirm this, postnatal pups were injected with the Calcineurin/NFAT inhibitor Cyclosporin A. Strikingly, pharmacological inhibition of WNT/Calcium signaling phenocopied the vasculature defects observed in conditional Rspo3 mutants. In summary, the authors in this study demonstrated a new function for RSPO3 in which it promotes WNT/Calcium signaling in the endothelium by stabilizing NFAT1 protein levels. Whether or not the three E3 ubiquitin ligases (RNF213, TRIM30α and USP18) identified in this study are universal targets of *Rspo3* is still unknown.

R-spondin3: versatile signaling molecule

The studies mentioned above demonstrate the amazing flexibility of *Rspo3* in promoting various cellular processes and signaling pathways within many organs. During embryonic development *Rspo3* has very specific spatial and temporal patterns of expression. Since R-spondins are poorly secreted, it is generally thought that they act in an autocrine manner ie. *Rspo3*'s role in the postnatal vasculature. However, *Rspo3* has also been demonstrated to act in a localized paracrine manner within the adrenal gland and the liver. Which cell types respond to *Rspo3* and R-spondins in general will inevitably be determined by which cell types express their receptors. In the case of the adrenal, LGR4 and LGR5 seem to be highly expressed in the zona glomerulosa and not the capsule (unpublished data), possibly explaining why it acts in a paracrine manner. The same can be said for the epithelial progenitors of the intestine, which express high levels of LGR4 and LGR5 and interact with R-spondins originating from the intestinal stroma (Barker et al., 2013; Kang et al., 2016).

In terms of which signaling pathways *Rspo3* acts through, there is variability as well. Most studies indicate RSPO3 promotes canonical Wnt/β-catenin signaling (Kazanskaya et al., 2008,

Vidal et al., 2016; Rocha et al., 2015). However, it is clear RSPO3 can also act through non canonical pathways (Scholz et al., 2016; Ohkawara et al., 2011). What determines RSPO3's mode of action is most likely related to additional components of the WNT pathway. Since RSPO3 cannot activate WNT signaling on its own, the presence of canonical or non-canonical WNTs may inevitably influence which pathway it exerts its actions through. In the placenta, several canonical WNTs are expressed alongside Rspo3, which may explain why it acts through canonical WNT signaling in the placental vasculature. This brings into doubt the universal notion proposed by Scholz et al. 2016 that *Rspo3*'s role in the endothelium is always through non canonical WNT/Calcium signaling. The concept of pathway flexibility can also be explained by the expression of WNT receptors. If the FZD receptors expressed near *Rspo3* tend to activate non canonical pathways then *Rspo3* will most likely signal though them. Although it must be noted that *Rspo3*'s interaction with *Sdc4* occurs through its TSR domain instead of its furin repeats and the receptors involved in *Rspo3*'s activation of the Wnt/Calcium pathway are unknown. Overall, *Rspo3* displays impressive versatility in terms of signaling capacity during embryonic development. Perhaps this explains why it is so essential and why the ablation of *Rspo3* in different organs almost always leads to severe developmental defects.

Receptors for Rspo3

As previously mentioned, R-spondins have been shown to bind and exert their actions through the three LGR receptors LGR4, LGR5 and LGR6. Hence, one would expect null mutants of the receptors to display similar phenotypes to the R-spondins. This is true in many cases; however, there are a few, albeit, important exceptions. In the developing intestine, both R-spondin and *Lgr* mutants display decreased proliferation of crypt stem cells (de Lau et al., 2012). In the developing gonad, *Lgr4* deletion recapitulates the masculinization of the ovary phenotype observed in *Rspo1* mutants (Koizumi et al., 2015). However, neither placental nor heart defects have been reported for *Lgr4* and *Lgr5* mutants. This is true even for *Lgr5* and *Lgr4* double mutants

which show slightly more severe phenotypes in the intestines and kidneys than the individual single nulls, but have no apparent heart defects (Kinzel et al., 2014). *Lgr6* nulls are viable (de Lau et al., 2012) and since it does not usually compensate for the LGRs in other organs, it is unlikely it does so in the heart or placenta. In the endothelium of the placenta it could be argued that *Rspo3* exerts its effects through a different receptor since, in addition to promoting β-catenin signaling, *Rspo3* may function through the NFAT pathway (Scholz et al., 2016). In the heart, however, *Rspo3* is suspected to function mainly through canonical Wnt signaling, suggesting it should be exerting its effects through the *Lgr* receptors.

A closer analysis of the *Lgr* mutants suggests there is a possibility that they could, at least in part, act as receptors for RSPO3 in the SHF. In the study by Kinzel et al., 2014, some of the Lgr4 and 5 dKOs were described as dying *In utero,* which contrasts with previous reports stating they die postnatally. *In utero* death could suggest placental or cardiac malformations, but since the timing of death was loosely described as being in the mid-late gestational phase rather than earlier (E9.5 for Rspo3 placental defects), it is possible that many of these *Lgr* mutants were dying from cardiac defects. In fact, a more thorough search through the literature confirms that *Lgr4* mutants on their own, do on occasion die during gestation (Mazerbourg et al., 2014). In this study *Lgr4* mutant hearts were described as being smaller and having an overall decrease in weight. A more thorough analysis of the mutant hearts was not performed. Despite this, it is still unclear if the *Lgr*s play a role in Rspo3's function in the heart and whether or not they are even expressed at early and/or later time-points in cardiac development. In essence, it is likely that the regulation of R-spondin-induced Wnt signaling is more complex than previously imagined and may involve different classes or receptors.

VII. Retinoic acid signaling in the heart

Vitamin A, through its active derivative, retinoic acid (RA), regulates major embryonic patterning decisions. As a result, deficient or excessive levels of vitamin A can result in congenital malformations and teratogenic effects. In humans, the importance of this vitamin extends into adulthood, where it has important roles in maintaining normal vision, regulating fertility and preventing neurodegenerative diseases. The developmental roles of RA have been studied using several vertebrate models, including zebrafish, *Xenopus laevis*, chicks and mice. These studies have uncovered highly pleotropic functions for RA ranging from early axial patterning, control of neurogenesis, regulation of limb development and many more. Since RA is a lipophilic molecule and is able to traverse cell membranes, it was initially thought that its action relied on diffusion gradients. However, several studies providing details about its transport, synthesis, metabolism, and target receptors have revealed that RA signaling is more complex than previously imagined (Niederreither and Dollé, 2008).

RA metabolic pathways

Vitamin A consists of a family of substances commonly referred to as retinoids. Retinoids, which include retinol, retinal and retinoic acid, are also referred to as preformed vitamin A. Preformed Vitamin A can be obtained directly from animal food sources. Plants provide precursor forms called carotenoids, which are converted in the body into usable retinoids. There are two major forms of Retinoic Acid: all-trans retinoic acid and 9-cis-retinoic acid. Both forms display unique characteristics (Napoli, 1996).

The canonical pathway for RA synthesis during embryonic development has been elucidated over the past few decades through gene targeting studies in the mouse. Retinol is obtained from the mother through the placenta, after which it is transported throughout the embryo by retinol binding protein (RBP) 4. In order to enter cells, the retinol-RBP4 complex must interact

with the cell surface receptor *Stra6* (stimulated by retinoic acid gene 6). *Stra6* facilitates intracellular transfer of retinol and its expression in the embryo is indicative of which tissues respond to RA signaling (Niederreither and Dolle, 2008). Homozygous mutations of human STRA6 have recently been found to cause a malformative syndrome associating *anophthalmia*, heart defects, lung hypoplasia and mental retardation (Pasutto et al., 2007).

Once inside the cell, retinol is transformed into retinaldehyde and then into RA through enzymatic reactions. Retinol to retinaldehyde conversion is catalyzed by cytosolic alcohol dehydrogenases (ADH) and microsomal retinol dehydrogenases (RDHs). Gene knockout studies initially suggested that this reaction occurred ubiquitously in the embryo, mainly via ADH7 (Molotkov *et al*., 2002). However, mutation of murine RDH10 has been shown to cause lethal abnormalities characteristic of RA-deficiency phenotypes; thus, demonstrating a first level of RA-synthesis regulation based on RDH10 expression (Sandell et al., 2007). The second step in RA synthesis, which involves retinaldehyde to RA conversion, is catalyzed by three retinaldehyde dehydrogenases: RALDH1, RALDH2, and RALDH3. This step is irreversible and is highly regulated in the embryo. Regulation is achieved by the very distinct expression patterns of the RALDH enzymes, whose presence or absence closely correlates with the dynamics of RA signaling (Niederreither and Dollé, 2008). Of the three enzymes, RALDH2 is the first to be expressed during development. It is initially induced in the primitive streak and mesodermal cells during gastrulation and is restricted to the posterior embryonic region. Following mesodermal differentiation, RALDH2 remains restricted to prospective cervical and trunk regions. Analysis of *Raldh2* null mice demonstrated that RALDH2 is responsible for almost all RA production during early embryogenesis (Niederreither et al., 1997). Its deficiency affects many developing systems, including the forebrain, hindbrain, heart, forelimbs and somites (Niederreither et al. 2001; Ribes et al., 2006; Mic et al., 2004). RALDH3 plays an important role in later stages of eye and nasal development (Dupé et al., 2003). RALDH1 mutants are viable, and so far this enzyme has only been demonstrated to act redundantly with RALDH3 in eye development (Matt et al., 2005).

RA metabolism

An important caveat about RA signaling relates to the regulation of its distribution and regional levels. Vitamin A deficiencies generally lead to severe deformations during embryonic development and in adult homeostasis. The same is true for excessive levels of Vitamin A (Niederreither and Dollé, 2008). Hence, apart from the regulation of RA synthesis, an additional level of control, in the form of RA-metabolizing enzymes, exists for its degradation. To date, three principal RA-metabolizing enzymes have been discovered belonging to the Cytochrome P450 26 (CYP26) family: CYP26A1, CYP26B1 and CYP26C1. These enzymes are responsible for transforming RA into the more polar and less active derivatives 4-OH-RA and 4-oxo-RA. All three enzymes display distinct expression patterns during embryogenesis and targeted disruption of *Cyp26a1* or *Cyp26b1* leads to developmental abnormalities that phenocopy the known teratogenic effects of excess Vitamin A (Abu abed et al., 2001; Yashiro et al., 2004). A main function of CYP26 enzymes might be to protect several proliferative progenitor zones from the differentiating effects of RA (Niederreither and Dollé, 2008).

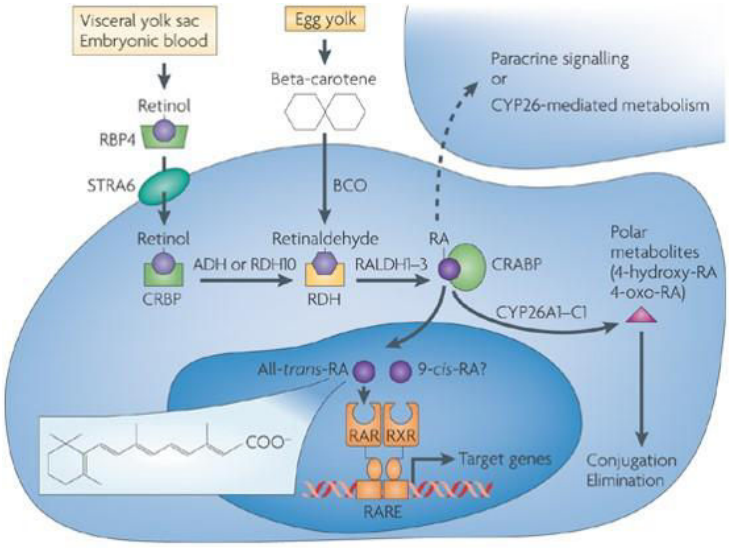

Figure 9, *Schematic demonstrating the RA signaling pathway*. Retinol is transported in the blood via RBP4. After interacting with the STRA6 receptor, retinol enters the cell and is then converted into Retinoic acid (RA) in a two step enzymatic process catalyzed by RDHs and RALDHs. Once synthesized, RA enters the nucleus and interacts with RAR-RXR heterodimers in an autocrine or paracrine manner. Excess RA is metabolized by CYP26 enzymes into polar metabolites (Neiderrether and Dollé, 2008).

Signal transduction

RA signaling is dependent on cells that have the ability to metabolize retinol to RA. RA-generating cells release RA, which is taken up by neighboring cells. Hence, RA signaling is generally considered to function in a paracrine manner, although autocrine RA signaling has also been detected in the embryonic heart epicardium and during spermatogenesis in the adult. Signal transduction involves binding of RA to a nuclear retinoic acid receptor (RAR), which forms a heterodimer complex with retinoid X receptor (RXR). RAR-RXR modulates transcription by binding to DNA at retinoic acid response elements (RARE) that are located in enhancer regions of RA target genes (Niederreither and Dollé, 2008).

In the absence of RA, the RAR-RXR heterodimer (already bound to a RARE element) recruits the nuclear receptor co-repressors (NCOR) 1 and 2, which then recruit histone deacetylase (HDAC) protein complexes and Polycomb repressive complex 2 (PRC2). This results in histone lysine 27 trimethylation, chromatin condensation and gene silencing. RA binding to RAR-RXR induces a conformational change in the heterodimer, which promotes the replacement of repressive factors by co-activators such as nuclear receptor co activator (NCOA) 1, 2 or 3. These co activators then recruit histone acetylase (HAT) complexes and Trithorax proteins, which mediate chromatin relaxation and gene activation. During activation, co activators bind to RAR, but not RXR, which is consistent with the observation that RAR is the key regulatory component of RAR-RXR heterodimers (Cunningham and Duester, 2015). In general, RA binding to RAR activates gene transcription; however, RA signaling has also been shown to repress the expression of certain genes. For example, a RARE sequence upstream of fibroblast growth factor 8 (*Fgf8*) mediates gene repression rather than activation (Kumar and Duester, 2014). This is generally attributed to RA binding leading to the recruitment of PRC2 and HDAC (Cunningham and Duester, 2015).

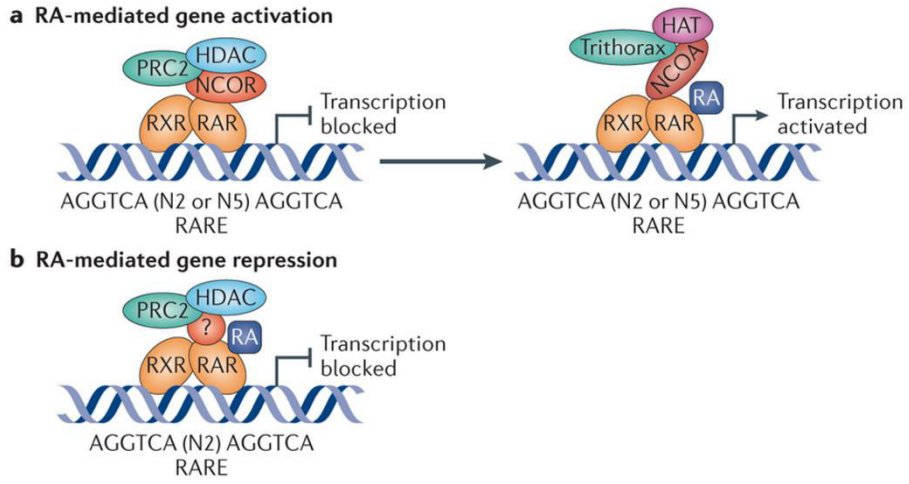

Figure 10, *RA-receptor mediated activation or repression of gene transcription.* **A,** In the absence of RA, RAR:RXR heterodimers recruit HDAC, NCOR and PRC2 and block transcription. Upon RA binding, repressor proteins are released and activator proteins (NCOA, HAT and Trithorax) are recruited resulting in gene transcription. **B,** RAR:RXR hetermodimers can also recruit repressive proteins upon binding to RA in order to block transcription (Cunningham and Duester, 2015).

A total of six receptors (RARα,β,γ and RXR α,β,γ) transduce the activities of RA (Niederreither and Dollé, 2008). Each RAR gene has two major isoforms (designated 1 and 2) that are derived by alternative promoter usage (Zaffran et al., 2014). RARs demonstrate high specificity to the RA pathway but RXRs have been reported to bind receptors from other pathways such as Vitamin D receptors, liver X receptors, thyroid receptors, and peroxisome proliferator-activated receptors (PPAR) (Zaffran et al., 2014) . In addition RXR receptors can act as homodimers while RARs only function as heterodimers with RXRs. RARα, RXRα, and RXRβ are found ubiquitously throughout the embryo and in adult tissues while RARβ, RARγ and RXRγ show more restricted patterns of expression (Stefanovic and Zaffran, 2016). Gene knockout studies on RARs and RXRs have demonstrated that they have crucial roles in many developmental processes. Combining receptor mutants such as RARα:RARγ or RARα:RXRα generally leads to more severe defects,

suggesting there is functional redundancy between RA receptors (Niederreither and Dollé, 2008).

For a list of phenotypes related to gene mutations in the RA signaling pathway refer to table 2.

Gene	Stage of lethality	Main structures and organs affected
*Null mutants for an individual gene**		
Rara	Early postnatal	Testis (degeneration of seminiferous tubules)
Rarb	Viable	Axial skeleton (vertebral transformations), eye (persistent retrolenticular membrane), lung (abnormal alveoli septation)
Rarg	Early postnatal	Axial skeleton (vertebral transformations), prostate and seminal vesicles (metaplasia), eye (absent Harderian glands)
Rxra	E13.5–E16.5	Heart (myocardial hypoplasia), eye (shortened ventral retina, thicker cornea, persistent retrolenticular membrane), placenta (disorganized labyrinthine zone)
Rxrb	Partial postnatal lethality	Testis (abnormal spermatogenesis, lipid accumulation in Sertoli cells)
Adh7	Partial postnatal lethality	Not determined
Rdh10[‡]	E13.5–E14.5	Otic vesicles (hypoplastic and/or ectopic), eye (absent ventral retina), posterior branchial arches (absent), forelimbs (hypoplastic), lung, pancreas (absent), kidney (hypoplastic)
Raldh2	E9.5–E10.5	Heart (impaired looping and myocardial differentiation), posterior hindbrain (abnormal patterning) and branchial arches (absent), forebrain, otic and optic vesicles (hypoplastic), forelimb buds (absent), somites (compacted and asymmetric)
Raldh3	Neonatal	Eye (shortened ventral retina, persistent retrolenticular membrane, absent Harderian gland), nasal region (choanal atresia)
Cyp26a1	Neonatal	Caudal region (severely truncated with spina bifida), axial skeleton (vertebral transformations), anterior hindbrain (abnormal patterning)
Cyp26b1	Neonatal	Maxillary-mandibular region and palate, limbs, male gonads
Compound null mutants for two genes		
Rara;Rarb	Neonatal	Axial skeleton (vertebral transformations and malformations), hindbrain (abnormal patterning), lung (agenesis and hypoplasia), outflow tract and large vessels (including persistent truncus arteriosus), kidney and female genital tract
Rara;Rarg	E18.5 and earlier	Craniofacial skeleton (severe deficiencies), axial skeleton (vertebral transformations and malformations), limbs (reduction defects), eye (coloboma, persistent retrolenticular membrane, abnormal cornea), Harderian and salivary glands (absent), hindbrain (abnormal patterning), outflow tract and large vessels (including persistent truncus arteriosus), kidney and genital tract
Rarb;Rarg	Neonatal	Axial skeleton (vertebral malformations), eye (shortened ventral retina, persistent retrolenticular membrane, sclera and iris defects), limbs (interdigital webbing)
Rarg;Rxra[§]	E13.5–E16.5	Heart, outflow tract and large vessels, eye (increase of $Rxra^{-/-}$ defects, coloboma)
Rxra;Rxrb	E9.5–E10.5	Caudal region (truncated), nasal region, posterior branchial arches (truncated), placenta (absence of labyrinthine zone)
Raldh1;Raldh3	Neonatal	Eye (severely shortened ventral retina, absent cornea, sclera, iris)
Raldh2;Raldh3[‖]	E9.5–E10.5	Forebrain, nasal region, optic vesicle (highly hypoplastic)
Cyp26a1; Cyp26c1	E9.5–E10.5	Forebrain, midbrain, branchial arches (reduced), hindbrain (expanded), cranial neural crest (deficient)

Table 2, *List of different phenotypes resulting from the deletion of the various enzymes and receptors involved in the RA-signaling pathways* (Niederreither and Dollé, 2008).

In the heart, RARα is ubiquitously expressed and is present in the myocardium while RARβ and RARγ show more complex regionalized expression. Isoform 1 of RARβ is found in the conotruncal mesenchyme while isoform 2 is expressed in the myocardium. RARγ is specifically expressed in the endocardial cushions (Dollé, 2009).

Retinoic acid response elements

RA mediated gene transcription is achieved by the binding of a RAR-RXR heterodimer to a motif composed of two direct hexameric repeats. In the classical model of RA signaling this motif consists of the sequence (A/G)G(T/G)TCA, with an interspacing of 5bp (DR5 elments) or 2bp (DR2 elements), followed by another sequence of (A/G)G(T/G)TCA. A more relaxed motif consisting of the sequence 5- (A/G)G(G/T)(G/T)(G/C)A-3 has also been described and represents a 10% consensus (Balmer and Blomhoff, 2005). The RXR receptor generally binds to the first repeat while RAR binds to the second one. The specificity of RAR-RXR binding to RAREs is regulated by various regulatory proteins and epigenetic factors (Stefanovic and Zaffran, 2016). Recently, a two-hybrid assay in yeast demonstrated that RXRα interacts with the cardiac transcription factor *Nkx2-5*. Mutations in *Nkx2-5* alter this interaction suggesting that some of the defects seen in *Nkx2-5* null mice and in humans with *Nkx2-5* mutations may be due to the disruption of this interaction (Prendiville et al., 2014). In terms of RA's role in activating or repressing gene transcription, it is thought that RARE elements with DR2 spacers have a higher probability of predicting a repressive function (Cunningham and Duester, 2015). However, this is not true for every gene and there is no universal rule for predicting gene activation or repression based on RARE sequences.

Recently, the use of chromatin immunoprecipitation (ChIP), with antibodies against RARs has demonstrated a greater diversity of RAREs than previously imagined. Novel hexameric repeats have been discovered in cell line studies involving ChIP coupled to sequencing (ChIP-seq) (Stefanovic and Zaffran, 2016). A recent ChIP-seq study in ES cells suggested that the

presence of RA might induce de novo RAR-RXR binding to several RAREs normally not bound by unliganded receptors (Mahony et al., 2011). There is also evidence that inverted repeats with no spacers can be targets for RARs. In total, ChIP-seq analyses have discovered up to 15000 potential RAREs, although many of these have not been attributed to endogenous RA signaling and may be off targets resulting from treatments with high amounts of RA (Stefanovic and Zaffran, 2016).

Retinoic acid reporter lines

In order to understand the effects of Retinoic acid signaling during embryonic development and in adult homeostasis it is necessary to determine the identity and spatiotemporal response of different cell types to RA. Although retinol is easily measured in the serum (Napoli, 1996), the distribution of its active derivative, retinoic acid, is difficult to measure accurately in tissues. Traditional methods to measure RA have relied on High Performance Liquid Chromatography-Mass spectrometry (HPLC/MS/MS) technologies; however, given the short half-life of RA as well as its inherent instability, obtaining accurate *in vivo* measurements has proven difficult (Niederreither and Dollé, 2008). Furthermore, measuring total RA levels provides no information regarding the cell types that respond to RA signaling, nor the degree of their response.

To address these issues researchers have developed several transgenic RA reporter lines by combining RARE elements with marker proteins. The rationale of these strategies is that most cells should produce at least one of the RARs that will activate the reporter upon binding to RA. The selection of RARE elements depends upon the faithfulness to which the genes carrying these elements recapitulate endogenous RA signaling. This inevitably depends upon the cell type as well as the epigenetic environment. Of all known RA targets, perhaps none are as faithful as the RARβ receptor (Niederreither and Dolle, 2008). As a result, many lines have taken advantage of the RARE elements found in the RARβ promoter to design RA-reporters. Overall, several RA-reporter lines have been established in various model organisms. For this section will focus on

three of these lines developed in the mouse: RARE-*hsp68-LacZ*, RARE-*Cre*, and RARE-*luciferase*.

The most utilized of the RARE-reporters is the RARE-*hsp68-LacZ* line (RARE-*LacZ*) (Rossant et al., 1991). The RARE-*LacZ* construct consists of three copies of the RARβ RARE element driving the *hsp68* promoter fused to a *LacZ* element. It is a transgenic line that has been shown to direct specific and temporal expression of the *hsp68-LacZ* gene in areas of high RA signaling during embryogenesis. During early embryogenesis it is highly expressed in the posterior domain and shows limited expression in anterior parts, an expression pattern that supports the well described role of RA in anterior-posterior patterning. Later on in development it shows a more restricted pattern of activation that coincides with the activities of RA signaling in various organs. Treatment of embryos with teratogenic doses of RA leads to near ubiquitous activation of the *hsp68-LacZ*, demonstrating a direct response to exogenous sources of RA (Figure 11). During early phases of heart development RARE-*LacZ* expression is limited to the venous pole, which demarcates the inflow tract region that gives rise to the atria and sinus venosus. This matches the known patterning roles of RA-signaling in which teratogenic doses of RA lead to expansion of the inflow tract at the expense of the outflow tract (Niederreither et al., 2001). During later phases of heart development RARE-*LacZ* expression becomes restricted to the epicardial and subepicardial layers, coinciding with RALDH2 expression in the epicardium (Shen et al., 2015). Overall, the RARE-*LacZ* line is expressed in various organs at various time-points and for the most part it seems to faithfully recapitulate endogenous RA-signaling. However, this line is limited by the fact that it cannot trace the fate of RA-responsive cells over time as it only transiently labels cells.

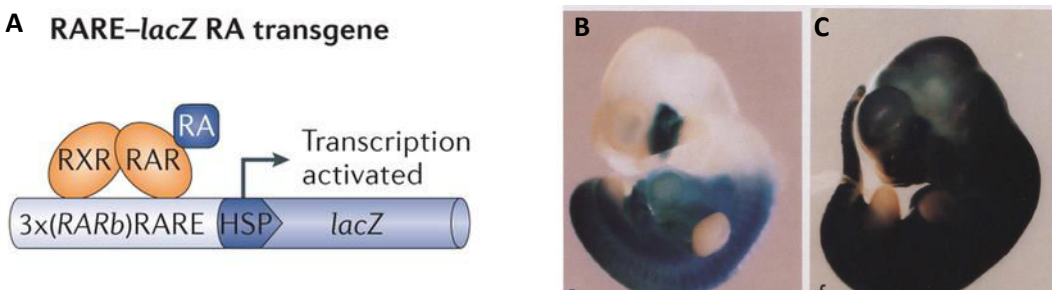

Figure 11, *The RARE-hsp68-LacZ line*. **A,** Graphic depicting the RARE-*hsp68-LacZ* construct that consists of three RARE elements from the RARβ gene fused to an *hsp68* promoter driving expression of a *LacZ* gene. **B,** RARE-LacZ embryo stained at E10.5 displaying anterio-posterior staining pattern. **C,** RARE-LacZ embryo treated with exogenous RA showing near ubiquitous staining (A: Neidertheier and Dollé 2008; B and C: Rossant et al., 1991)

In order to permanently label cells that respond to RA signaling *in vivo,* Dolle et al. developed a novel RARE reporter using *Cre* technology. The RARE-*Cre* line takes advantage the same RARE-*hsp68* construct as the RARE-*LacZ* except the *LacZ* element has been replaced with a *Cre*-recombinase. By crossing RARE-*Cre* mice with a reporter line, such as the ROSA26-*LacZ*, RA stimulation of the transgene leads to permanent *LacZ* activation. As a result, the responsive cell along with its progeny express the *LacZ*, allowing one to trace the distribution of RA-activated cells at later stages. When tested during embryogenesis the pattern of *LacZ* activation induced by the RARE-*Cre* correlated very highly with known sites of RA activity. These included the embryonic caudal region, limb buds, hind brain, and sensory organs. In accordance with the RARE-*LacZ*, RARE-*Cre* activation in the heart was very high in the venous pole at early stages and in the epicardium at later stages.

A third important, albeit less used, RARE reporter is the RARE-luciferase line (Bilbija et al., 2012). This transgenic line utilizes three copies of the RARE element from the RARβ promoter attached to the firefly luciferase gene. The advantage of this reporter is that, compared to the RARE-LacZ or RARE-Cre lines, it provides an easy read out and allows for rapid *in vivo* imaging of RA signaling without the need for tissue processing. When tested on mice subjected to permanent coronary artery ligation strong luciferase activity was detected in the heart, indicating

a role for RA-signaling post MI. Interestingly, the authors compared the intensity of luciferase activation at various time-points and observed that the RA-response peaked one week after surgery. The disadvantage of this line is that it does not provide any *in vivo* information on the cell types responding to RA. Plating of isolated cells from operated hearts can provide some insight on the activity within different cell types but this can be heavily biased by difficulties associated with the isolation procedures. Tracing these cells over time is also not possible and is something that would be very useful in the context of cardiac repair.

Overall, despite the availability of various RA-reporter lines there is still no universal read out for determining whether a cell or region is responsive to RA-signaling. Since these lines are transgenic and use different reporters (*LacZ* vs. *R26LacZ*) their responses do not overlap 100%. Perhaps this may be due to different sites of insertion or, alternatively, to different mechanisms of reporter activation ie. *hsp68-Cre* vs *hsp68-LacZ*. Hence, one must interpret results obtained using RARE reporters with caution. In essence, an RA-reporter line is but one of many effective tools for analyzing RA-responses. Only by using a combination of these tools can one get a realistic picture of the role of Retinoic acid signaling during embryogenesis and in adult tissue homeostasis.

Retinoic acid signaling in early heart development

RA signaling is intimately linked to heart development. Early studies in the quail revealed that vitamin A deficiency (VAD) led to cardia bifida along with severe heart tube formation defects (Heine et al., 1985; Dersch and Zile, 1993). In mice, it was later revealed that the RA synthesis enzyme, RALDH2, was highly expressed in the embryonic heart (Niederreither et al., 2001) and that a high level of RA-induced activity could be detected with RA-reporter lines at early stages of heart development (Rosant et al., 1991). Subsequent studies using gene knockout models of *Raldh2* and the various RA-receptors helped elucidate the sequential and multifaceted role of RA-signaling in heart development. It was discovered that RA-signaling is responsible for three key

events in early cardiac formation: (1) Modulation of the cardiac progenitor pool, (2) pre-patterning of the heart and atrial specification, and (3) formation of the outflow tract (Zaffran et al., 2014).

Perhaps the earliest heart developmental program influenced by RA-signaling is progenitor size control. Through a series of studies in chicks and zebrafish it was shown that increasing concentrations of exogenous retinoids lead to ever decreasing heart sizes (Drysdale et al., 1997). Consistent with this, treatment of zebrafish embryos with a pan-RAR antagonist during gastrulation produced oversized cardiac precursor domains (Jiang et al., 1999). In the mouse, RALDH2 seems to play an important role in heart patterning. At E6.5 RALDH2 is expressed in the lateral mesoderm located posteriorly to the cardiac crescent. RA-produced from this region acts directly on the expanding secondary heart field to limit its growth. This is supported by the observation that *Raldh2* null embryos display a caudal expansion of SHF-specific genes such as *Isl1*, *Nkx2.5* and *Tbx1* (Sirbu et al., 2008). As a result of this expansion, *Raldh2* mutant hearts fail to undergo proper looping and die around E10.5 (Niederreither, 2001). Interestingly, explant culture experiments suggest that the function of RA is to inhibit specification rather than to limit the proliferative capacity of cardiac progenitors (Ryckebusch et al., 2008). In fact, *Raldh2* null embryos display precociously differentiated myocytes at E8.5 (Sucov et al., 1994). These cells are flattened and already show organized sarcomeres. Interestingly, no RA-activity is detected in the mouse ventricles using the RARE-*LacZ* line at E8.5, suggesting that the precocious differentiation seen in *Raldh2* null hearts is the result of a much earlier requirement of RA in ventricular precursors (Xavier Neto et al., 2015).

Mechanistically, it is thought that RA's effect on limiting SHF expansion is mediated via FGF signaling. In *Raldh2* null mice, *Fgf8* expression is expanded caudally in a similar fashion to *Isl1* (Sirbu et al., 2008). In the SHF, *Fgf8* generally promotes *Isl1* expression, which is important in maintaining both the stemness and proliferative capacity of SHF progenitors (Kelly et al., 2012). Hence, it is thought that normal RA production from the posterior lateral mesoderm downregulates FGF8 in the SHF, which then restricts *Isl1* expression and the abnormal expansion of SHF

progenitors. This is supported by the fact that treatment of *Raldh2* null embryos with exogenous RA led to decreased *Fgf8* expression and, as a result, a reduction in SHF expansion (Sirbu et al., 2008). Furthermore, recent work has demonstrated that *Fgf8* does indeed have a functional RARE element in its promoter region and that RA signaling represses *Fgf8* expression in several *in vivo* and *in vitro* models (Kumar and Duester, 2014). However, a recent study in which CRISPR/Cas9 was used to delete the *Fgf8* RARE showed no defects in heart development or cardiac *Fgf8* expression, bringing into question the validity of this model (Kumar et al., 2016).

Proper anterior-posterior patterning is an essential part of heart chamber formation. At E8.0, the linear heart tube can be divided into the venous (caudal) and arterial (rostral) poles, which give rise to the sinus venosus/atria (inflow tract) and the ventricles/outflow tract respectively (Zaffran et al., 2014). RA-signaling, promoted by RALDH2 expression in the posterior lateral mesoderm, has been shown to promote specification of the venous pole of the heart. This is supported by several studies in chick and zebrafish in which exogenous RA lead to an expansion of the atrial domain while RA-antagonism lead to reductions in inflow tract size (Zaffran et al., 2014). In concordance, *Raldh2* null mouse embryos fail to undergo heart looping and have impaired atrial and sinus venosus development (Niederreither et al., 2001). In terms of timing, RA-induced partitioning of the cardiac field is believed to occur immediately after gastrulation. This was confirmed by a study conducted by Xavier-Neto et al. in which they showed that a single pulse of exogenous RA given around E7 produced hearts with marked atrial dominance. Further work has shown that within the cardiac field, a progenitor population of *Tbx5* expressing atrial progenitors responds directly to a caudal-rostral wave of RA-signaling, leading to the differentiation and maturation of these cells (Sirbu et al., 2008).

RA-signaling has also been shown to promote the proper formation of the outflow tract. As mentioned previously, the recruitment of cells from the SHF contributes to the elongation of the cardiac outflow tract (Zaffran et al., 2014). Interestingly, *Raldh2* null mouse embryos show reduced deployment of SHF cells, which subsequently causes outflow tract malformations (Niederreither,

2010). A more direct role for RA signaling in outflow tract development is supported by studies using RARE reporter lines in combination with RAR receptor knockouts. Under normal conditions, *LacZ*-positive cells from the RARE-*LacZ* line are found in the inferior wall of the outflow tract. However, in RARα:RARβ mutants, these *LacZ*-positive cells are lost, resulting in outflow tract deformations such as common arterial trunk (Li et al., 2010). RXRα and RARα:RXRα mutants also develop outflow tract defects, although there is a varying degree of severity amongst them that is most likely attributable to functional redundancy (Lee et al., 1997). In terms of timing, conditional deletion of a floxed RXRα allele in combination with the full RARα KO demonstrated that the period during which RA signaling is require for OFT development is E9-10.5 (Li et al., 2010). Mechanistically, RARα:RARβ mutants are not able to activate a *Mef2C* enhancer in SHF cells at E9.5, suggesting a failure in renewal of distal outflow tract progenitors within the SHF. In addition, elevated levels of TGFβ2, which has been shown to retain proximal outflow tract tissue in the distal region of the heart, have also been detected in RARα:RARβ mutants. Interestingly, reducing the levels of TGFβ2 in RARα:RARβ KOS leads to a partial rescue of the observed outflow tract defects (Li et al., 2010). Overall, the roles of RA-signaling in the various aspects of early heart development are interconnected. Retinoids produced by Raldh2 expression set a caudal boundary for the expanding SHF progenitors while at the same time promoting the development of the venous pole and, at a later point, the formation of the outflow tract.

Epicardial retinoic acid signaling and myocardial growth

The epicardium is essential for normal growth and maturation of the underlying compact myocardium. Indeed, removal of the epicardium in avian systems leads to an arrest in cardiomyocyte proliferation and embryonic death due to a reduction in the heart's ability to perform its functions (Zaffran et al., 2014). The epicardium facilitates myocardial compaction via the secretion of soluble and diffusible growth factors. Several lines of evidence suggest that RA-

signaling is essential for this process. The first line of evidence arises from the observation that RALDH2 is highly expressed in the epicardium (Guadix et al., 2011). The second comes from analyzing RARE reporter lines, which clearly show RA activity in the epicardial and sub-epicardial layers from E11.5 onwards (Dollé et al., 2010). The third comes from the fact that genetic alteration of RA receptors (RXRα or RARα:RARγ) causes embryonic lethality around E15.5 due to severe hypoplasia of the compact myocardium (Soco et al., 1994; Jenkins et al., 2005; Romeih et al., 2003). Hence, it is thought that RA-signaling promotes cross talk between two adjacent layers of the heart, the epicardium and myocardium.

In the mouse, RXRα mutant embryos display defective epicardial development and fail to expand their compact myocardial layer (Jenkins et al., 2005). To determine if the defects observed were specific to RXRα expression in the epicardium, Merki et al. 2005, performed an epicardial-specific deletion of RXRα using the *Gata5-Cre* line. Overall, myocardial thinning and epicardial defects were observed in the *Gata5-Cre* RXRα conditional KOs, although the severity of the defects was less than that observed in full RXRα-nulls. Recent studies using maternal based food supplementation at E7.5-9.5 to overcome the early lethality of *Raldh2* nulls showed that E12.5 rescued hearts exhibited thin myocardial layers, similar to the phenotype observed in RXRα mutants. Importantly, the epicardium was properly formed in *Raldh2* rescue mutants, suggesting the observed myocardial thinning to be due to epicardial-induced RA signaling and not defective formation of the epicardium (Lin et al., 2009).

Since then several approaches have been taken to identify the molecular pathways through which RA signaling regulates myocardial growth. Studies using epicardial cell cultures demonstrated that RA treatment promoted the secretion of soluble mitogens that stimulate cardiomyocyte proliferation (Lavine et al., 2005). Using RAR antagonism and an anti-erythopoetin (*Epo*) receptor antibody on heart slice cultures, Stuckmann et al. 2003, demonstrated that RA and EPO act in concert to induce myocardial growth. Interestingly, RA and EPO treatment did not

directly stimulate the proliferation of cardiomyocytes in vitro, instead they both stimulated the production of mitogens from epicardial cultures. Even more interesting, the addition of RA and EPO-treated media to cultures of cardiomyocytes stimulated their growth (Stuckmann et al., 2003). In terms of the mitogens produced, several FGFs such as FGF2, FGF9, FGF16 and FGF20 have been identified as major players (Lavine et al., 2005; Lin et al., 2010). Indeed, *Fgf9* null mice and mice carrying a myocardial-specific deletion of the *Fgf* receptors 1 and 2 display myocardial thinning (Lavine et al., 2005). Consistent with these findings, Raldh2 rescue mutants display decreased *Fgf2* and *Fgf9* mRNA levels in the compact myocardium (Lin et al., 2010). However, it must be noted that at the time-points during which myocardial compaction occurs (E10-14) *Fgf9* is primarily expressed in the endocardium and not the epicardium.

Despite all this data, a more recent series of studies have brought into question the role of epicardial-derived RA signaling in promoting cardiomyocyte proliferation. In the first of two studies, it was discovered that hepatic expression of *Epo* is dependent upon a RALDH2:RXRα signaling axis (Brade et al., 2011). *Epo* has been previously shown to be indispensable for cardiomyocyte proliferation as *Epo*-null mice die *in utero* due to severe thinning of the compact myocardial layer (Wu et al., 1999). RXRα mutants show decreased *Epo* expression in the liver (Brade et al., 2011). By showing that *Epo* expression was dependent upon RA signaling in the liver the authors suggested that an extra cardiac source of RA played an important part in cardiomyocyte growth. The authors then went on to show that *Epo* exerted its functions on the heart by binding to its receptor EPOR in the epicardium and promoting the expression of IGF2, another soluble ligand essential for cardiomyocyte growth (Brade et al., 2011).

In their second study, the authors decided to examine the activity of the RARE-*LacZ* line in both the *Raldh2* rescue KOs and RXRα nulls. Interestingly, they found that only the *Raldh2* rescue nulls showed a decrease in epicardial-specific RARE-*LacZ* activation (Shen et al., 2015). This indicated that the proposed RXRα-mediated RA-response in the epicardium was not essential for cardiomyocyte growth as epicardial RARE-*LacZ* activation was still present in RXR

KOs. The authors then went on to demonstrate that regulation of epicardial IGF2 expression by RA signaling occurs in a biphasic manner. Until E11.5, the heart and liver are adjacent to each other and *Epo* produced in the liver can easily diffuse to the epicardium and stimulate IGF2 expression. However, after E11.5, the membrane of the diaphragm closes and the communication between the liver and heart ceases. This coincides with the onset of placental function and the ensuing distribution of glucose to organs such as the heart. By performing an endothelial-specific deletion of the RARα receptor, the authors observed impaired formation of the placental labyrinth layer. They argued that this defect lead to a decrease in glucose production that ultimately affected epicardial IGF2 production. To prove their hypothesis, the authors treated epicardial cultures with increasing concentrations of glucose and observed a correlational rise in IGF2 expression (Shen et al., 2015). Hence, it was demonstrated that by stimulating EPO production in the liver as well as by promoting proper placental function, extra cardiac sources of RA signaling were the primary drivers of myocardial growth in the mid-late gestational phase of heart development.

Although these studies provided very compelling evidence of extra cardiac RA signaling being the primary driver for cardiomyocyte growth, they failed to deal with some minor details. First, deletion of RXRα with the *Gata5-Cre* deletion leads to myocardial thinning (Merki et al., 2005). Although RXRα plays an essential role in placental development, deletion of RXRα with the *Gata5-Cre* should not have affected its expression in the placenta. So the fact that epicardial deletion of RXRα leads to such a severe phenotype may suggest that it does have an important role in the epicardium. However, it could be argued that RXRα is acting via other pathways since RXRα has also been shown to interact with Vitamin D, PPAR and liver X receptors (Zaffran et al., 2014). Or perhaps it could be that there is a specific requirement for RXRα in epicardial RA signaling that other RAR/RXR receptors cannot meet (Xavier-neto et al., 2015). Hence, although they continue to activate RARE-*LacZ* expression in the absence of RXRα, the other 5 RA receptors cannot fully compensate for the unique capabilities of RXRα. Nevertheless, regardless of which model one chooses, the literature seems to point towards the fact that RA signaling does

not directly act on cardiomyocytes to promote their proliferation. Whether it is through an epicardial or extra cardiac source, retinoids support myocardial growth by promoting the secretion of soluble ligands, and not by directly interacting with cardiomyocytes. This is further supported by the fact that RXRα defects are not rescued by transgenic expression of RXRα in the myocardium and that RXRα-null cardiomyoblasts are normally integrated into a wildtype heart (Chen et al., 1998; Tran et al., 1998).

In addition to supporting myocardial growth, the epicardium is also a source of essential epicardial derived cells (EPDCs) that support the heart during mid-late gestation. These EPDCs include vascular smooth muscle cells, cardiac fibroblasts and a subset of coronary endothelial cells (Zaffran et al., 2014). In order to migrate into the heart, the EPDCs must first undergo an epithelial to mesenchymal transition (EMT). The Wilm's tumour (WT1) protein is specifically expressed in the epicardium and is essential for the EMT process occurring in EPDCs (Guadix et al., 2011). *Wt1*-deficient mice have reduced numbers of EPDCs and die from subsequent coronary defects (Moore et al., 1999). In addition, *Wt1*-deficient mice show reduced expression of RALDH2 in the epicardium. In fact, *Raldh2* has been demonstrated to be a direct target of WT1 (Guadix et al., 2011). Interestingly, the EMT defect observed in *Wt1*-deficient mice is partially rescued by RA supplementation, suggesting that RA signaling may be involved in epicardial EMT (Guadix et al., 2011). Furthermore, there is a possibility that the WT1 and RA signaling pathways are cross-inductive as epicardial RA has been shown to induce WT1 expression.

In order for the coronary arteries to develop properly, endothelial tube formation and vascular smooth muscle differentiation must occur in a coordinated fashion. As mentioned previously, EPDCs cells give rise to vascular smooth in a process involving migration from the epicardium into the myocardium, followed by differentiation. Differentiation of vascular smooth muscle cells corresponds to the time when RALDH2 expression is lost in EPDCs. An interesting study by Braitsch et al. 2012, proposed that before RALDH2 expression is lost in EPDCs, it induces TCF21 to inhibit smooth muscle cell differentiation in subepicardial EPDCs.

Mechanistically, it was suggested that upon invasion into the myocardium RALDH2 and, consequently, TCF21 expression are down regulated. As a result, EPDCs differentiate into vascular smooth muscle cells that support the coronary arteries. The authors then argued that this delay in smooth muscle cell differentiation was necessary for coronary vessel development since it allowed the endothelium of the coronary vasculature to form functional tubes before being surrounded by a smooth muscle layer.

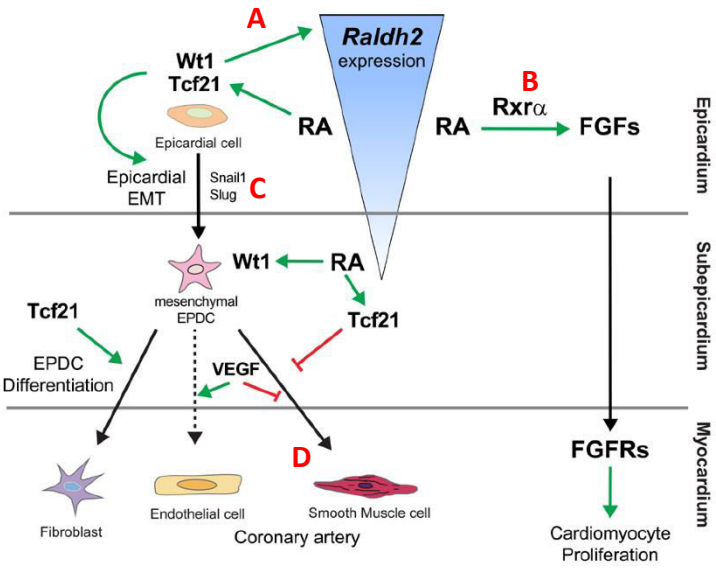

Figure 13, *Schematic demonstrating the roles of RA-signaling in the epicardium and in cardiomyocyte growth.* **A,** Raldh2 is activated by Wt1 in the epicardium to produce RA. **B,** RA promotes FGF production which is secreted to the myocardium to promote growth. **C,** By promoting WT1 expression RA facilitates epicardial EMT. **D,** RA delays smooth muscle differentiation by promoting TCF21 expression long enough for endothelial tubes to correctly form (Zaffran et al., 2014).

Retinoic acid signaling in cardiac remodeling and repair

One of the key issues with treating patients suffering from heart disease is that cardiomyocytes have a very limited potential to proliferate and repair the damaged heart. Hence, in order to improve the outcomes of patients recovering from acute myocardial infarction scientists have focused on two strategies: (1) Replacing damaged tissue though the stimulation of endogenous repair mechanisms or by transplanting new cardiomyocytes from exogenous sources, and (2) limiting the extent of the damage by surgical (reperfusion) or protective treatments (drugs) (Garbern and Lee, 2013). Of the two strategies, it is suspected that RA-signaling may play a role in protecting the heart from excessive damage. Experimental studies have for a long time suggested that RA suppresses the morphological alterations in cardiomyocytes normally induced by endothelin, angiotensin II and phenylephrine supplementation (Palm-Leis et al., 2004). In addition, RA signaling has been shown to inhibit apoptosis in cardiomyocytes exposed to cellular stress (Zhu et al., 2015). This protective role has been linked to RA-induced suppression of the mitogen activated-protein kinases (MAPK) pathway, a well-described signaling cascade responsible for promoting programmed cellular death in damaged or stressed cells (Palm-Leis et al., 2004; Zhu et al., 2015).

The first direct evidence that RA played a role in the cardiac remodeling and repair process came from a study performed in rats. The objective of the study was to evaluate the role of RA in experimental post-infarction myocardial remodeling. Wistar rats subjected to permanent ligation of the left anterior artery were fed either a RA-supplemented diet or a control diet and analyzed 6 months post-surgery. The authors looked at several variables such as cardiomyocyte cross sectional area, interstitial collagen, infarct size and heart function. Overall, it was determined that RA-fed rats showed a smaller cardiomyocyte cross sectional area as well as a reduction in interstitial collagen. Furthermore, the maximum rate rise of left ventricular pressure was greater in the RA-supplemented mice. Hence, RA supplementation seemed to play a protective role in the

damaged heart by regulating cardiomyocyte hypertrophy and interstitial collagen production (Paiva et al., 2005).

A few years later a similar study was performed, except this time the rats were fed a vitamin A deficient (VAD) diet for several months before surgery. Three months post MI, many of the same variables from the previous study were examined and compared between the VAD and control groups. From their analyses, the authors detected an increase in cardiomyocyte hypertrophy and interstitial collagen in the VAD group. They also determined that VAD rats displayed worsening diastolic dysfunction. Infarct sizes were similar as in the previous study. Overall, this study confirmed the majority of the observations made in the previous one. RA-signaling appeared to play an important role in attenuating the adverse remodeling process occurring post-MI. However, there were several limitations concerning the findings of these studies. First, the authors did not provide any molecular insight as to how RA could be attenuating the cardiac remodeling response post MI. Second, although the cardiomyocytes (hypertrophic response) and cardiac fibroblasts (interstitial collagen differences) seemed to be affected by RA-levels, there was no evidence showing these cell types were directly responding to RA (Minicucci et al., 2010).

In order to deal with these issues, two main studies using mice were carried out by separate groups. In the first study, the authors generated a RARE-luciferase reporter line (described in a previous section) to track the RA response post-surgery (Bilbija et al., 2012). Rather than examining mice at late time-points (3 and 6 months post MI), the authors focused on the first week following surgery. With their RA-reporter line an RA response in the heart was detected just 24 hours after surgery. A time course analysis of the ensuing days revealed that the response peaked 7 days post MI. This coincided with their molecular analyses showing increased expression of *Raldh2* and several RA-targets at these time-points. To determine which cell types were responding, the authors isolated cardiomyocytes and cardiac fibroblasts from post MI hearts and measured luciferase activity. From these measurements the authors determined that cardiac fibroblasts displayed a higher response than cardiomyocytes. Treatment of cultured primary

fibroblasts with all-trans Retinoic acid (atRA) resulted in decreased proliferation rates, leading the authors to conclude that part of the protective role of RA post MI was to limit collagen production by attenuating fibroblast proliferation. While this observation matched some of the ones made by previous studies (Paiva et al., 2004; Minicucci et al., 2010), it only accounted for part of the story. Perhaps, the reason why the authors detected a significantly smaller response in cultured cardiomyocytes compared to fibroblasts, related to the difficulties associated with isolating viable adult cardiomyocytes.

In the second study conducted by Zhu et al. 2015, mice were subjected to ischaemia/reperfusion surgeries and then injected with atRA for one week before being sacrificed and analyzed. Ischaemia/reperfusion consists of ligating the artery for a small period of time then reperfusing it. The authors argued that this model was more realistic than permanent LAD as it more closely mimics the process occurring in human patients after acute MI. Furthermore, reperfusion, although generally seen to reduce the infarct area in patients, has been shown to increase apoptosis in border zone myocytes (Vinten et al., 2004; Zhao 2004). Since RA is known to display anti-apoptotic activity in cultured cardiomyocytes, the authors wanted to determine if it played a similar role *in vivo* post MI/reperfusion. Analysis of mice seven days post-surgery revealed that atRA-treated mice showed significantly smaller infarct zones and less apoptosis. Analysis of gene expression changes showed a significant increase in the metalloprotease ADAM10 in atRA treated hearts. This protease had been previously shown to regulate MAPK activation by cleaving the advanced glycation end-products (RAGE) receptor, a well described activator of MAPK signaling (Raucci et al., 2008). Indeed, analysis of atRA –treated hearts lead to decreased activation of the three MAPK pathways (p38, pJNK and pERK). To confirm a potential link between RA treatment and increased RAGE cleavage, the authors performed MI on RAGE null mice and then treated them with atRA. Strikingly, the protective effects of atRA were abolished in RAGE KOs, who without atRA treatment, showed smaller infarcts compared to non-atRA-treated wildtype mice. A molecular analysis using *in vitro* systems confirmed these molecular links

and also demonstrated RA to play an antioxidant role in cardiomyocytes exposed to hypoxic conditions. Hence, a new model for the role of RA in the cardiac repair and remodeling process through which RA, by stimulating ADAM10 expression, reduces MAPK signaling, leading to decreased apoptosis and improved outcomes post MI.

A role for RA signaling in Cardiomyocytes

Developmental studies seem to suggest that the RA pathway does not directly affect cardiomyocyte growth during mid-late gestational phases of heart development (Zaffran et al., 2014; Xavier Neto et al., 2015). Instead, RA signaling originating from the epicardium and/or from extra cardiac sources (liver and placenta) stimulate the production of soluble mitogens that then promote cardiomyocyte differentiation and proliferation. This is supported by data showing that RXRα, the main RA receptor associated with the functions of RA during embryonic development, is dispensable in cardiomyocytes (Chen et al., 1998). It also seems to be supported by data using the RARE-LacZ which shows a response in the epicardium and subepicardium but nothing within the compact myocardium itself (Chen et al., 2015). Furthermore, direct treatment of cardiomyocytes with exogenous RA does not elicit a proliferative response (Stuckmann et al., 2002). While it is difficult to dispute the validity of this data, one must be careful in universally applying it to all stages of embryonic development. Furthermore, denying a role for RA-signaling on cardiomyocytes in different contexts such as the post-natal period or during cardiac remodeling and repair, would be counter-productive and oversimplified.

The first argument for a direct role of RA signaling in cardiomyocytes would involve looking at earlier time-points of heart development. Deletion of *Raldh2* along with several of the RA receptors leads to precocious differentiation of progenitors in the arterial and venous poles (Zaffran et al., 2014). These observations point to a clear effect of RA signaling on cardiac progenitors. At this point the epicardium is not present suggesting that production of RA in the posterior lateral mesoderm must be traveling towards and acting on the cardiac crescent/linear

heart tube in a direct manner. In the venous pole, this is supported by activation of the RARE-*LacZ* line. However, no *LacZ*-positive cells are detected in the arterial pole at these time-points (Xavier Neto et al., 2015) suggesting one of two things: (1) The effect on arterial pole progenitors is the result from an earlier function of RA signaling, and (2) the RARE-*LacZ* line is not sensitive enough to pick up this response. While there is evidence to support the first hypothesis, much less is known about the putative limitations of the RARE-*LacZ* line. Which brings us to our second point regarding the fact that no RARE-*LacZ* activation is detected in the myocardium during mid-late gestation. One of the issues regarding the analyses of RARE-*LacZ* activation in the mid-gestational heart is the fact that the majority of images from the tracing studies do not show any co-staining of the *LacZ* positive cells with epicardial markers (WT1 or TBX18) to prove that the epicardium and subepicardial cells are the only cell types responding to RA-signaling (Chen et al., 2015). In fact, by analyzing RARE-*Cre* activation at later time-points P7 one can easily notice a very broad signal extending well into the compact myocardium (Dolle et al., 2010). Whether this staining pattern encompasses cardiomyocytes or not is unclear; however, it would be worth taking a closer a look at the the activities of the RARE-LacZ and RARE-Cre lines during earlier stages with specific markers to see if, indeed, there is no cardiomyocyte response.

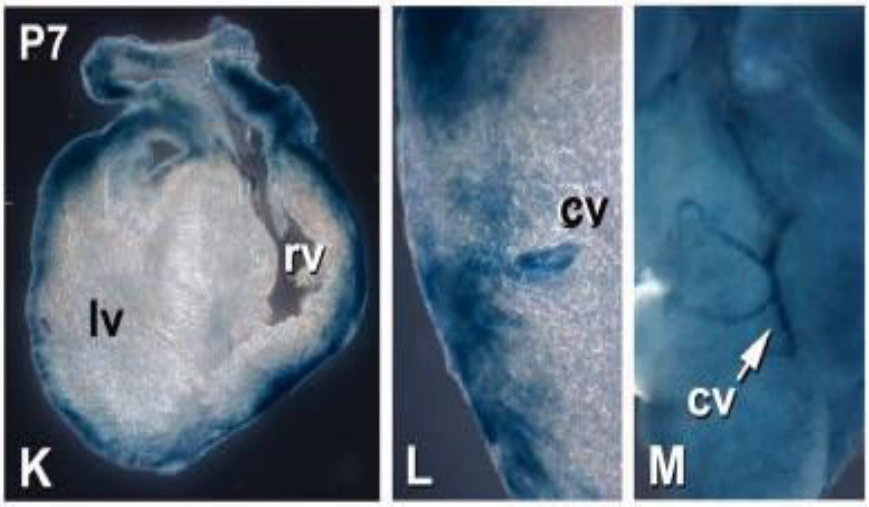

Figure 12, *Analysis of lacZ staining with the RARE-Cre:R26LacZ line in P7 hearts*. Notice the staining pattern extending well into the compact myocardium. The wall of a coronary vessel (cv) is labelled at this timepoint. rv=right ventricle, lv =left ventricle (Dollé et al., 2010).

Another line of reasoning is derived from a more detailed analysis of the phenotypes resulting from the various RA-receptor knockouts along with the *Raldh2* rescue nulls. The fact that RARE-*LacZ* staining is not abolished in the epicardium of *Gata5-Cre*-RXRα mutants (Merki et al., 2005) seems to suggest that the myocardial thinning resulting from RXRα deletion is unrelated to epicardial-specific RA-signaling. This would not be surprising considering that RXRα does not directly bind atRA and can interact with receptors from different pathways. Furthermore, RXRα receptors can activate the transcription of various genes independently of RAR receptors by forming homodimers (Zaffran et al., 2014). The RAR receptors are more faithful at transducing RA-dependent transcription and can provide a much more accurate depiction of the cell types involved in RA-signaling. However, a substantial amount of functional redundancy exists between them and only by deleting both the RARα and RARγ receptors can the myocardial thinning phenotype observed in mouse embryos be recapitulated (Zaffran et al., 2014). The fact that compaction defects are reproducible with the RARα and RARγ KOs suggests they do play an important role, but whether or not this is related to an extra cardiac or epicardial source of RA signaling is not clear. To address this issue one would have to perform a cardiomyocyte-specific deletion of RARα and RARγ and determine if there were any resulting phenotypes.

A detailed analysis of the rescue *Raldh2* KOs further complicates the picture. Supplementation of pregnant dams with RA during a specific time period delays the embryonic lethality observed in *Raldh2* nulls from E10.5 to E13.5 (Lin et al., 2010). At E12.5 *Raldh2* KOs exhibit severe myocardial thinning. On the surface, this observation seemed to support the hypothesis of epicardial RA-signaling promoting myocardial growth through the production of soluble mitogens. However, a closer analysis of the phenotype revealed that the overall proliferation levels within the compact myocardium of *Raldh2* rescue nulls were not actually decreased, instead, they increased slightly. This increase was attributed to a “side population” of cardiac progenitors which, in the absence of Raldh2, failed to differentiate and continued to proliferate. Interestingly, this lack of differentiation ended up being considered the prime reason

for the myocardial thinning defect observed in the *Raldh2* rescue KOS, which was contrary to the RXRα KOs that clearly displayed decreased overall cardiomyocyte proliferation (Jenkins et al., 2005). Surprisingly, the effects of *Raldh2* deletion during early stages of differentiation compared with later stages seem to contradict each other. *Raldh2* null embryos display precocious cardiac progenitor differentiation (Xavier-Neto et al., 2015) while Radh2 rescue KOs display a delay and/or reduction in progenitor differentiation. Nevertheless, both of these defects point towards RALDH2-induced RA production acting directly on cardiomyocytes to influence their differentiation states.

A further line of evidence supporting a direct role for RA-signaling on cardiomyocytes comes from studies performed during the post-natal period and adulthood. As mentioned before, a series of older studies performed in primary postnatal cardiomyocyte cultures suggested a protective effect of RA treatment in response to endothelin and angiotensin II-induced damage (Palm-Leis et al., 2004). These studies showed that RA limited the damage induced from these agents by inhibiting MAPK pathways. This was an interesting find since the renin-angiotensin system's (RAS) damaging effects on the heart post MI are well described and several drugs targeting this pathway have even been designed to help improve the outcomes of patients recovering from acute MI. These drugs include angiotensin converting enzyme inhibitors such as zofenopril, captopril and Ramipril (Murdoch and McMurray, 1998).

Since then, more data linking RA signaling with a protective effect from the RAS has emerged. In a study by Guleria et al., postnatal and adult cardiomyocytes (CMs) were exposed to high glycemic (HG) conditions to induce the RAS. The link between HG and the RAS has been previously described in diabetic patients, who face higher risks of developing cardiac diseases due to increased serum glucose levels promoting RAS activation in the heart. In this study the authors discovered that exposing CMs to high levels of glucose led to decreased RARα and RXRα expression, as well as increased apoptosis. Interestingly, the increase in apoptosis resulting from HG was recovered by treating CMs with RAR and RXR agonists. RARα and RXRα treatment also lead to a decrease in ROS production. Silencing of RARα and RXRα with siRNA promoted

apoptosis and increased ROS under normal conditions. Finally, RARα and RXRα agonists were shown to block HG induced expression of angiotensinogen and Angiotensin II synthesis, suggesting a direct link between RA, cardiomyocytes, the RAS and apoptosis.

A recent study has confirmed the protective role of RA on cardiomyocytes *in vivo*. By performing a myocardial specific deletion of the RARα receptor in adult mice, Zhu et al., successfully showed that basal level RA signaling through RARα was responsible for preventing cardiomyocyte hypertrophy, excessive ROS production and calcium reuptake deficiencies. Mechanistically, RARα deficient CMs were shown to express decreased levels of the superoxide dismutases (SOD) 1 and 2 (normally responsible for reducing ROS in the cell by converting them to hydrogen peroxide) and increased levels of NADPH oxidases (NOX) 2 and 4 (indicators of cellular stress due to excessive ROS). In regards to calcium reuptake, decreased levels of sarcoplasmic reticulum Ca ATPase2a (SERCA2a), an enzyme normally responsible for removing Ca from the cytosol, were detected in RARα myocytes. These causal relationships were all supported with *in vitro* data from neonatal CMs. Interestingly, induction of diabetes in adult mice with streptozotocin (a drug which kills pancreatic β-cells) led to decreased levels of RARα, once again providing a link between RA-signaling, diabetes and cardiac disease.

Overall, the data described above suggests that the role of RA signaling in the developing and adult heart is more complex than previously imagined. Various cell types, receptors and enzymes are involved. Deciphering which cells are responding to RA and defining that response is very much dependent on the physiological context and the efficiency of the genetic tools being used. Nevertheless, RA's role on the early phases of cardiac development as well its protective functions during adult homeostasis and in cardiac repair seems to indicate its effects on cardiac progenitors and cardiomyocytes are indispensable. However, further studies are needed to settle this debate.

CHAPTER II: THE ROLE OF R-SPONDIN3 IN CORONARY ARTERY FORMATION

I. Project description

Coronary artery anomalies (CAA) are common congenital defects that predispose to heart disease (Riley and Smart, 2011). Understanding the processes leading to the development of coronary arteries and identifying the signaling pathways that drive their specification is, therefore, of utmost importance.

Coronary vessel development begins at E11.5 with the formation of a vascular plexus on the dorsal aspect of the atrioventricular groove. The coronary plexus then expands and encompasses the entire heart, eventually giving rise to mature coronary veins, capillaries and arteries (Red Horse et al., 2010). The left and right coronary arteries connect to the coronary orifices at highly stereotyped locations (Tian et al., 2013). They are remodeled from the primitive coronary plexus in a complex process involving endothelial migration, proliferation and specification. Exactly how this process occurs is unclear, although several signaling pathways have been shown to be involved.

R-spondins (RSPO1-4) are secreted activators of Wnt/β-catenin signaling with various roles in embryonic patterning and organ development. They potently enhance WNT signaling by binding leucine-rich repeat-containing G protein-coupled receptors (LGR) and increasing the availability of WNT receptors (de Lau et al., 2012). Of particular interest in R-spondin3, which plays an important role in placental vasculature remodeling (Aoki et al. 2007; Kazanskaya et al., 2008) and development of the secondary heart field (Cambier et al., 2014).

Given Rspo3's essential role in remodeling the placental vasculature as well as its importance in SHF progenitors, I asked whether or not Rspo3 could be involved in coronary vessel development. A preliminary analysis of *Rspo3* expression demonstrated it was expressed at later time-points (E14.5) during cardiac development (Genepaint.org). Furthermore, *Rspo3* seemed to

be expressed in highly angiogenic regions of the heart, where the vascular plexus first emerges. Overall, the main goal of my principal PhD project was to understand the role of *Rspo3* in coronary vessel development. More specifically, I wanted to:

1) Study the expression pattern of *Rspo3* during mid-late gestation
2) Temporally delete *Rspo3* at critical time-points in coronary vessel development
3) Analyze and characterize any heart phenotypes resulting from *Rspo3* deletion
4) Understand the molecular mechanisms through which *Rspo3* affects coronary vessel formation

I began this project with a detailed analysis of *Rspo3*'s expression pattern during mid-late gestation. Since there are no reliable antibodies specific for RSPO3, I utilized *in situ* hybridization (ISH) to detect *Rspo3* mRNA in the heart. I decided to focus on embryonic days 11.5-14.5 (E11.5-14.5), since it is at these time-points that the heart's vasculature plexus is remodeled into mature arteries and veins.

Next I decided to delete *Rspo3* in the embryo to see if it had a role in coronary vessel formation. In order to avoid the early embryonic lethality observed in *Rspo3*-null embryos I crossed an *Rspo3* floxed line with the *CAGGCre-ER*^{TM} line (Hayashi and McMahon, 2002). The *CAGGCre-ER*^{TM} line contains the chicken β-actin promoter and the cytomegalovirus (CMV) enhancer upstream of a *Cre* recombinase, driving its ubiquitous expression. The *Cre* is fused to the mutated estrogen receptor (ER) and can only enter the nucleus upon binding synthetic forms of estrogen such as hydroxy-tamoxifen. Using this strategy I was able to deplete *Rspo3* in a temporal and ubiquitous manner by supplementing the pregnant dam with tamoxifen at desired time-points. I chose to delete *Rspo3* at E11.5 since it is at this time-point that the vascular plexus of the heart begins to develop. In addition, at E11.5 SHF development is complete; thus, avoiding potential progenitor defects. Analysis of the hearts was performed at E15.5 and E17.5 since both the coronary arteries and veins are mature at these time-points.

To understand the mechanisms underlying any potential phenotypes I decided to study the transcriptional changes occurring at earlier time-points. For this I performed several qPCR analyses on E13.5 mutant hearts with specific primers for WNT signaling target genes as well as many genes involved in angiogenesis. Immunostaining on paraffin sections of any potential hits was also carried out at this time-point to verify the results obtained from the qPCR analyses.

To delineate which pathway *Rspo3* was going through I looked at specific targets of both canonical and non-canonical WNT pathways. I also performed recovery experiments with the canonical WNT activator Lithium Chloride to see if pharmacological β-catenin stabilization could compensate for the loss of RSPO3. Finally, in order to determine if *Rspo*3 could directly influence either of these pathways in the endothelial compartment of the heart, I isolated primary endothelial cells from E15.5 hearts. Following isolation, I cultured and treated them with recombinant RSPO3 and then extracted RNA to examine differences in gene expression levels.

Overall, the aim of this project was simple. I hypothesized that Rspo3, through similar mechanisms observed in the placenta vasculature, was essential for coronary vessel development. Hence, disruption of Rspo3 at critical time-points during the remodeling of the coronary vasculature would lead to defects in the formation of the arterial and/or venous trees.

II. The role of R-spondin3 in coronary artery formation (Schematic for project design)

Part 1: Expression pattern of *Rspo3*

Murine Coronary Vessel development (Red Horse et al., 2010)

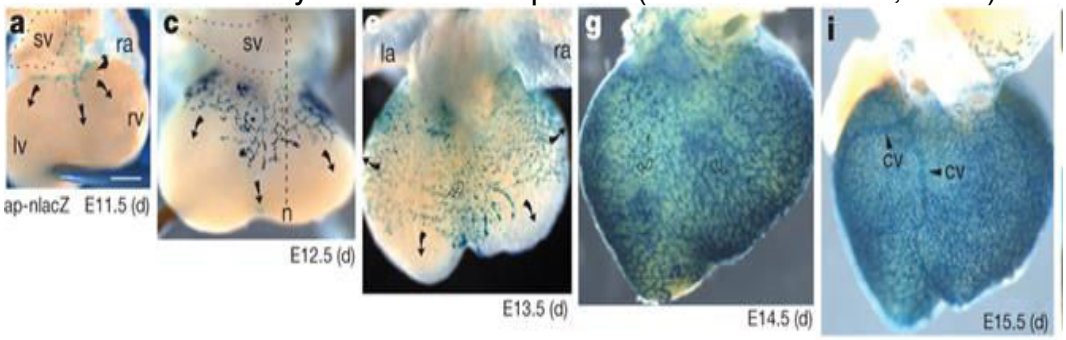

Analyze *Rspo3* expression by *in situ* hybridization during coronary vessel development

Part 2: Temporal deletion of *Rspo3*

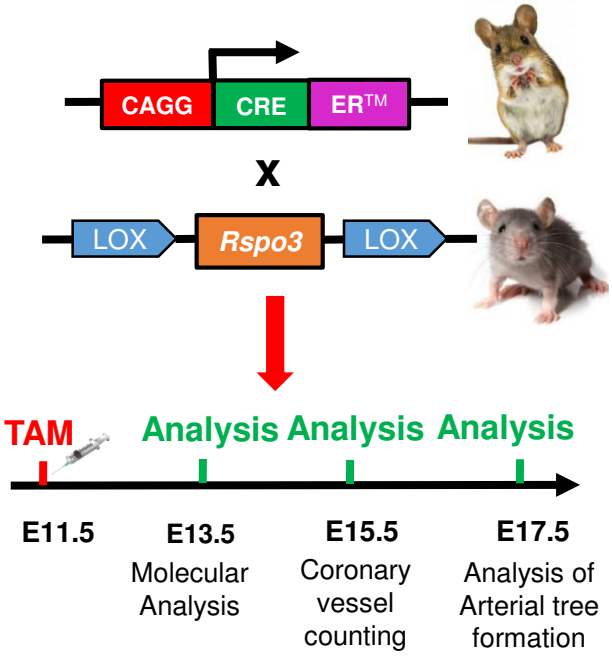

Study effects of *Rspo3* deletion on coronary vessel formation

III. Manuscript entitled “Coronary artery formation is driven by localized expression of R-spondin3

Report

Cell Reports

Coronary Artery Formation Is Driven by Localized Expression of R-spondin3

Graphical Abstract

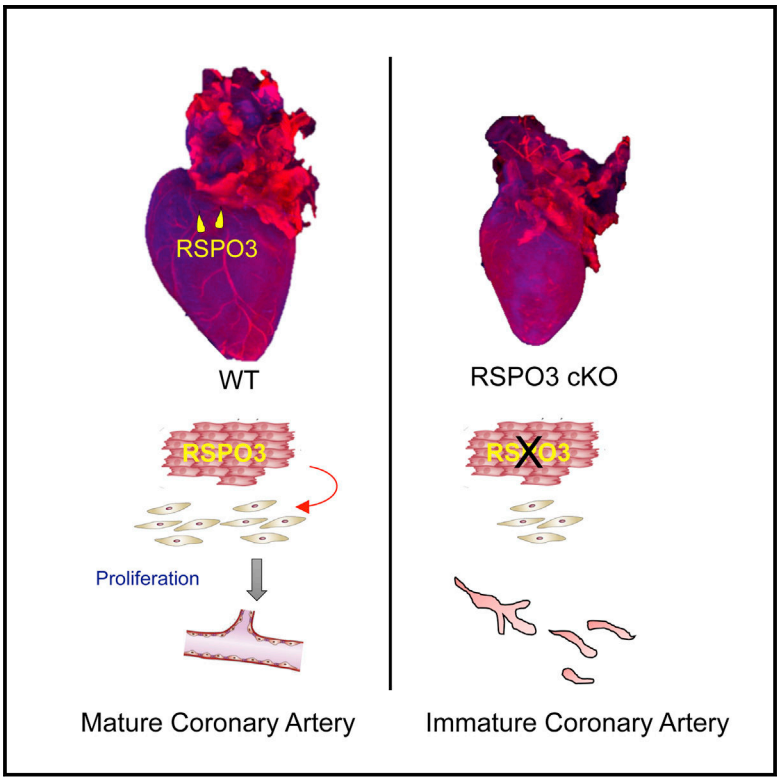

Authors

Fabio Da Silva, Ana Sofia Rocha, Fariba Jian Motamedi, ..., Harris Morrison, Kay Dietrich Wagner, Andreas Schedl

Correspondence

schedl@unice.fr

In Brief

Coronary arteries supply the heart with blood, and coronary diseases are one of the leading causes of death worldwide. Da Silva et al. find that RSPO3 is specifically expressed around the developing stems of the left and right coronaries, where it promotes their formation by stimulating arterial-specific proliferation through Wnt/β-catenin signaling.

Highlights

- *Rspo3* is expressed in angiogenic regions around developing coronary arteries
- *Rspo3* promotes localized arterial proliferation through Wnt/β-catenin signaling
- *Rspo3* deletion leads to defective coronary stem and improper arterial tree formation

Da Silva et al., 2017, Cell Reports *20*, 1745–1754
August 22, 2017
http://dx.doi.org/10.1016/j.celrep.2017.08.004

Cell Reports
Report

Coronary Artery Formation Is Driven by Localized Expression of R-spondin3

Fabio Da Silva,[1] Ana Sofia Rocha,[1,3] Fariba Jian Motamedi,[1] Filippo Massa,[1] Cem Basboga,[1] Harris Morrison,[2] Kay Dietrich Wagner,[1] and Andreas Schedl[1,4,*]
[1]Université Côte d'Azur, Inserm, CNRS, iBV, Nice, 06108, France
[2]MRC Human Genetics Unit, Western General Hospital, Edinburgh EH42XU, UK
[3]Present address: Institut d'Investigació Biomédica de Bellvitge (IDIBELL), L' Hospitalet de Llobregat 08908, Barcelona, Spain
[4]Lead Contact
*Correspondence: schedl@unice.fr
http://dx.doi.org/10.1016/j.celrep.2017.08.004

SUMMARY

Coronary arteries are essential to support the heart with oxygen, and coronary heart disease is one of the leading causes of death worldwide. The coronary arteries form at highly stereotyped locations and are derived from the primitive vascular plexus of the heart. How coronary arteries are remodeled and the signaling molecules that govern this process are poorly understood. Here, we have identified the Wnt-signaling modulator *Rspo3* as a crucial regulator of coronary artery formation in the developing heart. *Rspo3* is specifically expressed around the coronary stems at critical time points in their development. Temporal ablation of *Rspo3* at E11.5 leads to decreased β-catenin signaling and a reduction in arterial-specific proliferation. As a result, the coronary stems are defective and the arterial tree does not form properly. These results identify a mechanism through which localized expression of RSPO3 induces proliferation of the coronary arteries at their stems and permits their formation.

INTRODUCTION

Coronary artery anomalies (CAAs) are common congenital defects that predispose to heart disease including sudden cardiac death (Riley and Smart, 2011). Moreover, coronary artery diseases are among the leading causes of mortality in Western societies. Understanding the processes and signaling pathways that drive the development of the coronary arteries is therefore of utmost importance.

Coronary vessel development begins at embryonic day (E) 11.5 with the formation of a vascular plexus on the dorsal aspect of the atrioventricular groove. The coronary plexus then expands and encompasses the entire heart, eventually giving rise to mature coronary veins, capillaries, and arteries (Red-Horse et al., 2010). Lineage tracing studies have determined the endothelial cells of the coronary plexus originate from three different sources: a subset of the proepicardium (Katz et al., 2012; Cano et al., 2016), the venous endothelium of the sinus venosus (Red-Horse et al., 2010), and the ventricular endocardium (Wu et al., 2012). Despite these recent advances, the precise molecular cues guiding the remodeling of mature coronary arteries from the primitive vascular plexus remains unclear.

R-spondins (RSPOs1–4) are secreted activators of Wnt/β-catenin signaling with various roles in embryonic patterning and organ development. They potently enhance WNT signals by binding leucine-rich repeat-containing G protein-coupled receptors (LGRs) and increasing the availability of WNT receptors (de Lau et al., 2012). Of particular interest is R-spondin3 (*Rspo3*), which plays an important role in vasculature remodeling and heart development. *Rspo3*-deficient embryos die in utero at E10 due to vascular defects in the placenta (Kazanskaya et al., 2008), and tissue-specific ablation of *Rspo3* in the heart with the *Islet1-Cre* line leads to defective secondary heart field development (Cambier et al., 2014). In the placenta, RSPO3 promotes angiogenesis and vessel sprouting by controlling expression of vascular endothelial growth factor A (VEGFA) through canonical Wnt/β-catenin signaling (Kazanskaya et al., 2008). More recently, RSPO3 was shown to activate the non-canonical Wnt/calcium pathway in the endothelial compartment of the postnatal retina and lungs to promote blood vessel maintenance (Scholz et al., 2016).

Here, we show that *Rspo3* is specifically expressed in angiogenic regions of the heart at critical time points during coronary vessel development, where it induces canonical Wnt/β-catenin signaling to promote arterial-specific proliferation in the peritruncal vessels of the coronary plexus. Temporal ablation of *Rspo3* at E11.5 leads to defective formation of the proximal coronary arteries and, as a result, the arterial tree fails to develop properly.

RESULTS AND DISCUSSION

Rspo3 Is Expressed around the Developing Coronary Arteries

To study the expression pattern of *Rspo3* in the heart during mid gestation we carried out in situ hybridization analyses from E12.5–E18.5. Throughout these stages, *Rspo3* was expressed in angiogenic regions surrounding the base of the outflow tract, where coronary plexus formation initially occurs. Closer inspection revealed that *Rspo3* was specifically and highly expressed around the deep vascular channels that give rise to the left and right coronary arteries, and that this pattern of expression was maintained throughout development (Figure 1).

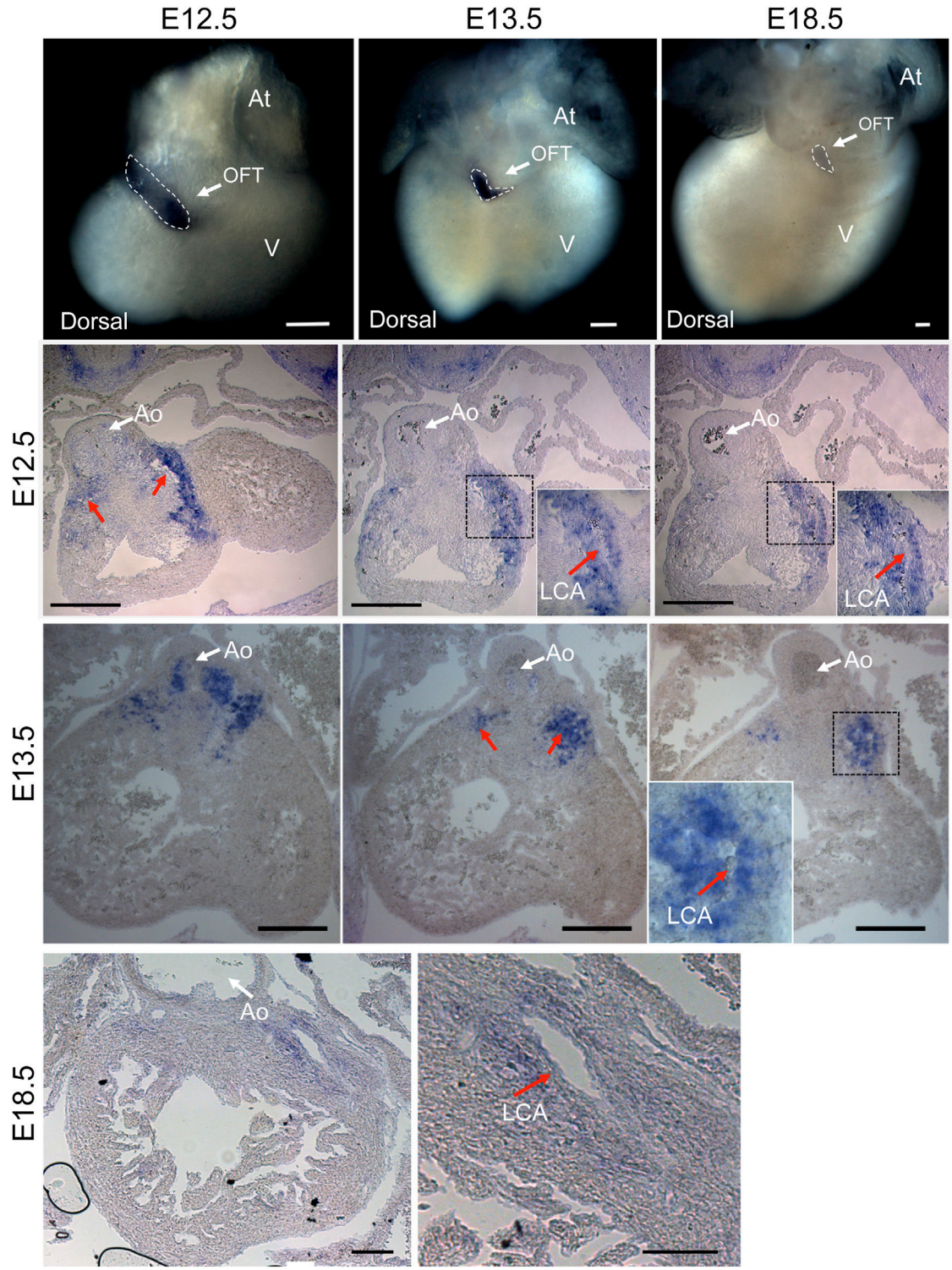

Figure 1. Rspo3 Is Expressed in Angiogenic Regions of the Heart around the Developing Coronary Arteries

Whole-mount in situ hybridization (ISH) analysis of embryonic hearts shows *Rspo3* is expressed around the base of the outflow tract from E12.5–E18.5 (top panels, dorsal view of hearts, *Rspo3* expression marked by dotted white lines). Closer inspection on sections near the aorta (white arrows) reveals *Rspo3* is highly expressed around the developing coronary arteries (red arrows) at E12.5 and E13.5. *Rspo3* continues to be expressed at lower levels around the left coronary artery at E18.5. Scale bars, 0.4 mm (whole mounts), 200 μM (sections). At = atrium, OFT = outflow tract, V = ventricle, Ao = aorta, LCA = left coronary artery.

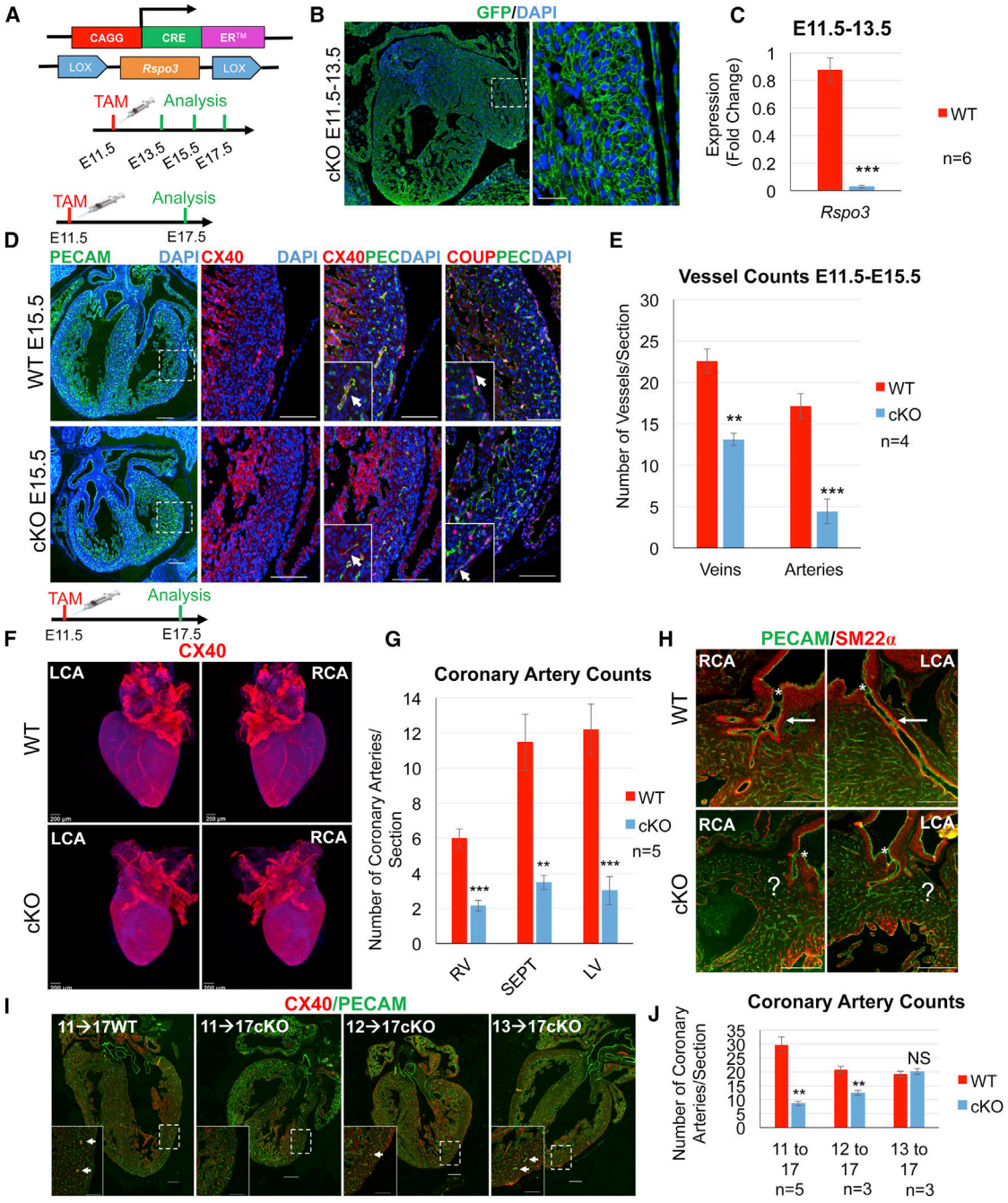

Figure 2. Coronary Artery Development Is Impaired in Rspo3-Deficient Hearts

(A) Schematic demonstrating the strategy used to delete loxP-flanked *Rspo3* in an inducible manner with the ubiquitously expressed *CAGGCre-ER*^{TM} line (CAGG = CMV enhancer + chicken β-actin promoter). *Rspo3* was deleted at E11.5 via tamoxifen (TAM) administration and sacrificed at various time points.

(B) GFP immunostaining on sections of *CAGGCre-ER*^{TM} *Rspo3fl/fl* (conditional knockout, cKO) hearts crossed with the mTmG reporter line demonstrates very efficient recombination in mutants when analyzed only 2 days after deletion.

(C) The *CAGGCre-ER*^{TM} line is very effective at deleting *Rspo3* in the heart, as demonstrated by qPCR analysis of *Rspo3* mRNA levels in *Rspo3*fl/fl (wild-type, WT) versus cKO embryos. Data are expressed as fold change versus controls and columns are means ± SEM (n = 6, 3 litters).

(D) Analysis of coronary vessel development in *Rspo3* mutant hearts. Veins were defined as COUPTFII(COUP)/PECAM-positive subepicardial vessels and arteries as connexin 40 (CX40)/PECAM-positive intra-myocardial vessels. The veins detected appear normal, while the arteries are grossly malformed in *Rspo3*-deficient hearts (white arrows, insets). Scale bars, 200 μM (mosaics), 100 μM (close ups).

(E) Coronary vessel counting reveals *Rspo3*-deficient hearts have significantly less coronary veins and arteries at E15.5. Columns are means ± SEM (n = 4, 2 litters).

(legend continued on next page)

Rspo3-Deficient Hearts Display Defective Coronary Vessel Development

The important role of *Rspo3* in placental vascularization prompted us to test whether it could play a similar role in the heart. To avoid the early embryonic lethality (E10) observed in full *Rspo3* knockouts, we opted for an inducible system by crossing a floxed allele of *Rspo3* (*Rspo3^{fl}*) with the ubiquitously expressed *CAGGCre-ER^{TM}* line (Hayashi and McMahon, 2002) (Figure 2A, schematic). Deletion of *Rspo3* was induced by tamoxifen administration at E11.5, a time point when the vascular plexus of the heart first appears. To test the efficiency of the *CAGGCre-ER^{TM}* line in the developing heart, we crossed it with the membrane targeted tandem dimer Tomato membrane targeted green fluorescent protein (mTmG) reporter allele (Muzumdar et al., 2007). GFP immunostaining demonstrated very efficient recombination in all compartments of the heart (Figure 2B). Furthermore, qPCR analysis of *Rspo3* mRNA in mutant hearts just 48 hr after deletion revealed a 97% reduction ($p = 0.0002$) in expression levels (Figure 2C).

To analyze coronary vessel development in *Rspo3* mutants, we performed immunofluorescent co-staining on E15.5 heart sections with platelet endothelial cell adhesion molecule (PECAM) and chicken ovalbumin upstream promoter-transcription factor 2 (COUPTFII) to identify the coronary veins and with PECAM and connexin 40 to identify the coronary arteries (Figure 2D). Serial counting revealed a 43% reduction ($p = 0.004$) in the number of veins and a drastic 75% reduction in the number of arteries in mutant hearts ($p = 0.001$) (Figure 2E). Upon closer inspection, the coronary veins showed normal morphology at E15.5 (Figure 2D, insets) and at E17.5 (Figure S3B) in mutant hearts, while the arteries were grossly malformed (Figure 2D, insets).

Defective coronary vessel development has been previously shown to lead to decreased proliferation resulting from inadequate blood supply to the myocardium (Ivins et al., 2015). In accordance, analysis of *Rspo3*-deficient hearts at E17.5 displayed hypoplastic hearts when compared to littermate controls. To determine the onset of the hypoplasticity in *Rspo3* mutant hearts, we injected pregnant dams with bromodeoxyuridine (BrdU) at E13.5 or E15.5 and calculated proliferation rates. Although there was a slight decrease of BrdU-positive cells in mutant hearts at E13.5, the difference only became significant at E15.5 (35%, $p = 0.001$) (Figure S1J), a time point that coincides with the appearance of the coronary arteries and veins. We next looked for evidence of hypoxia in mutant hearts by injecting pregnant dams with the hypoxia marker pimonidazole. Immunostaining on sections with an anti-pimonidazole antibody revealed a significant increase in hypoxic cells (45%, $p = 0.026$) in *Rspo3*-deficient hearts at E17.5. Increased apoptosis levels were also detected by active caspase-3 (59%, $p = 0.01$) and TUNEL staining (84%, $p = 0.03$) at this time point in mutant hearts (Figures S1K and S1L). Control embryos (*CAGGCre-ER^{TM}*-positive no *Rspo3^{fl}* allele) injected with tamoxifen showed no heart abnormalities (Figures S1A–S1C), demonstrating that the effects observed were specific to *Rspo3* deletion.

To exclude non-specific effects from other organs due to ubiquitous deletion of *Rspo3*, we analyzed mutant livers and placentas, two organs previously shown to directly affect heart development by controlling epicardial insulin-like growth factor 2 (*Igf2*) expression through erythropoetin (*Epo*) production and glucose/oxygen regulation, respectively (Shen et al., 2015). *Rspo3*-deficient placentas showed no obvious vascular abnormalities when deletion was performed at E11.5 (Figures S1D and S1E), and mutant livers did not display a significant decrease in *Epo* expression levels at all time points analyzed (Figure S1F). Furthermore, *Igf2* gene expression levels were not affected in mutant hearts (Figure S1G), thus demonstrating that the vascular abnormalities observed were not due to non-specific effects arising from ubiquitous deletion of *Rspo3*.

The Arterial Tree and Coronary Stems Are Malformed in Rspo3 Mutant Hearts

To visualize the extent of the coronary artery defect more clearly, we performed whole-mount immunohistochemistry on E17.5 hearts with the arterial-specific connexin 40 antibody and then scanned them with optical projection tomography (OPT). Strikingly, the left and right coronary arteries were almost completely absent in mutant hearts (Figure 2F; Movies S1 and S2). Quantification of the defect by serial counting revealed a significant decrease of coronaries in all compartments of the heart in *Rspo3* mutants, with the greatest decrease being detected in the left ventricle (75%, $p = 0.001$) (Figure 2G). We then examined sections where the coronary arteries establish a connection with the aorta, an area with particularly high levels of *Rspo3* expression. Immunostaining with antibodies against PECAM and the smooth muscle marker SM22α revealed that the proximal left and right coronaries of *Rspo3* mutants were largely absent from their stereotyped locations. In both cases, the coronary orifices formed normally, but were connected to smaller vessels arising from ectopic locations (interventricular septum for left coronary artery) (Figures 2H, S2A, and S2B). To determine the time window in which *Rspo3* promoted coronary development,

(F) OPT analysis of E17.5 hearts stained with a connexin 40 antibody clearly displays the absence of the left and right coronary arteries in *Rspo3* mutants. Scale bars, 200 μM.

(G) Quantification of coronary arteries on sections reveals a drastic reduction in the right and left ventricles, as well as the interventricular septum (n = 5, 2 litters). Columns are means ± SEM. RV = right ventricle, LV = left ventricle.

(H) Immunofluorescent staining with PECAM and the smooth muscle marker SM22α reveals defective formation of the proximal left and right coronary arteries (white arrows) in *Rspo3* mutants at E17.5. The right and left coronary orifices (asterisks) are formed, but are connected to immature vessels. Scale bars, 100 μM. LCA = left coronary artery, RCA = right coronary artery.

(I) Deletion of *Rspo3* at E12.5 leads to a decreased defect in coronary artery formation when compared to deletion at E11.5, while deletion at E13.5 results in no obvious coronary phenotype when compared to controls.

(J) Quantification of coronary arteries in mutants and controls at different deletion time points. Columns are means ± SEM (11 to 17: n = 5, 2 litters; 12 to 17: n = 3, 1 litter; and 13 to 17: n = 3, 1 litter). For all statistical analyses, two-tailed t test assuming unequal variances, $^{**}p < 0.01$, and $^{***}p < 0.001$. For additional information see Figures S1–S3.

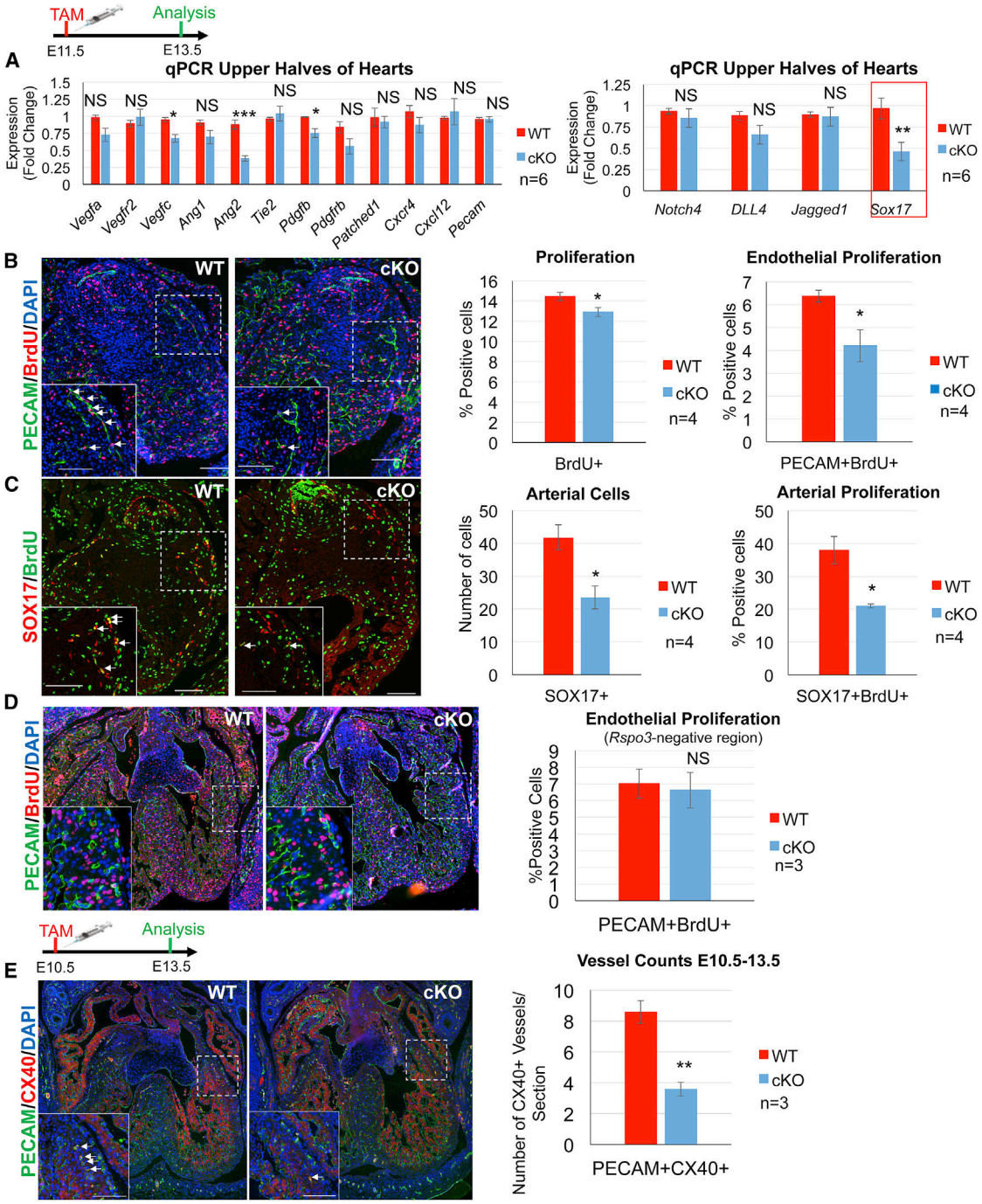

Figure 3. Endothelial Cell Proliferation Is Reduced in the Developing Coronaries of Rspo3 Mutant Hearts

(A) qPCR analysis of upper halves of *Rspo3*-deficient hearts at E13.5 reveals a significant downregulation of *Pdgfb*, *Vegfc*, Angiopoetin 2, and the arterial-specific transcription factor *Sox17*, when compared to WT hearts. Data are expressed as fold change versus controls and columns are means ± SEM (n = 6, 3 litters).

(B) BrdU labeling of Rspo3-deficient hearts reveals a significant reduction in endothelial (PECAM positive) proliferation on consecutive sections of the developing left coronary artery. Only a minor reduction in overall proliferation levels was detected (n = 4, 2 litters). Values were normalized on PECAM area measured (ImageJ) for the ventricular coronary vessels. Columns are means ± SEM.

(C) Immunostaining with an anti-SOX17 antibody reveals a large reduction in SOX17-positive cells around the developing left coronary artery. SOX17 cells also exhibit decreased proliferation rates in *Rspo3* mutants as evidenced by SOX17/BrdU co-immunostaining (n = 4, 2 litters). Columns are means ± SEM.

(legend continued on next page)

we performed deletions at later time points (E12.5 and E13.5). Although deletion at E12.5 still led to a decrease in the number (40%, p = 0.004) and size (Figure 2I, insets) of intra-myocardial arteries, the severity of the phenotype was decreased when compared to the deletion at E11.5 (70%, p = 0.0013) (Figure 2J). Deletion at E13.5 did not result in any apparent decrease in coronary arteries, altogether, suggesting that *Rspo3* promotes arterial formation during a very specific time period (E11–E13).

To better comprehend the underlying causes of the coronary artery phenotype, we extracted RNA from the upper halves of E13.5 hearts and analyzed gene expression levels by qPCR. From our analyses, we noticed a drastic reduction in the transcription factor *Sox17* (50%, p = 0.003) (Figure 3A). In a previous study, *Sox17* was shown to be specifically expressed in arteries during embryonic development and to promote arterial specification (Corada et al., 2013). *Sox17* was also shown to function upstream of Notch signaling, a pathway that is essential for arterial differentiation (Lawson et al., 2001). Surprisingly, no differences were observed in the Notch signaling pathway genes Notch4, *Dll4*, or Jagged1 (Figure 3A), suggesting the primary cause of the vascular phenotype to be unrelated to arterial-venous specification.

Interestingly, we did not observe any differences in the expression of *Vegfa*, a growth factor previously shown to be directly regulated by RSPO3 in the developing placenta. This was confirmed by immunostaining with an anti-VEGFA antibody on sections near the left coronary artery (Figure S3F).

To investigate putative proliferation defects in mutant hearts, we analyzed consecutive sections around the developing left coronary artery and observed decreased rates of endothelial proliferation (BrdU/PECAM-positive cells) in *Rspo3* mutants (35%, p = 0.045) (Figure 3B). Interestingly, total cell proliferation showed only a minor decrease (11%, p = 0.045), suggesting a specific paracrine effect of *Rspo3* on the endothelial cells of the developing coronaries. A paracrine action of RSPO3 has been reported previously in the liver (Rocha et al., 2015) and adrenal gland (Vidal et al., 2016).

We next examined SOX17 expression by immunostaining and noticed a reduction in both the number of SOX17-positive cells (44%, p = 0.049), as well as in the proliferation rates of these cells (45%, p = 0.048) (Figure 3C). SOX17 expression levels in individual cells remained high in *Rspo3* mutants, indicating a reduction in the number of SOX17-positive cells, rather than decreased expression in individual cells. Furthermore, ectopic expression of the venous transcription factor COUPTFII was not detected in the endothelium of *Rspo3*-deficient arteries, suggesting arterial differentiation was unaffected in mutant hearts (Figure S3C).

To determine if vascular defects could be detected at earlier time points, we performed a deletion of *Rspo3* at E10.5 and analyzed the hearts at E13.5. Serial counting revealed a drastic decrease of connexin 40/PECAM-positive intra-myocardial vessels in *Rspo3* mutants, suggesting RSPO3 has an early effect on the vascularization of the heart (Figure 3E). To look for putative smooth muscle abnormalities, we performed co-staining with PECAM and SM22α antibodies on sections around the developing left coronary artery. Overall, SM22α-positive cells were detected at normal levels and were able to envelop the developing vasculature, suggesting the effects of *Rspo3* deletion to be unrelated to smooth muscle defects (Figure S3D).

RSPO3 Promotes Coronary Artery Formation through Wnt/β-Catenin Signaling

A recent publication described an important role for *Rspo3* in vascular stability of the postnatal retina and lungs by activating the WNT/calcium pathway through suppression of the ubiquitin ligases *Rnf213*, *Trim30*α, and *Usp18*, factors that induce degradation of the WNT/calcium effector nuclear factor of activated T cells 1 (NFAT1) (Scholz et al., 2016). In this paper, endothelial-specific deletion of *Rspo3* led to increased endothelial apoptosis and vascular pruning. In addition, an essential role for NFAT signaling in coronary plexus formation has been previously shown (Zeini et al., 2009). Here, the authors demonstrated that NFAT/calcineurin signaling promoted initial tube formation in the primitive plexus, and that *Nfatc3* and *Nfatc4*, but not *Nfatc1* or *Nfatc2*, were expressed in the coronary vasculature. To investigate whether RSPO3 was acting through the NFAT/calcineurin pathway in coronary artery development, we analyzed the expression of NFAT1 and its target genes in the developing heart. In accordance with Zeini et al. (2009), no coronary-specific expression of NFAT1 could be detected by immunostaining (Figure S4A). In addition, through in situ hybridization analyses, we did not observe any upregulation of the main NFAT1 target *Rnf213* around the coronaries in *Rspo3* mutant hearts (Figure S4B). Furthermore, immunostaining with an anti-active caspase-3 antibody on sections around the developing left coronary did not reveal a significant difference in endothelial apoptosis in *Rspo3* mutants (p = 0.61) (Figures S4E and S4F). Next, we looked for differences in NFATc3 levels in Rspo3 mutant hearts. Although we could detect endothelial-specific expression of NFATc3 in the developing coronaries, we did not observe any differences between control and mutant hearts (Figures S4C and S4D). Overall, this data suggest that RSPO3 acts via an NFAT-independent pathway in coronary development.

To determine if RSPO3 was activating canonical Wnt/*β-catenin* signaling in the developing coronaries, we investigated the expression of the β-catenin target *Axin2*. qPCR analysis of RNA extracted from the upper halves of mutant hearts revealed a 50% (p = 0.004) reduction in expression levels when compared to controls (Figure 4A). We then analyzed active β-catenin (ABC) levels by performing an immunoblot on protein lysates from the upper halves of mutant hearts with an antibody specific to dephosphorylated β-catenin. A 50% (p = 0.049) reduction in ABC

(D) Endothelial proliferation in *Rspo3* mutants is not reduced in sections of the heart where *Rspo3* is not expressed, as shown by co-immunostaining with anti-PECAM and BrdU antibodies (n = 3, 1 litter). Values were normalized on PECAM area measured (ImageJ) for the ventricular coronary vessels. Columns are means ± SEM. Two-tailed Student's t test assuming unequal variances, *p < 0.05, **p < 0.01, and ***p < 0.001.

(E) Deletion of *Rspo3* at E10.5 followed by analysis at E13.5 reveals a reduction in the amount of CX40/PECAM-positive intra-myocardial vessels (white arrows) in mutant hearts. Columns are means ± SEM. All scale bars in this figure represent 100 μM. For all statistical analyses, two-tailed t test assuming unequal variances, *p < 0.05, **p < 0.01, and ***p < 0.001. For additional information see Figure S4.

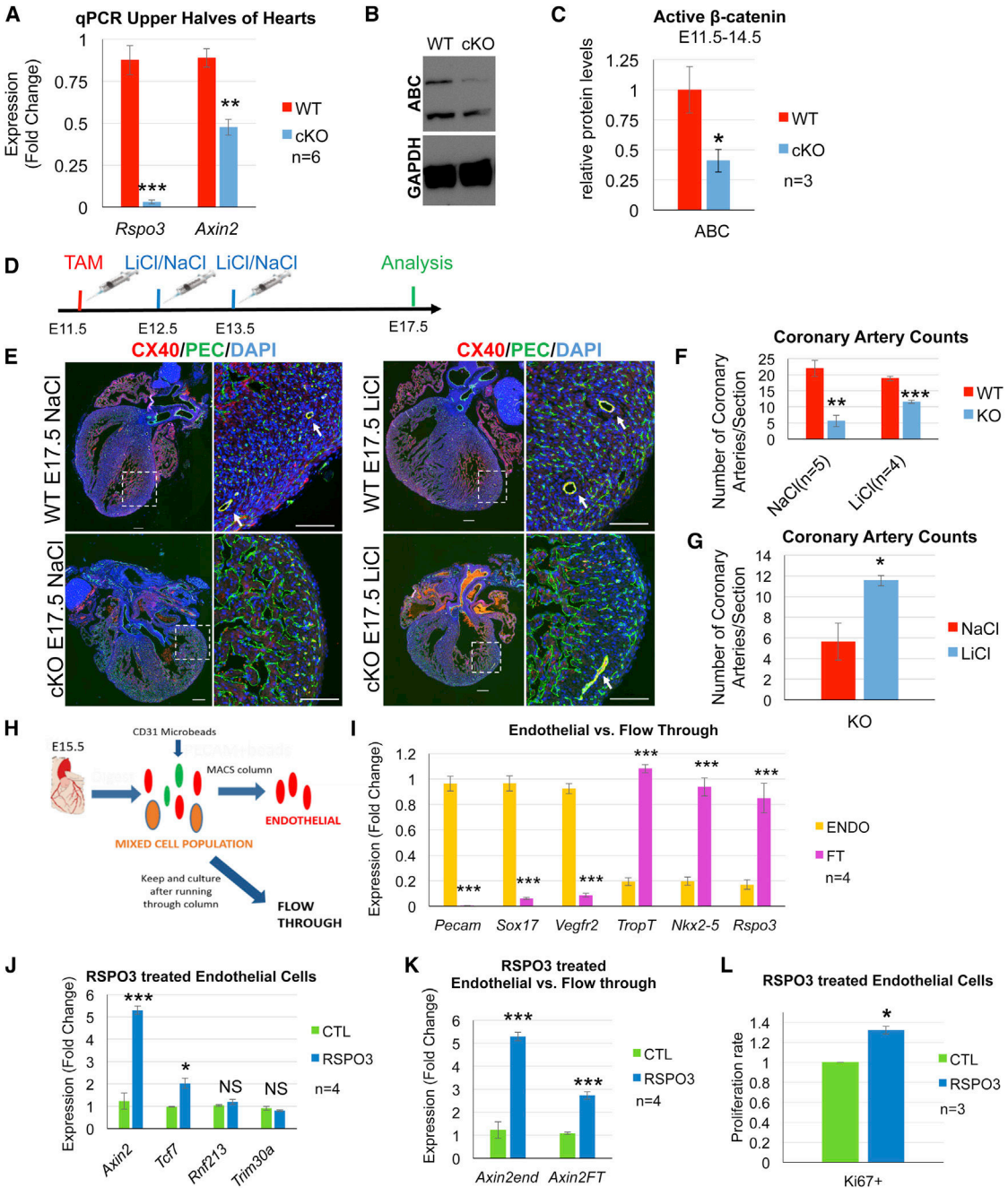

Figure 4. RSPO3 Acts through the Wnt/β-Catenin Signaling Pathway to Promote Coronary Artery Formation

(A) qPCR analysis of RNA extracted from the upper halves of *Rspo3*-deficient hearts at E13.5 reveals a significant downregulation of the canonical β-catenin target *Axin2* when compared to controls. Data are expressed as fold change versus controls and columns are means ± SEM (n = 6, 3 litters).

(B) Active β-catenin (ABC) levels are reduced in the upper halves of mutant hearts, as demonstrated by immuno-blotting with an antibody specific to dephosphorylated β-catenin.

(C) Quantification of protein levels was performed using ImageJ software (n = 3, 1 litter). Data are expressed as fold change versus controls and columns are means ± SEM.

(D) Schematic of recovery experiments showing administration of 100 mg/kg lithium chloride (LiCl), a GSK3β inhibitor, or sodium chloride (NaCl), as a control, to pregnant dams at E12.5 and E13.5.

(E) LiCl administration increased coronary artery number (white arrows) in *Rspo3* mutants when compared to NaCl controls. Scale bars, 100 μM.

(F) Quantification of coronary arteries in the ventricles of *Rspo3* cKOs demonstrates that LiCl-treated hearts have decreased coronary defects when compared to NaCl controls (NaCl n = 5, 3 litters; LiCl n = 4, 2 litters). Columns are mean ± SEM.

(legend continued on next page)

protein levels was detected in mutant hearts (Figures 4B and 4C). Finally, to determine if the coronary artery phenotype observed in *Rspo3* mutants could be recovered by pharmacological β-catenin activation, we injected pregnant dams with the glycogen synthase kinase 3 beta (GSK3β) inhibitor lithium chloride (LiCl) at E12.5 and E13.5 (Figure 2I). Strikingly, LiCl administration led to a drastic recovery in the number of coronary arteries when compared to mutants injected with sodium chloride, further demonstrating that *Rspo3* is acting through canonical WNT/β-catenin signaling on the developing coronaries (Figures 4D–4G).

We next wanted to know whether RSPO3 could directly activate β-catenin signaling in the endothelial cell compartment of the heart. To address this question, we isolated primary endothelial cells from embryonic hearts at E15.5 (Figure 4H, schematic). qPCR analysis revealed that the purified fraction was highly enriched in endothelial-specific genes (*Pecam*, *Vegfr2*, and *Sox17)* and expressed significantly lower levels of cardiomyocyte genes (*Nkx2–5* and *TroponinT*, *TropT*) when compared to the non-bound, flow through (FT) cells. Analysis of *Rspo3* expression levels showed very low expression in the endothelial compartment compared to the FT (Figure 4I). Interestingly, qPCR analysis revealed that *Wnt8a* expression, a known activator of β-catenin signaling, was highly enriched in isolated endothelial cells (Figure S4I). Treatment of isolated cells with recombinant RSPO3 protein caused a significant upregulation of *Axin2* (5-fold, p = 0.0003) and *Tcf7* (2-fold, p = 0.0189), another canonical *β-catenin* target previously shown to be upregulated in adult brain endothelial cells by treatment with the GSK3β inhibitor bromoindirubinoxime (BIO) (Aisagbonhi et al., 2011). Expression levels of the NFAT targets *Rnf213* and Trim30α were not significantly altered in treated cells (Figure 4J). EphrinB2 (arterial marker) and EphrinB4 (venous marker) expression levels were also not significantly altered (Figure S3E). To ensure that the effects on the canonical Wnt pathway were specific to the endothelial cells in culture, we also treated non-bound (flow through) cells from the isolation with recombinant RSPO3. The increase in *Axin2* expression observed in the endothelial cells was greater than that observed in the FT cells, indicating the upregulation in *β-catenin* signaling to be independent from contaminating cardiomyocytes or other cell types in the cultures (Figure 4K). Next, to see if RSPO3 could promote proliferation in our endothelial cell cultures, we isolated and grew them on coverslips and then performed immunostaining with a Ki67 antibody. As expected, RSPO3-treated cells showed significantly higher levels of proliferation when compared to controls (Figure 4L).

Apart from proliferation, *Rspo3* has also been shown to promote tube formation in cultured human umbilical vein endothelial cells (HUVECs), and it is likely that *Rspo3* may play a similar role in the developing coronaries. It is also possible that *Rspo3* may play a role in guiding the migration of endothelial cells toward the coronary orifices. Further work is needed to clarify these hypotheses.

In conclusion, our study has provided mechanistic insights into how localized activation of β-catenin through Rspo3 expression induces formation of the proximal coronary arteries. This information may in the long run prove invaluable to regenerative medicine therapies aimed at treating coronary heart disease.

EXPERIMENTAL PROCEDURES

Mice

All animal work was conducted according to national and international guidelines and was approved by the local ethics committee (PEA-NCE/2013/88). The *Rspo3^{flox}*, *mTmG*, and *CAGGCre-ER^{TM}* lines have been described previously (Rocha et al., 2015; Muzumdar et al., 2007; Hayashi and McMahon, 2002). Cre activation was obtained by a single administration (gavage) of 200 mg/kg tamoxifen (Sigma-Aldrich) dissolved in corn oil (Sigma-Aldrich) to pregnant females aged around 8 weeks carrying E11.5 embryos. Embryos were analyzed at various time points (E13.5, E15.5, and E17.5) and gender was not taken into consideration. For in vivo pharmacological rescues, pregnant mice were injected intraperitoneally (i.p.) with 100 mg/kg LiCl once a day at the indicated times.

In Situ Hybridization

Tissues were fixed overnight in 4% paraformaldehyde, progressively dehydrated, and embedded in paraffin. 7 μm thick sections were cut then rehydrated, and hybridization was performed as described in Wilkinson, (1992). Hybridized digoxigenin (DIG)-RNA probes were detected with alkaline phosphatase-coupled anti-digoxygenin antibody (1:4,000, Roche). After washing, the chromogenic reaction was performed with nitro blue tetrazolium bromo-chloro-indolyl-phosphate (NBT-BCIP) substrate (Promega) for several days at room temperature. The protocol for whole-mount in situ hybridization is described in the Supplemental Experimental Procedures.

Immunofluorescence and Histological Analysis

For immunofluorescence experiments, tissues were fixed overnight in 4% paraformaldehyde, progressively dehydrated, and embedded in paraffin. 5 μm thick sections were rehydrated, boiled in a pressure cooker for 2 min with antigen unmasking solution (Vector Labs), and blocked in PBS solution containing 10% normal donkey serum and 3% BSA. All antibodies were applied overnight at 4°C at the concentrations listed in the antibody table (see Table S1). Secondary antibodies were diluted 1:400 and applied at

(G) LiCl-treated cKO hearts have significantly more coronary arteries when compared t NaCl controls. Columns are mean ± SEM. Two-tailed Student's t test assuming unequal variances, *p < 0.05, **p < 0.01, and ***p < 0.001.

(H) Schematic demonstrating the strategy used to isolate endothelial cells from E15.5 hearts using magnetic microbeads coupled to CD31 antibody.

(I) Isolated cells are enriched in endothelial-specific genes (*Pecam*, *Sox17*, and *Vegfr2*) and express much lower levels of cardiomyocyte-specific genes (*Nkx2-5* and TroponinT, *TropT*) when compared to non-bound, FT cells. *Rspo3* is much more highly expressed in the FT than the isolated endothelial cells. Data are expressed as fold change versus controls and columns are means ± SEM (n = 4, 2 experiments).

(J) Treatment of endothelial cells with RSPO3 (200 ng/mL) induced *Axin2* (5-fold upregulation, p = 0.0003) and *Tcf7* (2-fold upregulation, p = 0.0182) expression. Expression of the RSPO3/NFAT targets *Rnf213* and *Trim30α* were not significantly altered. Data are expressed as fold change versus controls and columns are means ± SEM (n = 4, 2 experiments).

(K) Treatment of non-bound cells (FT) shows significant upregulation of *Axin2* expression, however, higher upregulation is observed in treated endothelial cells. Data are expressed as fold change versus controls and columns are means ± SEM (n = 4, 2 experiments).

(L) Culturing of endothelial cells on coverslips followed by immunostaining with KI67 antibody demonstrates increased proliferation in RSPO3-treated (200 ng/mL) endothelial cells. Proliferation rates of non-treated endothelial cells were considered as 1 for each individual experiment. Columns are means ± SEM (n = 3, 3 experiments). For all statistical analyses, two-tailed t test assuming unequal variances, *p < 0.05, **p < 0.01, and ***p < 0.001. For additional information see Figure S4.

room temperature for 1 hr. For histological analysis, 5 μm thick sections were stained with H&E, according to standard procedures.

OPT

For OPT, embryos were dissected at E17.5, fixed, and stained with the connexin 40 antibody, as described in Supplemental Experimental Procedures. Processing and OPT were performed as described elsewhere (Sharpe et al., 2002) using a Bioptonics 3001 system (Bioptonics, Edinburgh, UK). Tissue autofluorescence was used to visualize anatomical structures.

Isolation and Treatment of Primary Endothelial Cells from Embryonic Hearts

Whole hearts from E15.5 embryos were dissected, minced, pooled together, and digested with 1 mg/mL collagenase (Worthington Biochem) for 30 min at 37°C. The cell suspension was then washed with DMEM (Gibco), supplemented with 10% fetal bovine serum (FBS) (Gibco), and incubated for 15 min at 4°C with magnetic CD31 microbeads (Miltenyi) in PBS supplemented with 2% FBS and 2 mM EDTA (running buffer). Cells were then washed once with running buffer before being passed through an MS column (Miltenyi) attached to a magnet. After three washes with running buffer, cells were passed through an additional column, washed 3×, and then eluted. The eluted cells were then washed with DMEM + 10% FBS, spun down, and the final pellet resuspended in endothelial cell growth medium (DMEM + 20% FBS + 100 μg/mL endothelial cell growth supplement [ECGS], Sigma-Aldrich). Cells were grown until confluence, after which the media was switched to DMEM + 4% FBS. Cells were then treated with 200 ng/mL recombinant RSPO3 (R&D) for 48 hr. RNA was extracted using the RNeasy Micro Kit (QIAGEN) according to the manufacturer's protocol, and gene expression levels were analyzed by qRT-PCR, as described below. For proliferation assays, cells were isolated then cultured on coverslips coated with 0.1% gelatin in 96-well plates. Cells were grown until 50% confluence then the media switched to DMEM + 4% FBS. Cells were then treated with 200 ng/mL RSPO3 for 24 hr. Following treatment, cells were fixed for 15 min in 100% methanol on ice and stained with an anti-Ki67 antibody, as described in the Immunofluorescence and Histological Analysis section.

Statistical Analyses

Statistical analyses were performed according to the two-tailed unpaired Student's t test, *$p < 0.05$, **$p < 0.01$, and ***$p < 0.001$. Error estimates are expressed as either SD or SEM. Details of the statistical analyses and the programs used for quantification can be found in the figure legends. The letter "n" refers to the number of individual samples/hearts (embryonic dissections) or the number of wells (in vitro experiments).

SUPPLEMENTAL INFORMATION

Supplemental Information includes Supplemental Experimental Procedures, four figures, two tables, and two movies and can be found with this article online at http://dx.doi.org/10.1016/j.celrep.2017.08.004.

AUTHOR CONTRIBUTIONS

F.D.S. and A.S. designed the project. F.D.S. carried out all experiments, if not otherwise stated. H.M. performed the OPT analysis. C.B., F.M., and F.J.M. provided technical support with various experiments. K.D.W. and A.S.R. provided critical input for experimental design and data analysis. F.D.S. and A.S. wrote the manuscript, and all authors provided editorial input.

ACKNOWLEDGMENTS

We would like to thank the staff of the animal facility for their dedication and Agnès Loubat (Cytometrie platform) for her expertise in cell sorting. We are indebted to Hitoshi Okamoto (Riken Institute, Japan) for providing the *Rspo3*^{fl} allele. This work was supported by grants from the Fondation du France (201200029515 and 00056856), ARC (SL22020605297), and the ANR (ANR-ADSTEM and ANR-11-LABX-0028-01).

Received: April 18, 2017
Revised: June 20, 2017
Accepted: July 27, 2017
Published: August 22, 2017

REFERENCES

Aisagbonhi, O., Rai, M., Ryzhov, S., Atria, N., Feoktistov, I., and Hatzopoulos, A.K. (2011). Experimental myocardial infarction triggers canonical Wnt signaling and endothelial-to-mesenchymal transition. Dis. Model. Mech. *4*, 469–483.

Cambier, L., Plate, M., Sucov, H.M., and Pashmforoush, M. (2014). Nkx2-5 regulates cardiac growth through modulation of Wnt signaling by R-spondin3. Development *141*, 2959–2971.

Cano, E., Carmona, R., Ruiz-Villalba, A., Rojas, A., Chau, Y.Y., Wagner, K.D., Wagner, N., Hastie, N.D., Muñoz-Chápuli, R., and Pérez-Pomares, J.M. (2016). Extracardiac septum transversum/proepicardial endothelial cells pattern embryonic coronary arterio-venous connections. Proc. Natl. Acad. Sci. USA *113*, 656–661.

Corada, M., Orsenigo, F., Morini, M.F., Pitulescu, M.E., Bhat, G., Nyqvist, D., Breviario, F., Conti, V., Briot, A., Iruela-Arispe, M.L., et al. (2013). Sox17 is indispensable for acquisition and maintenance of arterial identity. Nat. Commun. *4*, 2609.

de Lau, W.B., Snel, B., and Clevers, H.C. (2012). The R-spondin protein family. Genome Biol. *13*, 242.

Hayashi, S., and McMahon, A.P. (2002). Efficient recombination in diverse tissues by a tamoxifen-inducible form of Cre: a tool for temporally regulated gene activation/inactivation in the mouse. Dev. Biol. *244*, 305–318.

Ivins, S., Chappell, J., Vernay, B., Suntharalingham, J., Martineau, A., Mohun, T.J., and Scambler, P.J. (2015). The CXCL12/CXCR4 axis plays a critical role in coronary artery development. Dev. Cell *33*, 455–468.

Katz, T.C., Singh, M.K., Degenhardt, K., Rivera-Feliciano, J., Johnson, R.L., Epstein, J.A., and Tabin, C.J. (2012). Distinct compartments of the proepicardial organ give rise to coronary vascular endothelial cells. Dev. Cell *22*, 639–650.

Kazanskaya, O., Ohkawara, B., Heroult, M., Wu, W., Maltry, N., Augustin, H.G., and Niehrs, C. (2008). The Wnt signaling regulator R-spondin 3 promotes angioblast and vascular development. Development *135*, 3655–3664.

Lawson, N.D., Scheer, N., Pham, V.N., Kim, C.H., Chitnis, A.B., Campos-Ortega, J.A., and Weinstein, B.M. (2001). Notch signaling is required for arterial-venous differentiation during embryonic vascular development. Development *128*, 3675–3683.

Muzumdar, M.D., Tasic, B., Miyamichi, K., Li, L., and Luo, L. (2007). A global double-fluorescent Cre reporter mouse. Genesis *45*, 593–605.

Red-Horse, K., Ueno, H., Weissman, I.L., and Krasnow, M.A. (2010). Coronary arteries form by developmental reprogramming of venous cells. Nature *464*, 549–553.

Riley, P.R., and Smart, N. (2011). Vascularizing the heart. Cardiovasc. Res. *91*, 260–268.

Rocha, A.S., Vidal, V., Mertz, M., Kendall, T.J., Charlet, A., Okamoto, H., and Schedl, A. (2015). The angiocrine factor Rspondin3 is a key determinant of liver zonation. Cell Rep. *13*, 1757–1764.

Scholz, B., Korn, C., Wojtarowicz, J., Mogler, C., Augustin, I., Boutros, M., Niehrs, C., and Augustin, H.G. (2016). Endothelial RSPO3 controls vascular stability and pruning through non-canonical WNT/Ca(2+)/NFAT signaling. Dev. Cell *36*, 79–93.

Sharpe, J., Ahlgren, U., Perry, P., Hill, B., Ross, A., Hecksher-Sørensen, J., Baldock, R., and Davidson, D. (2002). Optical projection tomography as a tool for 3D microscopy and gene expression studies. Science *296*, 541–545.

Shen, H., Cavallero, S., Estrada, K.D., Sandovici, I., Kumar, S.R., Makita, T., Lien, C.L., Constancia, M., and Sucov, H.M. (2015). Extracardiac control of embryonic cardiomyocyte proliferation and ventricular wall expansion. Cardiovasc. Res. *105*, 271–278.

Vidal, V., Sacco, S., Rocha, A.S., da Silva, F., Panzolini, C., Dumontet, T., Doan, T.M., Shan, J., Rak-Raszewska, A., Bird, T., et al. (2016). The adrenal capsule is a signaling center controlling cell renewal and zonation through *Rspo3*. Genes Dev. *30*, 1389–1394.

Wilkinson, D.G. (1992). Whole mount *in situ* hybridisation of vertebrate embryos. In *In Situ* Hybridization, D.G. Wilkinson, ed. (Oxford: Oxford University Press), pp. 75–83.

Wu, B., Zhang, Z., Lui, W., Chen, X., Wang, Y., Chamberlain, A.A., Moreno-Rodriguez, R.A., Markwald, R.R., O'Rourke, B.P., Sharp, D.J., et al. (2012). Endocardial cells form the coronary arteries by angiogenesis through myocardial-endocardial VEGF signaling. Cell *151*, 1083–1096.

Zeini, M., Hang, C.T., Lehrer-Graiwer, J., Dao, T., Zhou, B., and Chang, C.P. (2009). Spatial and temporal regulation of coronary vessel formation by calcineurin-NFAT signaling. Development *136*, 3335–3345.

Cell Reports, Volume *20*

Supplemental Information

Coronary Artery Formation Is Driven by Localized Expression of R-spondin3

Fabio Da Silva, Ana Sofia Rocha, Fariba Jian Motamedi, Filippo Massa, Cem Basboga, Harris Morrison, Kay Dietrich Wagner, and Andreas Schedl

SUPPLEMENTAL INFORMATION INVENTORY

Figure S1, related to Figure 2: *Ubiquitous deletion of Rspo3 at E11.5 does not indirectly affect coronary artery formation and Rspo3-deficient hearts are hypoplastic.* This figure examines the effects of *CAGGCre-ER*^{TM} activation in the absence of an *Rspo3* floxed allele as well as the effects of deleting *Rspo3* in the placenta and liver. It also demonstrates that *Rspo3*-deficient hearts are hypoplastic and exhibit increased levels of hypoxia and apoptosis.

Figure S2, related to Figure 2: *Development of the proximal left and right coronary arteries is severely impaired in Rspo3 mutants.* This figure provides more detail on the defective formation of the coronary stems observed in *Rspo3* mutant hearts.

Figure S3, related to Figures 2 and 3: *Coronary veins develop normally, arterial specification is not impaired and Vegfa expression is unchanged in Rspo3 mutant hearts.* This figure looks at coronary vein formation, arterial specification and VEGFA expression in *Rspo3* mutant hearts.

Figure S4, Related to Figure 4: *Rspo3 does not signal via the Wnt/Calcium pathway in coronary artery formation and various canonical and non-canonical Wnt ligands are expressed in the heart and coronary vasculature.* This figure looks at the effects of *Rspo3* deletion on the NFAT/Wnt-calcium pathway in the developing coronaries. It also analyzes the expression of several Wnt ligands in E13.5 hearts and isolated endothelial cells.

Antibodies table: List of antibodies used in this study.

Primers table: Complete list of primers used for qPCR analysis in this study.

Supplemental Methods: Description of supplementary experimental procedures not included in the main text.

Supplemental Videos: Optical Projection Tomography (OPT) videos of wholemount wildtype and Rspo3-mutant hearts immunostained with the connexin40 antibody.

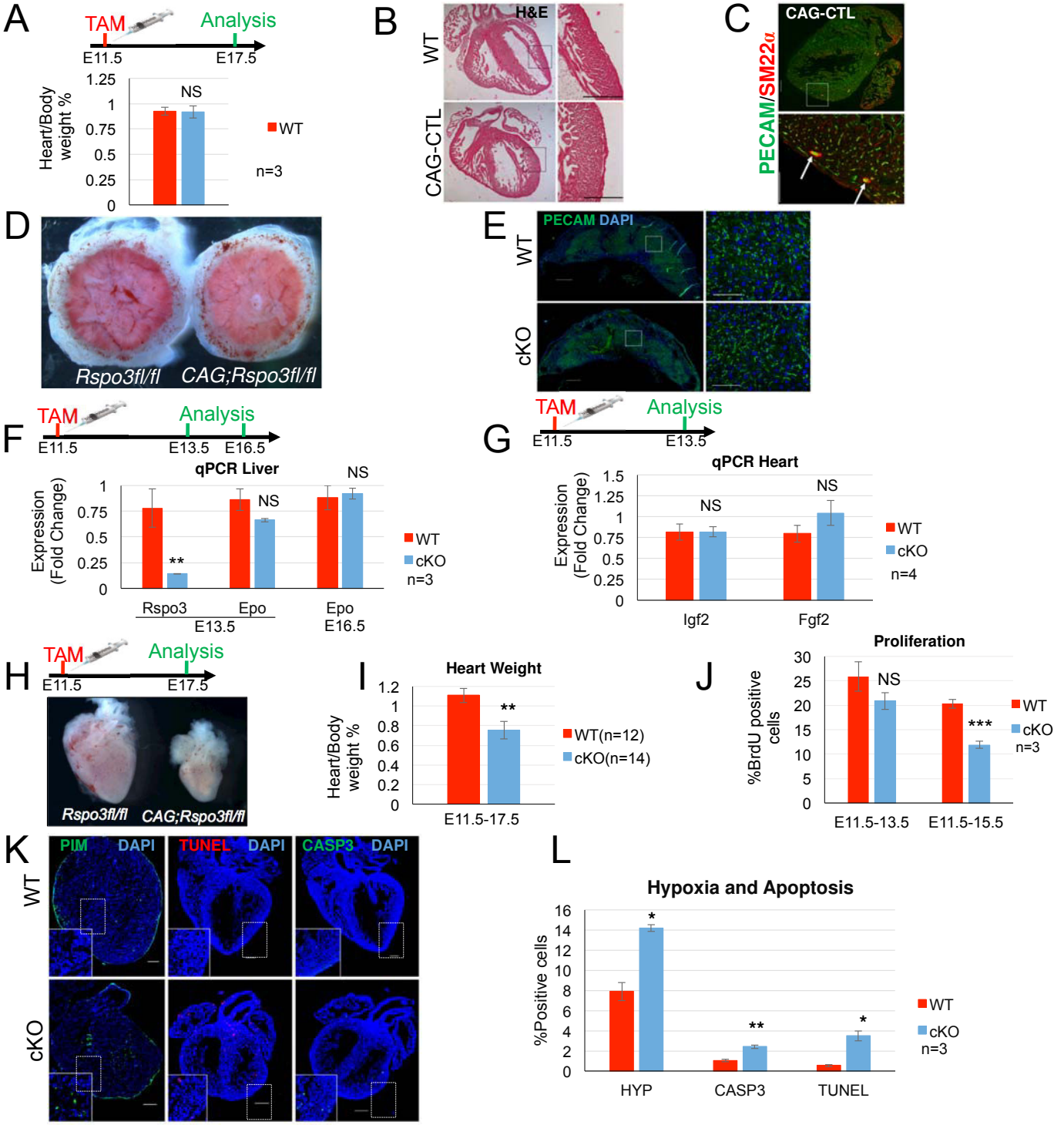

Figure S1, related to Figure 2: *Ubiquitous deletion of Rspo3 at E11.5 does not indirectly affect coronary artery formation and Rspo3-deficient hearts are hypoplastic.* (A-C) *CAGGCre-ER*^{TM} recombinase activation in the absence of an *Rspo3* floxed allele does not affect heart weight (A) or myocardial compaction as shown by HE staining (B). It also does not affect coronary artery formation (white arrows) as shown by PECAM/SM22α immunostaining (C). (D) *Rspo3* mutant placentas appear normal when analyzed 6 days after deletion. (E) Vascularization of the placenta is not impaired in *Rspo3*-mutants as demonstrated by PECAM staining (3 placentas analyzed). All scale bars 200μM. (F) Erythropoetin (*Epo*) expression is not significantly changed in livers of *Rspo3* mutants at all time-points analyzed (n=3, 1 litter). Data are expressed as fold change vs. controls and columns are means ± SEM. (G) *Igf2* and *Fgf2* expression in the heart are not significantly altered in *Rspo3* mutants at E13.5 (n=4, 2 litters). Data are expressed as fold change vs. controls and columns are means ± SEM. (H-I) *Rspo3*-deficient hearts are hypoplastic when analyzed 6 days after deletion. Columns are means ± SEM. (J) Labeling of hearts with BrdU demonstrates a decrease in proliferation in *Rspo3* mutants that is significant at E15.5 (n=3, 1 litter). Columns are means ± SEM. (K) Injection of the hypoxia marker Pimonidazole (PIM) followed by immunostaining with a Pimonidazole-specific antibody reveals an increase in hypoxic cells in *Rspo3* mutants at E17.5. Tunel and active caspase 3 (CASP3) staining reveal an increase in apoptosis in mutant hearts. (L) Quantification of hypoxia (HYP) and apoptosis (CASP3 and TUNEL). Columns are means ± SEM (n=3, 1 litter). All scale bars 200μM. For all statistical analyses two-tailed t-test assuming unequal variances, *p<0.05, **p<0.01, ***p<0.001.

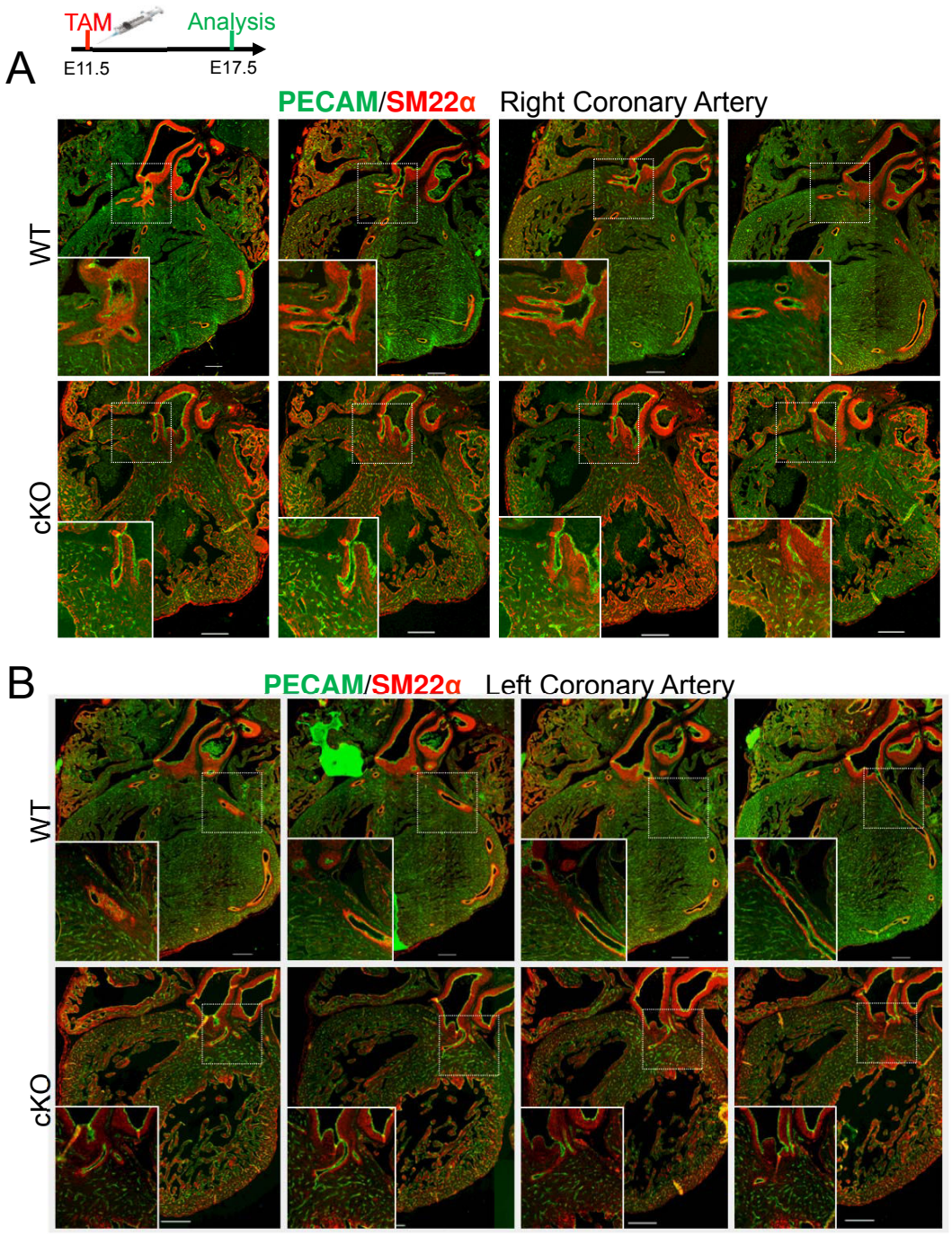

Figure S2, related to Figure 2: *Development of the proximal left and right coronary arteries is severely impaired in Rspo3 mutants.*
(A,B) Consecutive sections stained with the endothelial marker PECAM and the smooth muscle marker SM22α demonstrates defective development of the proximal right (A) and left (B) coronary arteries in *Rspo3*-deficient hearts. In both cases the coronary orifices are formed but are connected to smaller vessels arising from the interventricular septum. All scale bars 200 μM.

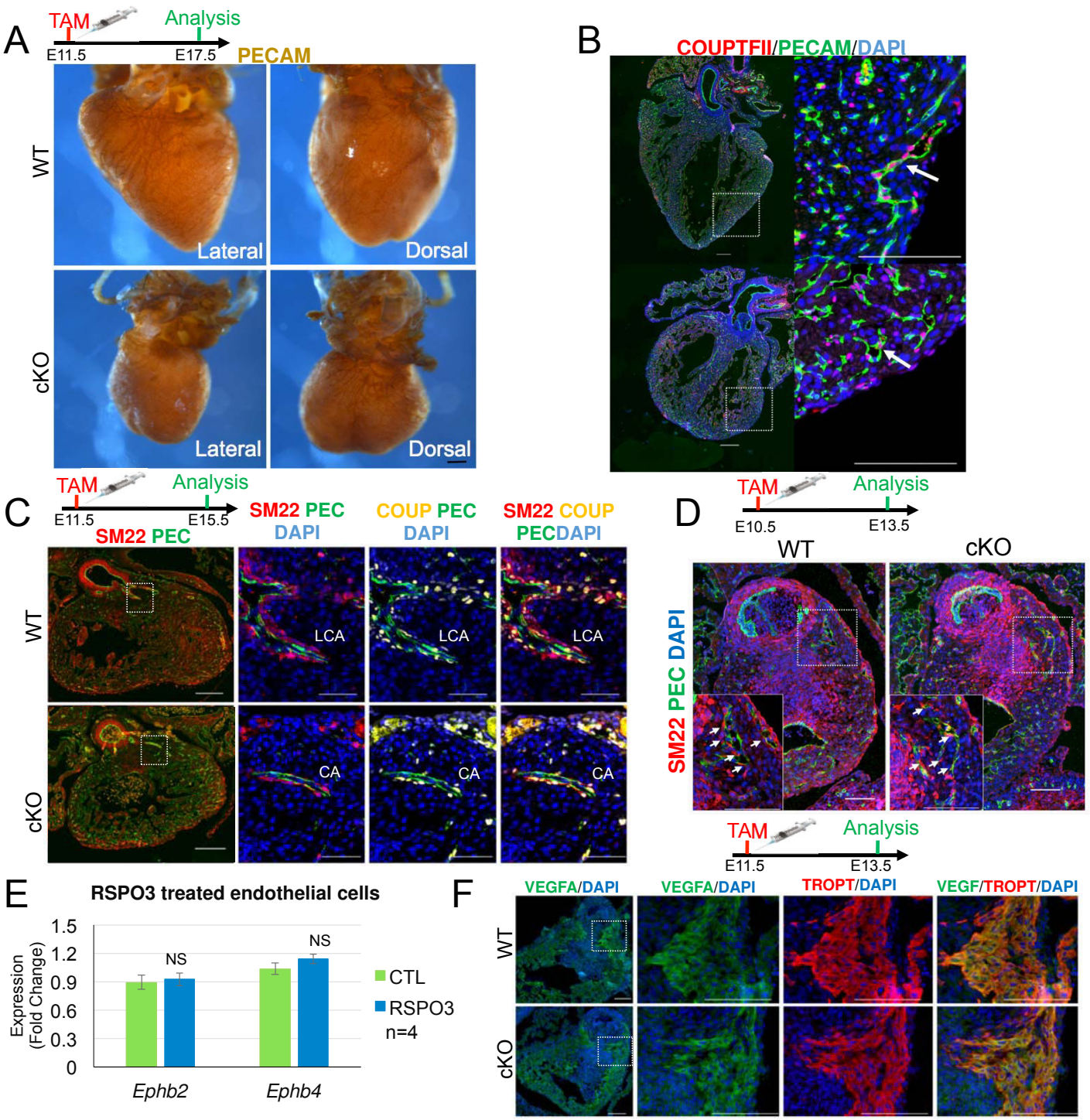

Figure S3, related to Figures 2 and 3: *Coronary veins develop normally, arterial specification is not impaired and Vegfa expression is unchanged in Rspo3 mutant hearts.* (A) Wholemount immunostaining with the endothelial-specific PECAM antibody reveals a drastic decrease in large diameter vessels on the lateral surface of *Rspo3* mutant hearts where coronary arteries are normally present. Large vessels representing the coronary veins were detected on the dorsal side of hearts and appear to be properly connected to the sinus venosus. Notice the presence of a mature venous tree in mutant hearts. (B) Co-immunostaining with PECAM and the venous-specific transcription factor COUPTFII reveals that vessels with venous identity (white arrows) form correctly in *Rspo3* mutants. Scale bars: wholemounts 0.5mm, mosaics 200 μM, close ups 100μM. (C) Co-immunostaining with PECAM (PEC) and SM22α (SM22) shows that the small arteries occasionally formed near the outflow tract in *Rspo3* mutants are able to recruit smooth muscle at E15.5. The endothelial cells (PECAM-positive) of these arteries do not ectopically express the venous marker COUPTFII indicating that their arterial identity is not lost. Normal COUPTFII expression in the smooth muscle (SM22 positive) of the arteries is found in *Rspo3* mutants. LCA=Left Coronary Artery, CA=Coronary Artery. Scale bars: mosaics 200μM, close ups 100μM. (D) Deletion of *Rspo3* at E10.5 followed by analysis at E13.5 reveals no obvious differences in smooth muscle (white arrows) recruitment to the developing coronaries in mutant hearts as demonstrated by PECAM/SM22α co-immunostaining. (E) Treatment of primary endothelial cells isolated from embryonic hearts with recombinant RSPO3 protein does not lead to significant changes in the arterial specific marker EphrinB2 nor the venous-specific marker EphrinB4. Data are expressed as fold change vs. controls and columns are means ± SEM (n=4, 2 experiments). (F) Immunofluorescence staining with an anti VEGF antibody shows no differences in VEGF expression between control and mutant hearts in the cardiomyocytes (TROPONINT (TROPT) positive) near the aorta which normally express high levels of *Rspo3*. Scale bars 100μM.

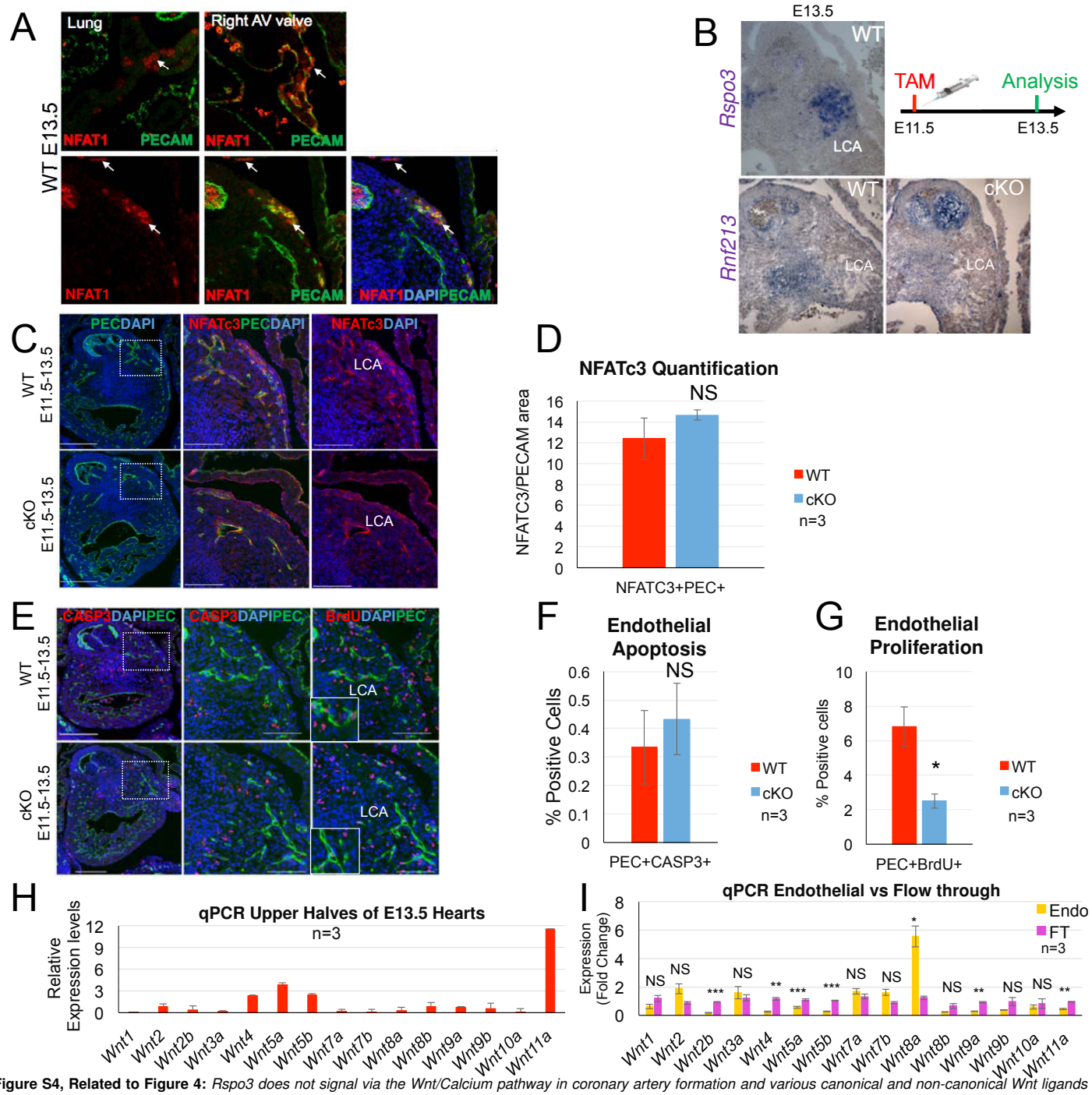

Figure S4, Related to Figure 4: *Rspo3 does not signal via the Wnt/Calcium pathway in coronary artery formation and various canonical and non-canonical Wnt ligands are expressed in the heart and coronary vasculature.*

(A) Immunostaining with an NFAT1 antibody shows specific staining (white arrows) in lung epithelia and endocardial cells (PECAM positive) of the right atrioventricular (AV) valve in E13.5 embryos. NFAT1 is not detected in the developing coronary arteries in E13.5 hearts. (B) *In situ* hybridization analysis of *Rspo3* and the ubiquitin ligase RNF213 reveals no increase in expression of *Rnf213* around the developing coronary arteries where *Rspo3* is highly expressed (3 hearts analyzed). LCA=Left Coronary Artery. (C) Co-immunostaining with NFATc3 and PECAM antibodies shows no obvious differences of NFATc3 protein levels in Rspo3 mutant endothelial cells when compared to controls. Scale bars: mosaics 200μM, close ups 100μM. (D) Quantification of NFATc3 protein levels in endothelial cells shows no significant differences between *Rspo3* mutants and controls. Values were normalized on PECAM (PEC) area measured for the ventricular coronary vessels (n=3, 1 litter). Columns are means ± SEM. (E) Active caspase 3 (CASP3) staining on mutant hearts reveals very few endothelial cells are apoptotic around the developing left coronary in mutant hearts at E13.5. PECAM/BrdU co-immunostaining shows a decrease in endothelial proliferation in Rspo3 mutants in the same hearts. Scale bars: mosaics 200μM, close ups 100μM. (F) Quantification of endothelial apoptosis reveals no significant differences between wildtype and mutant hearts. Quantification of endothelial proliferation rates of the same hearts reveals a significant reduction in mutant hearts. Values were normalized on PECAM area measured for the ventricular coronary vessels (n=3, 1 litter). Data are expressed as fold change vs. controls and columns are means ± SEM. (G) qPCR analysis of relative expression levels of various Wnt ligands in the upper halves of E13.5 wildtype hearts reveals high expression of *Wnt4*, *Wnt5a*, *Wnt5b* and *Wnt11a*. Values were normalized on *Gapdh* levels of expression. Fold change is relative to *Wnt2* levels of expression. Columns are means ± SEM (n=3, 1 litter). (I) qPCR analysis of Wnt ligand expression in isolated endothelial cells demonstrates a high enrichment of *Wnt8a* levels when compared to non-bound flow through (FT) cells. Columns are means ± SEM (n=3, 1 experiment). For all statitiscal analyses two-tailed t-test assuming unequal variances, *p<0.05, **p<0.01, ***p<0.001.

SUPPLEMENTAL TABLES:

Antibodies table, related to Experimental Procedures: List of Antibodies used in this study

Protein	**Host**	**Type**	**Dilution**	**Secondary**	**Manufacturer**
PECAM	Goat	polyclonal	1:200	AlexaFluor 647	Santa Cruz
CONNEXIN40	Rabbit	polyclonal	1:400	AlexaFluor 555	Alpha Diagnostic International
SM22α	Rabbit	polyclonal	1:400	AlexaFluor 555	Abcam
SOX17	Goat	polyclonal	1:200	AlexaFluor 647	R & D Systems
GAPDH	mouse	monoclonal	1:1000	Donkey-HRP	Santa Cruz
ACTIVE β -CATENIN	mouse	monoclonal	1:500	Donkey-HRP	Millipore
BrdU	mouse	monoclonal	1:250	AlexaFluor 555	BD Bioscience
NFAT1	mouse	monoclonal	1:200	AlexaFluor 555	Abcam
NFATc3	Rabbit	polyclonal	1:200	AlexaFluor 555	Santa Cruz
VEGFA	Rabbit	polyclonal	1:200	AlexaFluor 647	Santa Cruz

Primers table, related to Experimental Procedures: List of primers used for qPCR analysis in this study

Name	Sequence	Direction	Usage
Rspo3 right	CAGCCATTGTAATCTGAACACG	antisense	qPCR
Rspo3 left	TCATTTTGAACTTTATGGAATACATTG	sense	qPCR
Axin2 right	GCCATTGGCCTTCACACT	antisense	qPCR
Axin2 left	CCATGACGGACAGTAGCGTA	sense	qPCR
Notch4 right	TCCCTGCACCAGTGTCCT	antisense	qPCR
Notch4 left	CCATCCAGCTGATGACTCCT	sense	qPCR
Dll4 right	GGGAGAGCAAATGGCTGATA	antisense	qPCR
Dll4 left	AGGTGCCACTTCGGTTACAC	sense	qPCR
Sox17 right	CCACCACCTCGCCTTTCAC	antisense	qPCR
Sox17 left	GATGCGGGATACGCCAGTG	sense	qPCR
Vegfa right	AGAGGTCTGGTTCCCGAAA	antisense	qPCR
Vegfa left	TTAAACGAACGTACTTGCAGATG	sense	qPCR
EphB2 right	AATGTGGCTGCTCGGATCT	antisense	qPCR
EphB2 left	AATCTGCTTTAGTTCCACATGACA	sense	qPCR
Tcf7 right	TGCTGTCTATATCCGCAGGAA	antisense	qPCR
Tcf7 left	CAGCTCCCCCATACTGTGAG	sense	qPCR
Vegfc right	TCTTGTTAGCTGCCTGACACTG	antisense	qPCR
Vegfc left	CAGACAAGTTCATTCAATTATTAGACG	sense	qPCR
Ang2 right	AGCTCTGCTTGGACACCAG	antisense	qPCR
Ang2 left	AAACAAGCTACAAAATAAGAACAGCTT	sense	qPCR

SUPPLEMENTAL METHODS:

Mice

For proliferation assays BrdU (Sigma-Aldrich) dissolved in 0.9% NaCl was administered to pregnant dams one hour before sacrificing via intraperitoneal (IP) injection at a dose of 50mg/kg. For measuring hypoxia pregnant mice were injected IP with 60mg/kg piminidazole hydrochloride 1 hour before sacrificing.

Wholemount *in situ* hybridization

Wholemount *in situ* hybridization was performed as described elsewhere. Briefly, hearts were fixed in 4% PFA overnight at 4°C and stored at -20°C in 100% MeOH until hybridization. Hybridization was performed at 70°C for 18h for each sample. The detection was performed with alkaline phosphatase-coupled anti-dioxygenin antibody (1:4000, Roche) overnight at 4°C. After washing, the chromogenic reaction was performed with NBT-BCIP substrate (Promega) for several days at 4°C.

RT-qPCR

RNA was extracted from the upper halves of E13.5 hearts using TRIzol® reagent (Invitrogen), following the manufacturer's instructions. Reverse transcription was performed using the M-MLV reverse transcriptase in combination with oligo (dT) primers (Invitrogen). The cDNA was used as a template for quantitative PCR analysis using the SybrGREEN® Master Kit (Roche) and a Light Cycler 1.5® (Roche). The expression levels

were normalized to *Gapdh*. For each litter or experiment ddCt values were normalized to one control dCt rather than the mean of control delta Cts. Primers (see primer table) were designed on the Universal Probe Library website (Roche).

BrdU quantification

Detection of BrdU-positive cells was performed by immunofluorescence as described in the experimental procedures section with an anti-BrdU antibody (BD Bioscience). Results were obtained after scoring the percentage of BrdU positive nuclei/total nuclei in four different matched areas of four histological sections per embryo. Three independent WT embryos were compared with three independent mutants from the same litter.

Endothelial/arterial proliferation quantification

Quantification of BrdU-positive endothelial and arterial cells was performed by immunofluorescence with anti-PECAM and anti-SOX17 antibodies respectively. PECAM/BrdU or SOX17/BrdU positive cells were counted on at least 10 consecutive sections in the area immediately surrounding the developing left coronary artery. Four embryos from two dissections at E13.5 were counted for each analysis. PECAM was quantified by calculating the amount of pixels in the ventricular coronary vessels using ImageJ software. Counting of endothelial proliferation in *Rspo3*-negative regions was done in a similar a manner as above in five different areas of five histological sections in a total of three embryos per genotype (1 litter).

Coronary Vessel Quantification

Coronary arteries were defined as Connexin40/PECAM-positive intramyocardial vessels and coronary veins were defined as COUPTFII/PECAM-positive subepicardial vessels. For the analysis at E15.5 the vessels from the free ventricular walls were counted for five representative sections per embryo. A total of 4 embryos from two different litters were analyzed per genotype.

For the analyses at E17.5 the coronary arteries were counted for the right and left ventricles as well as for the interventricular septum. Six sections were analyzed per embryo and a total of 5 embryos from two different litters were analyzed per genotype. For the recovery experiments 6 sections from 5 (NaCl, 3 litters) or 4 (LiCl, 2 litters) embryos per genotype were counted.

Wholemount immunohistochemistry

Hearts were fixed in 4% PFA for 1 hour, washed in PBS, incubated in methanol/hydrogen peroxide (8:1) for 1 hour and then blocked in PBSST (5% Skim milk powder/PBS, 0.5%Triton X-100) for five hours. The primary antibodies used were Rabbit anti-mouse Connexin40 (Alpha Diagnostic International, 1:200) and Goat anti-PECAM (Santa Cruz, 1:50). Donkey anti-Rabbit IgG and Donkey anti-Goat (Santa Cruz, 1:100) were used as secondary antibodies and visualization was performed by incubating with DAB substrate (Sigma Aldrich). All antibodies were diluted in PBSST and incubations were carried out at 4°C overnight. Following each overnight incubation, tissues were washed three times 1 hour each at 4°C with PBSST.

Western Blot

Upper halves of hearts were lysed in RIPA buffer and protein lysates were separated on 10% polyacrylamide-SDS page gels, blotted on PVDF (Biorad) membranes and incubated with the indicated primary antibodies. Horseradish peroxidase-conjugated secondary antibodies were used for chemiluminescent detection.

IV. Future perspectives

The role of Rspo3 in coronary artery formation

In this study I have shown that the Wnt signaling modulator *Rspo3* is essential for murine coronary artery formation. *Rspo3* is specifically expressed around the developing coronary stems at key time-points during their formation. Ablation of *Rspo3* with the *CAGGCreER*^{TM} line at E11.5 leads to defective formation of the arterial tree. Mechanistically *Rspo3* was shown to promote arterial proliferation in the coronary stems through activation of the β-catenin signaling pathway.

The key points demonstrated in this study are the location and timing of *Rspo3* expression. Although *Rspo3* expression is very restricted, the location of its expression is so critical that ablation of local *Rspo3* leads to a global phenotype ie. the entire coronary tree is affected. It's specific pattern of expression ultimately leads to many novel questions which, if addressed in the future, would undoubtedly shed new and important insight into *Rspo3*'s role in coronary development. These questions are as follows: 1) What are the cell types that express *Rspo3* around the coronaries?, 2) What factors are activating *Rspo3* expression around the coronaries? ie. Is it physical stimuli? Is it transcriptional?, and 3) Which receptor/s does Rspo3 exert its actions through in the coronaries?

According to a study by Cambier et al., 2014, *Rspo3* is directly activated by the transcription factor NKX2-5 in cardio-myoblasts of the secondary heart field. Analysis of the expression pattern of *Rspo3* around the coronaries at E12-14 seems to suggest it continues to be expressed by cardiomyocytes at these time-points. Whether or not there is some expression in pericytes, endothelial cells or smooth muscle is not entirely clear at E12.5-13.5. However, at E14.5 there is a clear boundary between the *Rspo3*-expressing cells and the smooth muscle and endothelium of the coronary stems. Hence, it appears as though *Rspo3* is mainly expressed by cardiomyocytes at this time-point (data not shown). Whether or not this is true for earlier time-points is uncertain. However, an analysis of *Rspo3* expression in isolated endothelial cells vs.

non-bound flow-through cells (mainly cardiomyocytes and fibroblasts) reveals *Rspo3* is not expressed in the endothelium of the heart.

In order to more accurately determine the cell-types expressing *Rspo3*, several cell-type specific deletions would have to be performed. For instance, the *WT1CreER^{T2}* and *Pax3Cre* lines could be used to delete *Rspo3* in the epicardial and cardiac neural crest lineages respectively. To delete *Rspo3* in the endothelium inducible endothelial-specific *Cres* such as the *VEcadherinCreER^{T2}* or *Tie2CreER^{T2}* lines could be used. Constitutive *Cres* would not be suitable since according to Scholz et al., 2016, the embryos would die prematurely from placental defects. To delete *Rspo3* in the myocardium either a constitutive or inducible myocardial Cre could be used. The inducible *Cre* would avoid any potential progenitor defects, but it may result in incomplete recombination. The constitutive *Cre* would work more effectively but may lead to progenitor defects such as hypomorphic right ventricles, and outflow tract deformations. In essence, by performing the cell-type specific deletions and looking for coronary defects one could determine which cell types express *Rspo3*.

Determining the factors that activate *Rspo3* expression around the coronaries is perhaps the most interesting question left to explore. Why *Rspo3* is so specifically expressed around the stems at such precise time-points is unclear. As mentioned previously, NKX2-5 regulates *Rspo3* in early cardio-myoblasts (Cambier et al., 2014). However, NKX2-5 is not the only factor regulating *Rspo3* otherwise *Rspo3* would be expressed in the entire myocardium at E12-13, which it is not. We have looked for other transcription factors with similar patterns but have not found any which mimic *Rspo3's* expression around the coronary stems.

Aside from transcriptional regulation, it may be possible that physical/chemical stimuli may activate *Rspo3*. For instance, we initially thought that hypoxia may be driving *Rspo3* expression. Since *Rspo3* is expressed in the central vein of livers (Rocha et al., 2015), which is highly hypoxic compared to the portal system, we thought it was possible that there could be a hypoxia gradient in the areas where *Rspo3* is expressed. We tested this by injecting mice with piminadazole but

did not detect hypoxia in the cells that normally express *Rspo3* around the coronaries. To confirm our findings, we treated isolated cardiomyocytes with Cobalt Chloride, which mimics hypoxic conditions, and found that *Rspo3* expression was not upregulated. In fact, *Rspo3* expression was downregulated (data not shown). Which leads to the next hypothesis that perhaps the vessels themselves, through the delivery of oxygen or glucose could be activating *Rspo3*. Since the connection of the peri-truncal vessels to the aortic orifices occurs at E12.5, it is possible that the ensuing blood flow may trigger *Rspo3* expression, which then promotes the proliferation of the coronary stems. This remains to be tested.

Finally, there is the question about which receptor/s *Rspo3* could be working through in coronary artery development. Traditionally, R-spondins bind to the three LGR receptors *Lgr4*, *Lgr5* and *Lgr6* (de Lau et al., 2012). However, no coronary defects have been reported for the individual LGR4/5/6 nulls. In fact, even the *Lgr4/Lgr5* double knockouts have no reported defects in coronary artery development (Kinzel et al., 2014). Hence, it is possible that *Rspo3* may be acting through alternative receptors. Aside from their furin repeats, R-spondins have thrombospondin domains which allow them to bind to cell-cell adhesion receptors such as syndecans (de Lau et al., 2012). For example, in Xenopus *Rspo3* has been shown to bind the Syndecan 4 receptor and promote non-canonical Wnt/PCP signaling (Ohkawara et al., 2011). In the mouse Syndecan 4-nulls have no obvious phenotype and this is most likely due to functional redundancy between the various syndecans. Hence, in order to test if Syndecan 4 is a major receptor for *Rspo3* in coronary formation multiple KOs would have to be generated. In addition to the PCP pathway, RSPO3 has also been shown to promote NFAT/Wnt Calcium signaling. However, which receptor this goes through is unclear. Nevertheless, it is unlikely that RSPO3 is acting through non canonical Wnt pathways since Lithium Chloride administration (a well described activator of β-catenin signaling) can recover the coronary phenotype observed in *Rspo3*-nulls.

Because of the fact that RSPO3 promotes canonical Wnt signaling I believe it would be worth having a closer look at the LGR receptors. In the study by Kinzel et al., 2014, where they deleted both Lgr4 and Lgr5 together, it was reported that some embryos died *In utero* around E16.5. Interestingly, *Rspo3* deletion at E11.5 with the *CAGGCreER*^{TM} resulted in occasional death at E16.5 as well. Furthermore, an older study looking only at the *Lgr4* KO reported that *Lgr4*-null mice displayed hypoplastic hearts (Mazerbourg et al., 2004), another common occurrence observed in *Rspo3*-nulls. Could it be that LGR4 is the principle receptor for Rspo3 during coronary formation? And could it be that the phenotype was missed by previous authors? Further testing would be needed to test this hypothesis. Another possibility would be that Lgr6, despite having no observable phenotype and being fully viable, could somehow compensate for LGR4 in the heart. A double KO of the two would ultimately resolve this question. Finally, Rspo3 could possibly be acting through a novel, hitherto unidentified receptor. This may explain why the LGRs or Syndecans do not display placental or secondary heart field defects.

In conclusion, the striking localized expression of Rspo3 around the coronaries leads to many questions that, if answered, would lead to very interesting results. Answering these questions could be the subject of further projects and doing so will undoubtedly improve our understanding of coronary artery formation in the heart.

CHAPTER III: NOVEL ROLES FOR RETINOIC ACID SIGNALING IN CARDIAC DEVELOPMENT AND REPAIR

I. Project description

Cardiovascular diseases are among the leading causes of death worldwide (Mozaffarian et al., 2015). Treating patients recovering from myocardial infarction is difficult because cardiomyocytes have a limited potential to proliferate and repair the damaged heart (Roij, 2016). During embryonic development several signaling pathways act in a coordinated fashion to stimulate the proliferation, patterning and differentiation of cardiac progenitors into a functional heart. Interestingly, many of these signaling pathways are reactivated in the adult heart after myocardial damage (Aisagbhoni et al., 2015). Understanding the functions as well as the physiological changes induced by these molecular cues are, thus, of utmost importance in developing novel regenerative treatments for heart disease.

The Retinoic Acid (RA) pathway is a complex signaling cascade that plays critical roles during embryogenesis and adult homeostasis. As mentioned previously, three enzymes catalyze the second step of RA synthesis from precursor retinoids and six different receptors transduce the signals of RA (Niederreither and Dollé, 2008). The enzymes (RALDH1, RALDH2 and RALDH3) display unique and interesting patterns of expression during embryonic development, while many of the receptors (ie. RARα and RXRα) are ubiquitously expressed and display functionally redundancy (Stefanovic and Zaffran, 2016).

In the heart, RA signaling is important for cardiac patterning and growth. Early on, RA acts on the venous pole of the heart to regulate the caudal extension of the secondary heart field (Sirbu et al., 2008). From E11.5 onwards, RALDH2 and the main RA receptor, RXRα, are highly expressed in the outer most layer of the heart, the epicardium. The epicardium is essential for promoting myocardial growth through the secretion of soluble mitogens such as FGFs and IGF2.

RA signaling promotes the expression of these mitogens, and by doing so it supports myocardial growth (Xavier-Neto et al., 2015).

Recent data has demonstrated that the RA pathway is reactivated in adult hearts after myocardial infarction (Bilibija et al., 2012). This was an interesting observation since RA signaling is known to play a protective role in cardiomyocytes subjected to cellular stress *in vitro* (Palm-Leis et al., 2004). In addition, Vitamin A supplementation to rats post MI attenuated cardiac remodeling and improved ventricular function (Minicucci et al., 2010). More recently, exogenous all-trans retinoic acid supplementation in mice subjected to ischaemia/reperfusion was shown to lead to decreased apoptosis and a reduction in infarct size (Zhu et al., 2015). Finally, myocardial-specific deletion of the RARα receptor resulted in increased cellular stress, calcium mishandling and cellular hypertrophy in the myocardium of adult mice (Zhu et al., 2016). All together this data suggests that RA plays a cardio-protective role post MI and that this role may be specific to cardiomyocytes.

Determining the cell types that respond to RA-signaling as well as the characteristics of the response has proven difficult in both development and the adult. Most researchers have relied on RARE-reporters such as the RARE-*LacZ* (Rossant et al., 1991) and the RARE-*Cre* (Dolee et al, 2010) lines. However, as with any transgenic mouse model, these lines have their limitations and at times their patterns of activity do not fully overlap.

The focus of this project was to look more closely at the role of RA-signaling in the heart during mid-late gestation and after myocardial damage. By using a series of genetic mouse models along with a novel RARE-reporter, I have focused on studying the cell types that respond to RA, as well as the effects of genetically depleting RA-signaling in the heart. The two time-points I focused on were embryonic development post E11.5, and 1 week after surgically induced myocardial infarction. More specifically, I worked towards accomplishing the following goals:

(1) Determine the precise cell types that respond to RA during mid-late cardiac development and after surgically induced myocardial infarction

(2) Carefully study the phenotypes resulting from genetic depletion of the Raldh enzymes in a temporally and spatially controlled manner during late development and after Myocardial infarction (4) Discover and validate novel transcriptional targets of RA in cardiomyocytes with cardio-protective effects

In order to track cells that are responsive to retinoic acid I utilized a novel Retinoic acid reporter line generated in our lab. This transgenic line is composed of three RARE elements from the RARβ gene fused to the *hsp68* promoter driving expression of a tamoxifen-inducible *Cre-ER*^{T2} recombinase. By crossing this line with the *mTmG* reporter line (Muzumdar et al., 2007), I was able to permanently label RA-responsive cells and trace their descendants over time. The advantage of the RARECreER^{T2} line was that it allowed me to temporally control the labeling of RA-responding cells. Through co immunostaining with GFP and cell type specific markers, it also allowed me to define the cell types responding.

I decided to test our line during mid-late gestational stages of heart development as well as in adult hearts post MI. More specifically, I wanted to see which cell types responded to RA during the early (E11.5-E13.5) and late stages (E14.5-18.5) of cardiac development. I also wanted to more precisely define the cell types responding to RA-signaling post MI. One study has suggested that RA acts on the cardiac fibroblast population to limit their proliferation (Bilbija et al., 2012) while another suggests that RA prevents apoptosis in cardiomyocytes (Zhu et al., 2015). None of these studies showed direct in vivo evidence of RA acting on either cell type, so my goal was to attempt to and shed some light on this issue.

To better comprehend the role of RA signaling on cardiac repair I crossed an inducible *CAGGCre-ER*^{TM} line (Hayashi and McMahon, 2002) with floxed alleles of the Raldh1, 2 and 3 enzymes. The *CAGGCre-ER*^{TM} line is well described and has been shown to function effectively in muscular tissue such as the heart (Zhou et al., 2014). It is ubiquitously expressed and usually ensures full deletion of all floxed genes it is crossed with, regardless of the cell type. More

importantly, it allows one to choose at which time-points to delete these floxed alleles. In the context of RA signaling, temporal control is extremely important since disruption of this pathways generally leads to severe phenotypes. Hence, by deleting the *Raldh* enzymes during adulthood I could avoid the early embryonic lethality associated with full *Raldh2* nulls. Using this strategy I was able to study the putative consequences in cardiac remodeling associated with RA-depletion before myocardial infarction.

To further explore the roles of RA-signaling on cardiomyocytes I isolated primary cardiomyocytes from E18.5 hearts, treated them with RA, extracted RNA and then sent the RNA for high-throughput sequencing. The hope was that some of the hits from the sequencing would have cardio-protective functions, which could potentially explain some of the benefits of RA on CMs exposed to cellular stress. The next goal was to characterize these hits as real RA transcriptional targets and test agonists and/or antagonists of these *in vitro* and *in vivo* in an attempt to discover novel protective treatments for cardiac disease

II. Retinoic Acid signaling in cardiac development and repair (Schematic for project design)

Part 1: Lineage Tracing with RARECreER^{T2}

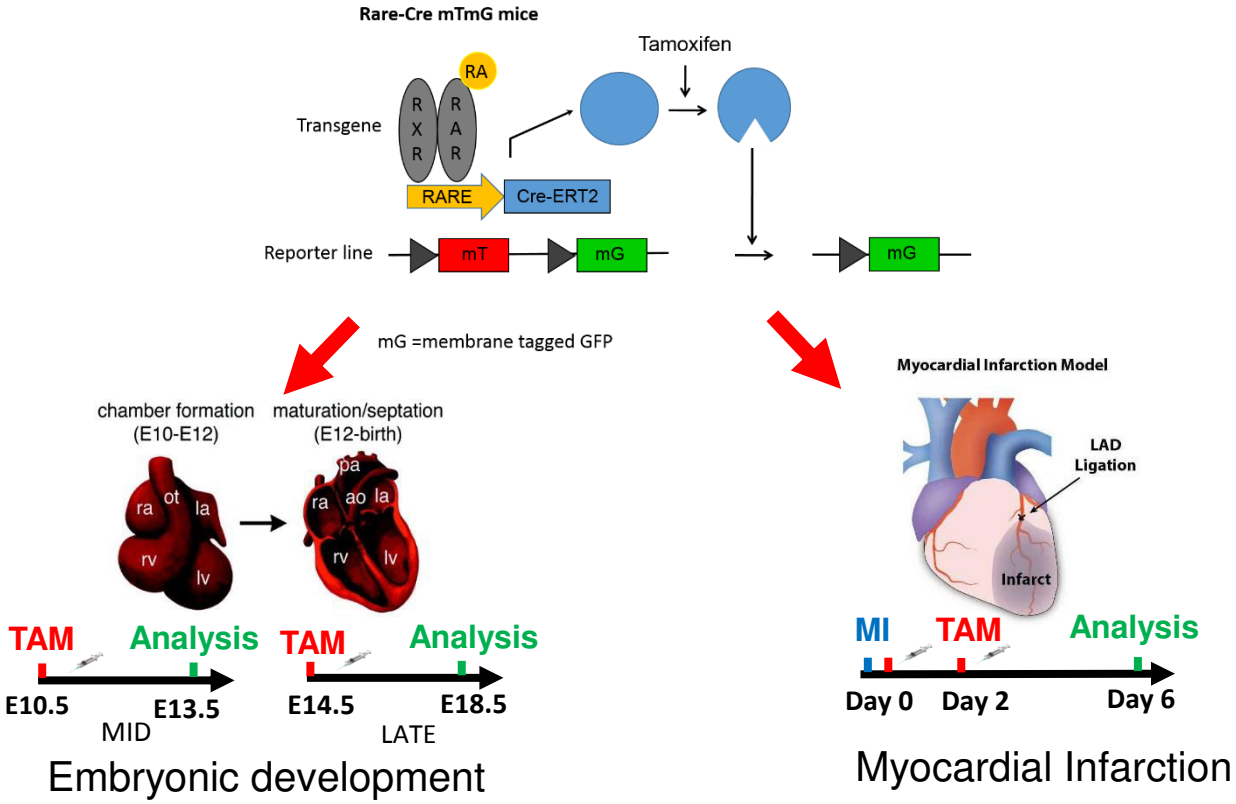

Embryonic development

Myocardial Infarction

Part 2: Genetic ablation of RA signaling

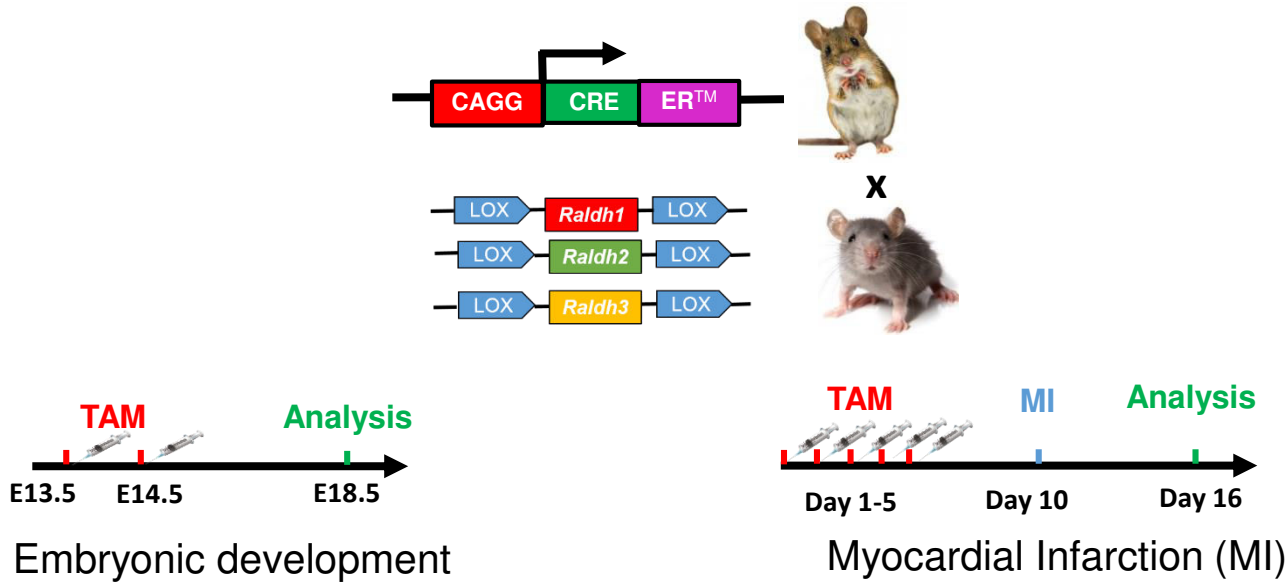

Embryonic development

Myocardial Infarction (MI)

III. Manuscript entitled: “Retinoic Acid promotes cardiomyocyte survival in cardiac development and repair”

Title:

Retinoic Acid signaling promotes cardiomyocyte survival in cardiac development and repair

Fabio Da Silva[1], *Fariba Jian Motamedi*[1], *Ana Sofia Rocha*[1#], *Jessica Ryler*[1], *Pascal Dollé*[2], *Norbert Ghyselinck*[2], *Kay Dietrich Wagner*[1] *and Andreas Schedl*[1*]

[1]Université Côte d'Azur, Inserm, CNRS, iBV, Nice, 06108, France
[2]IGBMC, Inserm, CNRS, Strasbourg, UMR7104, France

[#]present address: Institut d'Investigació Biomédica de Bellvitge (IDIBELL), Barcelona, Spain

Key Words: Retinoic Acid, cardiomyocytes, apoptosis, Angiotensin converting enzyme 1 (Ace1), Retinaldehyde dehydrogenase (*Raldh)*

***Corresponding author:**
Andreas Schedl
Inserm UMR1091
Centre de Biochimie
Parc Valrose
06108 Nice
France
Tel.: ++33492076401
FAX: ++33492076402
Email: Schedl@unice.fr

SUMMARY

Treatment of patients recovering from myocardial infarction (MI) is difficult since cardiomyocytes have a very limited capacity to proliferate and regenerate the damaged heart. Manipulation of the embryonic pathways normally reactivated after MI may be a promising way to develop novel regenerative treatments. The Retinoic Acid (RA) signaling pathway is essential for cardiac development and appears to play a protective role in damaged hearts. The exact mechanisms and cell types involved in this protective response is unclear. Here we have developed a novel inducible RA reporter line using CreER^{T2} technology. With this line we have observed a cardiomyocyte-specific response during mid-late gestation as well as after MI. Ablation of RA signaling through genetic deletion of the *Raldh1/2/3* enzymes leads to increased myocyte apoptosis both during late development and after MI. RNA sequencing analysis of primary cardiomyocytes reveals atRA treatment represses *Ace1* expression, providing a novel link between RA signaling and the Renin Angiotensin System in the context of heart repair.

INTRODUCTION

Cardiovascular diseases are the leading cause of death worldwide. Treating patients recovering from myocardial infarction (MI) is inherently difficult due to the fact that cardiomyocytes, the principal cell-type of the heart, have a limited potential to proliferate and repair the damaged heart (Aisagbonhi et al. 2011). Hence, developing novel treatments aimed at minimizing ischaemic damage are of the utmost importance.

Retinoic acid (RA), the active derivative of vitamin A, is involved in various aspects of embryonic development and adult homeostasis (Zaffran et al., 2014). RA is synthesized by three retinaldehyde dehydrogenases (RALDHs) encoded by *Raldh1*, *Raldh2* and *Raldh3.* RA can activate or repress the transcription of various genes by binding to nuclear retinoic acid receptors (RARα, RAR*β*, RARγ) which form heterodimers with retinoid X receptors (RXRα, RXR*β*, RXRγ) (Niedereither and Dolle, 2008).

An essential step in mammalian cardiac development involves the formation of the compact myocardial layer. Myocardial compaction occurs between E10-14 and involves the proliferation and differentiation of cardio-myoblasts (Zaffran et al., 2014). Both *Raldh2* and *Rxr*α mutants display severe hypoplasia of the compact layer (Lin et al., 2010; Jenkins et al., 2005; Merki et al., 2005). Mechanistically, it has been suggested that RA, synthesized by RALDH2 in the epicardium, works in an autocrine manner with RXRα functioning as the principle receptor (Zaffran et al., 2014). The RALDH2:RXRα axis stimulates the production of mitogens such as FGFs, which are then secreted to the myocardium to promote proliferation (Tran and Sucov 1998; Lavine et al., 2005, Stuckmann et al., 2003). It has also been suggested that RALDH2:RXRα signaling in the liver and placenta promote the production of EPO and the distribution of glucose respectively, both of which sequentially activate epicardial *Igf2* expression (Brade et al., 2011; Shen at al., 2015). IGF2 then promotes myocardial proliferation and compaction. Hence, whether the effects of RA are epicardial or derived from extra cardiac sources, RA signaling does not seem to directly act on the myocardium. This is supported by the fact that myocardial-specific deletion

of RXRα does not lead to cardiac defects (Xavier Neto et al., 2015). Whether or not RA signaling plays a role at later time-points (ie. post E14.5) remains to be investigated.

Many studies conducted in adult rats and mice suggest RA signaling plays an essential role in cardiac repair post MI. Vitamin A-deficient rats subjected to ligation of the left anterior descending artery (LAD) exhibit increased cardiomyocyte hypertrophy and interstitial collagen deposition (Minicucci et al., 2010). Furthermore, supplementation of all-trans Retinoic Acid (atRA) to mice following ischaemia/reperfusion surgery results in decreased apoptosis and smaller infarct zones (Zhu et al., 2015). In this study RA's anti-apoptotic effect appeared to be transduced through the MAP kinase pathway (Zhu et al., 2015; Palm-Leis et al., 2004).

Direct evidence that RA signaling is reactivated in the heart post MI comes from a study done with the RARE luciferase reporter line. In this study the authors detected RA signaling in damaged hearts 24 hours to 1 week post MI. Cardiac fibroblasts, and not cardiomyocytes, were determined to be the principle cell-types responding to RA (Bilibija et al., 2012).

Although the literature seems to suggest that cardiomyocytes do not respond directly to RA, additional studies show there may be minor, albeit important roles for RA signaling in the myocardium. In a recent study by Guleria et al. 2010, it was demonstrated that stimulation of the RA pathway in cultured neonatal cardiomyocytes subjected to high-glucose conditions led to decreased apoptosis. The protective effect was attributed to RA-induced modulation of the Renin-angiotensin system (RAS). More recently, cardiomyocyte-specific deletion of the RARα receptor in adult mice led to increased cardiomyocyte hypertrophy, excessive reactive oxygen species (ROS) accumulation and calcium mishandling defects (Zhu et al., 2016).

In this study we have developed a novel RA reporter line using *CreER*^{T2} technology (*RARECreER*^{T2}). With our *RARECreER*^{T2} line we have detected a novel cardiomyocyte-specific response during mid-late stages of development (E11-18). Furthermore, we have detected RA activity in cardiomyocytes of adult mice subjected to MI. In order to understand these responses more clearly, we have crossed floxed alleles of the *Raldh* enzymes (*Raldh1, Raldh2* and *Raldh3*)

(Fan et al., 2003; Vermot et al., 2006; Molotkov, 2006) with the ubiquitously expressed and inducible *CAGGCreER^{TM}* line (Hayashi and McMahon, 2002). By temporally deleting the Raldh enzymes at late stages (E13-14) we have observed decreased proliferation and increased apoptosis. In addition, by employing the same strategy in adult mice subjected to MI we observed a drastic increased in cardiomyocyte-specific apoptosis in *Raldh*-null mice. This increase in apoptosis may be correlated with a specific effect on the Renin-angiotensin system as RA supplementation to primary cardiomyocytes represses the expression of Angiotensin converting enzyme 1 (ACE1). Here we have shown that RA signaling acts directly on cardiomyocytes, and that this response is important at late stages of cardiac development. More importantly we have identified a novel protective role for RA signaling after MI.

RESULTS

A novel RARECreER^{T2} line displays a dynamic RA response during cardiac development

The Retinoic acid signaling pathway is extremely dynamic, acting on various tissues at different stages of embryonic development (Niedereither and Dolle, 2008). In order to better understand the timing and identity of the cell types responding to RA, we developed a novel tamoxifen-inducible RA reporter line using *CreER^{T2}* technology. Administration of tamoxifen at E6 to embryos carrying the Rosa26LacZ (R26L) line (Soriano, 1999) followed by analysis at E9 demonstrated very strong caudal X-gal staining (Figure 1B). A similar pattern was observed with administration of tamoxifen at E7 followed by analysis at E10 (Figure 1B). The X-gal staining at both time-points closely matched the staining pattern observed in *RARECre* R26L embryos (Dolle et al. 2010), a similar type of line with permanent rather than temporal labeling of RA-responsive cells. However, there was a noticeable absence of X-gal positive cells in the forebrains of our *RARECreER^{T2}* embryos. To see if we could label this region with additional pulses we administered tamoxifen at both E7 and E9. With the extra pulse at E9 we observed forebrain-

specific labeling (Figure 1B; red arrow), suggesting the differences seen with our reporter line to be related to the timing of the labeling rather than with the transgenic line itself.

A closer look at the hearts of the E6-9 and E7-10 *RARECreER^{T2}* embryos revealed specific labeling of the venous pole derivatives (atria and outflow tract) of the heart. The labeling pattern faithfully recapitulated that seen with other RA reporters (Rossant et al., 1991, Dolle et al., 2010), although the intensity of the labeling was not as strong and was observed to be more efficient with the E6.5 pulse compared to the E7.5 one (Figure 1 C-D). These discrepancies can most likely be attributed to variability in the efficiency of recombination resulting from differences in tamoxifen processing and distribution.

Next, we decided to look at RA activity at later time-points when myocardial compaction occurs (E10-13). RA signaling is thought to activate the synthesis of mitogens in the epicardium in an autocrine manner, suggesting the major cell types that respond to RA are epicardial cells rather than cardiomyocytes (Zaffran et al., 2014). Interestingly, with a single pulse of tamoxifen at E10.5 followed by analysis of E13.5, the *RARECreER^{T2}* line labelled a significant portion of the ventricles, with almost no labeling of the atria or outflow tract. Even more interesting, the principle cell-types responding to RA were located within the compact ventricular layer. Labeling of the outer epicardial layer was also observed, although to a significantly smaller extent (Figure 1E, whole-mounts and insets).

Cardiomyocytes respond directly to RA signaling during mid-late phases of gestation and RALDH2 is expressed by cardiac fibroblasts after E14.5

To determine more precisely which cell-types were being labelled by the *RARECreER^{T2}* line, we crossed our mice with the *mTmG* reporter allele (Muzumdar et al 2007) (Figure 2A) and performed co-immunostaining with epicardial-specific (Wilms tumour protein (WT1)) and myocardial-specific (MF20) antibodies. Administration of tamoxifen at E9.5 followed by analysis two days later revealed sparse labeling of both WT1-positive epicardial cells and MF20-positive cardio-myoblasts (Figure 2B). However, tamoxifen administration at E10.5 followed by analysis

at E13.5 revealed very strong labeling of MF20 positive cardio-myoblasts with very little labeling of WT1-positive epicardial cells (Figure 2C). The myocyte-specific labeling was highest in the compact layer with very little labeling observed in trabecular myocytes (Figure 2C, insets). GFP-positive endothelial cells and fibroblasts were occasionally observed, but at very low frequencies (data not shown).

The very strong and specific labeling of cardio-myoblasts contradicts previous reports which suggest RA's activity to be restricted to the epicardial and sub-epicardial layers at these time-points (Brade et al., 2011; Shen et al., 2015; Dolle et al., 2010). To determine if the myocyte response was real, we decided to validate our *RARECreER^{T2}* line using both *in vivo* and *in vitro* methods. Interestingly administration of exogenous all-trans Retinoic Acid (atRA) at E10.5 increased the RA–response significantly in *RARECreER^{T2}* E13.5 hearts (Figure 2D). In addition, a substantially larger portion of trabecular myocytes were labelled in comparison to controls (Figure 2D). Treatment of embryos with low doses of the RA reverse agonist BMS493 prior to and following tamoxifen administration lead to a very strong decrease in GFP-positive cells (Figure 2E). Isolation of primary cardiomyocytes from E18.5 *RARECreER^{T2}* hearts followed by atRA treatment lead to specific labelling of Troponin-T-positive cardiomyocytes *in vitro* (Figure 2F-G). To ensure the response was not an artifact specific to our transgenic line, we performed lineage tracing experiments with a second *RARECreER^{T2}* line (Line B). Administration of tamoxifen at E10.5 followed by analysis at E14.5 revealed a nearly identical pattern of GFP expression when compared to our original line (Figure S1A). Altogether, this data suggests the myocyte-specific labeling observed with the *RARECreER^{T2}* line to be a real response that can be influenced by exogenous activation or inactivation of the RA signaling pathway.

Although the role of RA signaling during heart looping and myocardial compaction is well described, it is unclear whether retinoids continue to play an important role after E13.5 (Zaffran et al., 2014). With our *RARECreER^{T2}* line we next decided to look at later time-points of heart development by administering tamoxifen at E14.5 and sacrificing embryos at E18.5. With this later

pulse, we observed a very high amount of GFP-positive cardiomyocytes (Figure 3A). We also observed that many of the myocytes labelled were located deep within the compact layer. To see if this labeling was due to clonal expansion of myocytes located near the epicardium, we labelled cells for a shorter period of time by giving a single pulse at E15.5 and analyzing at E17.5 (Figure 3B). Once again we observed myocyte-specific labeling, both near the epicardium as well as deeper within the compact layer. Interestingly, many of the GFP positive myocytes located further away from the epicardium were separated from other cells, suggesting their response to arise from a local source of RA, independent from the epicardium.

During cardiac development, RALDH2 is the main enzyme responsible for RA synthesis and disruption in its expression leads to both early and mid-stage cardiac defects (Niedereither and Dolle, 2008). Whether or not RALDH2 has a role at later time-points is unknown since both the full *Raldh2*-nulls as well as the *Raldh2*-rescue nulls die at E9.5 and E13.5 respectively (Niederreither et al., 2001; Lin et al., 2010). Since we detected RA signaling post E13.5, we decided to perform immunostaining with an anti-RALDH2 antibody during later stages of gestation. Interestingly, while RALDH2 was indeed restricted at to the epicardium at E12.5, after E14.5 RALDH2 protein could be detected in cells located within the ventricular and interventricular walls. This expression pattern seemed to increase at later time-points, peaking at E18.5 (Figure 3C). To determine which cell-types were expressing RALDH2 we performed co-immunostaining with various antibodies. Interestingly, we did no detect any co-immunostaining with myocyte (MF20), endothelial (PECAM1) or smooth muscle-specific (SM22α) markers (data not shown). To determine if the RALDH2-expressing cells were cardiac fibroblasts, we performed co-immuno-staining with VIMENTIN and observed a near complete overlap in expression. Since VIMENTIN also marks endothelial cells, we performed triple staining with PECAM1, VIMENTIN and RALDH2. None of the PECAM1/VIMENTIN positive cells expressed RALDH2 suggesting the identity of the RALDH2-expressing cells within the ventricular wall to be cardiac fibroblasts (Figure 3D). Finally, since fibroblasts originate from the pro-epicardial organ (PEO), we next wanted to see if the

RALDH2-expressing cells also arose from the epicardium. Lineage tracing with the *WT1CreER^{T2}* line (Zhou et al., 2008) crossed with the *mTmG* reporter revealed a significant portion of RALDH2-positive cells were positive for GFP, suggesting they originated from the PEO (Figure 3E).

Late stage ablation of the RA signaling pathway leads to myocardial thinning and increased apoptosis

The late response observed with our *RARECreER^{T2}* line coupled with the observation that RALDH2 is expressed by cardiac fibroblasts at late stages of gestation prompted us to question whether or not there was an additional later role for RA signaling in heart development. In order to test this, we crossed floxed alleles of the three *Raldh* enzymes (*Raldh1*, *Raldh2*, and *Raldh3*) with the ubiquitously expressed and inducible *CAGGCreER^{T2}* line (Figure 4A, schematic). In a previous study from our group, we demonstrated that the *CAGGCreER^{T2}* line displays efficient recombination in all cell-types in the heart with tamoxifen administration at E11.5 (Da Silva et al., 2017). In accordance, administration of tamoxifen at E13.5 and E14.5 led to very efficient deletion of all three RALDH enzymes as demonstrated by qPCR analysis from whole hearts at E16.5, as well as RALDH2 immunostaining at E18.5 (Figure 4B-C).

Next we wanted to check for defects in the compact layer as well as in the proliferation rates of cardiomyocytes. H&E staining of Raldh-null hearts demonstrated a slight thinning of the myocardial layer (Figure 4B) and BrdU injection followed by immuno-staining with an anti-BrdU antibody demonstrated a small but significant decrease in total cell proliferation (Figure 4D). We then decided to look for differences in apoptosis. Immunostaining with an active-caspase 3 antibody along with TUNEL staining demonstrated a large increase in apoptotic cells in *Raldh*-null hearts (Figure 4E). Interestingly, many of the apoptotic cells were cardiomyocytes (Figure 4E 3rd panel). To exclude non-specific effects arising from ubiquitous deletion of the *Raldh* enyzmes we analyzed mutant livers and placentas. Both organs displayed no obvious abnormalities (data not shown). Finally, we decided to look at *Igf2* levels in the heart to see if the proliferation or apoptosis defects observed were due to extra-cardiac RA signaling. No differences were

observed in mutant hearts suggesting the defects to be unrelated to the control of Igf2 expression from EPO or glucose stimulation (data not shown).

The RARECreER^{T2} line labels several cell-types in adult hearts subjected to Myocardial Infarction

Next we wanted to test our *RARECreER^{T2}* line in adults subjected to surgical ligation of the left coronary artery (Myocardial infarction model). For this we administered two pulses of tamoxifen, one immediately after surgery, and another 48 hours later (Figure 5A, schematic). Strikingly, analysis of hearts 6 days post MI revealed an upregulation of both RALDH2 and GFP expression in infarct hearts when compared to sham controls (Figure 5B). *Raldh1* and *Raldh3* were also upregulated as determined by qPCR analysis (Figure 5C). A closer look at the expression patterns revealed RALDH2 and GFP positive cells were highly upregulated within the injury and border zones of damage (Figure 5B). Most RALDH2-expressing cells were not GFP-positive suggesting a paracrine rather than autocrine mode of action (Figure 5E). Co-immunostaining of GFP with various markers demonstrated that many different cell-types seemed to be responding to RA. These included PECAM1-positive vessels, αSMA positive cells and Troponin-T-positive cardiomyocytes (Figure 5D). Interestingly, a substantial proportion of cardiomyocytes in the injury border zone were GFP-positive (Figure 5E). To see if the GFP response could be detected prior to 1 week, we analyzed infarct hearts three days after MI. From our analyses we observed a substantial amount of GFP expression in infarct hearts and minimal staining in sham mice (Figure 5F). We also performed long-term lineage tracing, this time providing an extra pulse of tamoxifen 6 days post MI. Analysis of hearts two months post MI revealed a much more robust labeling efficiency with many GFP positive cells in areas far away from the injury site (Figure 5G). Interestingly, nearly all of the cells labelled in the long-term studies were cardiomyocytes, with very few PECAM1 or αSMA positive cells detected at this time-point (Figure 5G).

Ablation of the RA signaling pathway prior to MI leads to larger infarct zones and increased apoptosis

We next wanted to test the effects of performing MI on RA-deficient adult mice. For this we utilized our *CAGGCreER^{TM} Raldh 1/2/3* floxed mice. To delete the enzymes we injected mice 5 times with tamoxifen 1 week prior to MI (Figure 6A, schematic). Analysis of hearts 1 week post MI determined a reasonable efficiency of deletion with a near 70% decrease of *Raldh1* and *Raldh2* mRNA levels (Figure 6D) and a 50% reduction in RALDH2 protein (Figure 6C). The reasons for the incomplete deletion is most likely attributable to the inaccessibility of the *Raldh* gene loci as testing of the *CAGGCreER^{TM}* crossed with the *mTmG* line, a Rosa26 based reporter, showed very efficient recombination in all cell types of the heart (Figure S4C). This inaccessibility may be correlated with the fact that the *Raldh* enzymes are expressed at very low levels under homeostatic conditions (Figure 5B).

To analyze the effects of depleting the RA pathway prior to MI we decided to measure the infarct zones of cKO mice. Strikingly, *Raldh* null mice exhibited significantly increased infarct zones as determined by collagen staining with the Sirius red dye (Figure 6E). Furthermore, cKO mice also exhibited increased rates of apoptosis as determined by active caspase 3 and Tunel staining (Figure 6G). Interestingly, many of the apoptotic cells in KO mice were cardiomyocytes and they tended to concentrate in clusters or so called “patches”. These patches were observed in 4 out of 7 KO mice and only 1 out of 8 control mice (Figure S5F, table).

atRA treatment represses Ace1 expression in cardiomyocytes

The labeling of cardiomyocytes with our *RARECreER^{T2}* line coupled with the increase in apoptosis observed in *Raldh* null mice both during development and after MI led us to believe that RA signaling indeed plays a protective role in cardiomyocytes. To try and decipher what this role could be we isolated primary cardiomyocytes from E18.5 hearts and then treated them with 100nM atRA for 48 hours to mimic the long-term exposure to RA experienced after MI. After treatment we extracted RNA and sent the samples for high-throughput sequencing (Figure 7A,

schematic). Analysis of the sequencing data determined that several canonical RA targets such as *Rarβ* and *Cyp26a1* were upregulated (Figure 7B, red arrows). It was also determined that several genes previously shown to be important in MI such as *Tgm2* (Szondy et al., 2006) were also upregulated (Figure 7B, green arrow). More importantly, we noticed the repression of Angiotensin converting enzyme 1 (*Ace1*) in our treated CMs (Figure 7C, red square). ACE1 is responsible for converting angiotensin 1 into angiotensin 2 (Gulleria et al., 2010). Upregulation of ACE1 has been observed in rodent hearts after MI and is generally considered to be harmful (Sun, 2010). This observation was very interesting due to the fact that a connection between RA signaling, the RAS system, and cardiomyocyte-specific apoptosis has been previously established *in vitro* (Palm-Leis et al., 2004; Gulleria et al., 2010). To test the repression of *Ace1* further we treated primary cardiomyocytes with BMS493 to inhibit the RA pathway. As expected *Ace1* expression was increased, validating the hypothesis that RA induces the repression of *Ace1* in cardiomyocytes (Figure 7F). We also observed increased *Ace1* expression in MI hearts when compared to shams, an observation made in previous publications (Figure 7G). (Sun, 2010).

A previous study using exogenous atRA supplementation in mice subjected to ischaemia/reperfusion determined that the RA pathway played an anti-apoptotic effect in damaged hearts by modulating the MAP kinase pathway. This modulation was hypothesized to be through the direct regulation of *Adam10*, a protease responsible for cleaving the RAGE10 receptor that promotes MAP kinase signaling cascades such as the ERK1/2 pathway (Zhu et al., 2010). In our *Raldh* null mice we did not observe any differences in *Adam10*, or phospho-ERK1/2 expression (Figure S6 E-F). Treatment of primary cardiomyocytes with atRA or BMS493 also did not lead to changes in the expression of *Adam10* (Figure S6 B-C) or phospho-ERK1/2 protein levels (data not shown), further suggesting the anti-apoptotic effects of RA post MI to be unrelated to Adam10/MAP Kinase signaling in our model of RA depletion.

DISCUSSION

RA signaling plays an essential role in cardiac development and repair. Here we have identified novel roles for RA in late stages of development and after myocardial infarction. Lineage tracing with a novel *RARECreER^{T2}* line demonstrates that cardiomyocytes are the principal cell types responding to RA signaling from E10-18 as well as after MI. Importantly, depletion of RA signaling through *Raldh1/2/3* deletion leads to increased myocyte apoptosis during late gestation and cardiac repair; suggesting RA plays a protective role in cardiomyocytes. Through RNA sequencing we show that this protective effect, at least after MI, may be due to repression of the *Ace1* enzyme, a principle component of the Renin angiotensin system (RAS).

Previous studies have shown that RA signaling is involved in myocardial compaction and that RA does not act directly on cardiomyocytes. With our novel *RARECreER^{T2}* line, we have shown that cardiomyocytes do indeed respond to RA. Furthermore, we have validated this response through *in vivo* and *in vitro* modulation of RA signaling (Figure 2). Whether or not this response plays an important role in myocardial compaction remains to be seen. One way of addressing this would be to perform a myocardial-specific deletion of the three RAR receptors. The deletion would have to target all three since functional redundancy between the RARs has been previously reported.

The late stage phenotype observed in our *Raldh1/2/3* cKOs is interesting and difficult to explain. RA signaling is important for the development of the placenta, liver and coronary vasculature. Defects in the formation of all these can all lead to myocardial thinning and, possibly, apoptosis. However, we would argue that the effects observed are independent of these for the following reasons: 1) The placenta, liver and coronary vasculature do not present any noticeable defects (data not shown) 2) *Igf2* expression is not affected in the hearts of *Raldh1/2/3* nulls (data not shown) and 3) The late nature of the E13.5 deletion makes it very unlikely that the apoptosis observed is due to indirect effects resulting from ubiquitous deletion of the *Raldh* enzymes.

Furthermore, analysis of hearts at E16.5, just three days after deletion already reveals increased apoptosis without any noticeable myocardial thinning (Figure S3).

The cause of the increased apoptosis has remained elusive in our studies. RA signaling has been previously shown to play an antioxidant role in cardiomyocytes during adult homeostasis. This was shown to be due to the regulation of the *Sod1* and *Sod2* enzymes (enzymes responsible for relieving oxidative stress) (Zhu et al., 2016). However, we did not detect any differences in *Sod1* or *Sod2* mRNA levels in our *Raldh1/2/3* null hearts, nor were they up-regulated in our RNA seq data (data not shown). Whether or not RA signaling plays an antioxidant role via SOD1/SOD2-independent mechanisms remains to be seen.

An RA-response following myocardial infarction has been previously reported. However, the precise identity and position of the cells responding were not accurately determined (Bilbija et al., 2012). Here we have shown that cardiomyocytes, along with many other cell-types respond directly to RA signaling. Given the fact that retinoinds have been shown to be involved in cardiomyocyte hypertrophy, proliferation and differentiation, (Minicucci et al., 2010; Zafran et al., 2014; and Lin et al., 2010) we believe this discovery is very valuable in the context of cardiac regeneration. The robust long term-labeling pattern in our hearts was unexpected. It is likely that this is due to the extra pulse of tamoxifen given 6 days post MI since at this time-point RALDH2 is very highly expressed in the damaged heart.

A previous study revealed atRA treatment given to mice recovering from ischaemia reperfusion improved cardiac function and reduced apoptosis. This was demonstrated to be due to regulation of *Adam10*, which cleaves the RAGE10 receptor. RAGE10 activates MAP Kinase signaling pathways such as ERK1/2 so its inhibition due to atRA treatment was thought to alleviate apoptosis post MI (Zhu et al., 2015). Our data on primary cardiomyocytes and *Raldh1/2/3* null infarct hearts did not show any changes of *Adam10* expression or ERK1/2 phosphorylation (Figure S6). This suggests the anti-apoptotic effects of RA post MI may arise though a different pathway in our model.

Since RA has been associated with the RAS on several occasions (Gulleria et al., 2010; Palm-Leis et al., 2004), we were not surprised to see *Ace1* come up as a top hit (repressed expression levels) in our RNA seq data (Figure 7). In fact, it has been already shown that atRA treatment represses the RAS in the context of cardiomyocyte apoptosis. Since ACE1 plays such a crucial role it is plausible that the RA induced regulation of RAS may, at least in cardiomyocytes, be related to *Ace1* repression. However, given the fact that the repression is relatively low (50%) in comparison to direct RA targets, it is likely that RA regulation of Ace1 may be indirect. This is supported by the fact that we did not identify any conserved RARE elements in the promoter regions of the Ace 1 gene via *in silico* analyses (data not shown). Nevertheless, in the context of cardiovascular disease, the connection between RA signaling and *Ace1* is an important one since there are already many treatments that work by targeting and inhibiting the ACE1 enzyme. In this context, it is thus possible that ACE1 inhibition coupled with atRA treatment may synergistically protect cardiomyocytes from apoptosis after acute events such as myocardial infarction.

EXPERIMENTAL PROCEDURES

Mice

All animal work was conducted according to national and international guidelines and was approved by the local ethics committee (PEA-NCE/2013/88). The *Rosa26LacZ*, *mTmG*, *Raldh1*^{fl}, *Raldh2*^{fl}, *Raldh3*^{fl}, and *CAGGCre-ER*^{TM} lines have been described previously (Soriano 1999; Muzumdar et al., Fan et al., 2003; Vermot et al., 2006; Molotkov, 2006; 2007; Hayashi and McMahon, 2002). For embryonic lineage tracing and *Raldh1/2/3* deletion experiments Cre activation was obtained by administration (gavage) of 200mg/kg tamoxifen (Sigma-Aldrich) dissolved in corn oil (Sigma-Aldrich) to pregnant females at the indicated time-points. For adult myocardial infarction experiments Cre activation was obtained by administration (Intraperitoneal Injection (IP)) of 100mg/kg tamoxifen at the indicated time-points. For BrdU experiments females were injected (IP) with BrdU dissolved in 0.9% NaCl 1 hour before sacrificing.

For generation of RARECreER^{T2} mice, fertilized zygotes were obtained from superovulated B6D2F1 females mated to B6D2F1 males. Linearized DNA, containing the RAREhsp68 cassete consisting of three copies of the RAR*β* DR5 RARE attached to the CreER^{T2} gene was injected into pronuclei of the zygotes. Zygotes were then transferred into the oviducts of pseudopregnant mice. All the mice used in these experiments were heterozygous for the transgene, and were back–crossed for more than five generations.

Myocardial Infarction surgeries

Mice were anesthesized with isofluorane and intubated. Mechanical ventilation was used to maintain a respiratory rate of 135/min with pure oxygen mixed with 1-2% isofluorane. A left-sided thoracotomy was performed, the pericardium was cut open, and permanent ligation of the descending branch of the left coronary artery was made roughly 2.5 mm under the tip of the left auricle using 8-0 silk suture. Sham operated mice underwent exactly the same procedure, except that the ligation around the left coronary artery was not made. Subsequently, the intercostal

space, muscles of the external thoracic wall and skin were sutured with 6/0 polyester. All animals received 0.5 ml saline IP post-surgery to compensate for fluid loss and 0.1 mg/kg of buprenorphrine hydrochloride subcutaneously for analgesia.

Whole-mount X-gal staining

For whole-mount X-gal analysis, embryos or dissected organs were fixed for 45 minutes in 0.1 % glutaraldehyde diluted in PBS, washed three times with wash buffer (2mM MgCl2, 0.2% NP-40, 0.1% Sodium deoxycholate in sodium phosphate buffer) and then incubated O/N at 37˚C in X-gal staining solution (washing buffer + 5mM potassium ferrocyanide, 5mM potassium ferricyanide and 1mg/ml X-Gal substrate). For analysis on sections samples were fixed O/N in 4% paraformaldehyde, embedded in paraffin, cut at 5µM on a microtome, de-paraffinized and counterstained with Eosin.

Immunofluorescence, histological analysis and Sirius red staining

For immunofluorescence experiments, tissues were fixed overnight in 4% paraformaldehyde, progressively dehydrated and embedded in paraffin. 5 µM thick sections were rehydrated, boiled in a pressure cooker for 2 minutes with Antigen Unmasking Solution (Vector laboratories) and blocked in PBS solution containing 10% normal donkey serum and 3% BSA. All antibodies were applied overnight at 4°C at the concentrations listed in the antibody table (see Table S1). Secondary antibodies were diluted 1:400 and applied at room temperature for 1 hour. For histological analysis 5 µM thick sections were stained with haematoxylin and eosin according to standard procedures. For Sirius red staining 5 µM thick sections were stained in Sirius red solution (DSRed powder (SIGMA) dissolved in picric acid) for 1 hour at room temperature. Samples were then washed in acidified water before being dehydrated with three EtOH 100% washes. Tunel stainings were performed as immunofluorescence experiments with the TMRRed *In situ* dell death detection kit (Roche).

Isolation of primary cardiomyocytes and treatment with atRA and BMS493

E18.5 hearts were dissected, minced and then digested in DMEM + Trypsin (100mg/ml) for three times 15 minutes at 37°C with shaking. After each 15 minute incubation, the supernatant was removed and 5ml FBS was added to stop the reaction. After the digestion, all solutions were pooled, run through a 70 µM filter and then spun down for 5 minutes at 1600 rpm at 4°C. The supernatant was then removed and the pellet resuspended in DMEM + 8% FBS. The cells were then plated for 1-2 hours on uncoated plastic wells of 6 well plates for the fibroblasts to adhere. The non-adhered cells containing the cardiomyocytes were then resuspended and plated on collagen coated (50 µg/ml) wells of 6 well plates. The next day the media was switched and the cardiomyocytes grown until 50-60% before being treated. For atRA (SIGMA) and BMS493 (TOCRIS) treatments, solutions were diluted in 100% EtOH at 10mM before being added directly to the media at final concentrations of 100nM (atRA (RNASseq) or 1µM (BMS493 and atRA (qPCR analysis)).

RT-qPCR

RNA was extracted from E16.5 hearts and primary cardiomyocytes using TRIzol® reagent (Invitrogen), following the manufacturer's instructions. Reverse transcription was performed using the M-MLV reverse transcriptase in combination with oligo (dT) primers (Invitrogen). The cDNA was used as a template for quantitative PCR analysis using the SybrGREEN® Master Kit (Roche) and a Light Cycler 1.5® (Roche). The expression levels were normalized to *Gapdh*. For each litter or experiment ddCt values were normalized to one control dCt rather than the mean of control delta Cts. Primers (see primer table) were designed on the Universal Probe Library website (Roche).

RNA Sequencing Analysis

Libraries for extracted RNA from primary E185 cardiomyocytes were prepared using the illumina TruSeq RNA IIbrary Kit according to the manufacturer's protocol. Paired end sequencing with an average of 20 million reads per sample was performed with the Illumina HiSeq 2000 at the EMBL sequencing center (Heidelberg, Germany). For gene expression analyses aligned BAM files were analyzed with proprietary Genomatix software with a cutoff value of $p<0.05$.

Quantification of collagen and immunostaining on sections

For the quantification of collagen staining the infarct areas of 7 sections per heart stained with Sirius red were measured with ImageJ software and the areas were then divided by the area of the left ventricular free wall. For RALDH2 and phospho-ERK1/2 expression the stained areas for 5 sections per heart were measured with ImageJ software and then divided by the area of the left ventricular free wall. For Tunel and BrdU stainings the number of positive cells were calculated for 5 sections per heart with ImageJ software and then divided by the total number of cells for the left ventricular free wall. All sections were spaced by at around 40 µM, covering a total area of at least 250-400 µM for all analyses.

Statistical Analyses

Statistical Analyses were performed according to the two tailed unpaired Student's t-test, $*p<0.05$ $**p<0.01$, $***p<0.001$. Error estimates are expressed as either Standard deviation (SD) or Standard error of mean (SEM). Details of the statistical analyses and the programs used for quantification can be found in the figure legends. The letter "n" refers to the number of individual samples/hearts (embryonic dissections and myocardial infarctions) or the number of wells (in vitro experiments).

AUTHOR CONTRIBUTIONS

F.D.S. and A.S. designed the project. F.D.S. carried out all experiments, if not otherwise stated. F.J.M performed all of the surgeries. The RARE transgenic construct was kindly provided by N.G and P.D. K.D.W. and A.S.R. provided critical input for experimental design and data analysis. F.D.S. and A.S. wrote the manuscript, and all authors provided editorial input.

ACKNOWLEDGEMENTS

We would like to thank the staff of the animal facility for their dedication. We are indebted to Pascal Dolle and Norbert Ghyselinck for providing the RARE construct.

SOURCES OF FUNDING

This work was supported by grants from the Fondation du France, ARC (SL22020605297) and the ANR (ANR-ADSTEM & ANR-11-LABX-0028-01).

REFERENCES

1) Aisagbonhi, O. et al. (2011). Experimental myocardial infarction triggers canonical Wnt signaling and endothelial-to-mesenchymal transition. Dis Mod and Mec. *483*, 469–483.
2) Bilbija, D. et al. (2012). Retinoic Acid Signalling Is Activated in the Postischemic Heart and May Influence Remodelling. PLoS ONE *7*, 1–9.
3) Brade, T. et al (2011). Retinoic acid stimulates myocardial expansion by induction of hepatic erythropoietin which activates epicardial Igf2. Development *138*, 139–148.
4) Dollé, P. et al. (2010). Fate of retinoic acid-activated embryonic cell lineages. Developmental Dynamics *239*, 3260–3274.
5) Fan, X. et al. (2003). Targeted disruption of Aldh1a1 (Raldh1) provides evidence for a complex mechanism of retinoic acid synthesis in the developing retina. Moll Cell Biol. *23*, 4637-4648.

6) Guleria, R.S. et al. (2011). Retinoic acid receptor-mediated signaling protects cardiomyocytes from hyperglycemia induced apoptosis: Role of the renin-angiotensin system. Journal of Cellular Physiology *226*, 1292–1307.

7) Hayashi, S. & McMahon, A.P. (2002). Efficient Recombination in Diverse Tissues by a Tamoxifen-Inducible Form of Cre: A Tool for Temporally Regulated Gene Activation/Inactivation in the Mouse. Developmental Biology *244*, 305–318.

8) Jenkins, S.J., Hutson, D.R. & Kubalak, S.W. (2005). Analysis of the proepicardium-epicardium transition during the malformation of the RXRα-/- epicardium. Developmental Dynamics *233*, 1091–1101.

9) Lavine, K.J. et al. (2005) Endocardial and epicardial derived FGF signals regulate myocardial proliferation and differentiation in vivo. Developmental Cell *8*, 85–95.

10) Lin, S.-C. et al. (2010). Endogenous retinoic acid regulates cardiac progenitor differentiation. Proceedings of the National Academy of Sciences of the United States of America *107*, 9234–9239.

11) Merki, E. et al. (2005). Epicardial retinoid X receptor alpha is required for myocardial growth and coronary artery formation. Proceedings of the National Academy of Sciences of the United States of America *102*, 18455–18460.

12) Minicucci, M.F. et al. (2010). Tissue vitamin A insufficiency results in adverse ventricular remodeling after experimental myocardial infarction. Cellular Physiology and Biochemistry *26*, 523–530.

13) Moloktov, A. et al., (2006). Retinoic acid guides eye morphogenetic movements via paracrine signaling but is unnecessary for retinal dorsoventral patterning. Development *133*, 1901-1910.

14) Muzumdar, M.D. et al. (2007). A global double-fluorescent Cre reporter mouse. Genesis (New York, N.Y. : 2000) *45*, 593–605.

15) Niederreither, K. & Dollé, P. (2008). Retinoic acid in development: towards an integrated view. Nat. Rev. Genet. *9*, 541–553

16) Niederreither, K. et al. (2001). Embryonic retinoic acid synthesis is essential for heart morphogenesis in themouse. Development *128,* 1019–1031.

17) Palm-Leis, A. et al. (2004). Mitogen-activated protein kinases and mitogen-activated protein kinase phosphatases mediate the inhibitory effects of all-trans retinoic acid on the hypertrophic growth of cardiomyocytes. Journal of Biological Chemistry *279*, 54905–54917.

18) Shen, H. et al. (2015). Extracardiac control of embryonic cardiomyocyte proliferation and ventricular wall expansion. Cardiovasc. Res. *105*, 271–278.

19) Soriano, P. (1999). Generalized *lacZ* expression with the ROSA26 Cre reporter strain. Nat Gen. *21*, 70-71.

20) Stuckmann, I., Evans, S. & Lassar, A.B. (2003). Erythropoietin and retinoic acid, secreted from the epicardium, are required for cardiac myocyte proliferation. Developmental Biology *255*, 334–349.

21) Sun, Y. (2010). Intracardiac Renin-Angiotensin system and myocardial repair/remodeling following infarction. J Mol Cell Card. *48*, 483-489.

22) Szondy, Z. et al. (2006). Tissue transglutaminase (TG2) protects cardiomyocytes against ischemia/reperfusion injury by regulating ATP synthesis. Cell Death and Differentiation *13*, 1827-1829.

23) Tran, C.M. & Sucov, H.M. (1998). The RXRalpha gene functions in a non-cell-autonomous manner during mouse cardiac morphogenesis. Development *125*, 1951–1956.

24) Vermot, J. et al. (2006). Conditional (loxP-flanked) allele for the gene encoding the retinoic acid-synthesizing enzyme retinaldehyde dehydrogenase 2 (RALDH2). Genesis *44*, 155-158.

25) Xavier-Neto, J. et al. (2015). Signaling through retinoic acid receptors in cardiac development: Doing the right things at the right times. Biochimica et Biophysica Acta - Gene Regulatory Mechanisms *1849*, 94–111.

26) Zaffran, S., Robrini, N. El & Bertrand, N. (2014). Retinoids and Cardiac Development. Journal of Developmental Biology *2*, 50–71.

27) Zhu, S. et al. (2016). Loss of myocardial retinoic acid receptor α induces diastolic dysfunction by promoting intracellular oxidative stress and calcium mishandling in adult mice. Journal of Molecular and Cellular Cardiology *99*, 100–112.

28) Zhu, Z. et al. (2015). All-trans retinoic acid ameliorates myocardial ischemia/reperfusion injury by reducing cardiomyocyte apoptosis. PLoS ONE *10,* 1–15.

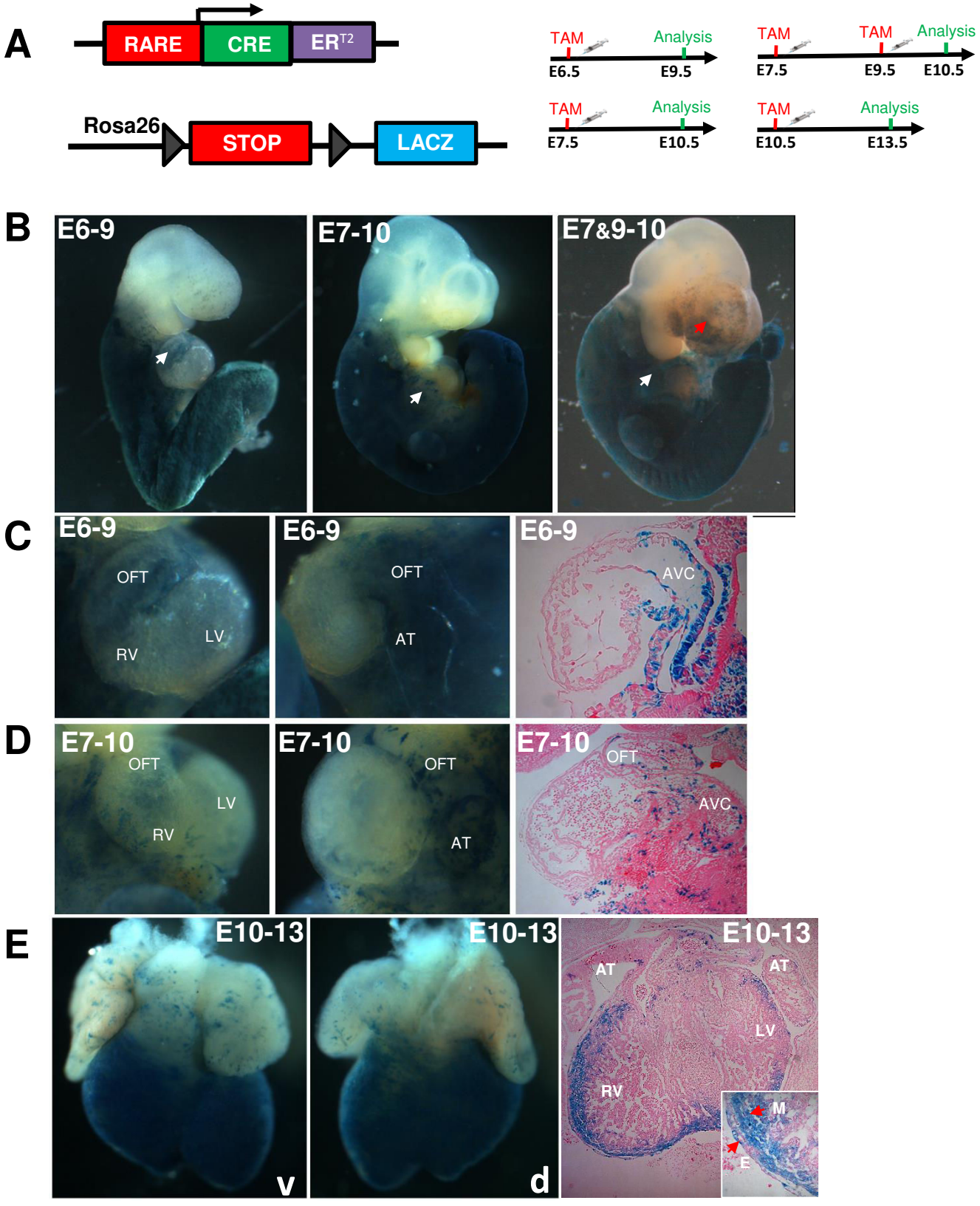

Figure 1, *Da Silva et al.*

Figure 1: *A novel RARECreER^{T2} line recapitulates endogenous Retinoic Acid signaling and reveals dynamic labeling in the heart during mid-late stages of gestation.*

(A) Schematic demonstrating the strategy used to test the novel *RARECreER^{T2}* line during various stages of embryonic development. The *RARECreER^{T2}* line was crossed with the *Rosa26LacZ* (*R26L*) reporter and recombination was induced via tamoxifen (TAM) administration at various time-points. **(B)** Whole-mount X-gal staining of *RARECreER^{T2} R26L* embyros induced at E6 and E7 followed by analysis at E9 and E10 respectively, demonstrates efficient labeling of the posterior region of embryos. An extra pulse at E9 labels parts of the forebrain as well (red arrows). **(C-D)** Analysis of *RARECreER^{T2}* labelled hearts reveals efficient labeling of the venous pole (outflow tract (OFT) and atria (At)) as shown by whole-mount X-gal staining and X-gal/eosin co-staining on sections of hearts at the indicated time-points. **(E)** Tamoxifen administration at E10 followed by analysis at E13 reveals very strong labeling in the ventricles of *RARECreER^{T2}* hearts as demonstrated by whole-mount X-gal staining. Closer inspection on sections stained with eosin reveals that both the myocardial (M) layer and epicardium (E) are positive for X-gal staining. RV= Right ventricle, LV = left ventricle, AVC = Atrioventricular canal, v=ventral, d=dorsal.

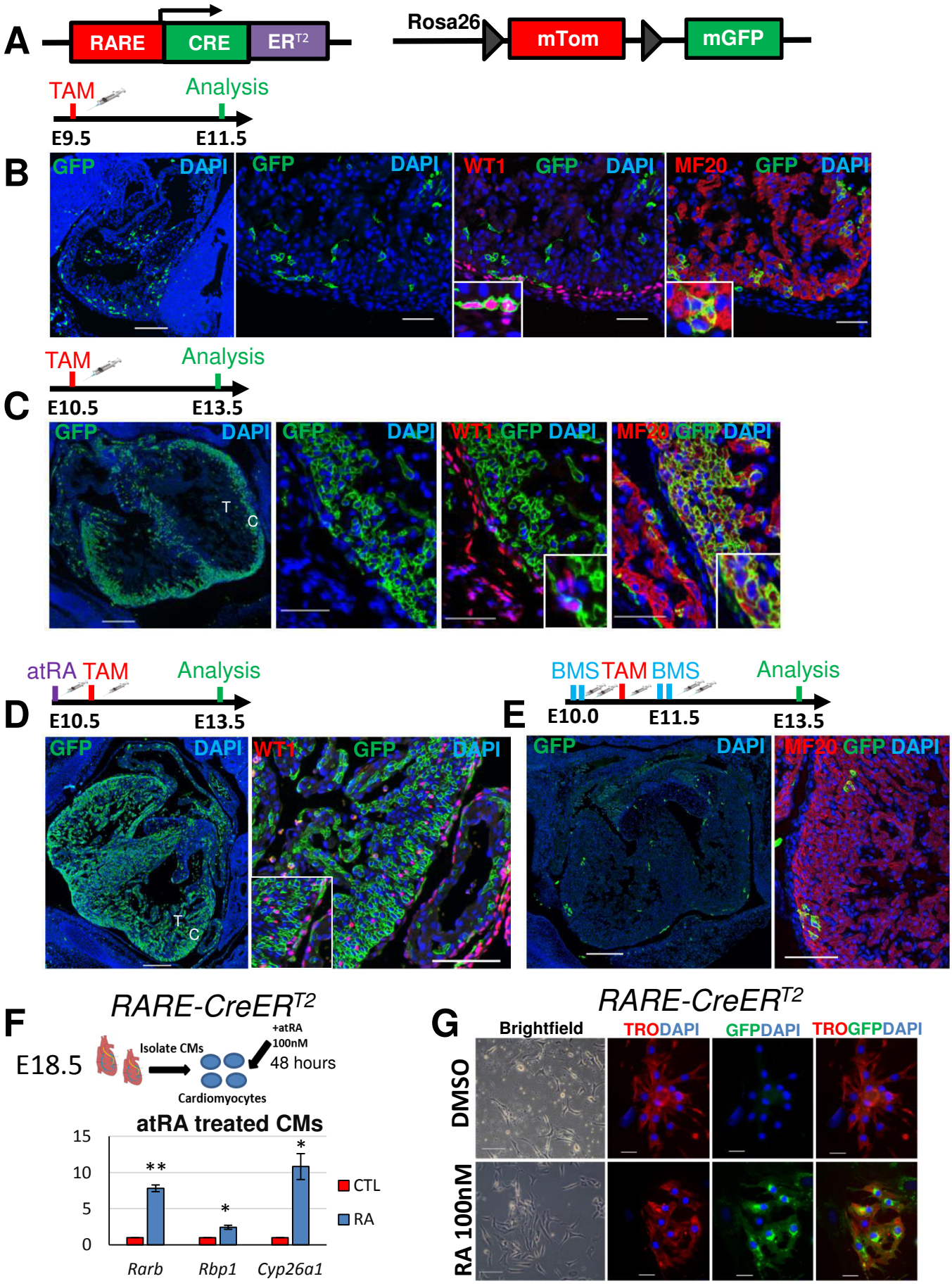

Figure 2, *Da Silva et al.*

Figure 2: *Cardiomyocytes respond directly to Retinoic Acid signaling during mid-late phases of gestation.* **(A)** Schematic demonstrating the use of the *mTmG* reporter line to determine the cell-types responding to RA signaling with the *RARECreER^{T2}* line. **(B)** Administration of tamoxifen (TAM) at E9.5 followed by analysis at E11.5 reveals partial labeling of the epicardium (GFP/Wilms' tumour protein (WT1)-positive cells) and myocardium (GFP/MF20-positive cells). **(C)** Tamoxifen administration at E10.5 followed by analysis at E13.5 reveals very efficient labeling of the compact myocardium (C) in comparison to the trabecular layer (T). The majority of cells labelled are postive for the myocyte marker MF20 and very few WT1-positive cells are positive for GFP. **(D)** Exogenous supplementation of all-trans Retinoic acid (atRA) prior to tamoxifen induction leads to a higher labeling efficiency of the epicardium (WT1-postive cells) at E13.5 when compared to controls. A higher labeling efficeincy of trabecular myocytes is observed as well. (E) Supplementation of the RA reverse agonist BMS493 both before and after tamoxifen induction reveals a drastic decrease in GFP-positive cells of *RARECreER^{T2}* hearts. **(F)** qPCR analysis of primary cardiomyocytes isolated from E18.5 hearts and treated with atRA leads to an upregulation of several canonical RA targets. Data are expressed as fold change vs. controls and columns are means ± SEM. **(G)** *RARECreER^{T2}; mTmG* cardiomyocytes respond directly to atRA treatment and express GFP. TRO = TroponinT, MF20 = Myosain heavy Chain. Scale bars mosaics: 200 µM, Close ups: 100 µM. Two tailed t-test assuming unequal variance, *p<0.05, **p<0.01.

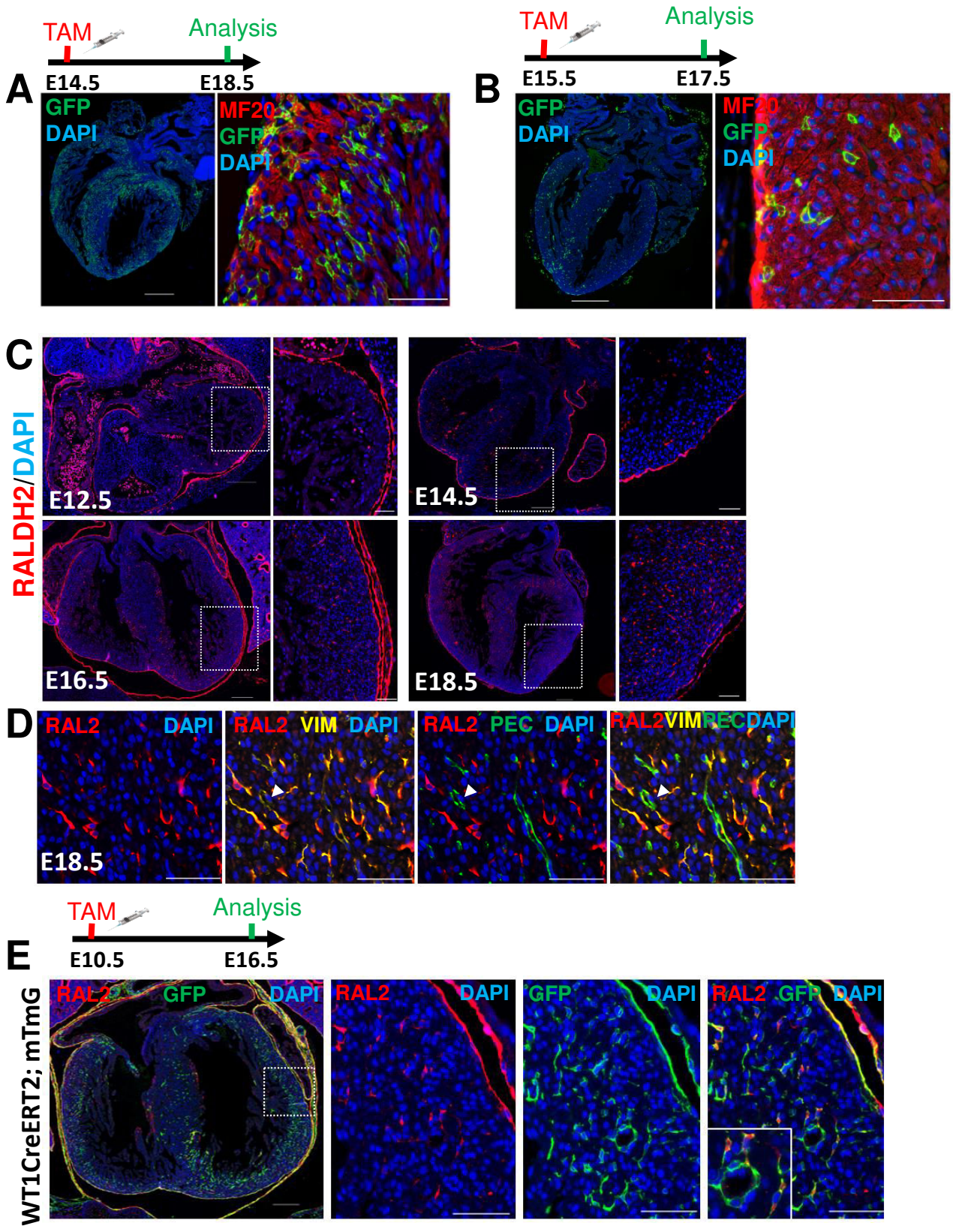

Figure 3, *Da Silva et al.*

Figure 3: *Cardiomyocytes respond to RA during late stages of development and RALDH2 is expressed by cardiac fibroblasts after E14.5* **(A)** Administration of tamoxifen (TAM) at E14.5 followed by analysis at E18.5 reveals cardiomyocyte-specific (MF20-positive) labeling with the *RARECreER^{T2}* line. **(B)** Tamoxifen administration at E15.5 labels cardiomyocytes deep within the ventricular wall when analyzed two days later. **(C)** Immunostaining with an anti-RALDH2 antibody reveals RALDH2 expression is restricted to the epicardium at E12.5. After E14.5 RALDH2 is expressed within the free ventricular wall. Very high RALDH2 expression in the ventricular wall is observed at E16.5 and E18.5. **(D)** Co-immunostaining with VIMENTIN and PECAM antibodies reveals RALDH2 is expressed by cardiac fibroblasts (VIMENTIN positive) and not by endothelial cells (VIMENTIN/PECAM positive, white arrowheads). **(E)** Administration of tamoxifen to embryos carrying the *WT1CreER^{T2}* and *mTmG* alleles followed by analysis at E16.5 reveals many of the RALDH2 positive cells within the ventricular free wall are derived from the epicardium (GFP-positive). Scale bars mosaics: 200 µM, Close ups: 100 µM.

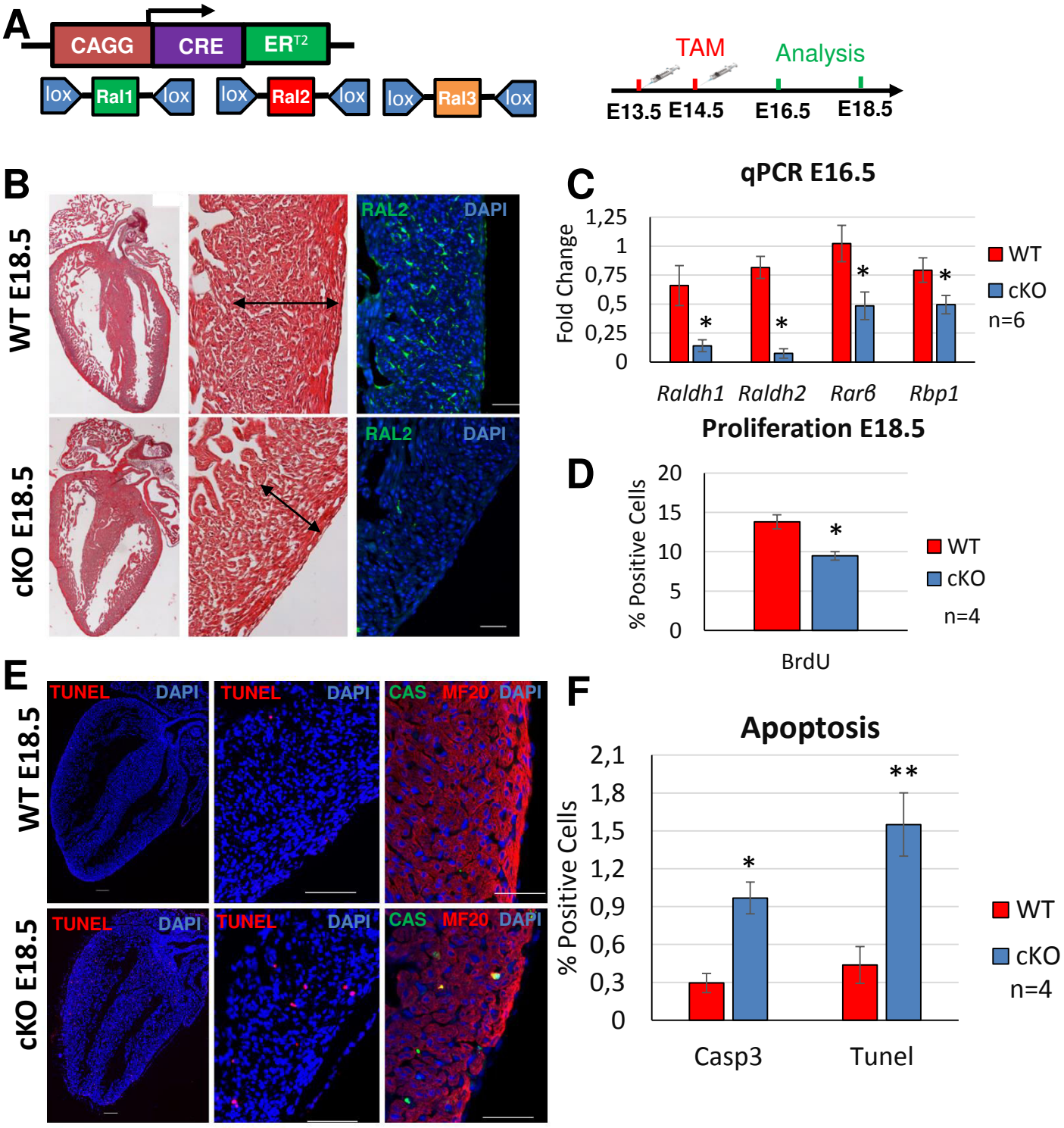

Figure 4, *Da Silva et al.*

Figure 4: *Late stage deletion of the Raldh enzymes leads to myocardial thinning and apoptosis* **(A)** Schematic demonstrating the strategy used to delete floxed alleles of the three *Raldh* enzymes (*Raldh1*, *Raldh2* and *Raldh3*) during late stages (E13.5) of embryonic development**. (B)** Administration of tamoxifen (TAM) at E13.5 and E14.5 followed by analysis at E18.5 reveals efficient deletion of RALDH2 levels in *Raldh1,2,3* conditional knockouts (cKO) as demonstrated by immunostaining with an anti-RALDH2 antibody. H&E staining demonstrates slight myocardial thinning in cKOs when compared to controls **(C)** qPCR analysis of cKO hearts reveals efficient deletion of *Raldh1* and *Raldh2.* The canonical RA target genes Rarβ and Retinol binding protein 1 (*Rbp1*) are also down-regulated in cKO hearts. Data are expressed as fold change vs. controls and columns are means ± SEM. **(D)** Immuostaining with an anti-BrdU antibody reveals decreased total proliferation rates in cKO hearts. **(E)** TUNEL and active caspase3 stainings reveal increased apoptosis in cKO hearts. Many of the aopototic cells are cardiomyocytes as demonstrated by active caspase3/MF20 co-staining**. (F)** Quantification of the percentage of apoptotic cells reveals a drastic increase in cKO hearts. Data are means ± SEM. All scale bars 100 μM. Two tailed t-test assuming unequal variance, *$p<0.05$, **$p<0.01$.

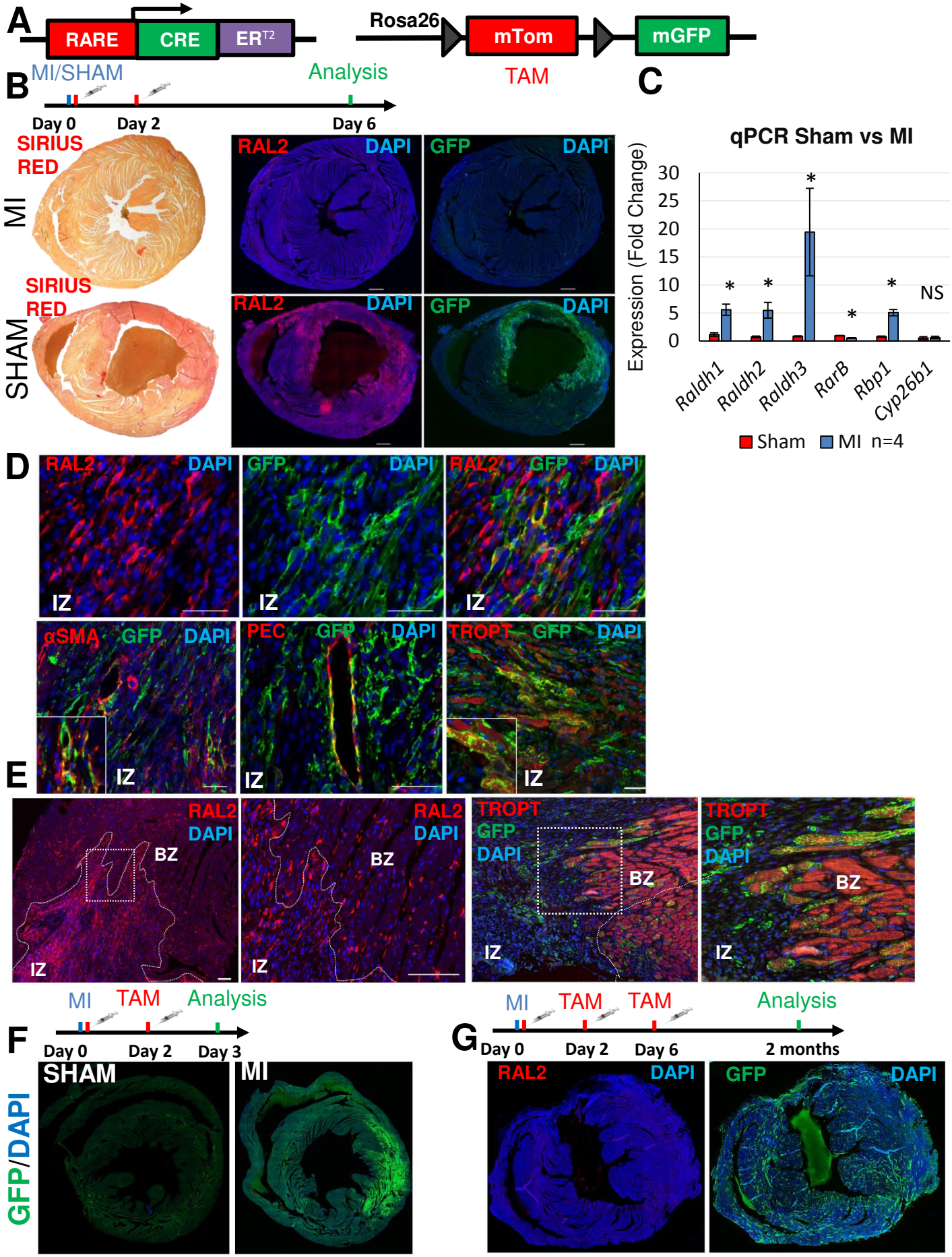

Figure 5, *Da Silva et al.*

Figure 5: *RA signaling is active in adult hearts post myocardial infarction* **(A-B)** Schematic demonstrating lineage tracing performed in *RARECreER^{T2}*: mTmG mice subjected to MI. Tamoxifen was administered twice (30 minutes and 48 hours after surgery) and hearts were analyzed 1 week post MI. Immunostaining reveals RALDH2 and GFP are highly expressed in and around the infarct zone (marked by Sirius Red staining). Very little RALDH2 or GFP staining is present in sham hearts. **(C**) qPCR analysis of the bottom halves of hearts demonstrates upregulation of the three *Raldh* enzymes in MI mice when compared to sham controls. The RA target *Rbp1* is also upregulated in MI hearts. Data are expressed as fold change vs. controls and columns are means ± SEM. **(D)** Immunostaining with RALDH2 and GFP antibodies demonstrates minimal co-staining suggesting the RA-response detected with the *RARECreER^{T2}* line works primarily in an autocrine manner. Co-staining of GFP with αSMA, PECAM1 and TROPONIN-T antibodies demonstrates an RA response in activated fibroblasts, coronary vessels and cardiomyocytes respectively. **(E)** Closer analysis of RALDH2 and GFP staining demonstrates both are expressed within the infarct zone as well as the border zone in MI hearts. **(F**) Analysis of infarct hearts 3 days after surgery shows high GFP staining around the infarct area. Very little staining in detected in sham hearts. **(G)** Long term lineage tracing (2 months) of *RARECreER^{T2}* mice subjected to MI demonstrates a strong and wide response to RA signaling that extends beyond the infarct zone. RAL2 = RALDH2, TROPT = TROPONIN-T, SMA=smooth muscle actin. Two tailed t-test assuming unequal variance, *$p<0.05$, **$p<0.01$.

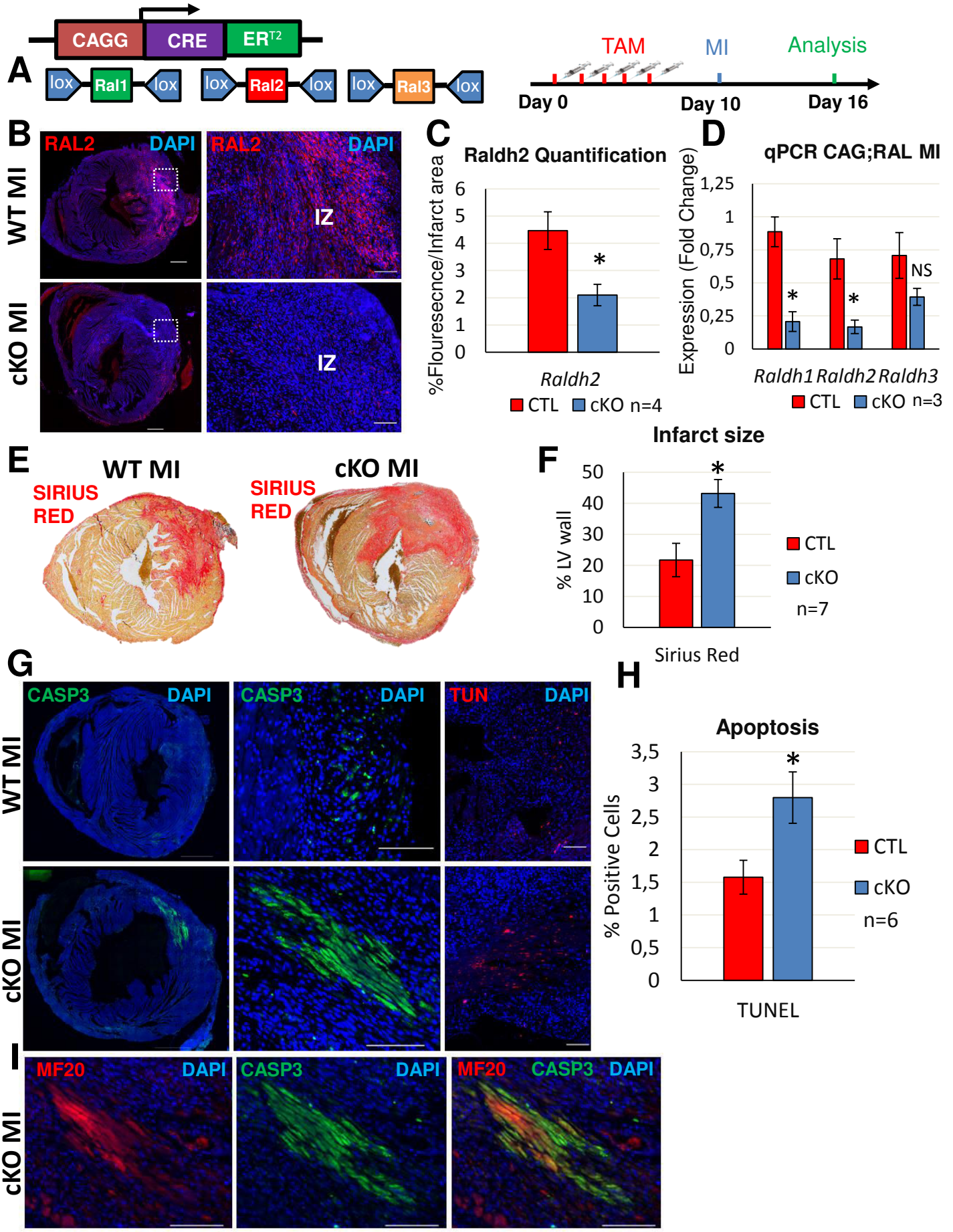

Figure 6, *Da Silva et al.*

Figure 6: *Ablation of Raldh enzymes leads to increased damage and apoptosis in cKO hearts subjected to MI.* **(A)** Schematic demonstrating strategy used to delete floxed alleles of the *Raldh* enzymes with the *CAGGCreERTM* line. Five doses of Tamoxifen were administered 1 week prior to surgery and operated hearts were analyzed 1 week post MI. **(B)** Immunostaining analysis reveals a significant decrease of RALDH2 expresssion in cKOs when compared to *CAGGCreER*^{TM} negative (Wildtype(WT)) hearts. **(C)** Quantification of RALDH2 staining reveals a 50% decrease in cKO hearts. RALDH2 area was measured using ImageJ software, and was then divided by the infarct area. Columns are means ± SEM. **(D)** qPCR analysis of RNA extracted from bottom halves of infarct hearts reveals significant decreases in *Raldh1* and *Raldh2* expression in cKOs when compared to WT controls. Data are expressed as fold change vs. controls and columns are means ± SEM. **(E)** Sirius red staining demonstrates an increase in collagen deposition and infarct size in cKO hearts when compared to WT controls. (F) Quantification of infarct size in cKOs and WT hearts. The infarct areas were measured with ImageJ software. Columns are means ± SEM. **(G)** Active caspase3 and Tunel stainings reveal increased apoptosis in cKO hearts when compared to WT controls. cKOs have visible “patches“ of apoptotic cells. (H) Quantification of Tunel positive cells was done using ImageJ software. Columns are means ± SEM. **(I)** Apoptotic “patches“ present in cKOs are positive for the cardiomyocyte marker MF20. RAL2 = RALDH2, CASP3 = active caspase 3, TUN = Tunel. Two tailed t-test assuming unequal variance, *$p<0.05$.

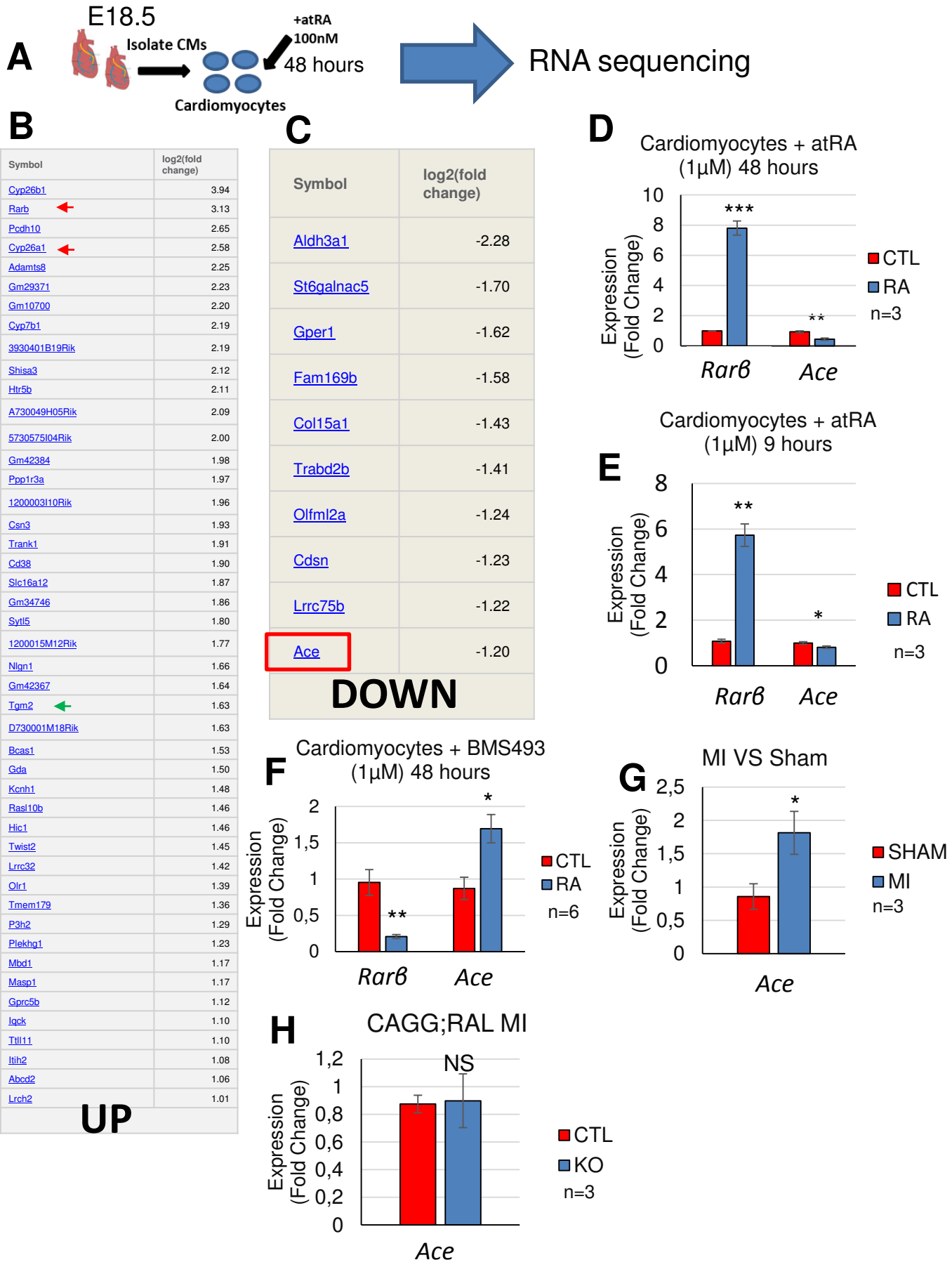

Figure 7, *Da Silva et al.*

Figure 7: *RNA sequencing of primary cardiomyocytes demonstrates Ace1 is down-regulated by atRA treatment.* **(A)** Schematic demonstrating strategy used to isolate primary cardiomyocytes from E18.5 hearts. Cultured cardiomyocytes were treated for 48 hours with 1μM atRA. RNA was extracted, libraries were prepared with oligodt primers and single paired end sequencing was performed on atRA-treated and control cells. **(B-C)** Analysis of RNA sequencing results reveals upregulation of several canonical RA targets (*Rarβ, Cyp26a1* etc.) (B) and repression of Angiotensin converting enzyme 1 (Ace1) **(C)**. Analysis was done using proprietary Genomatix software. **(D-E)** qPCR analysis of atRA treated cardiomyocytes confirms repression of *Ace1* mRNA levels both with long 48 hour **(D)** and short 9 hour **(E)** treatments. **(F)** Treatment of cardiomyocytes with the RA signaling reverse agonist BMS493 for 48 hours reveals an increase in *Ace1* expression levels according to qPCR analysis. **(G)** qPCR analysis of the bottom halves of MI hearts reveals an increase in *Ace1* expression when compared to sham controls. (H) cKO MI bottom halves of hearts show no differences in *Ace1* mRNA levels when compared to controls. For all graphs data are expressed as fold change vs. controls and columns are means ± SEM. ACE = angiotensin converting enzyme 1. Two tailed t-test assuming unequal variance, *$p<0.05$.

SUPPLEMENTAL INFORMATION INVENTORY

Figure S1, related to Figures 1, 2 and 5: *A secondary RARECreER^{T2} B line demonstrates a similar response as the original line and treatment of adults with atRA and BMS493 elicits strong RA activation and repression respectively, in cardiomyocytes.* This figure examines the RA response of a second RARECreER^{T2} line (line B). It also tests the activation/repression of the RARE line in adults with atRA and BMS493 treatments respectively.

Figure S2, related to Figure 4: *Deletion of Raldh enzymes during late gestation leads to myocardial thinning and decreased proliferation.* This figure provides more detail on the myocardial thinning and decreased proliferaton (BrdU staining) observed in *Raldh1/2/3*-null E18.5 hearts.

Figure S3, related to Figure 4: *Analysis of Raldh1/2/3 cKO hearts reveals decreased proliferation and increased apoptosis just 3 days after deletion* This figure looks at apoptosis and myocardial thinning in Raldh1/2/3 null hearts at an earlier time-point (E16.5).

Figure S4, Related to Figure 6: *The CAGGCreER^{TM} line works very effectively in adult hearts.* This figure looks at the recombination efficiency of the *CAGGCreER^{TM}* in adult hearts using the mTmG reporter line.

Figure S5, Related to Figure 6: *Raldh1/2/3fl cKO sham hearts do not display any adverse effects and have consistently larger infarcts when compared to wildtype controls.* This figure looks at the effects of deleting the Raldh genes on sham operated hearts. It also provides more details about the infarct areas of several *Raldh1/2/3* cKO and control hearts.

Figure S6, Related to Figure 6: *Primary cardiomyocytes treated with atRA and BMS493 do not display differences in Adam10 expression and Raldh1/2/3 cKO hearts do not display any significant differences in phospho-ERK1/2 expression.* This figure looks at Adam10 expression in cell culture experiments. It also looks at phopho-ERK1/2 expression in *Raldh1/2/3* cKO and control hearts.

Antibodies table: List of antibodies used in this study.

Primers table: Complete list of primers used for qPCR analysis in this study.

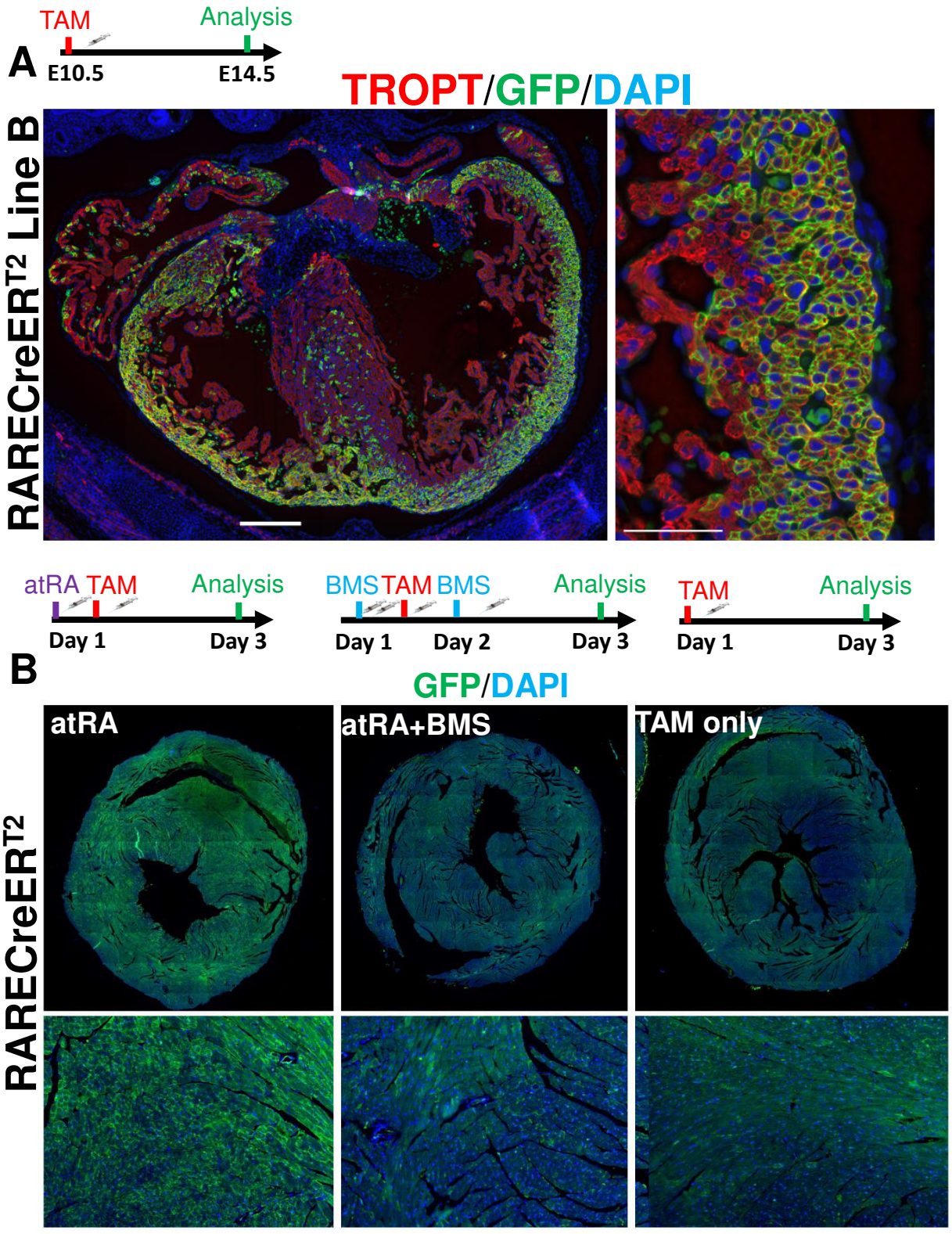

Figure S1, *Da Silva et al.*

Figure S1: *A second RARECreER^{T2} B line demonstrates a similar response as the original line and treatment of adults with atRA and BMS493 elicits strong RA activation and repression respectively, in cardiomyocytes.* **(A)** Administration of tamoxifen at E10.5 to embryos containing the *RARECreER^{T2}* B allele demonstrates a strong cardiomyocyte response in the compact zone when analyzed at E14.5. **(B)** *In vivo* atRA and BMS493 treatment up and down-regulate respectively a cardiomyocyte-specific response in adult hearts. Treatments were performed as described in figure schematics. TROPT = Troponin-T, BMS = BMS493. Scale bars mosaics: 200µM, close ups 100µM.

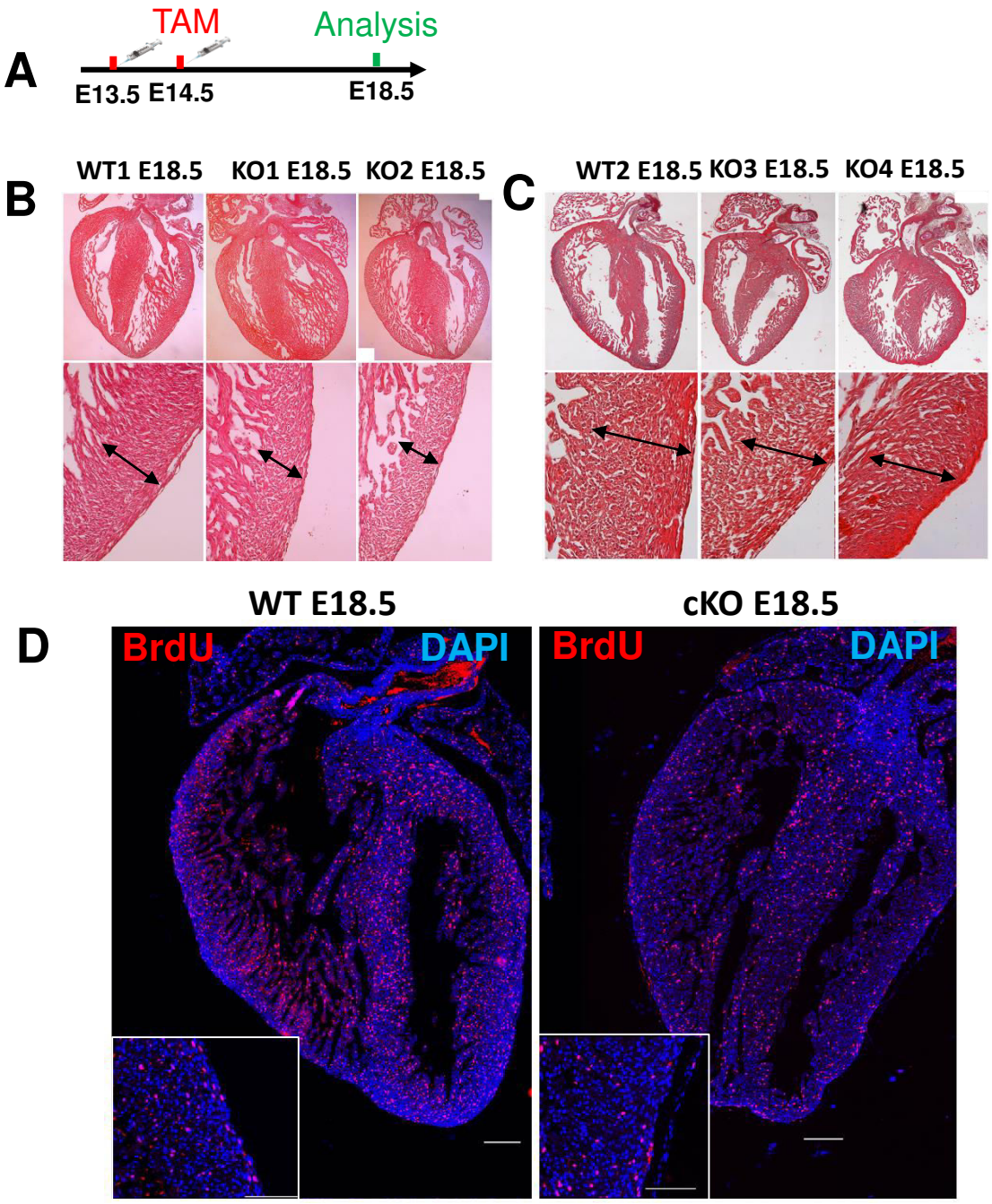

Figure S2, *Da Silva et al.*

Figure S2: *Deletion of Raldh enzymes during late gestation leads to myocardial thinning and decreased proliferation.* **(A)** Schematic demonstrating deletion of *Raldh* enzymes with *CAGGCreER*^{TM} line during late development. **(B-C)** H&E staining of cKO and WT hearts at E18.5 from two different litters (B = 1st litter; C = 2nd litter) demonstrates variable myocardial thinning in cKO hearts. **(D)** BrdU staining demonstrates decreased proliferation rates in cKO hearts at E18.5. Scale bars mosaics: 200μM**.**

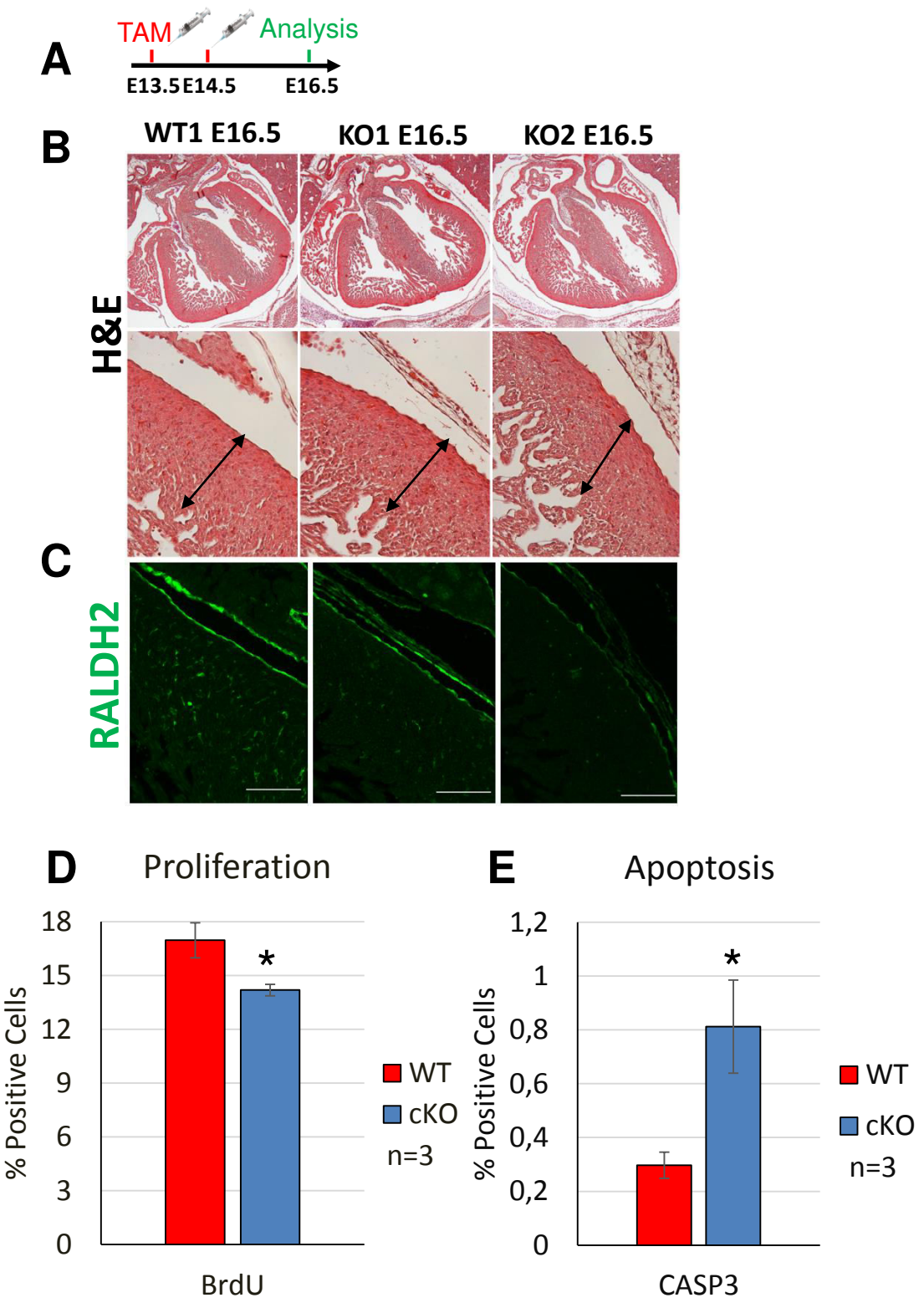

Figure S3, *Da Silva et al.*

Figure S3: *Analysis of Raldh1/2/3 cKO hearts reveals decreased proliferation and increased apoptosis just 3 days after deletion*. (A) Schematic demonstrating early analysis of *Raldh1/2/3* cKO hearts. **(B)** H&E staining does not demonstrate any serious differences in the thickness of the compact layer in cKO hearts when compared to controls. (C) Although RALDH2 levels are significantly reduced in cKOs, the enzyme is still detectable. **(D-E)** Despite detectable levels of RALDH2 decreased proliferation and increased apoptosis is detected in cKO hearts as demostrated by BrdU and Active Caspase 3 stainings respectively. Columns are means ±SEM. Two tailed t-test assuming unequal variances, *$p<0.05$.

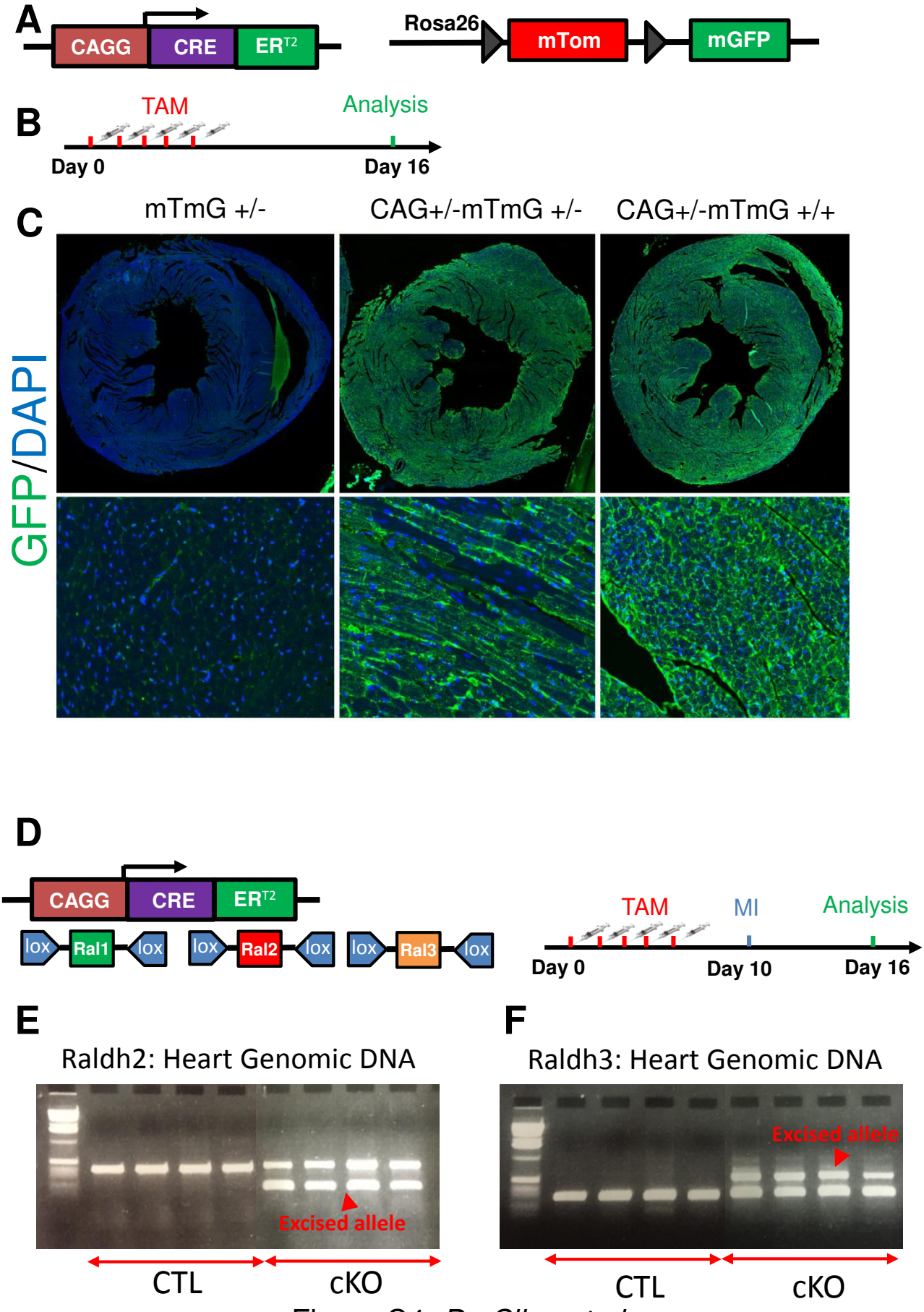

Figure S4, *Da Silva et al.*

Figure S4: *The CAGGCreER^{TM} line works very effectively in adult hearts.* **(A)** Schematic demonstrating strategy used to test the recombination efficiency of the *CAGGCreER^{TM}* line with the *mTmG* reporter allele. **(B)** Tamoxifen was administered 5 times to *CAGGCreER^{TM}:mTmG* adult males and hearts were sacrificed two weeks later. **(C)** GFP immunostaining of *CAGCreER^{TM}:mTmG* hearts reveals very efficient recombination. **(D-F)** Analysis of genomic heart DNA from *Raldh1,2,3* cKO adults subjected to MI reveals efficient excision of floxed *Raldh2* **(E)** and *Raldh3* **(F)** alleles (red arrowheads). Amplification of the non-excised alleles still occurs suggesting incomplete recombination in cKO hearts.

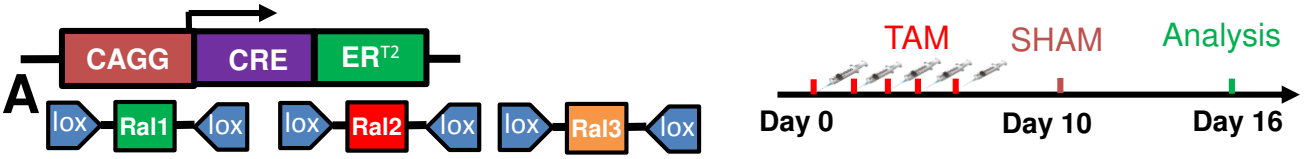

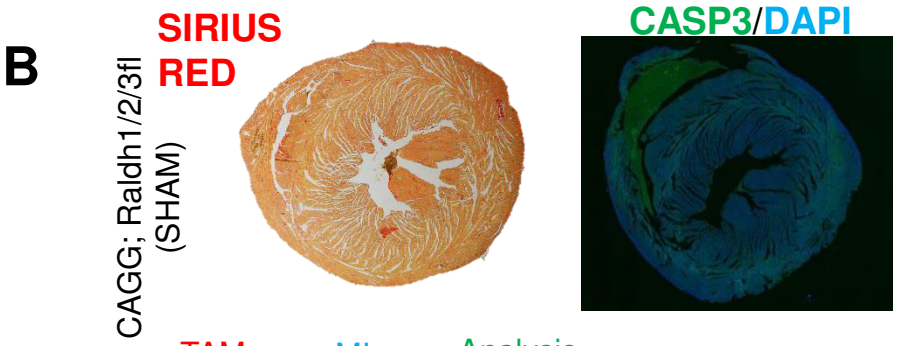

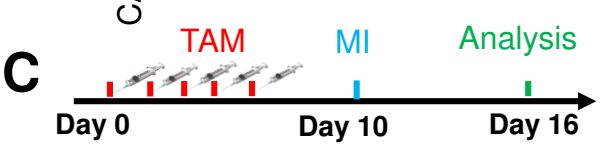

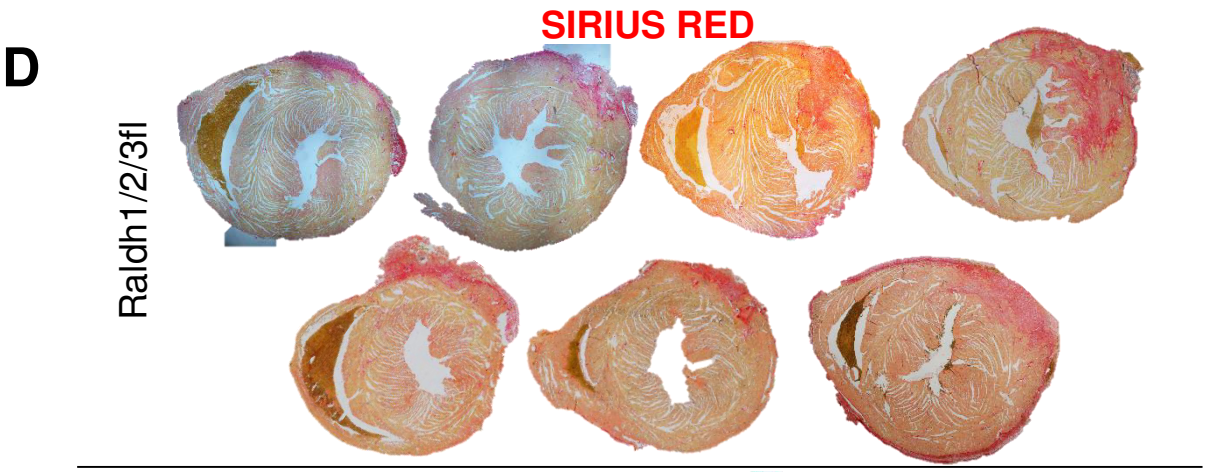

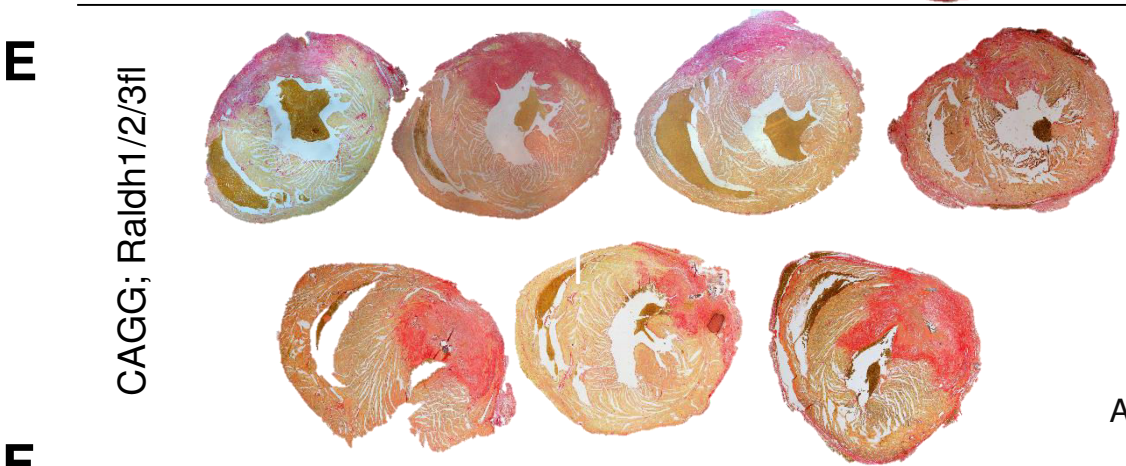

F

Genotype	No. of Surgeries	Early Death	Apoptotic Patches
Raldh1/2/3 fl	11	0	1
CAGG;Raldh1/2/3 fl	10	3	4

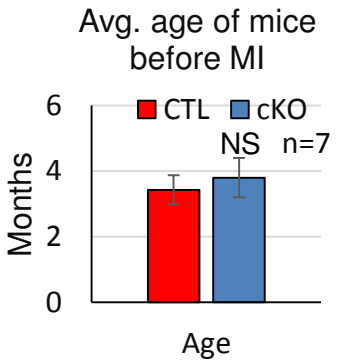

Figure S5, *Da Silva et al.*

Figure S5: *Raldh1/2/3fl cKO sham hearts do not display any adverse effects and cKO hearts subjected to MI have consistently larger infarcts when compared to controls* **(A)** Schematic demonstrating deletion of *Raldh* alleles with the *CAGGCreER^{TM}* line. **(B)** cKO sham hearts do not display any adverse remodeling defects or apoptosis as shown by sirius red and active caspase 3 immunostaining. **(C-E)** Sirius red staining of various MI hearts reveals consistently larger infarct sizes in cKO (CAGG; Raldh1/2/3fl) **(D)** hearts when compared to wildtype (Raldh1/2/3fl) hearts. **(F)** cKO MI hearts exhibit a higher incidence of early death (prior to analysis at 6 days post MI) and more “apoptotic patches”. Surgeries were performed on mice of similar age for cKOs and WTs.

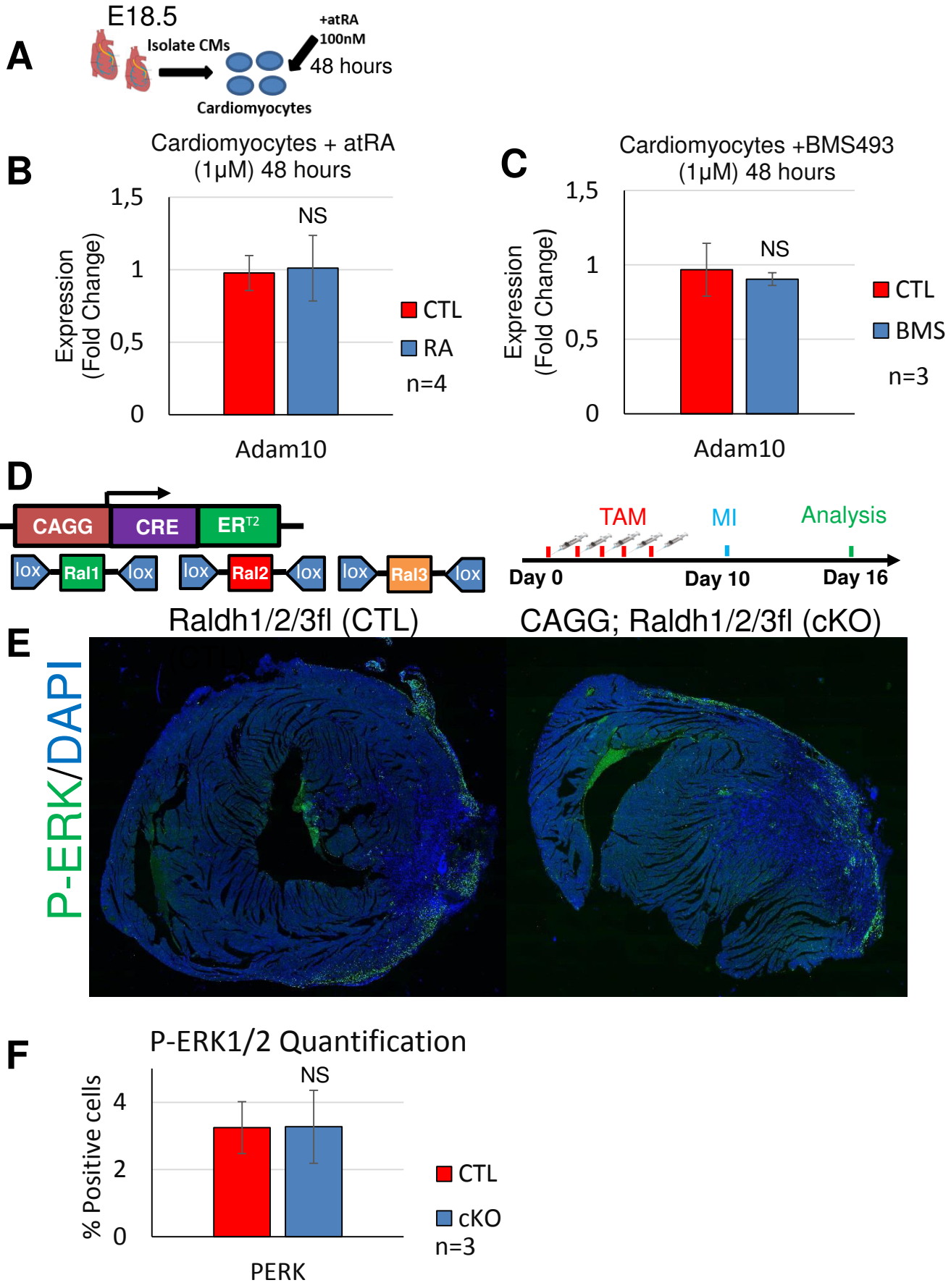

Figure S2, *Da Silva et al.*

Figure S6: *Primary cardiomyocytes treated with atRA and BMS493 do not display differences in Adam10 expression and Raldh1/2/3 cKO hearts subjedted to MI do not display any significant differences in phospho-ERK1/2 expression* **(A)** Schematic demonstrating isolation of primary cardiomyocytes from E18.5 hearts. **(B)** qPCR analysis of primary cardiomyocytes treated with atRA demonstrates no difference in *Adam10* expression. **(B)** qPCR analysis of primary cardiomyocytes treated with the RA reverse agonist inhibitor BMS493 demonstrates no difference in *Adam10* expression. **(D-E)** No differences in phospho-ERK1/2 expression is detected between *Raldh1/2/3* cKO and control MI hearts as demonstrated by immunostaining. (F) Quantification of phospho-ERK1/2 levels displays no significant differences between cKO and WT hearts. Phospho-ERK1/2 areas were measured using ImageJ software. Columns are means ± SEM.

SUPPLEMENTAL TABLES:

Antibodies table, related to Experimental Procedures: List of Antibodies used in this study

Protein	**Host**	**Type**	**Dilution**	**Secondary**	**Manufacturer**
PECAM	Goat	polyclonal	1:200	AlexaFluor 647	Santa Cruz
RALDH2	Rabbit	polyclonal	1:300	AlexaFluor 555	Sigma
SM22α	Rabbit	polyclonal	1:400	AlexaFluor 555	Abcam
GFP	Chicken	polyclonal	1:400	AlexaFluor 647	Abcam
MF20	mouse	monoclonal	1:20	AlexaFluor 555	DSHB
αSMA	mouse	monoclonal	1:500	AlexaFluor 555	Santa Cruz
BrdU	mouse	monoclonal	1:250	AlexaFluor 555	BD Bioscience
WT1	mouse	monoclonal	1:100	AlexaFluor 555	Dako
VIMENTIN	Chicken	Abcam	1:1000	AlexaFluor 555	Abcam
Active caspase3	Rabbit	polyclonal	1:200	AlexaFluor 647	R & D
Phospho-ERK1/2	Rabbit	polyclonal	1:400	Donkey anti Rabbit HRP Santa Cruz	Cell Signaling
TROPONIN-T	Mouse	monoclonal	1:300	AlexaFluor 555	Invitrogen

Primers table, related to Experimental Procedures: List of primers used for qPCR analysis in this study

Name	**Sequence**	**Direction**	**Usage**
Rarβ right	GTCAGCGCTGGAATTCGT	antisense	qPCR
Rarβ left	CACCGGCATACTGCTCAA	sense	qPCR
Rbp1 right	TCTCCCTTCTGCACACACTG	antisense	qPCR
Rbp1 left	GCCATTGGCCTTCACACT	sense	qPCR
Cyp26a1 right	GGAGCTCTGTTGACGATTGTT	antisense	qPCR
Cyp26a1 left	CCGGCTTCAGGCTACAGA	sense	qPCR
Raldh1 right	CATCTTGAATCCACCGAAGG	antisense	qPCR
Raldh1 left	GCCATCACTGTGTCATCTGC	sense	qPCR
Raldh2 right	GGCAGGATATTGACGACTCC	antisense	qPCR
Raldh2 left	TGAGCAGACACCGCTCAGT	sense	qPCR
Raldh3 right	AGTCGGTGCTATTCGCTCTC	antisense	qPCR
Raldh3 left	TGAGGATTGCCAAAGAGGA	sense	qPCR
Cyp26b1 right	CACTTTGCCCAGGAGGAAT	antisense	qPCR
Cyp26b1 left	CAGAAGGAAGTCTGGGCTTG	sense	qPCR
Ace1 right	TGCAGCTCCTGGTACAGTTTT	antisense	qPCR
Ace1 left	AAGATTGCCAAGCTCAATGG	sense	qPCR
Adam10 right	CTCAGGACCACTACTAGCAGCA	antisense	qPCR
Adam10 left	CCGTTTTTGAAAGGATGAGG	sense	qPCR

IV. Future perspectives

Novel functions for Retinoic Acid in cardiac development and repair

For this project I have shown that cardiomyocytes respond directly to Retinoic Acid (RA) signaling by performing a series of lineage tracing experiments with the novel *RARECreER^{T2}* line. Furthermore, by deleting the *Raldh1/2/3* enzymes I demonstrated that RA plays a protective role in cardiomyocytes by preventing apoptosis during late development and after Myocardial Infarction (MI).

A key point demonstrated here is that, contrary to previous studies, RA signaling acts directly on cardiomyocytes during myocardial compaction (E11.5-14.5). A second key point is that this role extends well beyond E14.5, to later phases of gestation. A third key point refers to cardio-protection, as deletion of the *Raldh1/2/3* enzymes leads to increased cardiomyocyte apoptosis in both late development and after MI. Unfortunately, for these studies I was not able to delve very deeply into the underlying mechanisms driving the cardio-protective effects of RA. Analysis of the RNA seq data did lead to the identification of some interesting targets such as *Ace1*, but it is likely that the scenario is much more complex. Hence, many questions remain to be answered.

One outstanding question can be phrased as follows: What are the mechanisms driving the increased apoptosis observed in *Raldh1/2/3* cKOs? A major issue with our strategy to ablate RA signaing relates to the *Cre* line used. The *CAGGCreER^{TM}* line deletes all three RALDH enzymes ubiquitously. Since the RALDH enzymes (especially RALDH2) play essential roles in many different organ systems, it is possible that the increase in cell death may be due to indirect effects. For example, RALDH ablation during development could affect the placenta, liver or vasculature of the embryo, and this could somehow be the primary cause of the observed heart defects. The late time-point of the deletion (E13-14), coupled with the fact that we observe no differences in *Igf2* expression would argue against this. The detection of apoptosis at E16.5, just

3 days after deletion, along with the high expression of RALDH2 in cardiac fibroblasts after E14.5 would also support the hypothesis that RA signaling prevents myocyte apoptosis.

The increase in apoptosis coupled with the slight decrease in proliferation suggests activation of the DNA damage response. This is in line with previous reports that suggest RA signaling alleviates oxidative stress in the heart. However, we did not detect any obvious differences in *Sod1* or *Sod2* expression in our cKO hearts or RNA seq data. Both of these genes play essential roles in the cell's response to free radical accumulation, and both have been shown to be regulated by RA in the myocardium of adult hearts (Zhu et al., 2016). Why they are not affected in our developmental and MI models is unclear. Interestingly, *Sod3* expression was determined to be down-regulated in the RNA-seq analysis. SOD3 is active in the extracellular space of cells and usually relieves oxidative stress. *Sod3* expression was increased in cKO hearts during development, but whether or not this is relevant remains to be seen. We did detect a slight increase in *Nox2* expression by qPCR, but this was not supported at the protein level as a western blot on lysates of cKO hearts did not yield any significant differences. We also did not detect any differences in phospho-Histone H2A, a faithful marker of DNA damage.

Aside from oxidative stress, RA has also been shown to regulate FGF signaling in the heart. We analyzed expression of several FGF ligands such as *Fgf2*, *Fgf9* or *Fgf16* and did not observe any differences. We also did not observe any differences in the FGFR receptors *Fgfr1* and *Fgfr2b/c*. As mentioned previously, *Igf2* expression was also not altered, nor was its receptor *Igf2r*.

The difficulty with identifying direct transcriptional targets in these studies may be related to the design of the RNA-seq experiments. We treated primary cardiomyocytes isolated from E18.5 hearts with atRA for 48 hours to mimic long-term exposure to RA. However, in hindsight, this was perhaps not the most suitable strategy, and there are two major reasons for this. The first, relates to the purity of the samples. Plating digested heart cells on uncoated wells ensures a large proportion of the fibroblasts adhere to the plastic, while the cardiomyocytes, which only

adhere to coated plates, remain suspended in solution. Re-plating the suspended cells on collagen-coated plates allows the cardiomyocytes to adhere. This leads to a partial enrichment of cardiomyocytes, but other cell types such as endothelial cells, smooth muscle and even some fibroblasts that did not initially bind to the plastic, may be carried over to the purified fraction. Hence, the changes in gene expression observed in the RNA seq analysis may be reflective of multiple cell-types rather than just cardiomyocytes. This could be resolved with more refined purification techniques such as FACS sorting. The second reason relates to the timing of the treatment. To identify direct transcriptional targets, shorter treatments are generally preferable to longer ones as long treatments may lead to the up/down-regulation of indirect targets. This may explain the repression of *Ace1*, which may not be a direct transcriptional target. Whether or not RAR receptors bind to potential RARE elements near the *Ace1* gene remains to be seen. In essence, repeating the RNA seq with a shorter treatment time to fully avoid indirect genes being activated/repressed may lead to more useful information regarding the role of RA signaling in cardiomyocytes in late development as well as after MI.

Another more effective way of determining the underlying mechanisms would be to look at the effects of specifically ablating RA signaling in the myocardium. This could be done by crossing floxed alleles of the three RAR receptors (RARα, RARβ, RARɣ) with an inducible myocardial-specific *Cre* line. This way, one can avoid non-specific effects resulting from other organs and/or cell types within the heart, and one could also choose which time-point/s to focus on. What is interesting about the RAR receptors is that the individual nulls do not develop cardiac defects. This is presumably due to functional redundancy as the loss of one receptor can be compensated for by expression of another. Combinations of two or more nulls (ie. RARα:RARβ or RARα:RARɣ) do lead to heart abnormalities so it would be interesting to see if these were related to myocardial-specific expression. Deletion of all three would remove any possibility of functional compensation and would resolve the issue of whether or not RA signaling plays a real role in cardiomyocytes. Furthermore, examining the changes in gene expression associated with

the removal of the RAR receptors in the myocardium would potentially shed light onto the mechanisms underlying the late roles of RA signaling in the heart. These same strategies could be applied to the MI experiments. This way, we could see if the myocyte-specific apoptotic patches are due to a direct effect of RA on the myocardium, or if it is indirect ie. influenced by the immune response, fibroblast activation, neoangiogenesis etc.

A second question relates to the expression of RALDH2. In the epicardium the transcription factor known as Wilms' tumour 1 (WT1) protein drives the expression of *Raldh2* (Guadix et al., 2012). However, the *Raldh2*-positive cardiac fibroblasts for the most part do not express WT1 (personal observation). Furthermore, RALDH2 expression in the fibroblasts is only activated after E14.5, well after their migration into the ventricular free walls (Zaffran et al., 2014). Why and how this expression is achieved remains a mystery. Another question is until when does RALDH2 continue to be expressed in the heart under normal conditions? In adults RALDH2 expression is almost undetectable. What about the post-natal period?

In the context of cardiac repair understanding the activation of RALDH2 is very important. After MI, RALDH2 expression becomes broadly expressed in and around the injury zone. Many of the cell types expressing RALDH2 are positive for VIMENTIN but their exact identities are unclear at this point. Understanding the regulation of RALDH2 expression may help us develop novel treatments based on RA synthesis, which may be more effective than simple administration of atRA.

A third question relates to the regulation of the RAS system by RA. RA signaling modulates various components of the renin angiotensin system in cardiomyocytes subjected to high glucose conditions (Gulleria et al., 2010). *Ace1* is one of those components. However, it does not seem to be a direct target. In fact, neither does *Ace2*, angiotensin I, angiotensin II etc. This is presumed by the fact that no such direct regulation has been reported, nor has anyone identified any functional RARE elements on any of these genes by ChIP-seq analysis. So how exactly does RA

regulate RAS-related genes? The answer to this question may lead to the development of novel treatments for cardiovascular diseases based on synergistic atRA + ACE inhibition strategies.

CHAPTER IV: CONCLUSION

Cardiovascular diseases resulting from occlusion of the coronary arteries are among the leading causes of death worldwide. Treating patients recovering from acute events such as myocardial infarction (MI), is inherently difficult since cardiomyocytes, the principal cell-type of the heart, have a limited potential to proliferate and repair the damaged heart. Hence, the development of novel regenerative treatments for coronary artery disease is of the utmost importance (Aisagbonhi et al. 2011). Interestingly, many embryonic signaling pathways are reactivated after MI and it has been suggested that the manipulation of these pathways through pharmacological means can lead to improved outcomes for patients suffering from heart disease (Garbern and Lee, 2014).

The mouse serves as an excellent model for studying heart development and regeneration. Through the use of various transgenic models, one can study the effects of deleting certain genes on heart development processes such as coronary artery formation. In addition, through the use of transgenic reporter lines with surgically induced MI mouse models one can delineate which pathways are re-activated after heart damage.

For the first part of my project I studied the effects of the Wnt signaling modulator, *Rspo3*, on coronary artery formation. By temporally ablating *Rspo3* at E11.5 I demonstrated that *Rspo3* is indispensable for coronary artery development. Mechanistically, *Rspo3* was shown to promote endothelial-specific proliferation of the coronary stems through canonical Wnt/β-catenin signaling. These findings are important in the context of coronary artery disease since it is plausible that *Rspo3* may also be involved in coronary remodeling post-MI. This, however, remains to be investigated.

For the second part of my project I have used a novel transgenic Retinoic acid reporter line (*RARECreER*^{T2}) to detect a cardiomyocyte-specific response during late development and after

surgically induced MI. In addition, by deleting the 3 RA-producing enzymes (*Raldh1, Raldh2,* and *Raldh3*) I have shown that RA-signaling appears to play an anti-apoptotic role during late gestation and acute phases of myocardial repair. Through RNA seq analysis I determined that RA repression of Angiotensin converting enzyme (*Ace1*) may partially explain the anti-apoptotic effects of RA-signaling post MI. Further studies are needed to more precisely delineate the molecular pathways involved in the cardio-protective response of RA-signaling.

CHAPTER V : BIBLIOGRAPHY

I. References for chapters I, II, III and IV

1) Abu-Abed, S. et al. (2001). The retinoic acid-metabolizing enzyme, CYP26A1, is essential for normal hindbrain patterning, vertebral identity, and development of posterior structures. Genes Dev. *15*, 226–240.
2) Acharya A. et al. (2012). The bHLH transcription factor Tcf21 is required for lineage-specific EMT of cardiac fibroblast progenitors. Development *139*, 2139–2149
3) Aisagbonhi, O. et al. (2011). Experimental myocardial infarction triggers canonical Wnt signaling and endothelial-to-mesenchymal transition. Dis Mod and Mec. *483*, 469–483.
4) Al Alam, D. et al. (2011). Contrasting expression of canonical wnt signaling reporters TOPGAL, BATGAL and Axin2 LacZ during murine lung development and repair. PLoS ONE, *6*.
5) Angelini, P. (2007). Coronary artery anomalies: An entity in search of an identity. Circulation Research *115*, 1296–1305.
6) Antman, E. M. and Braunwald, E. (2001). Acute myocardial infarction. In *Harrison's Principles of internal medicine* (ed. A. S. Fauci, E. Braunwald, K. J. Isselbacher, J. D.Wilson, J. B. Martin, D. L. Kasper, S. L. Hauser, D. L. Longo and T. R. Harrison), New York: McGraw-Hill, pp.1386-1399.
7) Aoki M., Mieda M., Ikeda T., Hamada Y., Nakamura H. & Okamoto H. (2007). R-spondin3 is required for mouse placental development. Dev Biol *301*, 218-226.
8) Arima, Y. et al. (2012). Preotic neural crest cells contribute to coronary artery smooth muscle involving endothelin signalling. Nature Communications *3*, 1267.
9) Arita, Y. et al. (2014). Myocardium-derived angiopoietin-1 is essential for coronary vein formation in the developing heart. Nature communications *5*, 1-14.
10) Assmus, B. et al. (2010). Clinical outcome 2 years after intracoronary administration of bone marrow-derived progenitor cells in acute myocardial infarction. Circ. Heart. Fail. *3*, 89-96.
11) Baenziger N.L., Brodie G.N. & Majerus P.W. (1971). A thrombin-sensitive protein of human platelet membranes. Proc Natl Acad Sci U S A *68*, 240-243.
12) Barandon, L. et al. (2005). Involvement of FrzA/sFRP-1 and the Wnt/frizzled pathway in ischemic preconditioning. *Circ. Res. 96*, 1299–1306.
13) Barandon, L., et al. (2003). Reduction of infarct size and prevention of cardiac rupture in transgenic mice overexpressing FrzA. Circulation *108*, 2282–2289.
14) Barker, N., Tan, S. & Clevers, H. (2013). Lgr proteins in epithelial stem cell biology. Development *140*, 2484–94.
15) Bell S.M., Schreiner C.M., Wert S.E., Mucenski M.L., Scott W.J. & Whitsett J.A. (2008) R-spondin 2 is required for normal laryngeal-tracheal, lung and limb morphogenesis. Development *135*, 1049-1058.
16) Bennett HS. (1936). The development of the blood supply to the heart in the embryo pig. Am. J. Anat. *60*, 27–53.
17) Bergmann et al. (2009). Evidence for cardiomyocyte renewal in humans. Science *324*, 98.
18) Bersell, K., Arab, S., Haring, B. & Kuhn, B. (2009). Neuregulin1/ErbB4 signaling induces cardiomyocyte proliferation and repair of heart injury. Cell *138*, 257.
19) Bettencourt-Dias, M., Mittnacht, S. & Brockes, J.P. (2003). Heterogeneous proliferative potential in regenerative adult newt cardiomyocytes. J. Cell Sci. *116*, 4001.
20) Bicknell, K.A., Coxon, C.H. & Brooks, G. (2004). Forced expression of the cyclin B1–CDC2 complex induces proliferation in adult rat cardiomyocytes. Biochem. J. *382*, 411.

21) Bilbija, D. et al. (2012). Retinoic Acid Signalling Is Activated in the Postischemic Heart and May Influence Remodelling. PLoS ONE *7*, 1–9.
22) Blaydon, D.C. et al. (2006). The gene encoding R-spondin 4 (RSPO4), a secreted protein implicated in Wnt signaling, is mutated in inherited anonychia. Nature genetics *38*, 1245–1247.
23) Blin, G. et al. (2010). A purified population of multipotent cardiovascular progenitors derived from primate pluripotent stem cells engrafts in portmyocardial infarcted nonhuman primates. J. Clin. Invest. *120*, 1125-1139.
24) Borycki A.G. & Emerson C.P. Jr. (2000). Study of skeletal myogenesis in cultures of unsegmented paraxial mesoderm. *Methods* Mol Biol *137*, 351-357.
25) Brade, T. et al (2011). Retinoic acid stimulates myocardial expansion by induction of hepatic erythropoietin which activates epicardial Igf2. Development *138*, 139–148.
26) Brade, T. et al. (2013). Embryonic heart progenitors and cardiogenesis. Cold Spring Harbor perspectives in medicine *3*, 1–18.
27) Braitsch C.M., Combs M.D., Quaggin S.E. & Yutzey K.E. (2012). Pod1/Tcf21 is regulated by retinoic acid signaling and inhibits differentiation of epicardium-derived cells into smooth muscle in the developing heart. Dev. Biol. *368*, 345–57
28) Bruneau, B. G (2008). The developmental genetics of congenital heart disease. Nature *451*, 943–948.
29) Bryan T. MacDonald; Keiko Tamai and Xi He (2010). NIH Public Access. *Developmental biology 17*, 9–26.
30) Buikema, J. et al. (2014). Wnt/β-Catenin Signaling during Cardiac Development and Repair. Journal of Cardiovascular Development and Disease *1*, 98–110
31) Buikema, J.W et al. (2013). Wnt/beta-catenin signaling directs the regional expansion of first and second heart field-derived ventricular cardiomyocytes. Development *140*, 4165–4176.
32) Buikema, J.W., Zwetsloot, P.P., Doevendans, P.A., Sluijter, J.P. & Domian, I.J. (2013). Expanding mouse ventricular cardiomyocytes through GSK-3 inhibition. Curr. Protoc. Cell Biol*. 61*.
33) Cadieu E. et al. (2009). Coat variation in the domestic dog is governed by variants in three genes. Science *326*, 150-153.
34) Cai C.L., Liang X., Shi Y., Chu P.H., Pfaff S.L., Chen J. & Evans S (2003). Isl1 identifies a cardiac progenitor population that proliferates prior to differentiation and contributes a majority of cells to the heart. Dev Cell *5*, 877–889
35) Cambier, L. et al. (2014). Nkx2-5 regulates cardiac growth through modulation of Wnt signaling by R-spondin3. Development *141*, 2959–2971.
36) Cano, E., Carmona, R., Ruiz-Villalba, A., Rojas, A., Chau, Y.-Y., Wagner, K. D., Wagner, N., Hastie, N. D., Muñoz-Chápuli, R. and Pérez-Pomares, J. M. (2016). Extracardiac septum transversum/proepicardial endothelial cells pattern embryonic coronary arterio-venous connections. Proceedings of the National Academy of Sciences of the United States of America *113*, 656–61.
37) Carmon K.S., Gong X., Lin Q., Thomas A. & Liu Q. (2011). R-spondins function as ligands of the orphan receptors LGR4 and LGR5 to regulate Wnt/beta-catenin signaling. Proc Natl Acad Sci U S A *108,* 11452-11457.
38) Chaudhry, H.W., et al. (2004). Cyclin A2 mediates cardiomyocyte mitosis in the postmitotic myocardium. J. Biol. Chem. *279*, 35858.
39) Chen H.I., Poduri A., Numi H., Kivel¨a R., Saharinen P., et al. (2014). VEGF-C and aortic cardiomyocytes guide coronary artery stem development. J. Clin. Investig. 124, 4899–914
40) Chen J., Kubalak, S.W. & Chien, K.R. (1998). Ventricular muscle-restricted targeting of the RXRalpha gene reveals a non-cell-autonomous requirement in cardiac chamber morphogenesis. Development *125*, 1943–1949.

41) Chen J.Z., Wang S., Tang R., Yang Q.S., Zhao E., Chao Y., Ying K., Xie Y. & Mao Y.M. (2002) Cloning and identification of a cDNA that encodes a novel human protein with thrombospondin type I repeat domain, hPWTSR. Mol Biol Rep *29*, 287-292.
42) Chen Q, Zhang H, Liu Y, Adams S, Eilken H, et al (2016). Endothelial cells are progenitors of cardiac pericytes and vascular smooth muscle cells. Nat. Commun. *7*, 12422
43) Chen, H.I. et al. (2014). The sinus venosus contributes to coronary vasculature through VEGFC-stimulated angiogenesis. Development (Cambridge, England) *141*, 4500–12.
44) Chen, H.I. et al. (2014). VEGF-C and aortic cardiomyocytes guide coronary artery stem development. Journal of Clinical Investigation *124*, 4899–4914.
45) Chen, P .-H., Chen, X., Lin, Z., Fang, D. & He, X. (2013). The structural basis of R-spondin recognition by LGR5 and RNF43. Genes Dev. *27*, 1345–1350.
46) Ching, S. & Vilain, E. (2009). Targeted disruption of sonic Hedgehog in the mouse adrenal leads to adrenocortical hypoplasia. Genesis *47*, 628–637.
47) Clark, R. (2005). Anatomy and Physiology: Understanding the Human Body. 1st ed. Sudbury, MA: Jones and Bartlett, pp.288-297.
48) Clevers, H. & Nusse, R. (2012). Wnt/β-catenin signaling and disease. Cell *149*, 1192–1205.
49) Cohen E.D., Tian Y. & Morrisey E.E. (2008). Wnt signaling: An essential regulator of cardiovascular differentiation, morphogenesis and progenitor self-renewal. *Development* 135: 789–798.
50) Cohen, E.D., Wang, Z., Lepore, J.J., Lu, M.M., Taketo, M.M., Epstein, D.J. & Morrisey, E.E. (2007). Wnt/beta-catenin signaling promotes expansion of Isl-1-positive cardiac progenitor cells through regulation of FGF signaling. J. Clin. Invest. *117*, 1794–1804
51) Cohen, E. D., Miller, M. F., Wang, Z., Moon, R. T. and Morrisey, E. E. (2012)/ Wnt5a and Wnt11 are essential for second heart field progenitor development. Development *139*, 1931–1940.
52) Cossu G. &Borello U. (1999). Wnt signaling and the activation of myogenesis in mammals. EMBO J *1*8, 6867-6872.
53) Cunningham, T.J. & Duester, G. (2015). Mechanisms of retinoic acid signalling and its roles in organ and limb development. Nature reviews Molecular cell biology *16*, 110–123.
54) DasGupta R. & Fuchs E. (1999). Multiple roles for activated LEF/TCF transcription complexes during hair follicle development and differentiation. Development *126*, 4557–4568.
55) David, R.et al. (2008). MesP1 drives vertebrate cardiovascular differentiation through Dkk-1-mediated blockade of Wnt-signalling. Nat. Cell Biol. *10*, 338–345.
56) de Lau W. et al. (2011). Lgr5 homologues associate with Wnt receptors and mediate R-spondin signalling. Nature *476*, 293-297.
57) Dersch, H. & Zile, M.H. (1993). Induction of normal cardiovascular development in the vitamin A-deprived quail embryo by natural retinoids. Dev. Biol. *160*, 424–433.
58) Di Stefano, V., Giacca, M., Capogrossi, M.C., Crescenzi, M. & Martelli, F. (2011). Knockdown of cyclin-dependent kinase inhibitors induces cardiomyocyte re-entry in the cell cycle. J. Biol. Chem. *286*, 8644
59) Dollé, P. (2009) Developmental expression of retinoic acid receptors (RARs). Nuclear Receptor Signaling *7*, 1-13.
60) Dollé, P. et al. (2010). Fate of retinoic acid-activated embryonic cell lineages. Developmental Dynamics *239*, 3260–3274.
61) Drysdale, T.A., Patterson, K.D., Saha, M. & Krieg, P.A. (1997) Retinoic acid can block differentiation of the myocardium after heart specification. Dev. Biol. *188*, 205–215.
62) Duan J et al. (2012). Wnt1/betacatenin injury response activates the epicardium and cardiac fibroblasts to promote cardiac repair. EMBO J. *31*, 429–42.

63) Dupe, V. et al. (2003). A newborn lethal defect due to inactivation of retinaldehyde dehydrogenase type 3 is prevented by maternal retinoic acid treatment. Proc. Natl Acad. Sci. USA *100*, 14036–14041.
64) Engel, F.B., et al. (2005). p38 MAP kinase inhibition enables proliferation of adult mammalian cardiomyocytes. Genes Dev. *19*, 1175.
65) Engleka, K. A., Gitler, A. D., Zhang, M., Zhou, D. D., High, F. A. & Epstein, J. A. (2005). Insertion of Cre into the Pax3 locus creates a new allele of Splotch and identifies unexpected Pax3 derivatives. Developmental Biology *280*, 396–406.
66) Ellison, G.M. et al. (2013). Adult c-kit(pos) cardiac stem cells are necessary and sufficient for functional cardiac regeneration and repair. Cell *154*, 827-842.
67) Fan, X. et al. (2003). Targeted disruption of Aldh1a1 (Raldh1) provides evidence for a complex mechanism of retinoic acid synthesis in the developing retina. Moll Cell Biol. *23*, 4637-4648.
68) Frangogiannis, N.G. (2014). The inflammatory response in myocardial injury, repair, and remodelling. Nature Reviews Cardiology *11*, 255–265.
69) Garbern, J.C. & Lee, R.T. (2013). Cardiac stem cell therapy and the promise of heart regeneration. Cell Stem Cell *12*, 689–698.
70) Gessert S. & Kuhl M. (2010). The multiple phases and faces of wnt signaling during cardiac differentiation and development. Circ Res *107*, 186–199.
71) Glinka A., Dolde C., Kirsch N., Huang Y.L., Kazanskaya O., Ingelfinger D., Boutros M., Cruciat C.M. & Niehrs C. (2011). LGR4 and LGR5 are R-spondin receptors mediating Wnt/beta-catenin and Wnt/PCP signalling. EMBO Rep *12*, 1055-1061.
72) Goldsmith JB & Butler HW (1937). The development of the cardiac-coronary circulatory system. Am. J.Anat. *60*, 185–201
73) Guadix, J.A. et al. (2011). Wt1 controls retinoic acid signalling in embryonic epicardium through transcriptional activation of Raldh2. Development *138*, 1093–1097.
74) Guleria, R.S. et al. (2011). Retinoic acid receptor-mediated signaling protects cardiomyocytes from hyperglycemia induced apoptosis: Role of the renin-angiotensin system. Journal of Cellular Physiology *226*, 1292–1307.
75) Haegel, H., Larue, L., Ohsugi, M., Fedorov, L., Herrenknecht, K., Kemler, R. (1995). Lack of beta-catenin affects mouse development at gastrulation. Development *121*, 3529–3537.
76) Hahn, J.-Y. et al. (2006). Beta-catenin overexpression reduces myocardial infarct size through differential effects on cardiomyocytes and cardiac fibroblasts. *J. Biol. Chem. 281*, 30979–30989.
77) Haq S et al. (2003). Stabilization of beta-catenin by a Wnt-independent mechanism regulates cardiomyocyte growth. Proc Natl Acad Sci U S A *100*, 4610–5.
78) Hare, J.M. et al. (2012). Comparison of allogeneic vs autologous bone marrow– derived mesenchymal stem cells delivered by transendocardial injection in patients with ischemic cardiomyopathy: the POSEIDON randomized trial. JAMA *308*, 2369–2379.
79) Hayashi, S. & McMahon, A.P. (2002). Efficient Recombination in Diverse Tissues by a Tamoxifen-Inducible Form of Cre: A Tool for Temporally Regulated Gene Activation/Inactivation in the Mouse. Developmental Biology *244*, 305–318.
80) He X., Semenov M., Tamai K. & Zeng X. (2004). LDL receptor-related proteins 5 and 6 in Wnt/beta-catenin signaling: arrows point the way. Development (Cambridge, England) *13,* 1663–1677.
81) He, W. et al. (2010) Exogenously administered secreted frizzled related protein 2 (Sfrp2) reduces fibrosis and improves cardiac function in a rat model of myocardial infarction, *Proceedings of the National Academy of Sciences*, 107, 21110–21115.
82) He, W., Zhang, L., Ni, A., Zhang, Z., Mirotsou, M., Mao, L., Pratt, R.E. & Dzau, V.J. (2010).

83) Heikkila, M. et al. (2002). Wnt-4 deficiency alters mouse adrenal cortex function, reducing aldosterone production. Endocrinology *143*, 4358–4365.
84) Heine, U.I., Roberts, A.B., Munoz, E.F., Roche, N.S. & Sporn, M.B. (1985). Effects of retinoid deficiency on the development of the heart and vascular system of the quail embryo. Virchows Archiv. B *50*, 135–152.
85) Hofmann, K. (2000). A superfamily of membrane-bound O-acyltransferases with implications for wnt signaling. Trends Biochem. Sci. *25*, 111–112.
86) Hsieh, P.C. et al. (2007). Evidence from a genetic fate-mapping study that stem cells refresh adult mammalian cardiomyocytes after injury. Nat. Med. *13*, 970.
87) Huang, G.N. et al. (2012). C/EBP transcription factors mediate epicardial activation during heart development and injury. Science *338*, 1599-1603.
88) Hutson MR, Kirby ML (2007). Model systems for the study of heart development and disease. Cardiac neural crest and conotruncal malformations. Semin Cell Dev Biol *18*, 101–110.
89) Ieda, M., Fu, J.D., Delgado-Olguin, P., Vedantham, V., Hayashi, Y., Bruneau, B.G., and Srivastava, D. (2010). Direct reprogramming of fibroblasts into functional cardiomyocytes by defined factors. Cell *142*, 375–386.
90) Ishii Y., Wajid M., Bazzi H., Fantauzzo K.A., Barber A.G., Blaydon D.C., Nam J.S., Yoon J.K., Kelsell D.P. & Christiano A.M. (2008). Mutations in R-spondin 4 (RSPO4) underlie inherited anonychia. J Invest Dermatol *128*, 867-870.
91) Ivins S., Chappell J., Vernay B., Suntharalingham J., Martineau A., et al. (2015). The CXCL12/CXCR4 axis plays a critical role in coronary artery development. Dev. Cell 33, 455–68
92) Jenkins, S.J., Hutson, D.R. & Kubalak, S.W. (2005). Analysis of the proepicardium-epicardium transition during the malformation of the RXRα-/- epicardium. Developmental Dynamics *233*, 1091–1101.
93) Jiang X., Rowitch D.H., Soriano P., McMahon A.P. & Sucov H.M. (2000). Fate of themammalian cardiac neural crest. Development *127*, 1607–1616.
94) Jiang, X., Choudhary, B., Merki, E., Chien, K.R.; Maxson, R.E. & Sucov, H.M. (2002). Normal fate and altered function of the cardiac neural crest cell lineage in retinoic acid receptor mutant embryos. Mech. Dev. *117*, 115–122.
95) Jiang, Y., Drysdale, T.A. & Evans, T. (1999). A role for GATA-4/5/6 in the regulation of Nkx2.5 expression with implications for patterning of the precardiac field. Dev. Biol. *216,* 57–71.
96) Jopling, C., et al. (2010). Zebrafish heart regeneration occurs by cardiomyocyte dedifferentiation and proliferation. Nature *464*, 606.
97) Kaga, S., Zhan, L., Altaf, E. & Maulik, N. (2006). Glycogen synthase kinase-3beta/beta-catenin promotes angiogenic and anti-apoptotic signaling through the induction of VEGF, Bcl-2 and surviving expression in rat ischemic preconditioned myocardium. J. Mol. Cell. Cardiol. *40*, 138–147.
98) Kamata T., Katsube K., Michikawa M., Yamada M., Takada S. & Mizusawa H. (2004) R-spondin, a novel gene with thrombospondin type 1 domain, was expressed in the dorsal neural tube and affected in Wnts mutants. Biochim Biophys Acta *1676*, 51-62.
99) Kang, E., Yousefi, M. & Gruenheid, S. (2016). R-spondins are expressed by the intestinal stroma and are differentially regulated during Citrobacter rodentium- and dss induced colitis in mice. PLoS ONE *11*, 1–13.
100) Katharina S Volz, Andrew H Jacobs, Heidi I Chen, Aruna Poduri, Andrew S McKay, Daniel P Riordan, Natalie Kofler, Jan Kitajewski & Irving Weissman, K.R.-H. (2015). Pericytes are progenitors for coronary artery smooth muscle. eLife, *1*, 1–22.
101) Katz, T.C. et al. (2012). Distinct Compartments of the Proepicardial Organ Give Rise to Coronary Vascular Endothelial Cells. Developmental Cell *22*, 639–650.

102) Kazanskaya O., Glinka A., del Barco Barrantes I., Stannek P., Niehrs C. & Wu W. (2004) R-Spondin2 is a secreted activator of Wnt/beta-catenin signaling and is required for Xenopus myogenesis. Dev Cell *7*, 525-534.
103) Kazanskaya O., Ohkawara B., Heroult M., Wu W., Maltry N., Augustin H.G. & Niehrs C. (2008) The Wnt signaling regulator R-spondin 3 promotes angioblast and vascular development. Development *135*, 3655-3664.
104) Keegan, B.R., Feldman, J.L., Begemann, G., Ingham, P.W. & Yelon, D. (2005). Retinoic acid signaling restricts the cardiac progenitor pool. Science *307*, 247–249
105) Kelly, R.G. (2012). The Second Heart Field. Current Topics in Developmental Biology *100*, 33-65.
106) Kim K.A., Wagle M., Tran K., Zhan X., Dixon M.A., Liu S., Gros D., Korver W., Yonkovich S., Tomasevic N., Binnerts M. & Abo A. (2008). R-Spondin family members regulate the Wnt pathway by a common mechanism. Mol Biol Cell *19*, 2588-2596.
107) Kim, K. A., Zhao, J., Andarmani, S., Kakitani, M., Oshima, T., Binnerts, M. E., Abo, A., Tomizuka, K. & Funk, W. D. (2006). R-spondin proteins: A novel link to β-catenin activation, *Cell Cycle 5*, 23–26.
108) Kimelman, D. (2006). Mesoderm induction: from caps to chips. Nature reviews Genetics *7*, 360–372.
109) Kinzel, B. et al. (2014). Functional roles of Lgr4 and Lgr5 in embryonic gut, kidney and skin development in mice. Developmental Biology *390*, 181–190.
110) Kobayashi, K. et al. (2009). Secreted Frizzled-related protein 2 is a procollagen C proteinase enhancer with a role in fibrosis associated with myocardial infarction. Nat. Cell Biol*. 11*, 46–55.
111) Koizumi, M. et al. (2015). Lgr4 Controls Specialization of Female Gonads in Mice 1. Biology of Reproduction *93*, 1–11.
112) Kuhn, B., et al. (2007). Periostin induces proliferation of differentiated cardiomyocytes and promotes cardiac repair. Nat. Med. *13*, 962.
113) Kumar, S. & Duester, G. (2014). Retinoic acid controls body axis extension by directly repressing Fgf8 transcription. Development *141*, 2972–2977.
114) Kumar, S., Cunningham & T.J., Duester, G. (2016). Nuclear receptor corepressors Ncor1 and Ncor2 (Smrt) are required for retinoic acid-dependent repression of Fgf8 during somitogenesis. Dev. Biol. *418,* 204-215.
115) Kuriyama S. & Mayor R. (2008). Molecular analysis of neural crest migration. Philos Trans R Soc Lond B Biol Sci *363*, 1349–1362.
116) Kwon, C., Qian, L., Cheng, P., Nigam, V., Arnold, J. and Srivastava, D. (2009). A regulatory pathway involving Notch1 / β -catenin / Isl1 determines cardiac progenitor cell fate. Nature Cell Biology *11*, 951–957.
117) Laeremans, H. et al. (2011). Blocking of frizzled signaling with a homologous peptide fragment of wnt3a/wnt5a reduces infarct expansion and prevents the development of heart failure after myocardial infarction. Circulation *124*, 1626–1635.
118) Laflamme, M.A. et al. (2007). Cardiomyocytes derived from human embryonic stem cells in pro-survival factors enhance function of infarcted rat hearts. Nat. Biotechnol. *25*, 1015–1024.
119) Lavine K.J., White A.C., Park C., Smith C.S., Choi K., et al. (2006). Fibroblast growth factor signals regulate a wave of Hedgehog activation that is essential for coronary vascular development. Genes Dev. *20*, 1651–66
120) Lavine, K.J. et al. (2005) Endocardial and epicardial derived FGF signals regulate myocardial proliferation and differentiation in vivo. Developmental Cell *8*, 85–95.
121) Lavine, K.J. et al. (2008). Hedgehog signaling to distinct cell types differentially regulates coronary artery and vein development. Development (Cambridge, England) *135*, 3161–3171.

122) Lee, R.Y., Luo, J., Evans, R.M., Giguere, V. & Sucov, H.M. (1997). Compartment-selective sensitivity of cardiovascular morphogenesis to combinations of retinoic acid receptor gene mutations. Circul. Res. *80*, 757–764.
123) Li, F. et al. (1996). Rapid transition of cardiac myocytes from hyperplasia to hypertrophy during postnatal development. J. Mol. Cell. Cardiol. *28*, 1737.
124) Li, P., Pashmforoush, M. & Sucov, H.M. (2010). Retinoic acid regulates differentiation of the secondary heart field and tgf beta-mediated outflow tract septation. Dev. Cell. *18*, 480–485.
125) Lin, S.-C. et al. (2010). Endogenous retinoic acid regulates cardiac progenitor differentiation. Proceedings of the National Academy of Sciences of the United States of America *107*, 9234–9239.
126) Linzbach, A.J. (1950). The muscle fiber constant and the law of growth of the human ventricles. Virchows Arch. *318*, 575.
127) Liu N. & Olson E.N. (2010). MicroRNA regulatory networks in cardiovascular development. Dev Cell *18*, 510–525.
128) Logan C.Y. & Nusse R.(2004). The Wnt signaling pathway in development and disease. Annual review of cell and developmental biology *20*, 781–810.
129) Lustig B et al. (2002). Negative feedback loop of Wnt signaling through upregulation of conductin/axin2 in colorectal and liver tumors. Mol Cell Biol *22*, 1184–1193.
130) Lyons, I., Parsons, L. M., Hartley, L., Li, R., Andrews, J. E., Robb, L. & and Harvey, R. P. (1995). Myogenic and morphogenetic defects in the heart tubes of murine embryos lacking the homeo box gene Nkx2-5. Genes Dev. *9*, 1654-1666.
131) Ma Q. et al. (2009). *Fog2* is critical for cardiac function and maintenance of coronary vasculature in the adult mouse heart. J. Clin. Investig. 119, 1462–76.
132) Macdonald, B.T. et al. (2009). Wnt/beta-catenin signaling: components, mechanisms, and diseases. Dev. Cell. *17*, 9-26.
133) MacGrogan, D., Nus, M. & Pompa, J.L. de la. (2010). Notch signaling in cardiac development and disease. Current Topics in Developmental Biology *92*, 333–365.
134) Mahony, S., Mazzoni, E.O., McCuine, S., Young, R.A., Wichterle, H. & Gifford, D.K. (2011). Ligand- dependent dynamics of retinoic acid receptor binding during early neurogenesis. Genome Biol. *12*, R2.
135) Malliaras, K. et al. (2013). Cardiomyocyte proliferation and progenitor cell recruitment underlie therapeutic regeneration after myocardial infarction in the adult mouse heart. EMBO Mol. Med. *5*, 191-209.
136) Manner J. (1999). Does the subepicardial mesenchyme contribute myocardioblasts to the myocardium of the chick embryo heart? A quail-chick chimera study tracing the fate of the epicardial primordium. Anat. Rec. *255*, 212–226
137) Manner J., Perez-Pomares J.M., Macias D. & Munoz-Chapuli R. (2001). The origin, formation and developmental significance of the epicardium: A review. Cells Tissues Organs *169*, 89–103.
138) Maretto S. et al. (2003). Mapping Wnt/beta-catenin signaling during mouse development and in colorectal tumors. Proc Natl Acad Sci U S A *100*, 3299–3304.
139) Mark, M., Ghyselinck, N.B. & Chambon, P. (2009). Function of retinoic acid receptors during embryonic development. Nucl. Recept. Sign. *7*
140) Matt, N. et al. (2005). Retinoic acid-dependent eye morphogenesis is orchestrated by neural crest cells. Development *132*, 4789–4800.
141) Mazerbourg, S. et al. (2004). Leucine-rich repeat-containing, G protein-coupled receptor 4 null mice exhibit intrauterine growth retardation associated with embryonic and perinatal lethality. Mol Endocrinol *18*, 2241–2254.

142) Merki, E. et al. (2005). Epicardial retinoid X receptor alpha is required for myocardial growth and coronary artery formation. Proceedings of the National Academy of Sciences of the United States of America *102*, 18455–18460.
143) Mic, F. A., Sirbu, I. O. & Duester, G. (2004). Retinoic acid synthesis controlled by *Raldh2* is required early for limb bud initiation and then later as a proximodistal signal during apical ectodermal ridge formation. J. Biol. Chem. *279*, 26698–26706.
144) Minicucci, M.F. et al. (2010). Tissue vitamin A insufficiency results in adverse ventricular remodeling after experimental myocardial infarction. Cellular Physiology and Biochemistry *26*, 523–530.
145) Mlodzik, M. (2002). Planar cell polarization: do the same mechanisms regulate Drosophila tissue polarity and vertebrate gastrulation? Trends Genet *18*, 564-571.
146) Mollova, M. et al. (2013). Cardiomyocyte proliferation contributes to heart growth in young humans. Proc. Natl. Acad. Sci. U.S.A. *110*, 1446-1451.
147) Molotkov, A. et al. (2002). Stimulation of retinoic acid production and growth by ubiquitously expressed alcohol dehydrogenase *Adh3*. Proc. Natl Acad. Sci. USA *99*, 5337–5342.
148) Moloktov, A. et al., (2006). Retinoic acid guides eye morphogenetic movements via paracrine signaling but is unnecessary for retinal dorsoventral patterning. Development *133*, 1901-1910.
149) Moore, A.W., McInnes, L., Kreidberg, J., Hastie, N.D. & Schedl, A. (1999). Yac complementation shows a requirement for wt1 in the development of epicardium, adrenal gland and throughout nephrogenesis. Development *126*, 1845–1857.
150) Moretti A. et al. (2006). Multipotent embryonic isl1þ progenitor cells lead to cardiac, smooth muscle, and endothelial cell diversification. Cell *127*, 1151–1165.
151) Mouse R-spondin2 is required for apical ectodermal ridge maintenance in the hindlimb. Dev Biol *311*, 124-135.
152) Mozaffarian, D. et al. (2015). Heart disease and stroke statistics-2015 update : A report from the American Heart Association. Circulation Research *131*, 29-39.
153) Murdoch, D.R. & McMurray, J.J. (1998). ACE inhibitors in acute myocardial infarction. Hospital Medicine *59*, 111–115.
154) Muzumdar, M.D. et al. (2007). A global double-fluorescent Cre reporter mouse. Genesis (New York, N.Y. : 2000) *45*, 593–605.
155) N., Binnerts M. & Abo A. (2008). R-Spondin family members regulate the Wnt pathway by a common mechanism. Mol Biol Cell *19*, 2588-2596
156) Nam J.S., Park E., Turcotte T.J., Palencia S., Zhan X., Lee J., Yun K., Funk W.D. & Yoon J.K. (2007).
157) Nam J.S., Turcotte T.J. & Yoon J.K. (2007) Dynamic expression of R-spondin family genes in mouse development. Gene Expr Patterns *7*, 306-312.
158) Napoli, L. & Sciences, B. (1996). Acid Biosynthesis. Nature, *10*, 993–1001.
159) Naqvi, N. et al. (2014) A proliferative burst during preadolescence establishes the final cardiomyocyte number. Cell. *157*, 795–807.
160) Niederreither, K. & Dollé, P. (2008). Retinoic acid in development: towards an integrated view. Nat. Rev. Genet. *9*, 541–553.
161) Niederreither, K. et al. (2001). Embryonic retinoic acid synthesis is essential for heart morphogenesis in the mouse. Development *128,* 1019–1031.
162) Niederreither, K. et al. (2001). Embryonic retinoic acid synthesis is essential for heart morphogenesis in themouse. Development *128,* 1019–1031.
163) Niederreither, K., McCaffery, P., Drager, U. C., Chambon, P. & Dollé, P. (1997). Restricted expression and retinoic acid-induced downregulation of the retinaldehyde dehydrogenase type 2 (RALDH‑2) gene during mouse development. Mech. Dev. *62*, 67–78.
164) Noordermeer, J., Klingensmith, J., Perrimon, N., & Nusse, R. (1994). Disheveled and armadillo act in the wingless signalling pathway in Drosophila. Nature *367*, 80–83.

165) Noseda M., Peterkin T., Simoes F.C., Patient R. & Schneider, M.D. (2011). Cardiopoietic factors: Extracellular signals for cardiac lineage commitment. Circ Res *108*, 129–152.
166) Nusse, R., & Varmus, H.E. (1982). Many tumors induced by the mouse mammary tumor virus contain a provirus integrated in the same region of the host genome. Cell *31*, 99–109.
167) Oerlemans MI et al. (2010). Active Wnt signaling in response to cardiac injury. Basic Res Cardiol. *105*, 631–41.
168) Ohkawara, B., Glinka, A. & Niehrs, C. (2011). Rspo3 Binds Syndecan 4 and Induces Wnt/PCP Signaling via Clathrin-Mediated Endocytosis to Promote Morphogenesis. Developmental Cell *20*, 303–314.
169) Ozhan, G. & Weidinger, G. (2015). Wnt/β-catenin signaling in heart regeneration. *Cell* Regeneration, *4*, 1–12.
170) Paiva, S. a R. et al. (2005). Retinoic acid supplementation attenuates ventricular remodeling after myocardial infarction in rats. The Journal of nutrition *135*, 2326–2328.
171) Palm-Leis, A. et al. (2004). Mitogen-activated protein kinases and mitogen-activated protein kinase phosphatases mediate the inhibitory effects of all-trans retinoic acid on the hypertrophic growth of cardiomyocytes. Journal of Biological Chemistry *279*, 54905–54917.
172) Pana kova, D., Sprong, H., Marois, E., Thiele, C., and Eaton, S. (2005). Lipoprotein particles are required for Hedgehog and Wingless signalling. Nature *435*,58–65.
173) Parma P., Radi O., Vidal V., Chaboissier M.C., Dellambra E., Valentini S., Guerra L., Schedl A. & Camerino G. (2006). R-spondin1 is essential in sex determination, skin differentiation and malignancy. Nat Genet *38*, 1304-1309.
174) Pasumarthi, K.B., Nakajima, H., Nakajima, H.O., Soonpaa, M.H. & Field, L.J. (2005). Targeted expression of cyclin D2 results in cardiomyocyte DNA synthesis and infarct regression in transgenic mice. Circ. Res. *96*, 110.
175) Pasutto, F. et al. (2007). Mutations in *STRA6* cause a broad spectrum of malformations including anophthalmia, congenital heart defects, diaphragmatic hernia, alveolar capillary dysplasia, lung hypoplasia, and mental retardation. Am. J. Hum. Genet. *80*, 550–560.
176) Perez-Pomares, J.M. & De La Pompa, J.L. (2011). Signaling during epicardium and coronary vessel development. Circulation Research *109*, 1429–1442.
177) Picco, G., Petti, C., Centonze, A., Torchiaro, E., Crisafulli, G., Novara, L., Acquaviva, A., Bardelli, A. and Medico, E. (2017) Loss of AXIN 1 drives acquired resistance to WNT pathway blockade in colorectal cancer cells carrying RSPO 3 fusions. EMBO Mol. Med. *9*, 293–303.
178) Pinto, A.R. et al. (2016). Revisiting cardiac cellular composition. Circulation Research *118*, 400-409.
179) Poelmann R.E, Gittenberger-deGroot A.C., Mentink M.M., B¨okenkamp R. & Hogers B. (1993). Development of the cardiac coronary vascular endothelium, studied with antiendothelial antibodies, in chicken-quail chimeras. Circ. Res. *73*, 559–68
180) Porrello, E.R., et al. (2011). Transient regenerative potential of the neonatal mouse heart. Science *331*, 1078.
181) Prendiville, T., Jay, P.Y. & Pu, W.T. (2014). Insights into the genetic structure of congenital heart disease from human and murine studies on monogenic disorders. Cold Spring Harb. Perspect. Med. *4*.
182) Qian, L. et al. (2012). In vivo reprogramming of murine cardiac fibroblasts into induced cardiomyocytes. Nature *485*, 593–598.
183) Qian, L., Huang, Y., Spencer, C.I., Foley, A., Vedantham, V., Liu, L., Conway, S.J., Fu, J.D., & Srivastava, D. (2012). In vivo reprogramming of murine cardiac fibroblasts into induced cardiomyocytes. Nature *485*, 593–598.

184) Qyang, Y. et al. (2007). The renewal and differentiation of Isl1+ cardiovascular progenitors are controlled by a Wnt/beta-catenin pathway. Cell Stem Cell *1*, 165–179.
185) Raucci A, Cugusi S, Antonelli A, Barabino SM, Monti L, Bierhaus A, et al. (2008). A soluble form of the receptor for advanced glycation endproducts (RAGE) is produced by proteolytic cleavage of the membranebound form by the sheddase a disintegrin and metalloprotease 10 (ADAM10). FASEB J. *22*, 3716–3727.
186) Red-Horse, K. et al. (2010). Coronary arteries form by developmental reprogramming of venous cells. Nature, *464*, 549–553.
187) Reese, D.E., Mikawa, T. & Bader, D.M. (2002). Development of the coronary vessel system. Circulation Research *91*, 761–768.
188) Ribes, V., Wang, Z., Dollé, P. & Niederreither, K. (2006). Retinaldehyde dehydrogenase 2 (RALDH2)-mediated retinoic acid synthesis regulates early mouse embryonic forebrain development by controlling FGF and sonic hedgehog signaling. Development *133,* 351–361.
189) Rijsewijk, F., Schuermann, M., Wagenaar, E., Parren, P., Weigel, D., & Nusse, R. (1987). The Drosophila homolog of the mouse mammary Oncogene int-1 is identical to the segment polarity gene wingless. Cell *50*, 649–657.
190) Riley, P.R. & Smart, N. (2011). Vascularizing the heart. Cardiovascular Research *91*, pp.260–268.
191) Rocha, A.S. et al. (2015). The Angiocrine Factor Rspondin3 Is a Key Determinant of Liver Zonation. Cell Reports, *13*, 1757–1764.
192) Romeih, M. et al. (2003). Function of RARγ and RARα2 at the Initiation of Retinoid Signaling Is Essential for Avian Embryo Survival and for Distinct Events in Cardiac Morphogenesis. Developmental Dynamics *228*, 697–708.
193) Rooij, E. Van (2016). Clinical Implications of Basic Research: Cardiac Repair after Myocardial Infarction. New England Journal of Medicine *374*, 2016–2018.
194) Rossant, J. et al. (1991). Expression of retinoic acid response element-hsp lacZ transgene defines specific domains of transcriptional activity during mouse embryogenesis. Genes & Development *5*, 1333–1344.
195) Ryckebusch, L., Wang, Z., Bertrand, N., Lin, S.C., Chi, X., Schwartz, R., Zaffran, S. & Niederreither, K. (2008). Retinoic acid deficiency alters second heart field formation. Proc. Nat. Acad. Sci. *105*, 2913–2918.
196) Saga, Y., Miyagawa-Tomita, S., Takagi, A., Kitajima, S., Miyazaki, J. & Inoue, T. (1999). MesP1 is expressed in the heart precursor cells and required for the formation of a single heart tube. Development *126*, 3437–3447.
197) Sandell, L. L. et al. (2007). RDH10 is essential for synthesis of embryonic retinoic acid and is required for limb, craniofacial, and organ development. Genes Dev. *21*, 1113–1124.
198) Schlueter J. & Brand T. (2012). Epicardial progenitor cells in cardiac development and regeneration. J Cardiovasc Transl Res *5*, 641–653.
199) Schmidt, D et al. (2007). Prenatally fabricated autologous human living heart valves based on amniotic fluid derived progenitor cells as single cell source. Circulation *116*, I64–I70.
200) Scholz, B. et al. (2016). Endothelial RSPO3 Controls Vascular Stability and Pruning through Non-canonical WNT/Ca(2+)/NFAT Signaling. Developmental cell *36*, 79–93.
201) Senyo, S. E., Lee, R. T. and Kühn, B. (2014). Cardiac regeneration based on mechanisms of cardiomyocyte proliferation and differentiation, Stem Cell Research *13*, 532–541.
202) Senyo, S.E. et al. (2013). Mammalian heart renewal by pre-existing cardiomyocytes. Nature *493*, 433-436.
203) Sharma, B., Chang, A. & Red-Horse, K. (2017). Coronary Artery Development: Progenitor Cells and Differentiation Pathways. Annual Review of Physiology *79*, 1-19.
204) Shen, H. et al. (2015). Extracardiac control of embryonic cardiomyocyte proliferation and ventricular wall expansion. Cardiovasc. Res. *105*, 271–278.

205) Shi, J. et al. (2016). Emerging Role and Therapeutic Implication of Wnt Signaling Pathways in Autoimmune Diseases. J. Immuno. Res.
206) Shiba, Y. et al. (2012). Human ES-cell-derived cardiomyocytes electrically couple and suppress arrhythmias in injured hearts. Nature *489*, 322–325.
207) Showell C., Binder O. & Conlon F.L. (2004). T-box genes in early embryogenesis. Dev Dyn *229*, 201–218.
208) Siegfried, E., Chou, T.B., & Perrimon, N. (1992). wingless signaling acts through zeste-white 3, the Drosophila homolog of glycogen synthase kinase-3, to regulate engrailed and establish cell fate. Cell *71*, 1167–1179.
209) Singh A., Ramesh S., Cibi D.M., Yun L.S., Li J., et al. (2016). Hippo signaling mediators Yap and Taz are required in the epicardium for coronary vasculature development. Cell Rep*. 15*, 1384–93.
210) Smart, N. et al. (2011). De novo cardiomyocytes electrically couple and suppress arrhythmias in injured hearts. Nature *489*, 322-325.
211) Smith C.L., Blaek S.T., Sung C.Y., Tallquist M.D. (2011). Epicardial-derived cell epithelial-to-mesenchymal transition and fate specification require PDGF receptor signaling. Circ. Res*. 108*, 15–26.
212) Soonpaa, M.H. and Field, L.J. (1997). Assessment of cardiomyocyte DNA synthesis in normal and injured adult mouse hearts. Am. J. Physiol. Heart Circ. Physiol. *272*, 220-226.
213) Soriano, P. (1999). Generalized *lacZ* expression with the ROSA26 Cre reporter strain. Nat Gen. *21*, 70-71.
214) Spater, D. et al. (2013). A HCN4+ cardiomyogenic progenitor derived from the first heart field and human pluripotent stem cells. Nat. Cell Biol. *15*, 1098–1106.
215) Stefanovic, S. & Zaffran, S. (2017). Mechanisms of retinoic acid signaling during cardiogenesis. Mechanisms of Development *143*, 9–19.
216) Stuckmann, I., Evans, S. & Lassar, A.B. (2003). Erythropoietin and retinoic acid, secreted from the epicardium, are required for cardiac myocyte proliferation. Developmental Biology *255*, 334–349.
217) Sucov H.M., Gu Y., Thomas S., Li P. & Pashmforoush M. (2009). Epicardial control of myocardial proliferation and morphogenesis. Pediatr Cardiol *30*, 617–625.
218) Sucov, H.M., Dyson, E., Gumeringer, C.L., Price, J., Chien, K.R. & Evans, R.M. (1994). RXR alpha mutant mice establish a genetic basis for vitamin A signaling in heart morphogenesis, Genes Dev. *8*, 1007–1018.
219) Sugimura, R. & Li, L. (2010). Noncanonical Wnt signaling in vertebrate development, stem cells, and diseases. Birth Defects Research Part C - Embryo Today: Reviews *90*, 243–256.
220) Sun, Y. (2010). Intracardiac Renin-Angiotensin system and myocardial repair/remodeling following infarction. J Mol Cell Card. *48*, 483-489.
221) Szondy, Z. et al. (2006). Tissue transglutaminase (TG2) protects cardiomyocytes against ischemia/reperfusion injury by regulating ATP synthesis. Cell Death and Differentiation *13*, 1827-1829.
222) Takeuchi, J. & Bruneau, B. (2009). Directed transdifferentiation of mouse mesoderm to heart tissue by defined factors. Nature *459*, 708–711.
223) Tanaka, K., Kitagawa, Y., and Kadowaki, T. (2002). Drosophila segment polarity gene product porcupine stimulates the posttranslational N-glycosylation of wingless in the endoplasmic reticulum. J. Biol. Chem. *277*, 12816–12823.
224) Tian, X. et al. (2013). Peritruncal coronary endothelial cells contribute to proximal coronary artery stems and their aortic orifices in the mouse heart. PLoS ONE *8*, 1–9.
225) Tian, X. et al. (2013). Subepicardial endothelial cells invade the embryonic ventricle wall to form coronary arteries. Cell research *23*, 1075–90.

226) Tian, X., Pu, W.T. & Zhou, B. (2015). Cellular origin and developmental program of coronary angiogenesis. Circulation Research *116*, 515–530.
227) Tomizuka K. et al. (2008). R-spondin1 plays an essential role in ovarian development through positively regulating Wnt-4 signaling. Hum Mol Genet *17*, 1278-1291.
228) Tomizuka K., Horikoshi K., Kitada R., Sugawara Y., Iba Y., Kojima A., Yoshitome A., Yamawaki K., Amagai M., Inoue A., Oshima T. & Kakitani M. (2008). R-spondin1 plays an essential role in ovarian development through positively regulating Wnt-4 signaling. Hum Mol Genet *17*, 1278-1291
229) Tran, C.M. & Sucov, H.M. (1998). The RXRalpha gene functions in a non-cell-autonomous manner during mouse cardiac morphogenesis. Development *125*, 1951–1956.
230) Traverse, J.H. et al. (2012). Effect of the use and timing of bone marrow mononuclear cell delivery on left ventricular function after acute myocardial infarction: the TIME randomized trial. JAMA *308*, 2380–2389.
231) Trembley M.A., Velasquez L.S., de Mesy Bentley K.L. & Small E.M. (2015). Myocardin-related transcription factors control the motility of epicardium-derived cells and the maturation of coronary vessels. Development *142*, 21–30.
232) Vermot, J. et al. (2006). Conditional (loxP-flanked) allele for the gene encoding the retinoic acid-synthesizing enzyme retinaldehyde dehydrogenase 2 (RALDH2). Genesis *44*, 155-158.
233) Vidal, V. et al. (2016). The adrenal capsule is a signaling center controlling cell renewal and zonation through Rspo3. Genes and Development *30*, 1389–1394.
234) Vincent, S.D. & Buckingham, M.E. (2010). How to make a heart. The origin and regulation of cardiac progenitor cells. Current Topics in Developmental Biology *90*, 1–41.
235) Vinten-Johansen J. (2004). Involvement of neutrophils in the pathogenesis of lethal myocardial reperfusion injury. Cardiovasc Res. *61*, 481–497.
236) Volz K.S. et al. (2015). Pericytes are progenitors for coronary artery smooth muscle. *eLife* 4:e10036
237) W.D. (2006). R-Spondin proteins: a novel link to beta-catenin activation. Cell Cycle *5*, 23-26
238) Webb, I., Sicard, P., Clark, J., Redwood, S. & Marber, M. (2010). Myocardial stress remodelling after regional infarction is independent of glycogen synthase kinase-3 inactivation. J. Mol. Cell. Cardiol. *49*, 897–900.
239) Wills, A.A., Holdway, J.E., Major, R.J. & Poss, K.D. (2008). Regulated addition of new myocardial and epicardial cells fosters homeostatic cardiac growth and maintenance in adult zebrafish. Development *135*, 183.
240) Woulfe, K.C. et al. (2010). Glycogen synthase kinase-3beta regulates post-myocardial infarction remodeling and stress-induced cardiomyocyte proliferation *in vivo*. Circ. Res. *106*, 1635–1645.
241) Wu H., Lee S. H., Gao J., Liu X. & Iruela-Arispe M. L. (1999). Inactivation of erythropoietin leads to defects in cardiac morphogenesis. Development *126*, 3597-3605
242) Wu, B. et al. (2012). Endocardial cells form the coronary arteries by angiogenesis through myocardial-endocardial VEGF signaling. Cell *151*, 1083–1096.
243) Xavier-Neto, J. et al. (2015). Signaling through retinoic acid receptors in cardiac development: Doing the right things at the right times. Biochimica et Biophysica Acta - Gene Regulatory Mechanisms *1849*, 94–111.
244) Xavier-Neto, J., Neville, C.M., Shapiro, M.D., Houghton, L., Wang, G.F., Nikovits, W., Jr., Stockdale, F.E. & Rosenthal, N. (1999). A retinoic acid-inducible transgenic marker of sino-atrial development in the mouse heart. Development *126*, 2677–2687.
245) Xiao, Q. et al. (2017). A p53 based genetic tracing system to follow postnatal cardiomyocyte expansion in heart regeneration. Development *144*, 580–589.

246) Yan, J., Zhang, L., Sultana, N., Park, D. S., Shekhar, A., Bu, L., Hu, J., Razzaque, S. & Cai, C. L. (2015). A murine Myh6^{MerCreMer} knock-in allele specifically mediates temporal genetic deletion in cardiomyocytes after tamoxifen induction. PLoS ONE *10*, 1–15.
247) Yan, K. S. et al. (2017) Non-equivalence of Wnt and R-spondin ligands during Lgr5 + intestinal stem-cell self-renewal. Nature *1,* 1–8.
248) Yang J.T., Rayburn H. & Hynes R.O. (1995). Cell adhesion events mediated by a4 integrins are essential in placental and cardiac development. Development *121*, 549–560.
249) Yashiro, K. et al. (2004). Regulation of retinoic acid distribution is required for proximodistal patterning and outgrowth of the developing mouse limb. Dev. Cell *6,* 411–422.
250) Ye, Z., Zhou, Y., Cai, H., and Tan, W. (2011). Myocardial regeneration: Roles of stem cells and hydrogels. Adv. Drug Deliv. Rev. *63*, 688–697.
251) Yu, J. & Virshup, D.M. (2014). Updating the Wnt pathways. Bioscience reports *34*, 593–607.
252) Zaffran, S., Robrini, N. El & Bertrand, N. (2014). Retinoids and Cardiac Development. Journal of Developmental Biology *2*, 50–71.
253) Zaidi, S. & Brueckner, M. (2017). Genetics and Genomics of Congenital Heart Disease. Circulation Research *120*, 923–940.
254) Zamora, M., Männer, J. & Ruiz-Lozano, P. (2007). Epicardium-derived progenitor cells require beta-catenin for coronary artery formation. Proceedings of the National Academy of Sciences of the United States of America *104*, 18109–14.
255) Zaruba, M.N. et al. (2010). Cardiomyogenic potential of C-kit(+)-expressing cells derived from neonatal and adult mouse hearts, Circulation *121*, 1992-2000.
256) Zebisch, M., Xu, Y., Krastev, C., Macdonald, B. T., Chen, M., Gilbert, R. J. C., He, X. & Jones, E. Y. (2013). Structural and molecular basis of ZNRF3/RNF43 transmembrane ubiquitin ligase inhibition by the Wnt agonist R-spondin. Nat. Commun. *4*, 2787
257) Zeini M., Hang C.T., Lehrer-Graiwer J., Dao T., Zhou B. & Chang C-P. (2009). Spatial and temporal regulation of coronary vessel formation by calcineurin-NFAT signaling. Development *136*, 3335–4
258) Zelarayán, L.C et al. (2008). Beta-Catenin downregulation attenuates ischemic cardiac remodeling through enhanced resident precursor cell differentiation. *Pr*oc. Natl.Acad. Sci. USA *105*, 19762–19767.
259) Zhang, H. et al. (2016). Endocardium Minimally Contributes to Coronary Endothelium in the Embryonic Ventricular Free Walls. Circulation Research *118*, 1880–1893.
260) Zhang, J., Wilson, G.F., Soerens, A.G., Koonce, C.H., Yu, J., Palecek, S.P., Thomson, J.A., & Kamp, T.J. (2009). Functional cardiomyocytes derived from human induced pluripotent stem cells. Circ. Res. *104*, e30–e41.
261) Zhao ZQ. (2004). Oxidative stress-elicited myocardial apoptosis during reperfusion. Curr Opin Pharmaco*l. 4*, 159–165.
262) Zhou B., von Gise A., Ma Q., Rivera-Feliciano J. & Pu W.T. (2008). Nkx2–5- and Isl1-expressing cardiac progenitors contribute to proepicardium. Biochem Biophys Res Commun *375*, 450–453.
263) Zhou, B., et al. (2008). Epicardial progenitors contribute to the cardiomyocyte lineage in the developing heart. Nature *454*, 109–13.
264) Zhou, B. et al. (2012). Thymosin beta treatment after myocardial infarction does not reprogram epicardial cells into cardiomyocytes. J. Mol. Cell. Cardiol. *52*, 43-47.
265) Zhou, Y., Zhang, T., Zhang, Q. K., Jiang, Y., Xu, D. G., Zhang, M., Shen, W. and Pan, Q. J. (2014) Unstable expression of transgene is associated with the methylation of CAG promoter in the offspring from the same litter of homozygous transgenic mice. Molecular Biology Reports *41*, 5177–5186.

266) Zhu, S. et al. (2016). Loss of myocardial retinoic acid receptor α induces diastolic dysfunction by promoting intracellular oxidative stress and calcium mishandling in adult mice. Journal of Molecular and Cellular Cardiology *99*, 100–112.
267) Zhu, Z. et al. (2015). All-trans retinoic acid ameliorates myocardial ischemia/reperfusion injury by reducing cardiomyocyte apoptosis. PLoS ONE *10,* 1–15.